ISSN 0021-9673

ISHED
LY

VOL. 192 NO. 1 APRIL 25, 1980

NAL OF

CHROMATOGRAPHY

INTERNATIONAL JOURNAL ON CHROMATOGRAPHY, ELECTROPHORESIS AND RELATED METHODS

ELSEVIER SCIENTIFIC PUBLISHING COMPANY
AMSTERDAM

PUBLICATION SCHEDULE FOR 1980

Journal of Chromatography (incorporating *Chromatographic Reviews*) and *Journal of Chromatography, Biomedical Applications*

MONTH	D 1979	J	F	M	A	M	J	J	A	S	O	N	D
Journal of Chromatography	185 186	187/1 187/2 188/1	188/2 189/1 189/2	189/3 190/1	190/2 191 192/1	192/2 193/1 193/2 193/3		The publication schedule for further issues will be published later.					
Chromatographic Reviews			184/1	184/2									
Biomedical Applications		181/1	181/2	181/ 3-4	182/1	182/2	182/ 3-4						

Scope. The *Journal of Chromatography* publishes papers on all aspects of chromatography, electrophoresis and related methods. Contributions consist mainly of research papers dealing with chromatographic theory, instrumental development and their applications. The section *Biomedical Applications*, which is under separate editorship, deals with the following aspects: developments in and applications of chromatographic and electrophoretic techniques related to clinical diagnosis (including the publication of normal values); screening and profiling procedures with special reference to metabolic disorders; results from basic medical research with direct consequences in clinical practice; combinations of chromatographic and electrophoretic methods with other physicochemical techniques such as mass spectrometry. In *Chromatographic Reviews*, reviews on all aspects of chromatography, electrophoresis and related methods are published.

Submission of Papers. Papers in English, French and German may be submitted, if possible in three copies. Manuscripts should be submitted to:

The Editor of *Journal of Chromatography*, P.O. Box 681, 1000 AR Amsterdam, The Netherlands

or to:

The Editor of *Journal of Chromatography, Biomedical Applications*, P.O. Box 681, 1000 AR Amsterdam, The Netherlands.

Reviews are invited or proposed by letter to the Editors and will appear in *Chromatographic Reviews* or *Biomedical Applications*. An outline of the proposed review should first be forwarded to the Editors for preliminary discussion prior to preparation.

Subscription Orders. Subscription orders should be sent to: Elsevier Scientific Publishing Company, P.O. Box 211, 1000 AE Amsterdam, The Netherlands. The *Journal of Chromatography, Biomedical Applications* can be subscribed to separately.

Publication. The *Journal of Chromatography* (including *Biomedical Applications* and *Chromatographic Reviews*) has 22 volumes in 1980. The subscription price for 1980 (Vols. 181–202) is Dfl. 2838.00 plus Dfl. 352.00 (postage) (total *ca.* US$ 1636.00). The subscription price for the *Biomedical Applications* section only (Vols. 181–183) is Dfl. 399.00 plus Dfl. 48.00 (postage) (total *ca.* US$ 229.25). Journals are automatically sent by air mail to the U.S.A. and Canada at no extra costs, and to Japan, Australia and New Zealand with a small additional postal charge. Back volumes of the *Journal of Chromatography* (Vols. 1 through 180) are available at Dfl. 140.00 (plus postage). Claims for issues not received should be made within three months of publication of the issue. If not, they cannot be honoured free of charge. For customers in the U.S.A. and Canada wishing additional bibliographic information on this and other Elsevier journals, please contact Elsevier/North-Holland Inc., Journal Information Centre, 52 Vanderbilt Avenue, New York, N.Y. 10017. Tel: (212) 867-9040.

For further information, see page 3 of cover.

Printed in The Netherlands

VOL. 192, NO. 1 JOURNAL OF CHROMATOGRAPHY APRIL 25, 1980

CONTENTS

(Continued overleaf)

Contents (continued)

Notes

JOURNAL OF ORGANOMETALLIC CHEMISTRY LIBRARY

A series of books presenting reviews of recent developments and techniques in the expanding field of organometallic chemistry.

Coordinating Editor: D. SEYFERTH, *Massachusetts Institute of Technology, Cambridge, Mass., U.S.A.*

Volume 9: ORGANOMETALLIC CHEMISTRY REVIEWS

CONTENTS: Applications of organomagnesium compounds in polymerization *(D. B. Malpass).* Formation and reactivity of the complexes of carbonyl compounds with organoaluminium compounds and aluminium chloride *(A. Sprozynski and K. B. Starowieyski).* Organofluorosilanes *(R. M. Pike and K. A. Koziski).* Structural evidence of coordination interactions in organic derivatives of mercury, tin and lead *(N. G. Furmanova, L. G. Kuz'mina and Yu. T. Struchkov).* The preparation of organotin compounds by the direct reaction *(J. Murphy and R. C. Poller).* Recent advances in the chemistry of arsonium ylides *(R. K. Bansal and S. K. Sharma).*

Selected plenary lectures from the Fifth International Symposium on Organosilicon Chemistry held in Karlsruhe, August 14-18, 1978: The environmental chemistry of liquid polydimethylsiloxanes, an overview *(C. L. Frye).* Cyclic silanes *(E. F. Hengge).* Silicon as a substituent and a link of heterocyclic rings *(L. Birkofer).* Recent developments in silyl-transition metal chemistry *(B. J. Aylett).* Mechanism of nucleophilic substitution at silicon. The nature of the driving force of stereochemistry *(R. Corriu).* Silicon-containing derivatives of carbonic acid *(V. F. Mironov).* Novel aspects of silicone chemistry *(W. Buechner).*

1980 viii + 432 pages US $105.00/Dfl. 215.00 ISBN: 0-444-41840-7

Volume 8: ORGANOMETALLIC CHEMISTRY REVIEWS; ANNUAL SURVEYS: SILICON - GERMANIUM - TIN - LEAD

CONTENTS: Silicon - Synthesis and reactivity; Annual Survey covering the year 1977 *(J. Y. Corey).* Organosilicon reaction mechanisms; Annual Survey for the year 1977 *(F. K. Cartledge).* Silicon: Bonding and Structure; Annual Survey covering the year 1977 *(P. R. Jones).* Silicon - Application to organic synthesis; Annual Survey covering the year 1977 *(G. M. Rubottom).* Germanium; Annual Survey covering the year 1977 *(D. Quane).* Tin; Annual Survey covering the year 1977 *(P. G. Harrison).* Lead; Literature Survey covering the year 1977 *(J. Wolters).*

1979 viii + 608 pages US $105.00/Dfl. 215.00 ISBN: 0-444-41789-3

ELSEVIER

P.O. Box 211,
1000 AE Amsterdam
The Netherlands

52 Vanderbilt Ave
New York, N.Y. 10017

The Dutch guilder price is definitive. US $ prices are subject to exchange rate fluctuations.

7157

JOURNAL OF CHROMATOGRAPHY

VOL. 192 (1980)

JOURNAL *of* CHROMATOGRAPHY

INTERNATIONAL JOURNAL ON CHROMATOGRAPHY,
ELECTROPHORESIS AND RELATED METHODS

ELSEVIER SCIENTIFIC PUBLISHING COMPANY
AMSTERDAM

Printed in The Netherlands

Journal of Chromatography, 192 (1980) 1–18

CHROM. 12,570

GRADIENT ELUTION IN LIQUID CHROMATOGRAPHY

XI. INFLUENCE OF THE ADJUSTABLE GRADIENT PARAMETERS ON THE CHROMATOGRAPHIC BEHAVIOUR OF SAMPLE COMPOUNDS

PAVEL JANDERA and JAROSLAV CHURÁČEK

Department of Analytical Chemistry, University of Chemical Technology, Pardubice (Czechoslovakia)

(First received February 26th, 1979; revised manuscript received July 20th, 1979)

SUMMARY

The influence of the initial concentration of the stronger eluting component in the mobile phase and of the slope and shape of the gradient on important retention characteristics, such as retention volume, band width, selectivity, resolution and the position of elution bands in the chromatogram, was investigated both theoretically and experimentally, with particular attention to normal adsorption and reversed-phase chromatography using gradient elution in a binary solvent system. The different effects of the adjustable gradient parameters on the above retention characteristics are discussed.

INTRODUCTION

Gradient elution is generally accepted as the most efficient means for the solution of the so-called "general elution problem" in liquid chromatography[1]. Increasing requirements for the analysis of complex samples of naturally occurring compounds and for pollution analysis have emphasized the practical utility of gradient elution[2–4].

A better understanding of the influence of various adjustable gradient parameters on the separation process is useful when making a rational choice of the gradient profile for a given practical system. Further, the quantitative approach to the problem can be used as an aid to the identification of individual sample compounds in gradient elution chromatograms.

The main aim of gradient elution is to adjust adequately the retention of sample compounds during elution. Most practical separation problems can be solved using two-component (binary) solvent systems in which one component (solvent b) is a much stronger eluent than the other (solvent a), so that the capacity ratios of chromatographed compounds can be varied over a wide range by changing the proportion of the stronger eluent b in the mobile phase from 0 to 1.

The concentration of the stronger eluent in the mobile phase can be changed discontinuously by isocratic steps (so-called "stepwise elution"), continuously according to one monotonous mathematical function (straight lines or convex or concave

curves) or in several subsequent gradient steps with different concentration–time functions. Stepwise elution is discussed in a separate paper[5]. Elution consisting of several gradient steps is rather complex to describe quantitatively. It is meant as a "tailor-made" gradient profile for given separation problems requiring different changes of solvent composition in different parts of a chromatogram. The influence of the gradient profile on the chromatographic behaviour of sample compounds can be studied most adequately for single-curve gradients, which are by far the most frequently used and the simplest for generating gradient profiles.

This study is concerned with simple gradients described by a single mathematical function of the concentration (c) of the stronger eluting component in the mobile phase with time or, better, with the volume (V) of the eluate from the beginning of gradient elution. Various arbitrary mathematical functions can be used for this purpose; the most popular are, however, linear, exponential and logarithmic curves.

It is advantageous to express the mathematical form of the gradient function in such a way that three features of a gradient profile can be clearly distinguished: the initial concentration of the stronger eluting component in the mobile phase (A), the slope (B) and the shape ($\varkappa$) of the gradient[6]:

$$c = (A^{\frac{1}{\varkappa}} + BV)^{\varkappa} \tag{1}$$

As the three parameters of the gradient function, A, B and $\varkappa$, can be adjusted independently one from the others in order to control separation, it is desirable to know how each of these parameters influences the important characteristics of gradient elution chromatographic behaviour (retention volumes, band width, resolution, etc.).

During the preparation of this manuscript we had the opportunity of studying the latest results of Snyder and co-workers on the above aspects of gradient elution, with particular emphasis on reversed-phase systems[7–9]. These workers used a similar approach and obtained results very similar to ours in many respects. Our treatment, however, is somewhat different and it may be useful to compare the results of the two approaches. In the following discussion the results of our previous experiments with gradient elution in normal adsorption and reversed-phase chromatography are used[6,10–13].

CHROMATOGRAPHIC BEHAVIOUR OF SAMPLE COMPOUNDS IN GRADIENT ELUTION EXPERIMENTS

Retention volume

A quantitative treatment of retention volumes and other characteristics in gradient elution chromatography requires that the relationship between the capacity ratios, k', of sample compounds and the concentration of the more efficient eluting component in the mobile phase, c, be known, at least in a simplified manner. As we have shown previously[14], two simple equations can be used to describe many practical chromatographic systems:

$$k' = k'_0 c^{-n} \tag{2}$$

for chromatography based on adsorption or ion-exchange mechanisms and

$$k' = k'_0 \cdot 10^{-cn} \tag{3}$$

for partition chromatography, reversed-phase chromatography and related systems. Here, k'_0 and n represent experimental parameters characteristic of a given column material, solute and binary mobile phase system and do not depend on the composition of the mobile phase.

Much can be discussed about the validity of eqns. 2 and 3 and deviations from these equations can be found in numerous practical systems. It should be stressed, however, that these equations provide a good fit to a great variety of practical chromatographic systems in the range of capacity ratios k' = 1–10.

The sample compounds in gradient elution chromatography migrate down the column with capacity ratios changing within the above range[9,13] and deviations from eqns. 2 and 3 for $k' > 10$ or $k' < 1$ are relatively small in practice. Some deviations at $k' < 1$ can be attributed to systematic errors in the measurement of V_m (the precision of the determination of k' is poor here). We found a good validity of eqn. 2 in different adsorption systems[10,12,15] and eqn. 3 was found to fit well in a variety of reversed-phase systems (see, for example, works cited in refs. 9, 13 and 14). Thus, the deviations from eqn. 3, such as those found by Schoenmakers *et al.*[16], are not very important in most instances.

We derived two equations making possible calculations of net retention volume, $V'_{R(g)}$, for gradient elution chromatography[6,13] using the gradient function defined by eqn. 1 for systems where eqn. 2 or 3 can be applied, provided the parameters k'_0 and n in eqn. 2 or 3 are known for the compounds to be separated.

We have verified the validity of the relationships derived in adsorption chromatography of azo dyes on silica with gradients in various binary solvent systems[10,12] and in the reversed-phase chromatography of xanthine alkaloids, barbiturates and substituted uracils with a concentration gradient of methanol in a methanol–water mobile phase[13]. These relationships were further verified by Hartwick *et al.*[17] for the reversed-phase chromatography of nucleosides and bases.

The approach of Snyder and co-workers[7–9] is based on the so-called linear solvent strength gradients[18], in which the capacity ratios for individual sample compounds decrease during gradient elution according to the equation

$$\log k' = \log k_a - b\left(\frac{t}{t_0}\right) \tag{1a}$$

where k_a refers to the k' value at the beginning of gradient elution (*i.e.*, for the starting eluent). In reversed-phase chromatography, Snyder and co-workers make use of eqn. 3, as we did[7–9,13]. A linear solvent strength gradient in reversed-phase chromatography means a linear change of c with time (or V)[7,9] *i.e.*, eqn. 1 can be used for $\varkappa = 1$. Combining this equation with eqn. 3 and comparing it with eqn. 1a, we obtain

$$\log k' = \log k'_0 - nA - nBV \tag{1b}$$

$$\log k_a = \log k'_0 - nA \tag{1c}$$

and

$$b = nBt_0F = nBV_m \tag{1d}$$

where F is the flow-rate of the mobile phase and V_m is the column void volume.

In this instance, the two approaches yield essentially identical equations for retention volumes (compare the derivations in refs. 6, 7, 9 and 13). The parameter b, used by Snyder and co-workers, involves both the adjustable slope of the concentration gradient and the parameter n, which is a property of the sample compound and the two solvents, a and b, forming the gradient.

The parameter n can be adjusted by changing the nature of solvent b or a. In our approach, the parameter B is the property of the gradient profile only and does not depend on the chromatographic system.

Good validity of the equation derived by Snyder and co-workers for reversed-phase gradient elution has been obtained[8,19]. The approach of Snyder and co-workers yields identical equations for retention volume in reversed-phase and in normal adsorption chromatography, provided a linear solvent strength gradient is employed. In normal adsorption chromatographic systems, where eqn. 2 can be applied, this means an exponential gradient, as can easily be demonstrated. Here, Snyder and co-workers' approach and the resulting equation differ essentially from our treatment using gradients according to eqn. 1. However, similar conclusions concerning the influence of the gradient profile on retention behaviour in both reversed-phase and normal adsorption systems result from our approach and that of Snyder and co-workers.

From the equations for retention volumes in gradient elution chromatography according to gradient function given by eqn. 1, *i.e.* in different possible linear and non-linear solvent strength gradients[6,13], it can clearly be seen that for a given gradient function the ratio $V'_{R(g)}/V_m$ remains constant when A, $\varkappa$ and BV_m are kept constant (in a given separation system of stationary phase and solvents a, b, the parameters k'_0 and n in eqns. 2 and 3 are always constant). This means that sample compounds are eluted with the same retention volume (in column void volume units) and with the mobile phase of the same composition, even if the flow-rate of the mobile phase is changed, but B (in % of solvent b per millilitre of the eluent) is kept constant. Retention behaviour in agreement with this theoretical conclusions was found experimentally by Engelhardt and Elgass[20]. On the other hand, if we require a constant $V'_{R(g)}/V_m$ ratio when the length or diameter of the column is changed, B should be adjusted so as to keep BV_m constant (constant parameter b of Snyder and co-workers, eqn. 1a), which is in agreement with suggestions in refs. 7 and 9.

For convenience, in the following discussion we shall refer to the slope of the gradient as represented by B, the shape (curvature) by $\varkappa$ and the initial concentration of solvent b at the beginning of the gradient by A.

According to the relationships for retention volumes derived using the two approaches discussed, the net retention volumes in gradient elution chromatography, $V'_{R(g)}$, decrease with increasing parameters A and B in eqn. 1. As predicted by this theory, a linear decrease in log $V'_{R(g)}$ with increasing log B was found to apply well in the adsorption chromatography of azo dyes in different solvent systems[10,12], but could also be found in the reversed-phase chromatography of alkaloids, barbiturates and substituted uracils, where eqn. 3 applies[13] (Figs. 1–3).

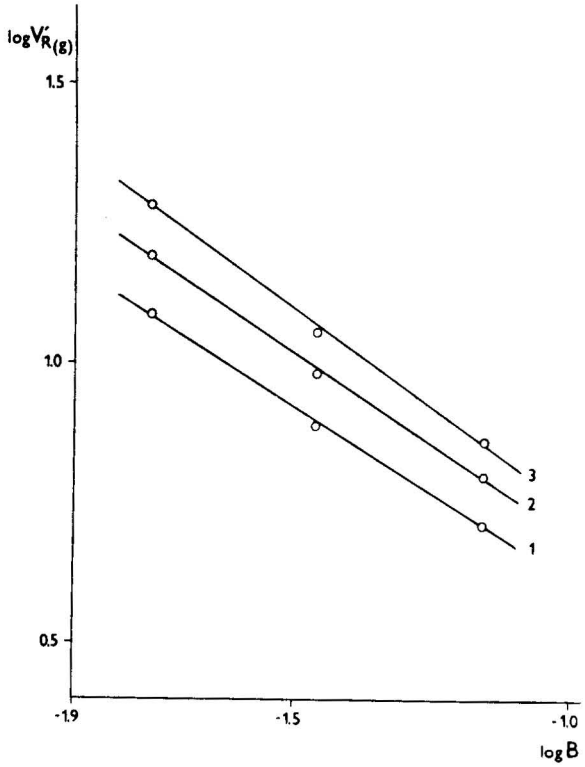

Fig. 1. Logarithmic plots of retention volumes $V'_{R(g)}$, of alkaloids *versus* the slope of the gradient, B, in reversed-phase gradient elution chromatography. Column: reversed-phase C_{18} on LiChrosorb Si-100 (10 μm), 300 × 4.2 mm; V_m = 3.2 ml. Mobile phase: gradient of methanol in water; $A = 0$; $\varkappa = 1$ (eqn. 1); flow-rate, 0.98 ml/min. $V'_{R(g)}$ in ml, B in % CH_3OH per millilitre of the mobile phase·10^{-2}. Compounds: 1 = theobromine; 2 = theophylline; 3 = caffeine.

The parameter A influences the retention volumes of later eluted peaks far less than those of earlier eluted peaks[7].

The parameter $\varkappa$ characterizes the shape of the gradient in such a way that as $\varkappa$ increases from 0 to 1, the concavity of the gradient diminishes; the gradient profile is linear at $\varkappa = 1$ and becomes more and more convex as $\varkappa$ increases further. Thus, with increasing $\varkappa$ and A and B constant, the actual concentration of more efficient eluting agent at a given time (or volume of the eluate) decreases and the net retention volumes, $V'_{R(g)}$, of sample compounds increase, as can be seen from the example of adsorption chromatography of azo dyes in Fig. 4.

Band width

The width of a peak in gradient elution chromatography results from three effects: the spreading of the solute band with time as it moves along the column, the instantaneous value of the capacity ratio at the moment of elution of the peak maximum and the compression of the band resulting from the fact that the front of the band moves in the mobile phase with a lower eluting strength than the end of the band[7–9,18].

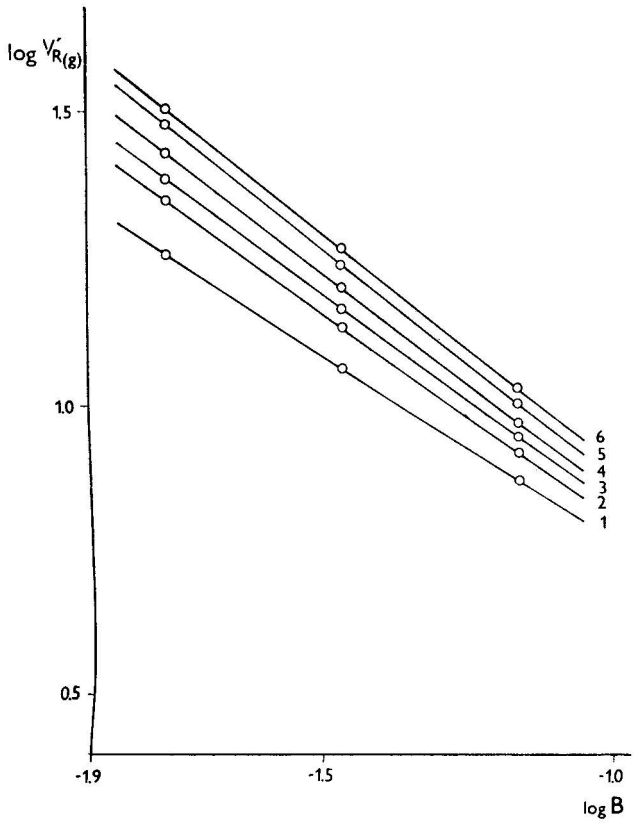

Fig. 2. Logarithmic plots of retention volumes, $V'_{R(g)}$, of barbiturates *versus* the slope of the gradient, B, in reversed-phase gradient elution chromatography. Conditions as in Fig. 1. Compounds: 1 = barbital; 2 = heptobarbital; 3 = allobarbital; 4 = aprobarbital; 5 = butobarbital; 6 = hexobarbital.

Neglecting the last effect, we derived the relationship for the band width, $w_{(g)}$, in gradient elution chromatography, where eqn. 2 or 3 applies[6].

The widths of peaks calculated when the band compression effect was neglected were approximately 10–20% higher than the experimental values measured in the gradient elution chromatography of azo dyes on silica[10,12] and in the gradient elution reversed-phase chromatography of barbiturates, substituted xanthines and uracils[13].

Snyder and Saunders[21] presented a method of calculation of the band compression factor, which expresses quantitatively the band compression effect, for linear solvent strength gradients, where this is only a function of b from eqn. 1a and can be determined for the corresponding value of b using a plot constructed by Snyder and co-workers[7,9,21] or by direct calculation[9]. The results of the experimental verification of the band width calculations according to Snyder presented in ref. 9 indicate that the calculated band widths are underestimated for $b > 0.2$, where the band compression factor acquires values lower than 0.8, while the agreement is satisfactory for $b < 0.2$. Thus, taking into account that complete neglect of band compression yields

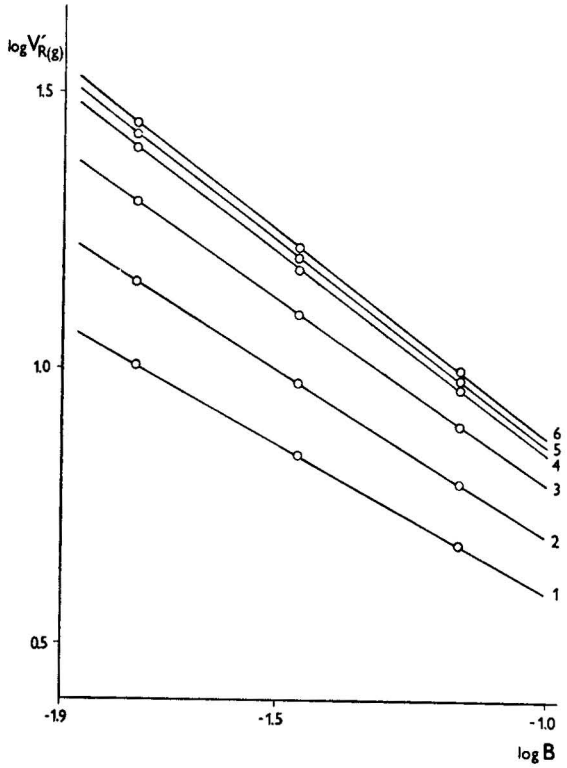

Fig. 3. Logarithmic plots of retention volumes, $V'_{R(g)}$, of substituted uracils *versus* the slope of the gradient, B, in reversed-phase gradient elution chromatography. Conditions as in Fig. 1. Compounds: 1 = 3,6-dimethyluracil; 2 = 3-ethyl-6-methyluracil; 3 = 3-*n*-propyl-6-methyluracil; 4 = 3-*sec.*-butyl-6-methyluracil; 5 = 3-*n*-butyl-6-methyluracil; 6 = 3-*tert.*-butyl-6-methyluracil.

overestimated calculated band widths, it might be expected that the use of a semi-empirical band compression factor of 0.8–0.9 for practically used gradient slopes would not introduce gross errors in comparison with more accurate determinations from the above-mentioned plot or calculation. However, this simplified approach would require further investigation.

Like retention volumes, peak widths in gradient elution chromatography decrease to a certain extent with increase in A and B in eqn. 1, as expected from both Snyder and co-workers' and our approaches, but this effect is less distinct here than with retention volumes. The rate of decrease in $w_{(g)}$ with increase in B in the adsorption chromatography of azo dyes on silica was dependent on the shape of the gradient ($\varkappa$) and the peak widths showed a tendency to reach constant values at high B[11]. In the reversed-phase chromatography of barbiturates, substituted xanthines and uracils, the peak widths, $w_{(g)}$ were far less influenced by the gradient slope, B[13]. Increasing the initial concentration of methanol in the mobile phase had a negligible effect on the peak width, and the values of $w_{(g)}$ were very similar for all the compounds studied with little regard to the differences in retention[13]. This is also in fair agreement with the behaviour predicted from Snyder's theory of linear solvent strength gradients[9].

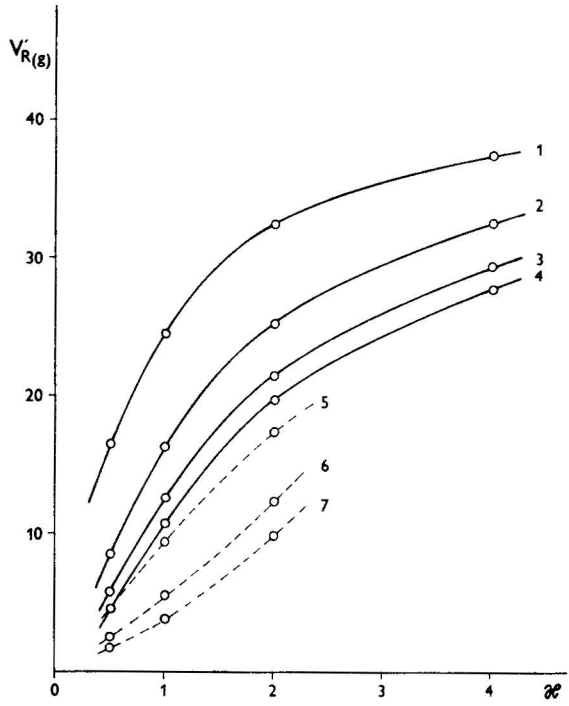

Fig. 4. Plots of the experimental retention volumes, $V'_{R(g)}$ (ml), of four azo compounds in gradient elution adsorption chromatography on Porasil A *versus* $\varkappa$ in eqn. 1. Column: Porasil A (60) (37–75 μm), 400 × 3 mm; V_m = 2.00 ml. Mobile phase: gradient of ethyl acetate in cyclohexane (curves 1–4) and of *n*-propanol in *n*-heptane (curves 5–7). Flow-rate, 0.64 ml/min; $A = 0$; $B = 0.026$ (% of alcohol per millilitre of mobile phase·10^{-2}). Compounds: dimethylamide (curve 1); diethylamide (curves 2 and 5); di-(*n*-propyl)amide (curves 3 and 6) and di-(*n*-butyl)amide (curves 4 and 7) of *p*-N,N-dimethyl-*p'*-aminobenzeneazobenzoic acid.

The influence of the shape (curvature) of the gradient on peak widths is complex and depends on the character of the compound and the mobile phase (parameters k'_0 and n in eqn. 2 or 3) and on the other parameters of the gradient (A, B). All of these parameters play a certain role in the determination of the actual composition of the eluent at the moment at which the peak maximum is eluted. Experimental plots of $w_{(g)}$ *versus* $\varkappa$ for four azo compounds in gradient elution chmatography on silica are shown in Fig. 5. In reversed-phase chromatographic experiments with gradient elution of barbiturates and other compounds, a change in the shape of the gradient ($\varkappa$) had only a minor effect on peak widths[13].

Thus, the parameters A, B and $\varkappa$ of the gradient function affected the peak widths in gradient elution in a relatively low-efficiency adsorption chromatographic system (non-linear solvent strength gradients) far more than those in a high-efficiency reversed-phase chromatographic system (linear solvent strength gradients), where the experimental peak widths were approximately constant (to within 20–40%) for all of the compounds and gradient functions studied[13].

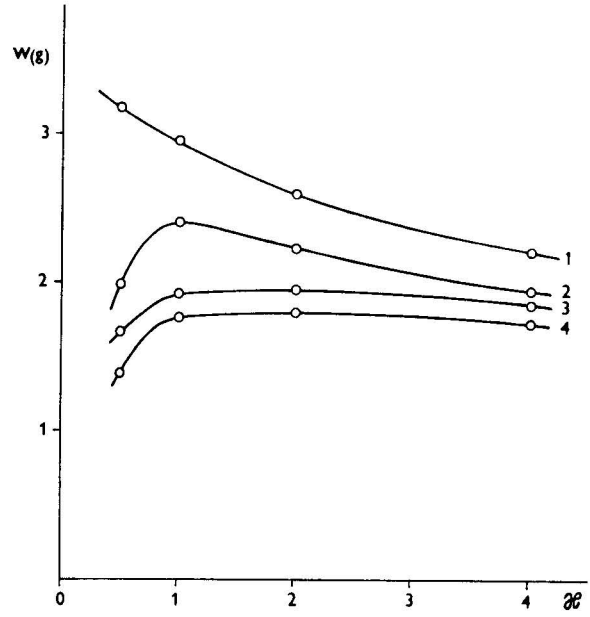

Fig. 5. Plots of the experimental peak widths, $w_{(g)}$, of four azo compounds *versus* $\varkappa$ in gradient elution adsorption chromatography on Porasil A. Conditions and numbers of compounds as in Fig. 4. Gradient of ethyl acetate in cyclohexane.

Retention ratio

By analogy with isocratic elution chromatography, we can calculate an apparent retention ratio in gradient elution chromatography, $\alpha_{(g)}$, as the ratio of net retention volumes for a pair of sample compounds 1 and 2, $V'_{R(g)1}$, $V'_{R(g)2}$, after substitution from the appropriate relationships[6,7,13] into

$$\alpha_{(g)} = \frac{V'_{R(g)2}}{V'_{R(g)1}} \tag{4}$$

In contrast to the isocratic retention ratio, $\alpha_{(g)}$ defined in this way does not represent the function of the parameters k'_{01}, k'_{02}, n_1 and n_2 only, but depends also on the parameters of the gradient (A, B and $\varkappa$). As a rule, relatively minor differences in n can be expected for most structurally similar compounds and their isocratic retention ratio is virtually independent of the composition of the mobile phase prepared from a given pair of solvents[9,10,14,15]. In systems where eqn. 3 applies, a more or less significant increase in $\alpha_{(g)}$ would be expected with decreasing B and increasing A in eqn. 1, and this could be observed in practical reversed-phase systems[13] (Table I). [Increasing A diminishes the retention volumes, whereas it does not cause great differences in $V'_{R(g)}$.]

In systems described by eqn. 2, $\alpha_{(g)}$ is not expected to depend on the slope B and decreases with increase in the parameter $\varkappa$ in eqn. 1, provided $A = 0$ (ref. 6).

TABLE I

INFLUENCE OF THE INITIAL CONCENTRATION OF THE MORE EFFICIENT ELUTING AGENT IN THE MOBILE PHASE AND OF THE SLOPE OF THE GRADIENT FUNCTION (PARAMETERS *A* AND *B* IN EQN. 1) ON THE RETENTION RATIOS OF BARBITURATES IN GRADIENT ELUTION REVERSED-PHASE CHROMATOGRAPHY

Column, mobile phase gradient and experimental conditions as in Table III. The retention ratios, $\alpha_{(g)i/1}$ of all of the compounds are relative to barbital (compound 1). The experimental values are compared with those calculated using eqn. 4 in ref. 13. Compounds: 1 = barbital, $k'_0 = 21.81$, $n = 3.2$; 2 = heptobarbital, $k'_0 = 58.44$, $n = 3.71$; 3 = allobarbital, $k'_0 = 69.44$, $n = 3.55$; 4 = aprobarbital, $k'_0 = 106.96$, $n = 3.66$; 5 = butobarbital, $k'_0 = 187.41$, $n = 3.78$; 6 = hexobarbital, $k'_0 = 252.29$, $n = 3.77$; 7 = pentobarbital, $k'_0 = 470.65$, $n = 4.07$ [k'_0 and n are the experimental parameters in eqn. 3 evaluated by linear regression from experimental $\log k' = f(c)$ plots; c = concentration of methanol in the mobile phase in isocratic elution experiments].

A	*Retention ratio*	*B*					
		0.06872		*0.03436*		*0.01718*	
		$\alpha_{(g)}$ *calc.*	$\alpha_{(g)}$ *exptl.*	$\alpha_{(g)}$ *calc.*	$\alpha_{(g)}$ *exptl.*	$\alpha_{(g)}$ *calc.*	$\alpha_{(g)}$ *exptl.*
0	$\alpha_{(g)2/1}$	1.13	1.12	1.19	1.17	1.26	1.24
	$\alpha_{(g)3/1}$	1.21	1.20	1.28	1.27	1.37	1.36
	$\alpha_{(g)4/1}$	1.29	1.28	1.38	1.37	1.50	1.49
	$\alpha_{(g)5/1}$	1.39	1.38	1.51	1.50	1.67	1.67
	$\alpha_{(g)6/1}$	1.46	1.46	1.60	1.59	1.78	1.78
	$\alpha_{(g)7/1}$	1.50	—	1.66	1.66	1.90	1.90
0.1	$\alpha_{(g)2/1}$	1.16	1.14	1.23	1.22	1.32	1.31
	$\alpha_{(g)3/1}$	1.26	1.25	1.35	1.34	1.47	1.49
	$\alpha_{(g)4/1}$	1.35	1.35	1.47	1.46	1.64	1.68
	$\alpha_{(g)5/1}$	1.48	1.48	1.64	1.64	1.87	1.94
	$\alpha_{(g)6/1}$	1.57	1.56	1.75	1.75	2.02	2.09
	$\alpha_{(g)7/1}$	1.61	1.61	1.84	1.84	2.18	2.26

Table II shows experimental results from a normal adsorption system, which are in agreement with these considerations.

For certain pairs of compounds, however, n_1 differs significantly from n_2 and, depending on the values of k'_{01} and k'_{02}, $\alpha = 1$ under isocratic conditions for a certain composition of the binary mobile phase, as we have discussed in detail and demonstrated on practical examples elsewhere [15]. In gradient elution chromatography the situation is analogous and $\alpha_{(g)} = 1$ for such a pair of compounds for certain combinations of A, B and $\varkappa$, where these compounds cannot be separated. This situation is illustrated by two practical examples of isocratic and gradient reversed-phase separations[13] in Table III and has been discussed qualitatively by Snyder[9].

A knowledge of the parameters of the gradient for which $\alpha_{(g)} = 1$ may be useful for appropriate selection of gradients for certain separation problems. These values can be calculated after substitution of the appropriate relationships into eqn. 4 while setting $\alpha_{(g)} = 1$. The resulting equations usually must be solved by using approximate methods and the relationships for the required parameters can be expressed in the explicit form in special instances only. Thus, if eqn. 2 applies in a given system and the gradient is started with pure solvent a, we obtain the value of B for which $\alpha_{(g)} = 1$:

TABLE II

INFLUENCE OF THE SHAPE OF THE GRADIENT FUNCTION (PARAMETER $\varkappa$ IN EQN. 1) ON THE RETENTION RATIOS OF AZO COMPOUNDS IN GRADIENT ELUTION ADSORPTION CHROMATOGRAPHY ON SILICA

Column: Porasil A (37–75 μm), 400 × 3.0 mm; V_m = 2.0 ml. Gradient of ethyl acetate in cyclohexane according to the gradient function given by eqn. 1 with different parameters B and $\varkappa$ (A = 0). $\alpha_{(g)2/1}$, $\alpha_{(g)3/1}$ and $\alpha_{(g)4/1}$ are the retention ratios for compounds 2–4 relative to compound 1. The experimental values are compared with those calculated using eqn. 10 in ref. 6. Flow-rate of mobile phase, 0.64 ml/min; detection, photometric (440 nm). Compounds, amides of *p*-N,N-dimethyl-*p'*-aminobenzeneazobenzoic acid: 1 = di(*n*-butyl) amide, k'_0 = 0.242, n = 1.68; 2 = di(*n*-propyl)-amide, k'_0 = 0.330, n = 1.68; 3 = diethylamide, k'_0 = 0.65, n = 1.76; 4 = dimethylamide, k'_0 = 1.94, n = 1.93 [k'_0 and n are the experimental parameters in eqn. 2 evaluated by linear regression from experimental log k' = f (log c) plots. The average value of n = 1.86 was taken for calculations of $\alpha_{(g)}$].

$\varkappa$	*Retention ratio*	*B*							
		0.00162		*0.00649*		*0.02597*		*0.1039*	
		$\alpha_{(g)}$ *calc.*	$\alpha_{(g)}$ *exptl.*	$\alpha_{(g)}$ *calc.*	$\alpha_{(g)}$ *exptl.*	$\alpha_{(g)}$ *calc.*	$\alpha_{(g)}$ *exptl.*	$\alpha_{(g)}$ *calc.*	$\alpha_{(g)}$ *exptl.*
0.5	$\alpha_{(g)2/1}$	1.24	1.25	1.24	1.24	1.24	1.25	1.24	1.19
	$\alpha_{(g)3/1}$	1.86	1.84	1.86	1.86	1.86	1.87	1.86	1.76
	$\alpha_{(g)4/1}$	3.68	—	3.68	3.57	3.68	3.62	3.68	3.50
1.0	$\alpha_{(g)2/1}$	1.16	1.15	1.16	1.16	1.16	1.17	1.16	1.16
	$\alpha_{(g)3/1}$	1.52	1.49	1.52	1.50	1.52	1.52	1.52	1.52
	$\alpha_{(g)4/1}$	2.41	2.18	2.41	2.22	2.41	2.29	2.41	2.39
2.0	$\alpha_{(g)2/1}$	1.09	1.08	1.09	1.09	1.09	1.09	1.09	1.09
	$\alpha_{(g)3/1}$	1.29	1.25	1.29	1.27	1.29	1.28	1.29	1.28
	$\alpha_{(g)4/1}$	1.70	1.59	1.70	1.62	1.70	1.64	1.70	1.66
4.0	$\alpha_{(g)2/1}$	1.05	1.05	1.05	1.05	1.05	1.06	1.05	1.05
	$\alpha_{(g)3/1}$	1.15	1.15	1.15	1.15	1.15	1.16	1.15	1.15
	$\alpha_{(g)4/1}$	1.35	1.34	1.35	1.34	1.35	1.35	1.35	1.35

$$B_{(a=1)} = \frac{1}{V_m}\left\{\frac{[k'_{01}(\varkappa n_1 + 1)]^{(\varkappa n_2+1)}}{[k'_{02}(\varkappa n_2 + 1)]^{(\varkappa n_1+1)}}\right\}^{\frac{1}{\varkappa(n_1-n_2)}} \tag{5}$$

For the systems described by eqn. 3, we can write under analogous conditions an approximate equation, assuming large k'_0 values and $\varkappa = 1$:

$$B_{(a=1)} \approx \frac{1}{2.31\ V_m} \cdot \frac{(k'_{02}n_2)^{\frac{n_1}{n_2-n_1}}}{(k'_{01}n_1)^{\frac{n_2}{n_2-n_1}}} \tag{6}$$

Resolution

As the main aim of chromatography is to separate substances, resolution is the most important characteristic of the chromatographic process. The resolution of two compounds 1 and 2 in gradient elution chromatography, $R_{s(g)}$, can be defined by analogy with isocratic elution as

$$R_{s(g)} \approx \frac{V'_{R(g)2} - V'_{R(g)1}}{w_{(g)2}} \tag{7}$$

TABLE III

INFLUENCE OF PARAMETERS A AND B OF THE GRADIENT FUNCTION (EQN. 1) ON THE ELUTION SEQUENCE IN GRADIENT ELUTION REVERSED-PHASE CHROMATOGRAPHY

Column: octadecylsilica bonded on LiChrosorb Si-100 (10 μm), 300 × 4.2 mm; V_m = 3.2 ml. Isocratic elution: mobile phase composed of methanol (different concentrations, c) in water; k'_1–k'_4 are experimental capacity ratios for compounds 1–4; $\alpha_{2/1}$, $\alpha_{4/3}$ are experimental retention ratios for compounds 2, 1 and 4, 3, respectively. Gradient elution: gradient of methanol in water according to the gradient function given by eqn. 1 with different parameters A and B ($\varkappa = 1$). $V'_{R(g)1}$–$V'_{R(g)4}$ are experimental net retention volumes for compounds 1–4; $\alpha_{(g)2/1}$, $\alpha_{(g)4/3}$ are retention ratios for compounds 2, 1 and 4, 3, respectively, found experimentally and calculated from eqn. 4 in ref. 13. Flow-rate of the mobile phase, 0.97 ml/min; detection, UV (254 nm), 0.16 a.u.f.s. Compounds: 1 = caffeine, k'_0 = 32.28, n = 3.78; 2 = barbital, k'_0 = 21.81, n = 3.20; 3 = 3-*n*-butyl-6-methyluracil, k'_0 = 67.20, n = 3.25; 4 = aprobarbital, k'_0 = 106.96, n = 3.66 [k'_0 and n are the experimental parameters of eqn. 3 evaluated by linear regression from experimental log k' = f(c) plots].

Isocratic elution

% CH_3OH (c)	k'_1	k'_2	$\alpha_{2/1}$	k'_3	k'_4	$\alpha_{4/3}$
20	5.82	5.12	0.88	21.89	21.06	0.96
30	1.78	2.29	1.29	7.49	8.42	1.12
40	0.90	1.16	1.29	3.24	3.47	1.07

Gradient elution

A	B	$V'_{R(g)1}$ (ml)	$V'_{R(g)2}$ (ml)	$\alpha_{(g)2/1}$		$V'_{R(g)3}$ (ml)	$V'_{R(g)4}$ (ml)	$\alpha_{(g)4/3}$	
				Exptl.	Calc.			Exptl.	Calc.
0	0.06872	7.26	7.25	1.00	1.02	9.58	9.28	0.97	1.00
	0.03436	11.39	11.56	1.01	1.00	15.97	15.88	0.99	1.01
	0.01718	19.21	17.92	0.93	0.96	26.63	26.75	1.00	1.04
0.1	0.06872	5.64	5.84	1.04	1.03	8.02	7.90	0.98	0.99
	0.03436	8.72	8.90	1.02	1.01	13.23	13.03	0.98	1.01
	0.01718	13.11	12.36	0.94	0.97	20.65	20.79	1.01	1.04

If the relationship between the capacity ratios of sample compounds and composition of the mobile phase is given by eqn. 2, the introduction of the corresponding relationships for $V'_{R(g)}$ and $w_{(g)}$ yields the following relationship for resolution:

$$R_{s(g)} = \underbrace{\frac{\sqrt{N_2}}{4}}_{\text{I}} \cdot \underbrace{\frac{\alpha_{(g)} - 1}{\alpha_{(g)}}}_{\text{II}} \cdot \underbrace{\frac{(\varkappa n_2 + 1)Bk'_{02}V_m + A^{\frac{\varkappa n_2+1}{\varkappa}} - A^{\frac{1}{\varkappa}}\left[(\varkappa n_2 + 1)Bk'_{02}V_m + A^{\frac{\varkappa n_2+1}{\varkappa}}\right]^{\frac{\varkappa n_2}{\varkappa n+1}}}{V_m B\left\{\left[(\varkappa n_2 + 1)Bk'_{02}V_m + A^{\frac{\varkappa n_2+1}{\varkappa}}\right]^{\frac{\varkappa n_2}{\varkappa n_2+1}} + k'_{02}\right\}}}_{\text{III}}$$

N_2 is the number of plates for compound 2, which is assumed not to depend significantly on the composition of the mobile phase.

By analogy with isocratic elution chromatography, three terms for different contributions to the resolution can be distinguished: I, the efficiency, is essentially the same as in isocratic elution operation; II, the selectivity, employs $\alpha_{(g)}$ instead of α; and III, the capacity, is a function only of the retention of compound 2 in gradient elution work.

Introducing the relationship for $\alpha_{(g)}$ into eqn. 8, we can express resolution as the function of the parameters k'_{01}, n_1, k'_{02} and n_2 of the two chromatographed compounds (eqns. 2) and of A, B and $\varkappa$:

$$R_{s(g)} = \frac{\sqrt{N_2}}{4V_m B} \times$$

$$\times \frac{\left[(\varkappa n_2 + 1)Bk'_{02}V_m + A^{\frac{\varkappa n_2+1}{\varkappa}}\right]\left[\frac{1}{\varkappa n_2+1} - \right](\varkappa n_1 + 1)Bk'_{01}V_m + A^{\frac{\varkappa n_2+1}{\varkappa}}\Big]^{\frac{1}{\varkappa n_1+1}}}{1 + k'_{02}\left[(\varkappa n_2 + 1)Bk'_{02}V_m + A^{\frac{\varkappa n_2+1}{\varkappa}}\right]^{-\frac{\varkappa n_1}{\varkappa n_2+1}}} \quad (9)$$

In systems described by eqn. 3, relationships analogous to eqns. 8 and 9 can be derived in the same manner ($\varkappa = 1$):

$$R_{s(g)} = \underbrace{\frac{\sqrt{N_2}}{4}}_{\text{I}} \cdot \underbrace{\frac{\alpha_{(g)} - 1}{\alpha_{(g)}}}_{\text{II}} \cdot \underbrace{\frac{\log(2.31 n_2 BV_m k'_{02} + 10^{n_2 A}) - n_2 A}{n_2 BV_m[1 + k'_{02}(2.31 n_2 BV_m k'_{02} + 10^{n_2 A})^{-1}]}}_{\text{III}} \quad (10)$$

and

$$R_{s(g)} = \frac{\sqrt{N_2}}{4V_m B} \times$$

$$\times \frac{\frac{1}{n_2} \cdot \log(2.31 n_2 BV_m k'_{02} + 10^{n_2 A}) - \frac{1}{n_1} \cdot \log(2.31 n_1 BV_m k'_{01} + 10^{n_1 A})}{1 + k'_{02}(2.31 n_2 BV_m k'_{02} + 10^{n_2 A})^{-1}} \quad (11)$$

The influence of A, B and $\varkappa$ on the resolution in gradient elution chromatography depends on combination of the parameters k'_{01}, k'_{02}, n_1 and n_2 of the two compounds 1 and 2, like the influence of the concentration of the more efficient eluting agent in the mobile phase on the resolution in isocratic elution chromatography.

As has been discussed above, there are certain combinations of A, B and $\varkappa$ which may yield $\alpha_{(g)} = 1$ and no resolution in gradient elution chromatography. In such an instance, as one of A and B increases while the other two parameters are held constant, the capacity term III decreases and the selectivity term II in eqn. 8 or 10 decreases first to zero [$\alpha_{(g)} = 1$] and then increases again, as when the concentration of the more efficient eluting agent in the mobile phase is increased in isocratic elution chromatography[15].

Consequently, a maximum occurs on the $R_{s(g)} = f(B)$ or $R_{s(g)} = f(A)$ curve, which can be calculated by solving the equation $dR_{s(g)} = 0$ for one of the above parameters. For example, the value of $B_{(max)}$ for maximum resolution can be solved by an approximate method using the relationship obtained from eqn. 9 for $A = 0$ and a constant value of $\varkappa$, in the following form:

$$B_{(max)} = \left\{ \frac{k'_{02}\left(\frac{\varkappa n_1}{\varkappa n_1 + 1} - \frac{\varkappa n_2}{\varkappa n_2 + 1}\right) \cdot \frac{[(\varkappa n_1 + 1)k'_{01}V_m]^{\frac{1}{\varkappa n_1 + 1}}}{[(\varkappa n_2 + 1)k'_{02}V_m]^{\frac{\varkappa n_2}{\varkappa n_2 + 1}}} + B^{\frac{\varkappa n_2}{\varkappa n_2 + 1}}_{(max)} \cdot \frac{\varkappa n_1}{\varkappa n_1 + 1}[(\varkappa n_1 + 1)k'_{01}V_m]^{\frac{1}{\varkappa n_1 + 1}}}{\frac{\varkappa n_2}{\varkappa n_2 + 1} \cdot [(\varkappa n_2 + 1)k'_{02}V_m]^{\frac{1}{\varkappa n_2 + 1}}} \right\}^{\frac{\varkappa n_1 + 1}{\varkappa n_1}} \quad (12)$$

In most practical systems, no reversal of the order of elution with changing composition of the mobile phase occurs. Here, A has no significant influence on the differences in retention volumes or peak widths, which leads to a relatively small influence of A on resolution. Thus, the increase in the selectivity term II and the decrease in the capacity term III with increasing A tend to counterbalance each other, up to a certain value of A, where the retention of the two compounds is decreased to such an extent that the resolution decreases with a further increase in A.

In these systems, the capacity term III is influenced by B more significantly than the selectivity term II and the resolution increases with decreasing B[11].

The shape of the concentration gradient characterized by the parameter $\varkappa$ in eqn. 1 has a more complex influence on resolution. It can be shown theoretically that maximal resolution can be found for certain values of $\varkappa$ even in the most simple instances, where $n_1 \approx n_2$ and $A = 0$ in eqn. 8. Here, the resolution approaches zero for very large $\varkappa$ and becomes identical with the resolution in isocratic elution using the pure, more efficient eluent for $\varkappa = 0$. The resolution obtained in gradient elution chromatography is always larger than in the above two extreme situations and a maximum on the $R_s = f(\varkappa)$ curve must occur. In practice, however, these maxima are likely to be rather flat and even a large change in $\varkappa$ would not influence the resolution very significantly, as shown by the example in Fig. 6.

Snyder *et al.*[7,9] published a relatively simple equation for linear solvent strength gradients, using certain simplifying assumptions, such as $n_1 = n_2$, low values of A and large values for k'_{01} and k'_{02}, but small differences between them. As a result of these simplifications, this equation is much simpler than eqn. 10, which can be applied to this system. Another difference is in the band compression factor, which is incorporated in the denominator of their equation as a function of the parameter b from eqn. 1a. Like eqn. 10, their relationship may be written in the form of terms I, II and III, where $\alpha_{(g)} = k'_{02}/k'_{01}$ and the term III is also much simpler (approximately equal to $1/(1 + 1.15\,b)$ (ref. 9). This equation allows for rapid estimations of resolution and its application requires only a rough guess of the parameter n (which is contained implicitly in b and is usually known in reversed-phase systems, see eqn. 1d). Eqns. 8–10 are much more complex but allow direct calculations of resolution without further simplifying assumptions, in linear and non-linear solvent strength gradients, for compounds with different values of n and for any values of A. The band compression factor can be incorporated into denominators of the above equations, either as a function of the gradient slope or as a semi-empirical factor of 0.8–0.9; see preceding discussion of band width.

To use Snyder's equation for the calculation of resolution in linear solvent systems where $n_1 \neq n_2$ and/or $A \gg 0$, a series of subsequent corrections have to be introduced, as suggested in ref. 9.

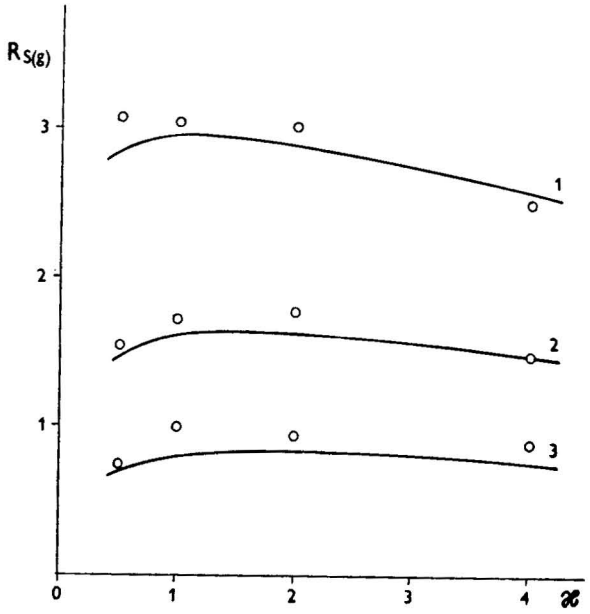

Fig. 6. Plots of the experimental (points) and calculated (eqn. 13, $A = 0$; full curves) resolution, $R_{s(g)}$, *versus* $\varkappa$ in gradient elution adsorption chromatography on Porasil A. Conditions and numbers of compounds as in Fig. 4. Gradient of ethyl acetate in cyclohexane. Curve 1, resolution of compounds 1 and 2, $R_{s(g)1,2}$; curve 2, resolution of compounds 2 and 3, $R_{s(g)2,3}$; curve 3, resolution of compounds 3 and 4, $R_{s(g)3,4}$.

Using his approach, Snyder[9] arrived at very similar conclusions about the influence of the initial concentration and gradient slope on resolution in systems where $n_1 = n_2$ and where $n_1 \neq n_2$.

Compression criterion

It is difficult to find a convenient criterion that is useful for the characterization of the chromatographic behaviour of more than two compounds during gradient elution. An important feature of gradient elution is its capability to compress the chromatogram, *i.e.*, to shorten the retention time of the last eluted compounds with respect to the early eluted solutes. We attempted to introduce a new appropriate criterion to characterize quantitatively this effect, namely the compression criterion, Q, which is defined as

$$Q = \frac{V'_{R(g)z} - V'_{R(g)1}}{V'_{R(g)2} - V'_{R(g)1}} = \frac{\alpha_{(g)z/1} - 1}{\alpha_{(g)2/1} - 1} \tag{13}$$

where $V'_{R(g)1}$, $V'_{R(g)2}$ and $V'_{R(g)z}$ denote the net retention volumes of the first, the second and the last eluted compound, respectively, and $\alpha_{(g)2/1}$ and $\alpha_{(g)z/1}$ are the retention ratios of the second and the last compounds with respect to the first compound. Thus, Q expresses the length of the chromatogram in multiples of its relative portions necessary for the elution of the first two sample compounds. If the first two

compounds are eluted with $R_{s(g)} = 1$ and the peak widths are equal for all of the compounds eluted, then Q becomes identical with peak capacity in gradient elution chromatography defined according to Horváth and Lipsky[22], but generally no limiting assumptions are involved in the definition of Q.

The compression criterion can be useful evaluating the influence of A, B and $\varkappa$ on the compression of a chromatogram, if $V'_{R(g)1}$, $V'_{R(g)2}$ and $V'_{R(g)z}$ are expressed from the appropriate equation[6,13]. An adequate compression of the chromatogram may be desirable with respect to the number of compounds to be resolved and the time of analysis.

Assuming that eqn. 2 applies and that the respective parameters n for all of the compounds are close to each other, and using gradient functions with zero initial concentration of the efficient eluting component, $A = 0$, we obtain the following relationship for Q:

$$Q = \frac{\left(\frac{k'_{0z}}{k'_{01}}\right)^{\frac{1}{\varkappa n + 1}} - 1}{\left(\frac{k'_{02}}{k'_{01}}\right)^{\frac{1}{\varkappa n + 1}} - 1} \tag{14}$$

According to eqn. 14, the compression of a chromatogram in this instance should depend on the curvature only, and not on the slope of the gradient function. This conclusion was confirmed experimentally in the adsorption chromatography of azo dyes on silica, as is shown in Fig. 7, where the calculated values of Q are plotted against $\varkappa$ together with the experimental points obtained at four different values of the slope of the gradient function (B).

As confirmed experimentally, the differences in retention volumes are not influenced much by the initial concentration of the efficient eluting agent at the beginning of gradient elution, A (see preceding discussion). It can also be assumed that Q is not influenced much by A.

This is not the case, however, in the relatively rare instances where the differences in the values of n are large for individual sample compounds. In reversed-phase chromatography, where eqn. 3 fits approximately to describe the dependence of capacity ratios on the composition of mobile phase, eqn. 14 cannot be used and the compression criterion Q depends on the slope of the gradient function, as shown in Table IV.

CONCLUSIONS

To summarize the influence of the gradient profile on the chromatographic behaviour of sample compounds in gradient elution chromatography, from the preceding discussion and from the comparison of the approaches of Snyder and co-workers and ourselves, we can draw the following conclusions:

(a) As the initial concentration of solvent b (parameter A in eqn. 1) is increased, retention volumes decrease, but band widths, differences in retention volumes of

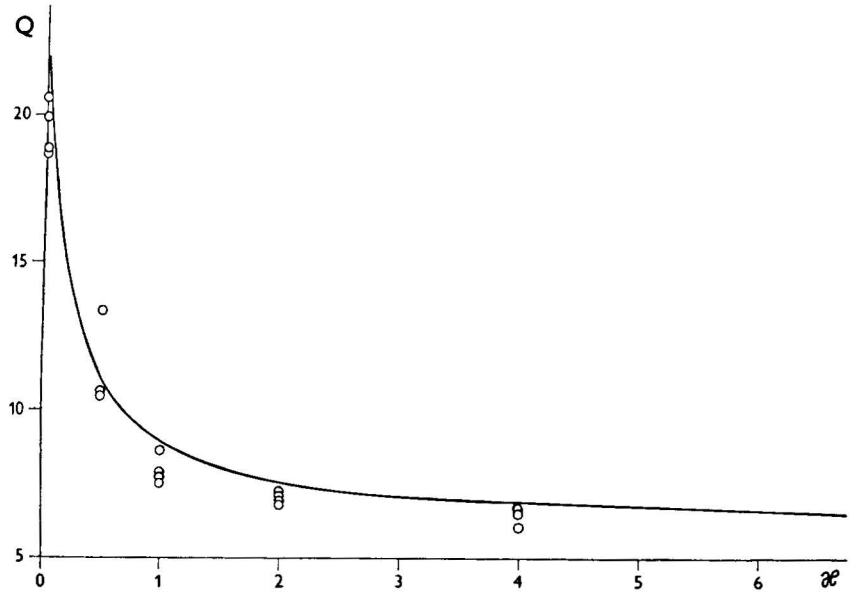

Fig. 7. Plots of the experimental (points) and calculated (full curve) values of the compression criterion, Q, *versus* $\varkappa$ in gradient elution adsorption chromatography on Porasil A. Experimental points were measured at different values of B (0.0016–0.1039); $A = 0$. Eqn. 14 was used for calculations; k_{01} is k_0' of compound 4; k_{0z}' is k_0' of compound 1; $n = 1.86$ is an average value for the four azo compounds studied. Conditions and numbers of compounds as in Fig. 4. Gradient of ethyl acetate in cyclohexane.

TABLE IV

INFLUENCE OF PARAMETERS A AND B OF THE GRADIENT FUNCTION (EQN. 1) ON THE COMPRESSION CRITERION, Q, IN GRADIENT ELUTION REVERSED-PHASE CHROMATOGRAPHY

Column, mobile phase gradient and experimental conditions as in Table III. The experimental values of Q are compared with those calculated using eqns. 13 and 4 in ref. 13. Compounds: barbiturates: 1 = barbital; 2 = heptobarbital; z = hexobarbital; the values of k_0' and n (eqn. 3) are given in Table I; substituted uracils: 1 = 3,6-dimethyluracil, $k_0' = 9.51$, $n = 4.40$; 2 = 3-ethyl-6-methyluracil, $k_0' = 15.63$, $n = 3.69$; z = 3-*n*-butyl-6-methyluracil, $k_0' = 67.20$, $n = 3.25$ [k_0' and n were evaluated by linear regression from experimental $\log k' = f(c)$ plots].

Compounds	*A*	*B*					
		0.06872		*0.03436*		*0.01718*	
		Q calc.	*Q exptl.*	*Q calc.*	*Q exptl.*	*Q calc.*	*Q exptl.*
Barbiturates	0	3.53	3.74	3.18	3.41	2.98	3.21
	0.1	3.63	3.92	3.31	3.48	3.16	3.49
Substituted	0	3.40	3.37	3.65	3.67	3.96	3.92
Uracils	0.1	3.43	3.39	3.70	3.76	4.08	4.26

sample compounds and resolution are usually not much influenced, if A does not exceed practically useful limits. In this range, A can be used to control the time of analysis, while the resolution is kept approximately constant.

(b) An increase in the gradient slope (parameter B in eqn. 1) usually results in a decrease in retention volumes, resolution and band width (the influence of B increases in this order). The chromatogram becomes more compressed. B can be utilized for control of resolution within certain limits, while other system parameters are kept constant. If the parameters n_1 and n_2 in eqns. 2 or 3 are significantly different for compounds to be separated, maxima and minima of resolution may be found occasionally when B (or A or $\varkappa$, to a lesser extent) is changed in a systematic manner, but this effect is likely to be of minor importance only.

(c) Increasing the parameter $\varkappa$ in eqn. 1 [changing the shape (curvature) of the gradient] leads to changes in the relative positions of sample bands in a chromatogram, usually corresponding to some increase in retention volumes. The compression of the whole chromatogram can be controlled, but the influence of $\varkappa$ on other retention characteristics is usually not as significant as that of A and B.

REFERENCES

1 L. R. Snyder, in J. J. Kirkland (Editor), *Modern Practice of Liquid Chromatography*, Wiley-Interscience, New York, 1971, p. 149.
2 K. Aitzetmüller, *J. Chromatogr. Sci.*, 13 (1975) 454.
3 W. E. May , S. N. Chesler, S. P. Cram, B. H. Gump, M. S. Hertz and S. M. Dyszel *J. Chromatogr. Sci.*, 13 (1975) 535.
4 C. G. Creed, *Res./Develop.*, 27 (1976) 40.
5 P. Jandera and J. Churáček, *J. Chromatogr.*, 170 (1979) 1.
6 P. Jandera and J. Churáček, *J. Chromatogr.*, 91 (1974) 223.
7 L. R. Snyder, J. W. Dolan and J. R. Gant, *J. Chromatogr.*, 165 (1979) 3.
8 J. W. Dolan, J. R. Gant and L. R. Snyder, *J. Chromatogr.*, 165 (1979) 31.
9 L. R. Snyder, in Cs. Horváth (Editor), *Liquid Chromatography*, Academic Press, New York, London, in press.
10 P. Jandera and J. Churáček, *J. Chromatogr.*, 93 (1974) 17.
11 P. Jandera and J. Churáček, *J. Chromatogr.*, 104 (1975) 9.
12 P. Jandera, M. Janderová and J. Churáček, *J. Chromatogr.*, 115 (1975) 9.
13 P. Jandera, J. Churáček and L. Svoboda, *J. Chromatogr.*, 174 (1979) 35.
14 P. Jandera and J. Churáček, *J. Chromatogr.*, 91 (1974) 207.
15 P. Jandera, M. Janderová and J. Churáček, *J. Chromatogr.*, 148 (1978) 79.
16 P. J. Schoenmakers, H. A. H. Billiet, R. Tijssen and L. de Galan, *J. Chromatogr.*, 149 (1978) 519.
17 R. A. Hartwick, C. M. Grill and P. R. Brown, *Anal. Chem.*, 51 (1979) 34.
18 L. R. Snyder, *Chromatogr. Rev.*, 7 (1965) 1.
19 H. Elgass, *Untersuchung zur Gradient Elution*, Thesis, Universität des Saarlandes, Saarbrücken, 1978.
20 H. Engelhardt and H. Elgass, *J. Chromatogr.*, 158 (1978) 249.
21 L. R. Snyder and D. L. Saunders, *J. Chromatogr. Sci.*, 7 (1969) 195.
22 C. G. Horváth and S. R. Lipsky, *Anal. Chem.*, 39 (1967) 1893.

Journal of Chromatography, 192 (1980) 19–36

CHROM. 12,571

GRADIENT ELUTION IN LIQUID CHROMATOGRAPHY

XII. OPTIMIZATION OF CONDITIONS FOR GRADIENT ELUTION

PAVEL JANDERA and JAROSLAV CHURÁČEK

Department of Analytical Chemistry, University of Chemical Technology, Pardubice (Czechoslovakia)

(First received February 26th, 1979; revised manuscript received July 20th, 1979)

SUMMARY

Different possibilities for the optimization of gradient elution conditions are discussed and compared. An approach is developed that permits calculations of the optimal initial concentration and slope of the gradient for the separation of mixtures containing compounds with known relationships of capacity ratio *versus* composition of the mobile phase. The approach was used for the selection of optimal conditions in the reversed-phase gradient elution chromatography of barbiturates and substituted uracils. The agreement between the experimental and expected chromatographic data is compared. A general approximate method is suggested for the prediction of the slope of the gradient in reversed-phase chromatography.

INTRODUCTION

Gradient elution is widely accepted as a highly efficient technique for adjusting adequately the retention of sample compounds during elution[1]. The conditions for gradient elution are usually selected by a trial-and-error method. In many instances it would be useful, however, if we were able to calculate the optimal gradient elution conditions for a given separation problem from the properties of the chromatographic system and compounds to be separated, without performing a number of preliminary experiments. Such a rational choice of the optimal gradient elution profile for a required separation is not possible without a good understanding of the influence of the profile of the concentration gradient on retention characteristics such as retention volume, peak width and resolution. This aspect has been treated quantitatively in Part XI[2] and elsewhere[3].

A few papers have been published in which the positions of the maxima and bandwidths in gradient elution chromatography were correlated with the profile of the concentration gradient in special instances[4–8], but such approaches cannot be used as the basis for the optimization of gradient elution chromatography because of the lack of general applicability and the complexity of the resulting equations.

Snyder and co-workers[9,10] developed the concept of so-called "linear solvent strength" gradients, which are relatively simple to understand and treat. This concept

was recently elaborated by this group and a method for the optimization of these gradients has been suggested[3,11,12].

In this paper another approach to gradient optimization is suggested and compared with the treatment of Snyder and co-workers.

OPTIMIZATION OF RESOLUTION IN GRADIENT ELUTION CHROMATOGRAPHY: COMPARISON OF DIFFERENT APPROACHES

Optimization of the chromatographic process means finding adequate conditions so as to obtain a required resolution of sample compounds in as short a time as possible. To meet this aim in gradient elution chromatography, the components (solvents) from which the gradient is formed and the profile of the gradient should be judiciously chosen. Most practical separation problems can be solved by using no more than two solvents of different elution strengths. After an appropriate choice of the weaker (a) and the stronger (b) solvent, the profile of the gradient should be selected, *i.e.*, the shape (curvature) and the slope (B) of the gradient and the starting concentration (A) of solvent a in the mobile phase. The optimization of the gradient profile requires different treatments if the sample compounds are known and if there is information available about their chromatographic behaviour under isocratic conditions, or if an essentially unknown sample is to be separated.

Approach according to Snyder and co-workers

Snyder and co-workers[3,11,12] suggested an optimization approach for "linear solvent strength" gradients in reversed-phase chromatography. In "linear solvent strength" gradients the logarithms of the capacity ratios of sample compounds, k_i', decrease linearly with time according to[9,10]

$$\log k_i' = \log k_a - b(t/t_0) \tag{1}$$

where k_a is k_i' in the mobile phase at the beginning of gradient elution, t_0 is the column dead time and b characterizes the slope of the gradient but depends also on the behaviour of sample compound i in a given chromatographic system (for a more detailed discussion, see refs. 3, 9 and 10). The concentration profile of a "linear solvent strength" gradient together with the character of the relationship between k_i' and the composition (isocratic) of the mobile phase (such as described by eqn. 2a or 2b in further discussion below) determine the shape of the concentration gradient. In reversed-phase chromatography, where eqn. 2b usually applies well, this means a linear concentration gradient (linear change of concentration of solvent b in the eluent with time)[11]. With certain simplifying assumptions (*e.g.*, k_a for all compounds very large, *i.e.*, $A \to 0$; constant separation factors for sample compounds during the gradient), a simplified equation for resolution in gradient elution chromatography as a function of b in eqn. 1 could be derived[3,10,11].

As in isocratic elution chromatography, where maximal resolution per time unit can be achieved at certain values of the capacity ratios of sample compounds, maximal resolution in a given separation time in gradient elution chromatography is obtained for a fixed value of b ($b \approx 0.2$; see detailed discussion in refs. 3, 11 and 12).

The optimization approach according to Snyder and co-workers[11,12] suggests

gradients using this value of b, from which the slope B of the linear concentration gradient can be calculated, provided that n in eqn. 2b is approximately constant in a given reversed-phase chromatographic system and its value can be estimated, which appears to be a realistic assumption in practice. The initial concentration of solvent b is $A = 0$.

This optimization approach can be applied generally in reversed-phase chromatography, but it cannot give the best utilization of the analysis time or the resolution required for each individual separation problem. Therefore, Snyder and coworkers[11,12] recommend the following "fine tuning" of the separation conditions using a trial-and-error method, for which they provide several hints. These should be tried subsequently in the following order:

(a) increase in the initial concentration, A, of solvent b (if sample compounds are eluted too late);

(b) variation in the parameter b in eqn. 1 to obtain a better resolution;

(c) increase in N by decreasing the flow-rate or by increasing the column length, if the resolution is still insufficient;

(d) changing the organic solvent b if the selectivity is too low or if the sample compounds are very strongly retained.

Present optimization approach

The optimization approach presented here allows the direct calculation of the best profile of the gradient necessary to achieve the separation of a mixture of known compounds in as short a time as possible with a gradient formed from two given solvents a and b. Thus, "tailor-made" gradients for each separation are calculated, in which the solvent strength does not necessarily change linearly. This approach can be used for both reversed-phase and normal adsorption and ion-exchange systems, but the relationships between the capacity ratios, k', of sample compounds and the concentration (c) of the stronger solvent b in the mobile phase under isocratic conditions must be known, in addition to the respective constants of this equation. In principle, different k' *versus* c functions may be used, but we shall restrict ourselves here to the two simplest and evidently most useful relationships:

$$k' = k_0' c^{-n} \tag{2a}$$

and

$$k' = k_0' 10^{-cn} \tag{2b}$$

where k_0' and n are experimental constants of the sample compound and system used.

Eqn. 2a can be used in many normal adsorption and ion-exchange systems, while eqn. 2b is suitable for reversed-phase chromatography. It is not the purpose of this paper to argue about the validity of and deviations from these equations; for a comprehensive discussion, see refs. 3, 11 and 13–19.

In our optimization approach it is assumed that the efficiency (plate number, N) of the column used does not depend significantly on the composition of the binary mobile phase, which seems to be a reasonable assumption in most situations. The optimization of separation by controlling N via the column length or flow-rate can be achieved by analogy with isocratic elution and is not considered in the present approach, where a fixed value of N is assumed (given column dimensions and flow-rate).

It is further assumed that there is no concentration change in the mobile phase caused by the column (solvent demixing is negligible) or by the geometry of the instrument.

Finally, it is assumed that the gradient-generating device used is capable of mixing two different liquids so as to produce a concentration gradient according to any mathematical function of concentration *versus* time. It is desirable that the concentration gradient be defined by a gradient function that should be simple and applicable to a wide variety of gradient profiles. The following gradient function is compatible with these requirements and has proved useful in practice[16]:

$$c = (A^{\frac{1}{\varkappa}} + BV)^{\varkappa} \tag{3}$$

where V is the volume of the mobile phase delivered by the gradient-generating device from the beginning of the gradient and A, B and $\varkappa$ are adjustable parameters of the gradient function; A denotes the initial concentration of the stronger eluting agent in the binary mobile phase at the beginning of the gradient, B is the gradient slope and $\varkappa$ characterizes the shape (curvature) of the gradient profile. Other forms of gradient function can be also used for the optimization approach.

Using eqns. 2a, 2b and 3, relationships for important retention characteristics in gradient elution chromatography (retention volume, peak width, resolution) were derived[16,17] and the influence of A, B and $\varkappa$ (eqn. 3) on these characteristics was determined[2]. The optimization approach suggested here is based on the conclusions from this previous work.

Resolution in gradient elution chromatography

Let us now consider the gradient elution separation of a two-component sample mixture. To achieve the resolution, R_S, required, the parameters A, B and $\varkappa$ in eqn. 3 can be calculated from the appropriate equation for R_S, by analogy with the approach for the selection of the optimal composition of the mobile phase necessary to obtain the resolution required in isocratic elution chromatography[13]. In part XI[2], the influence of A, B and $\varkappa$ on the resolution is discussed in detail. It has been shown that there are certain values of the slope of the gradient function, B and/or of the initial concentration of the efficient eluting agent in the mobile phase, A, at which maximal or zero resolution of compounds 1 and 2 can eventually occur in gradient elution chromatography, if $n_1 \neq n_2$ in eqn. 2a or 2b.

The occurrence of an extreme in the $R_{S(g)} = f(A)$ or $R_{S(g)} = f(B)$ function within the practically useful range of these functions, however, is likely only with major differences in n_1 and n_2, which rarely happens in practical systems. Maxima of $R_{S(g)} = f(\varkappa)$ functions are more likely to occur, but they are rather flat. By analogy with isocratic elution chromatography, the resolution in gradient elution chromatography using a given pair of solvents is limited by minimal and maximal values, which cannot be exceeded at any practical combination of A, B and $\varkappa$.

A can be varied within the possible concentration limits of the more efficient eluting agent in the mobile phase (from 0 to c_{max}). The slope of the concentration gradient is limited by the requirement that the retention volume of the last compound eluted, $V'_{R(g)z}$, must not exceed the volume of the mobile phase delivered on to the column from the beginning of the gradient until the maximal possible concentration of

the more efficient eluting agent in the mobile phase is achieved, otherwise the elution is finished under isocratic conditions with the pure, more efficient eluting agent, and that the two components of the mobile phase must remain miscible. If two of the parameters A, B and $\varkappa$ are known, the maximal admissible (m.a.) value of the remaining parameter can be calculated, *e.g.*, the parameter $B_{\text{m.a.}}$ or $A_{\text{m.a.}}$ assuming the gradient function according to eqn. 3:

$$B_{\text{m.a.}} = \frac{c_{\max}^{\frac{1}{\varkappa}} - A^{\frac{1}{\varkappa}}}{V'_{R(g)z}} \tag{4a}$$

$$A_{\text{m.a.}} = (c_{\max}^{\frac{1}{\varkappa}} - V'_{R(g)z}B)^{\varkappa} \tag{4b}$$

The values of $B_{\text{m.a.}}$ or $A_{\text{m.a.}}$ can be calculated after the introduction of the appropriate relationship for $V'_{R(g)z}$ in accordance with the validity of eqn. 2a or 2b for the experimental system studied[16].

METHODS OF CALCULATION

If the required resolution of a two-component mixture is in principle possible in a given chromatographic system, it can be achieved using optimized isocratic elution and the application of gradient elution chromatography is unnecessary. On the other hand, it is extremely difficult to programme the composition of the mobile phase so as to obtain just the resolution necessary for baseline separation of all of the components of a complex, multicomponent mixture. This aim, if necessary at all often cannot be achieved by using a simple monotonous gradient function and the elution conditions have to be programmed separately, step-by-step, for the resolution of subsequent neighbouring compounds. Stepwise elution can be used to give an approximate solution to this problem.

Gradient elution using a simple gradient function with three parameters (like eqn. 3) can be suitably optimized so that two, or maximally three, independent requirements could be satisfied. Thus, the parameters of a gradient function could be calculated for two or three required values of the resolution at different points on a chromatogram or for a required resolution of two compounds and a required retention volume of another compound. Such an approach to the optimization of gradient elution would not only be very complex, but also unlikely to be meaningful, as the values of A, B and $\varkappa$ for one of the requirements could often fall into the range precluded by another requirement and the calculation would fail. In our opinion, it is more reasonable to base the optimization approach on only one required value for the resolution of the two components of a sample mixture that are most difficult to resolve. Consequently, one of the parameters A, B and $\varkappa$ is determined and the other two can be varied, as is illustrated in Figs. 1 and 2. Fig. 1. shows the relationship between B and $\varkappa$ at a fixed value of A and the required value of the resolution of two neighbouring substances in adsorption gradient elution chromatography, and Fig. 2 shows a plot of B *versus* A at a fixed value of $\varkappa$ and with the same required resolution. In both figures, a plot of the retention volume of another sample compound against

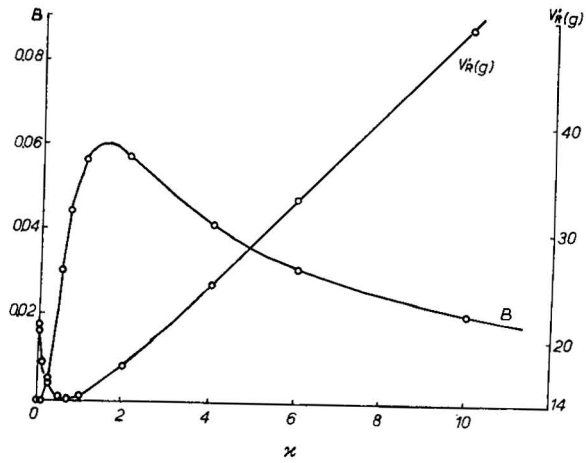

Fig. 1. Influence of $\varkappa$ in eqn. 3 on B and the retention volume of the last-eluted compound ($V'_{R(g)4}$) in the adsorption chromatography of four azo compounds. Column, Porasil A; binary mobile phase composed of cyclohexane and ethyl acetate. Compounds: 1 = di-(*n*-butyl)amide, 2 = di-(*n*-propyl)-amide, 3 = diethylamide and 4 = dimethylamide of *p*-N,N-dimethylamino-*p'*-azobenzoic acid. A in eqn. 3 = 0. $R_{s(g)1,2} = 0.5$ required. Eqns. 5, 6 and 7 were used in calculations. $V_m = 2.0$ ml; $N = 137$; $k'_{01} = 0.242$; $k_{02} = 0.330$; $k'_{03} = 0.65$; $k'_{04} = 1.94$; $n_1 \approx n_2 \approx n_3 \approx n_4 \approx n = 1.68$.

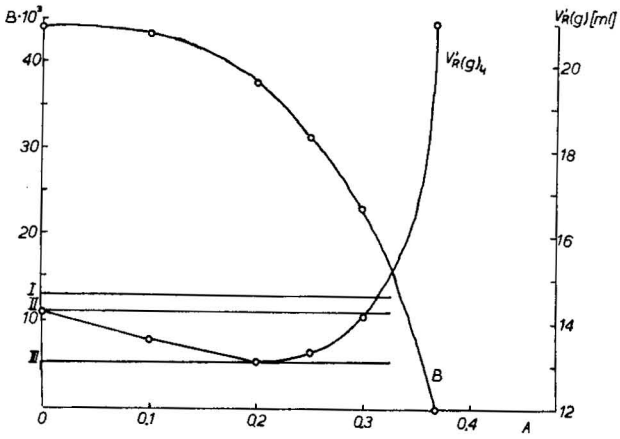

Fig. 2. Influence of A in eqn. 3 on B and the retention volume of the last-eluted compound ($V'_{R(g)4}$) in the adsorption chromatography of four azo compounds. Chromatographic system, compounds and operating conditions as in Fig. 1. $\varkappa$ in eqn. 3 = 0.68. $R_{s(g)1,2} = 0.5$ required. Eqns. 5, 6 and 7 were used in calculations. For comparison, the values of $V'_{R(g)4}$ are given for gradients with different A and $\varkappa$, where B is optimized with respect to the achievement of $R_{s(g)1,2}$ required: I, $c = 0.0564V$ (linear gradient, $\varkappa = 1$); II, $c = (0.0441V)^{0.68}$ (gradient with zero initial concentration of ethyl acetate, A = 0); III, $c = (0.1302 + 0.0378V)^{0.68}$ (gradient optimized with respect to the minimal time of separation) (c = %, v/v·10^{-2} of methanol in the mobile phase at the inlet of the column at V ml of the eluate from the beginning of the gradient elution).

$\varkappa$ and A is shown. The plots of retention volume show a minimum at a certain value of $\varkappa$ and A. Thus, it seems reasonable to accept the achievement of the minimal retention volume of an arbitrary compound as the second condition of the optimization approach. These two requirements are sufficient to determine A and B.

The parameter $\varkappa$ is less significant than the other two with respect to the requirements of the optimization approach, but it determines the compression of a chromatogram expressed by means of a compression criterion, Q (ref. 2), (if eqn. 2a applies) and, if necessary, it can be determined from the required value of Q before the optimization of A and B.

The optimization of A and B consists in an appropriate choice of the compound i, the retention volume of which should be minimal, the determination of the minimum of function $V'_{R(g)i} = f(A,B)$ at given value of $\varkappa$, while A and B are further interrelated so that the required value of resolution $R_{S(g)1,2}$ of two appropriately chosen compounds with adjacent bands is kept constant. The usual Lagrange mathematical solution to the problem would suffer from severe difficulties and a modified method of solution is therefore preferred. An interval of possible values of A is defined, $A > 0$; $A < A_{max}$, where A_{max} represents the concentration of the more efficient eluting agent in the mobile phase, at which the resolution required is just achieved in isocratic elution chromatography. From this interval, the values of A that are used for calculation of the corresponding values of B necessary to achieve the required $R_{s(g)1,2}$ are subsequently chosen. Then, the corresponding values of the retention volume, $V'_{R(g)i}$, are calculated and compared. The comparison of the values of $V'_{R(g)i}$ corresponding to the chosen values of A is used for a subsequent reduction of the interval of values of A (the interval is halved in each step) until the minimal value of $V'_{R(g)i}$ is found with a pre-set precision (*e.g.*, 1 %). Then, the arithmetic mean of this interval represents the required solution for A with the corresponding value of B. This approach is based on the assumption that there is only one minimum of $V'_{R(g)i}$ in the interval of the values of A, as in Fig. 2; it is universal and can be applied with different $k' = f(c)$ and gradient functions. However, a computer is required for the optimization calculations. In the present work, a TI 58 programmable pocket calculator with a program capacity of 480 steps was used. Fig. 3 shows the block diagram of the calculation.

The equations used for the calculations in the above optimization approach will differ according to the gradient function and the function $k' = f(c)$ that apply for a given system.

I. Gradient function according to eqn. 3: eqn. 2a applies for a given chromatographic system. Then,

$$B = \frac{\sqrt{N}(X_2 - X_1)}{2V_m R_{s(g)1,2}\left(\frac{k'_{01}}{X_1^{\varkappa n_1}} + \frac{k'_{02}}{X_2^{\varkappa n_2}} + 2\right)} \tag{5}$$

$$V'_{R(g)i} = \frac{X_i - A^{\frac{1}{\varkappa}}}{B} \tag{6}$$

where N is the number of plates of the column, which is assumed to be approximately equal for all the sample components, V_m is the volume of the mobile phase in the column, $\varkappa$ is selected before the calculation and

$$X_j = \left[(\varkappa n_j + 1)Bk'_{0j}V_m + A^{\frac{\varkappa n_j + 1}{\varkappa}}\right]^{\frac{1}{\varkappa n_j + 1}} \tag{7}$$

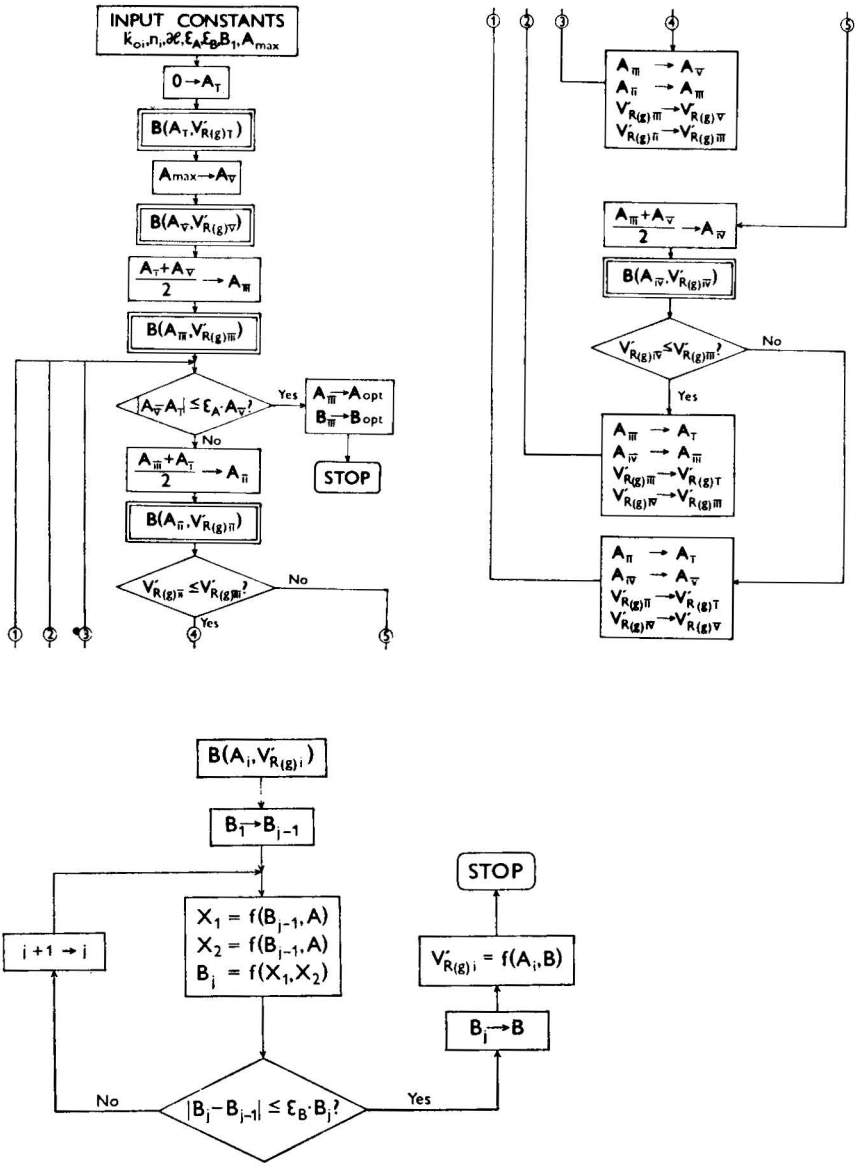

Fig. 3. Block diagram of the program used in the optimization approach.

The subscript $j = 1$, 2 or i relates to compound 1, 2 or i, respectively. The parameter B must be calculated from eqn. 5 using an iteration method (see the block diagram in Fig. 3).

The upper limit of the interval of A, A_{max}, is calculated as the concentration of the more efficient eluting agent in the mobile phase for a required resolution $R_{s1,2}$ in isocratic elution chromatography[13]:

(1) by an iteration method if $n_1 \neq n_2$:

$$A_{max} = \left[\frac{k'_{02}\left(1 - \frac{2R_{s1,2}}{\sqrt{N}}\right)}{\frac{k'_{01}}{A_{max}^{n_1}} \cdot \left(1 + \frac{2R_{s1,2}}{\sqrt{N}}\right) + \frac{4R_{s1,2}}{\sqrt{N}}} \cdot \right]^{\frac{1}{n_2}} \tag{8}$$

(2) if $n_1 \approx n_2 = n$:

$$A_{max} = \left\{ \left[\frac{\sqrt{N}}{2R_{s1,2}} \cdot (k'_{02} - k'_{01}) - k'_{01} - k'_{02} \right] \cdot \frac{1}{2} \right\}^{\frac{1}{n}} \tag{9}$$

II. Gradient function according to eqn. 3 with $\varkappa = 1$; eqn. 2b applies for a given chromatographic system. Then,

$$B = \frac{\sqrt{N}(\log X_2 - \log X_1)}{2V_m R_{s(g)1,2}\left(\frac{k'_{01}}{X_1^{n_1}} + \frac{k'_{02}}{X_2^{n_2}} + 2\right)} \tag{10}$$

$$V'_{R(g)i} = \frac{\log X_i - A}{B} \tag{11}$$

Here,

$$X_j = [2.31BV_m n_j k'_{0j} + 10^{n_j A}]^{\frac{1}{n_j}} \tag{12}$$

and the meaning of the subscripts j, i, 1, 2, and of V_m and N is as above. Eqn. 10 is solved for B by an iteration method.

The upper limit of the interval of A, A_{max}, is calculated as the concentration of the more efficient eluting agent in the mobile phase necessary to achieve the resolution $R_{s1,2}$ under isocratic conditions. Using an approach analogous to that in ref. 13 for eqn. 2a. we can derive the following relationships based on eqn. 2b:

Eqn. 13 for $n_1 \neq n_2$, which is solved using an iteration method:

$$A_{max} = \frac{1}{n_1} \cdot \log \left[\frac{k'_{01}\left(1 + \frac{2R_{s1,2}}{\sqrt{N}}\right)}{\frac{k'_{02}}{10^{n_2 A_{max}}} \cdot \left(1 - \frac{2R_{s1,2}}{\sqrt{N}}\right) - \frac{4R_{s1,2}}{\sqrt{N}}} \right] \tag{13}$$

(2) eqn. 14 for $n_1 \approx n_2 = n$:

$$A_{max} = \frac{1}{n} \cdot \log \left\{ \left[\frac{\sqrt{N}}{2R_{s1,2}} (k'_{02} - k'_{01}) - k'_{01} - k'_{02} \right] \cdot \frac{1}{2} \right\} \tag{14}$$

The same approach can be used for other gradient functions. For example, if eqn. 2a applies and we use a logarithmic gradient function:

$$c = \log(A^{\frac{1}{\varkappa}} + BV)^{\varkappa} \tag{15}$$

we can calculate B, $V'_{R(g)i}$ and X_j from eqns. 5–7, as in case I above. The value of

A_{max}, however, should be calculated from the equation

$$A_{max} = 10^{A'_{max}} \tag{16}$$

where A'_{max} represents the value of A_{max} calculated from eqn. 13 or 14.

EXPERIMENTAL

The same gradient elution instrumentation was used as in Part X[17]. A reversed-phase column, packed with an octadecylsilica reversed phase and a mobile phase composed of water and methanol was treated as described in Part X[17], and the same samples, substituted alkyluracils and barbiturates, were also used.

RESULTS AND DISCUSSION OF THE VERIFICATION OF THE OPTIMIZATION APPROACH

Reversed-phase chromatography of substituted uracils and barbiturates on an octadecylsilica column using methanol and water as the components of the binary mobile phase was used for verification experiments. To illustrate the optimization approach suggested above, three model mixtures were chosen. The first mixture contained homologous lower alkyluracils, 3,6-dimethyluracil, 3-ethyl-6-methyluracil, 3-*n*-propyl-6-methyluracil and 3-*n*-butyl-6-methyluracil. The second mixture contained 3-*sec.*-butyl-6-methyluracil and 3-*tert.*-butyl-6-methyluracil in addition to the components of the first mixture. The third mixture was composed of barbital, heptobarbital, allobarbital, aprobarbital, butobarbital, hexobarbital and amobarbital.

For each of these mixtures, the concentrations of methanol in the mobile phase necessary to achieve the required resolution for each pair of the compounds with adjacent chromatographic bands were calculated first. An iteration method of solution of eqn. 13 was used. The separation of the most difficult to separate pair required the lowest concentration of methanol in the mobile phase, which represented the optimal concentration for isocratic elution, c_{opt}.

Then, the optimized conditions for gradient elution with a linear gradient function were calculated using eqns. 10–12. The required resolution of the most difficult to resolve pair of compounds should be obtained and the minimal elution volume of the last-eluted compound was required simultaneously. The calculated optimized gradient functions are shown in Fig. 4. The chromatographic experiments were performed under optimized isocratic and gradient elution conditions and the important retention data from these experiments are summarized and compared with calculated values in Tables I –III. The method of calculation of retention volumes, peak widths and resolution in reversed-phase chromatography under isocratic and gradient elution conditions was described in Parts IX[14] and X[17] and elsewhere[3,11,18].

The parameters k'_0 and n in eqn. 2 for the individual compounds in the chromatographic system used were determined from the values of the capacity ratios, k', in isocratic experiments using mobile phases with different concentrations of methanol (linear regression analysis of the experimental log k' *versus* c function; see ref. 17). These values of k'_0 and n are given in Tables I–III and were used in both optimization calculations and calculations of retention characteristics.

TABLE I

COMPARISON OF EXPERIMENTAL AND CALCULATED RETENTION VOLUMES, PEAK WIDTHS AND RESOLUTION FOR THE REVERSED-PHASE SEPARATION OF A MIXTURE OF HOMOLOGOUS SUBSTITUTED URACILS UNDER OPTIMIZED ISOCRATIC AND GRADIENT ELUTION CONDITIONS

Column: octadecylsilica chemically bonded on LiChrosorb Si-100 (10 μm), 300 × 4.2 mm; V_m = 3.20 ml, N = 3350. Mobile phase, methanol–water; flow-rate, 0.96 ml/min. Sample compounds: 1 = 3,6-dimethyluracil; 2 = 3-ethyl-6-methyluracil; 3 = 3-*n*-propyl-6-methyluracil; 4 = 3-*n*-butyl-6-methyluracil. The optimal concentration of methanol in the mobile phase (c_{opt}) was calculated from eqn. 13 for isocratic resolution, R_s = 1.95, of compounds 1 and 2 and the optimal values A_{opt} and B_{opt} for gradient elution according to the function given by eqn. 3 ($\varkappa$ = 1) were calculated for the required optimal conditions, $R_{s1,2}$ = 2.15, $V'_{R(g)4}$ = minimum, using eqns. 10–12. The parameters k'_0 and n in eqn. 2 were determined according to ref. 17 and the values of V'_R, w, R_s, $V'_{R(g)}$, $w_{(g)}$ and $R_{s(g)}$ (retention volumes, peak widths and resolution under isocratic and gradient elution conditions) were calculated according to refs. 14 and 17.

Compound	k'_0	n	A_{opt}	B_{opt}	$V'_{R(g)}$ *(ml)*		$w_{(g)}$ *(ml)*		$R_{s(g)}$	
					Calc.	*Exptl.*	*Calc.*	*Exptl.*	*Calc.*	*Exptl.*
1	9.51	4.40	0.358	0.165	0.51	0.79	0.24	0.23		
2	15.63	3.69			1.05	1.37	0.26	0.24	2.15	2.47
3	29.98	3.31			1.74	2.05	0.27	0.26	2.60	2.72
4	67.20	3.25			2.40	2.72	0.27	0.30	2.44	2.39
			c_{opt} *(%, v/v* × 10^{-2}*)*		V'_R *(ml)*		*w (ml)*		R_s	
					Calc.	*Exptl.*	*Calc.*	*Exptl.*	*Calc.*	*Exptl.*
1	9.51	4.40	0.509		0.17	0.38	0.23	0.25		
2	15.63	3.69			0.66	0.93	0.27	0.30	1.95	2.00
3	29.98	3.31			1.98	2.06	0.36	0.37	4.19	3.37
4	67.20	3.25			4.78	4.54	0.55	0.54	6.15	5.45

TABLE II

EXPERIMENTAL AND CALCULATED RETENTION VOLUMES, PEAK WIDTHS AND RESOLUTION FOR THE REVERSED-PHASE SEPARATION OF A MIXTURE OF LOWER ALKYL-SUBSTITUTED URACILS UNDER OPTIMIZED ISOCRATIC ELUTION CONDITIONS

Column, operating conditions, methods of calculation and meaning of symbols as in Table I. Sample compounds: 1 = 3,6-dimethyluracil; 2 = 3-ethyl-6-methyluracil; 3 = 3-*n*-propyl-6-methyluracil; 4 = 3-*sec.*-butyl-6-methyluracil; 5 = 3-*n*-butyl-6-methyluracil; 6 = 3-*tert.*-butyl-6-methyluracil. Conditions of optimization: isocratic elution, $R_{s4,5}$ = 1.95.

Compound	k'_0	n	c_{opt} *(%, v/v·*10^{-2}*)*	V'_R *(ml)*		*w (ml)*		R_s	
				Calc.	*Exptl.*	*Calc.*	*Exptl.*	*Calc.*	*Exptl.*
1	9.51	4.40	0.392	0.57	0.93	0.26	0.28		
2	15.63	3.69		1.79	2.02	0.34	0.38	4.07	3.32
3	29.98	3.31		4.85	4.79	0.56	0.55	6.80	5.96
4	54.56	3.21		9.66	9.78	0.89	0.91	6.63	6.83
5	67.20	3.25		11.51	11.99	1.02	1.04	1.95	2.27
6	96.25	3.40		14.39	14.44	1.22	1.18	2.57	2.21

TABLE III

COMPARISON OF EXPERIMENTAL AND CALCULATED RETENTION VOLUMES, PEAK WIDTHS AND RESOLUTION FOR THE REVERSED-PHASE SEPARATION OF A MIXTURE OF BARBITURATES UNDER OPTIMIZED ISOCRATIC AND GRADIENT ELUTION CONDITIONS

Column, operating conditions, methods of calculation and meaning of symbols as in Table I. Sample compounds: 1 = barbital; 2 = heptobarbital; 3 = allobarbital; 4 = aprobarbital; 5 = butobarbital; 6 = hexobarbital; 7 = amobarbital. $N \approx 2330$. Conditions of optimization: isocratic elution, $R_{s1,2} = 1.60$; gradient elution, (a) $R_{s(g)1,2} = 1.70$; $V'_{R(g)7}$ = minimum; (b) $R_{s(g)6,7} = 1.75$; $V'_{R(g)1}$ = minimum.

Compound	k'_0	n	c_{opt}		V'_R *(ml)*		w *(ml)*		R_s	
			(%, v/v·10^{-2})		*Calc.*	*Exptl.*	*Calc.*	*Exptl.*	*Calc.*	*Exptl.*
1	21.81	3.20	0.523		1.48	1.53	0.39	0.42		
2	58.44	3.71			2.15	2.08	0.44	0.47	1.60	1.24
3	69.44	3.55			3.11	3.03	0.52	0.52	2.00	1.92
4	106.96	3.66			4.18	4.14	0.61	0.61	1.89	1.96
5	187.41	3.78			6.38	6.16	0.79	0.75	3.14	2.97
6	252.29	3.77			8.69	8.10	0.98	0.92	2.61	2.32
7	617.73	4.29			11.36	10.80	1.21	1.06	2.44	2.73
			A_{opt}	B_{opt}	$V'_{R(g)}$ *(ml)*		$w_{(g)}$ *(ml)*		$R_{s(g)}$	
					Calc.	*Exptl.*	*Calc.*	*Exptl.*	*Calc.*	*Exptl.*
1	21.81	3.20	0.368*	0.061*	2.51	2.58	0.39	0.29		
2	58.44	3.71			3.17	3.27	0.39	0.29	1.70	2.38
3	69.44	3.55			3.76	3.96	0.41	0.29	1.48	2.38
4	106.96	3.66			4.26	4.56	0.41	0.29	1.23	2.07
5	187.41	3.78			4.98	5.32	0.41	0.30	1.76	2.58
6	252.29	3.77			5.53	5.95	0.41	0.30	1.34	2.10
7	617.73	4.29			5.79	6.29	0.40	0.31	0.64	1.11
1	21.81	3.20	0.523**	0.0082**	1.41	1.40	0.38	0.32		
2	58.44	3.71			2.00	1.86	0.42	0.35	1.48	1.37
3	69.44	3.55			2.82	2.67	0.48	0.37	1.82	2.28
4	106.96	3.66			3.66	3.55	0.53	0.43	1.66	2.23
5	187.41	3.78			5.23	4.98	0.62	0.48	2.73	3.14
6	252.29	3.77			6.72	6.32	0.70	0.55	2.26	2.60
7	617.73	4.29			7.99	7.70	0.75	0.57	1.75	2.46

* Conditions of optimization: (a).
** Conditions of optimization: (b).

The optimal (maximal) isocratic concentration of methanol necessary to achieve $R_s = 1.95$ for 3,6-dimethyluracil and 3-ethyl-6-methyluracil is 50% (v/v) (Table I). Fig. 4 (curve 1) shows the gradient function optimized for the required resolution, $R_{s(g)} = 2.15$, for these two compounds and the minimal retention volume of 3-*n*-butyl-6-methyluracil. The retention volume of the last-eluted compound in gradient elution chromatography is half that in optimized isocratic elution.

In the chromatography of the six-component mixture of lower alkyluracils, the separation of 3-*sec.*-butyl-6-methyluracil from 3-*n*-butyl-6-methyluracil is more difficult than the separation of the other pairs of compounds and requires a lower concentration of methanol in the mobile phase for isocratic elution than the separation

of the homologous mixture, *ca.* 40% (v/v) (Table II). If gradient elution is optimized for this resolution of the two butyl isomers and the minimal retention time of 3-*tert.*-butyl-6-methyluracil is required, the calculation gives the values $A = 0.392$ and $B = 0$, which represents isocratic elution with the same composition of mobile phase as above. Thus, gradient elution chromatography cannot diminish the time of separation for this mixture in comparison with isocratic elution.

The resolution of barbital and heptobarbital requires a lower concentration of methanol in the mobile phase under isocratic conditions than the separation of the other pairs from the mixture of barbiturates, 52% (v/v), for a resolution $R_s = 1.6$ (Table III). If a resolution of barbital and heptobarbital of $R_s = 1.7$ and a minimal retention volume of the last-eluted amobarbital are required, the optimization calculation yields $A = 0.368$ and $B = 0.061$ for the linear gradient function (curve 2 in Fig. 4) and the time of separation is almost half that in the optimized isocratic experiment.

The resolution of hexobarbital from amobarbital is too low, however (Fig. 5).

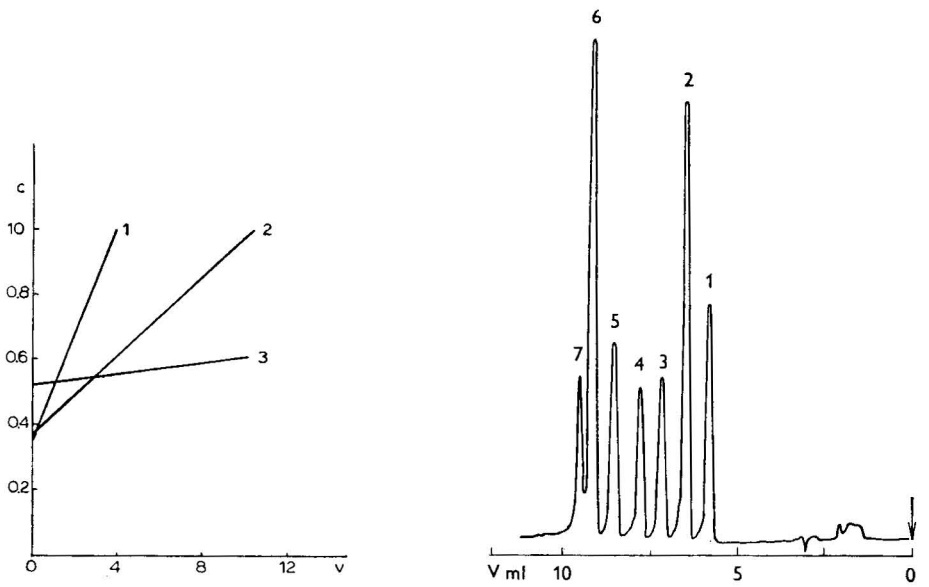

Fig. 4. Plots of optimized linear gradient functions for separation of homologous alkyluracils and barbiturates. Curve 1: $c = 0.358 + 0.165V$, optimized for separation of alkyluracils (optimization and operating conditions in Table I). Curve 2: $c = 0.368 + 0.061V$, optimized for separation of barbiturates; resolution of barbital and heptobarbital, $R_{s(g)} = 1.7$ required [optimization and operating conditions in Table III, conditions (a)]. Curve 3: $c = 0.523 + 0.0082V$, optimized for separation of barbiturates; resolution of hexobarbital and amobarbital, $R_{s(g)} = 1.75$ required [optimization and operating conditions in Table III, conditions (b)]. c = Concentration of methanol in the mobile phase at the inlet of the column, %, v/v·10^{-2}; V ml = volume of the mobile phase delivered on to the column from the beginning of gradient elution.

Fig. 5. Optimized gradient elution reversed-phase separation of a mixture of seven barbiturates. Numbers of compounds and operating conditions as in Table III [conditions (a)]; resolution of barbital and heptobarbital (compounds 1 and 2), $R_{s(g)} = 1.7$ required; elution according to linear gradient function (curve 2 in Fig. 4). V ml = volume of the eluate from the beginning of gradient elution. Detection: UV (254 nm), range 0.32 a.u.f.s.

Therefore, the optimization approach was repeated with other requirements: the resolution of hexobarbital and amobarbital should be $R_s = 1.75$ and the retention volume of the first-eluted compound, barbital, should be minimal. The calculated gradient function ($A = 0.523$ and $B = 0.0082$, curve 3 in Fig. 4) is much less steep and begins at a higher concentration of methanol in the mobile phase than in the previous optimization. The separation of all of the components in the mixture is satisfactory (Fig. 6) and the separation time is slightly increased (*ca.* 75% of the time for isocratic elution) in comparison with the above optimized experiment.

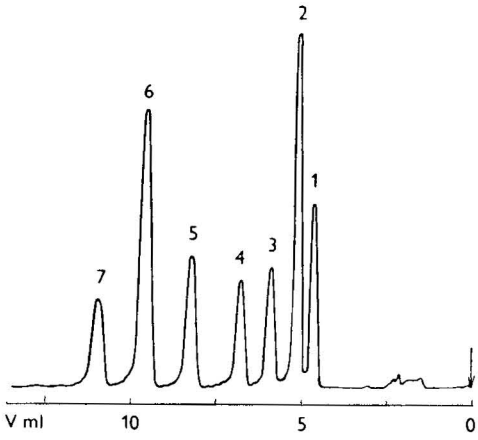

Fig. 6. Optimized gradient elution reversed-phase separation of a mixture of seven barbiturates. Numbers of compounds and operating conditions as in Table III [conditions (b)]; resolution of hexobarbital and amobarbital (compounds 6 and 7), $R_{s(g)} = 1.75$ required; elution according to linear gradient function (curve 3 in Fig. 4). V ml = volume of the eluate from the beginning of gradient elution. Detection: UV (254 nm); range 0.32 a.u.f.s.

The calculated and experimental retention characteristics under isocratic and gradient elution conditions, compared in Tables I–III, are in satisfactory agreement. The maximal difference in retention volumes is *ca.* 0.3–0.4 ml, which is an error comparable to that in the previous experiments with gradient elution reversed-phase chromatography[17]. The differences between the experimental and calculated peak widths were less than 0.1–0.15 ml.

Using the same optimization requirements as for the second gradient curve, we calculated the optimized logarithmic gradient function for the separation of the mixture of barbiturates (eqn. 15, $\varkappa = 1$). The parameters of this function are given in Table IV, where the profiles of the logarithmic and linear gradient functions are compared. It is obvious that the two gradient functions are essentially identical in the part of gradient useful for the separation of the mixture of barbiturates. This result seems to give further support to the opinion that the curvature of the gradient function is much less important than the slope and the initial conditions for the optimization of gradient elution.

TABLE IV

COMPARISON OF THE OPTIMIZED LINEAR AND LOGARITHMIC GRADIENT FUNCTIONS FOR THE REVERSED-PHASE SEPARATION OF A MIXTURE OF BARBITURATES

Operating conditions as in Table I, sample compounds in the mixture as in Table III. Conditions of optimization as in Table III, (b), *i.e.*, $R_{s(g)6,7} = 1.75$; $V'_{R(g)1}$ = minimum; $N \approx 2330$. Gradient function: (I), $c = A + BV$ (eqn. 3), $A = 0.523$, $B = 0.0082$, calculated with use of eqns. 10–13; (II) $c = \log (A + BV)^{\varkappa}$ (eqn. 15), $\varkappa = 1$, $A = 3.331$, $B = 0.067$, calculated with use of eqns. 5–7, 13 and 16. V = ml of the eluate from the beginning of the gradient elution; c = concentration of methanol (%, v/v·10^{-2}) in the mobile phase at the inlet of the column, corresponding to gradient functions I(c_I) and II(c_{II}).

Concentration	*V (ml)*										
	0	*1*	*2*	*3*	*4*	*5*	*6*	*7*	*8*	*9*	*10*
c_I	0.523	0.531	0.539	0.547	0.555	0.564	0.572	0.580	0.588	0.596	0.605
c_{II}	0.523	0.531	0.540	0.548	0.556	0.564	0.572	0.580	0.587	0.595	0.602

SIMPLIFIED GENERAL APPROACH FOR OPTIMIZATION OF REVERSED-PHASE GRADIENT ELUTION CHROMATOGRAPHY

Let us now examine the possibilities for the optimization of gradient elution in the reversed-phase chromatography of an unknown sample mixture in a different way to that of Snyder *et al.*[11]. In this instance, significant simplifications of the theory must be accepted. Firstly, identical values of n in eqn. 2a will be assumed. Then, the equation for the difference in retention volumes, $\Delta V'_{R(g)}$, of two compounds, 1 and 2, can be written as follows:

$$\Delta V'_{R(g)} = V'_{R(g)2} - V'_{R(g)1} = \frac{1}{nB} \cdot \log \left(\frac{2.31 nBV_m k'_{02} + 10^{nA}}{2.31 nBV_m k'_{01} + 10^{nA}} \right) \tag{17}$$

Assuming a low value of A, we neglect the term 10^{nA} as a first approximation:

$$\Delta V'_{R(g)} \approx \frac{1}{nB} \cdot \log \left(\frac{k'_{02}}{k'_{01}} \right) \approx \frac{\log \alpha_0}{nB} \approx \frac{\log \alpha}{nB} \tag{18}$$

where α_0 denotes the retention ratio of compounds 1 and 2 in the pure, less efficient eluting agent in the binary mobile phase under isocratic conditions, which should be equal to the retention ratio α at an arbitrary composition of the binary mobile phase (α should not depend on the composition of the mobile phase in isocratic elution if $n_1 = n_2 = n$). In practice, however, n is not strictly constant for the members of a homologous series and, consequently, α depends to certain extent on the composition of the binary mobile phase. Therefore, it is reasonable to consider α in eqn. 18 as the retention ratio in the mobile phase with a composition corresponding to the arithmetic mean in the composition interval effective during the gradient elution.

In a homologous series, the plots of log k' *versus* the number of carbon atoms in aliphatic substituents are close to straight lines. Thus, the logarithms of the retention ratios remain approximately constant for two neighbouring homologues differ-

ing by one CH_2 group ($\log \alpha_c \approx$ constant). Further, it can be reasonably expected that the values of α_c and n do not depend much on the type of organic compound in a given system of reversed phase and binary mobile phase. Thus, in agreement with other workers, we found $n \approx 3.0$–4.0 and $\log \alpha_c \approx 0.3$ for octadecylsilica reversed phase in a water–methanol mobile phase containing 50% of methanol[17].

From eqn. 18, it follows that, with known $\log \alpha_c$ and n, we can estimate the slope of the concentration gradient in reversed-phase chromatography necessary for achievement of the required difference in retention volumes between neighbouring members of a homologous series. The difference in retention volumes, $\Delta V'_{R(g)}$ can be correlated with the resolution, $R_{s(g)}$, if we assume that the peak widths in gradient elution chromatography, $w_{(g)}$, are approximately equal to peak widths under isocratic conditions with $k' = 1$:

$$\Delta V'_{R(g)} = R_{s(g)} w_{(g)} \approx \frac{8 V_m R_{s(g)}}{\sqrt{N}} \tag{19}$$

where V_m is the volume of the mobile phase in the column and N is the number of plates (isocratic conditions).

The use of eqn. 18 is illustrated by Table V. The values of n and $\log \alpha_c$ were taken from the experiments in Part X[17]. The estimated values of the differences between the retention volumes of the two compounds differing by one CH_2 group in the aliphatic substituent are compared with the experimental values for three different slopes, B, of the linear gradient function (start of the gradient in pure water, $A = 0$, system I).

A similar correlation was shown for experiments performed by Elgass[20] and Engelhardt and Elgass[21] on the gradient elution chromatography of phenacyl esters of saturated fatty acids on a C_8 reversed-phase column using a binary mobile phase composed of water and acetonitrile. The values of n and $\log \alpha_c$ for this system were estimated from two isocratic experiments with C_8–C_{12} acids using 100% and 70% acetonitrile – water. The parameter n was calculated as the average of the ratio of the difference in $\log k'$ and the corresponding difference in the concentration of acetonitrile in the mobile phase; $\log \alpha_c$ was estimated as the arithmetic mean of the differences in $\log k'$ between two neighbouring homologous acids in the two mobile phases. These calculations are shown in the bottom section of Table V.

The experimental differences in the retention volumes for two neighbouring homologues in Table V are in satisfactory agreement with the estimated values, if we take into account the simplifications involved in the estimation approach.

CONCLUSIONS

The experimental results of reversed-phase gradient elution chromatography suggest a good validity of the optimization approaches described. The exact calculation procedure requires that the parameters of the function $k' = f(c)$ be known for sample compounds in a given chromatographic system. Under this condition, the calculations with the use of a computer or a programmable calculator make it possible to plan the conditions for gradient elution with a required resolution of a chosen pair of sample compounds with minimal retention volume of another chosen compound

TABLE V

OPTIMIZATION OF GRADIENT ELUTION OF HOMOLOGOUS MIXTURES IN REVERSED-PHASE CHROMATOGRAPHY

System I. Column: C_{18} on LiChrosorb Si-100 (10 μm). Mobile phase: methanol–water. Sample compounds: barbiturates, substituted uracils. The values of log α_c and n were taken as average values from experiments under isocratic conditions; log α_c is the average difference in log k' between two compounds differing by one CH_2 group in 50% methanol–water from the two series of compounds[17].

System II. Column: C_8 on LiChrosorb Si-100 (10 μm). Mobile phase: acetonitrile–water. Sample compounds: phenacyl esters of saturated fatty acids, n-C_6–C_{18}. The values of log α_c and n were taken from two isocratic experiments in 70% ($c = 0.7$) and 100% ($c = 1.0$) acetonitrile–water, as shown in the bottom section. These two experiments and two experiments with linear gradient elution were performed by Elgass[20] and Engelhardt and Elgass[21].

B represents the slope of linear gradient function [eqn. 3; $\varkappa = 1$, $A = 0$ (0–100% CH_3OH) in system I; $A = 0.7$ (70–100% CH_3CN) in system II].

System	*Compounds*	*Reversed phase*	*Mobile phase*	*Log* α_c'	n	B	$\Delta V'_{R(g)}$ *(ml)*	
							Calc.	*Exptl.*
I	Barbiturates; substituted uracils	C_{18}	CH_3OH–H_2O	0.3	3.5	0.069	1.2	0.8
						0.035	2.4	1.8
						0.017	5.0	4.0
II	Saturated fatty acid derivatives	C_8	CH_3CN–H_2O	0.1	3.9	0.0075	3.5	3.0
						0.015	1.7	1.6

Fatty acid	*Concentration of acetonitrile in the mobile phase (%, v/v·10⁻²)*				$P = \log k'_{0.7} - \log k'_{1.0}$	$n = \frac{P}{\Delta c}$
	$c = 0.7$		$c = 1.0$			
	log k'	$\Delta \log k'_{CH_2}$	*log* k'	$\Delta \log k'_{CH_2}$		
C_8	0.32		−0.77		1.09	3.63
		0.13		0.09		
C_{10}	0.58		−0.59		1.17	3.90
		0.125		0.07		
C_{12}	0.83		−0.45		1.28	4.27
Arithmetic mean	—	0.127*	—	0.08*	—	3.93

* Log $\alpha_c = 0.103$ (arithmetic mean of $\Delta \log k'_{CH_2}$ at $c = 0.7$ and $c = 1.0$).

(if this resolution can be achieved under isocratic conditions in the given system). The slope of the gradient in the reversed-phase chromatography of homologous mixtures for the achievement of a required difference in retention volumes between two neighbouring homologues can be estimated.

REFERENCES

1 C. Liteanu and S. Gocan, *Gradient Liquid Chromatography*, Wiley, Chichester, New York, 1974.
2 P. Jandera and J. Churáček, *J. Chromatogr.*, 192 (1980) 1.
3 L. R. Snyder, in C. Horváth (Editor), *Liquid Chromatography*, Academic Press, New York, London, in press.
4 H. Schwab, W. Rieman and P. A. Vaughan, *Anal. Chem.*, 29 (1957) 1357.
5 E. C. Freiling, *J. Phys. Chem.*, 61 (1957) 543.
6 S. Ohashi, N. Tsuji, Y. Ueno, M. Takeshita and M. Muto, *J. Chromatogr.*, 50 (1970) 349.

7 F. Molnár, A. Horváth and V. A. Khalkin, *J. Chromatogr.*, 26 (1967) 215.
8 D. L. Massart and W. Bossaert, *J. Chromatogr.*, 32 (1968) 195.
9 L. R. Snyder, *Chromatogr. Rev.*, 7 (1965) 1.
10 L. R. Snyder and D. L. Saunders, *J. Chromatogr. Sci.*, 7 (1969) 195.
11 L. R. Snyder, J. W. Dolan and J. R. Gant, *J. Chromatogr.*, 165 (1979) 3.
12 J. W. Dolan, J. R. Gant and L. R. Snyder, *J. Chromatogr.*, 165 (1979) 31.
13 P. Jandera, M. Janderová and J. Churáček, *J. Chromatogr.*, 148 (1978) 79.
14 P. Jandera and J. Churáček, *J. Chromatogr.*, 170 (1979) 1.
15 P. Jandera and J. Churáček, *J. Chromatogr.*, 91 (1974) 207.
16 P. Jandera and J. Churáček, *J. Chromatogr.*, 91 (1974) 223.
17 P. Jandera, J. Churáček and L. Svoboda, *J. Chromatogr.*, 174 (1979) 35.
18 P. J. Schoenmakers, H. A. H. Billiet, R. Tijssen and L. de Galan, *J. Chromatogr.*, 149 (1978) 519.
19 P. Jandera and J. Churáček, *J. Chromatogr.*, 93 (1974) 17.
20 H. Elgass, unpublished results.
21 H. Engelhardt and H. Elgass, *J. Chromatogr.*, 158 (1978) 249.

Journal of Chromatography, 192 (1980) 37–51

CHROM. 12,572

GRADIENT ELUTION IN LIQUID CHROMATOGRAPHY

XIII. INSTRUMENTAL ERRORS IN GRADIENT ELUTION CHROMATOGRAPHY

PAVEL JANDERA, JAROSLAV CHURÁČEK and LADISLAV SVOBODA
Department of Analytical Chemistry, University of Chemical Technology, Pardubice (Czechoslovakia)
(First received February 26th, 1979; revised manuscript received July 20th, 1979)

SUMMARY

Instrumental sources of experimental errors in gradient elution liquid chromatography are considered. The performance of the equipment generating the concentration gradient in the low-pressure part has been investigated and it is shown that the equipment is able to reproduce the required ratio of the two components of the mobile phase and to maintain the flow-rate with an error of less than 1%. The deviations from the gradient profile due to the mixing in a reciprocating high-pressure pump are negligible under normal gradient elution conditions.

INTRODUCTION

The importance of the gradient elution technique in the liquid chromatography of mixtures of compounds with a wide range of capacity ratios is widely acknowledged. With increasing requirements on precise and reproducible quantitative results, it is important to evaluate and, as far as possible, to eliminate errors connected with the application of gradient elution. If the sample size and the chromatographic system are sufficiently stable and appropriately chosen, the errors in retention volumes and peak widths are due primarily to the limits of precision and reproducibility of three chromatographic variables: the composition and the flow-rate of the mobile phase and the temperature[1], their relative importance decreasing in that order. In order to achieve sufficiently reproducible results, it is important that the three variables can be reproduced in repeated experiments and their random fluctuations should be minimized. These three variables, however, should also be kept as close as possible to the expected values, otherwise the results are influenced by additional parameters that are properties not of the chromatographic system but of the instrumental design, are often very difficult to predict and hinder any comparison of results achieved with different instruments. In general, the reproducibility and accuracy of the experimental conditions can be far more easily controlled in isocratic elution chromatography than in gradient elution chromatography, but the latter technique can yield results as reproducible and accurate as those obtained under isocratic con-

ditions if appropriate attention is paid to the instrumental design and to the operation of the chromatographic system.

INSTRUMENTAL DESIGN AND ERRORS IN GRADIENT ELUTION CHROMATOGRAPHY

From the three parameters that influence the reproducibility in gradient elution chromatography, the temperature can be easily and satisfactorily controlled by simple thermostating of the column by means of a water-jacket connected to a circulating constant-temperature bath, if necessary[2].

The actual flow-rate and the change in the composition of the mobile phase with time (the profile of the gradient) may deviate from the required pre-set values for a number of reasons:

(a) The more efficient eluting component of the mobile phase is preferentially retained on the column, its content in the mobile phase decreases and consequently the gradient profile deviates from the pre-set value (solvent demixing effect). This effect is much more significant in adsorption than in reversed-phase chromatography and increases with the difference in polarities between the two components of the mobile phase[3]. The retention behaviour of the early eluted compounds may be subject to serious deviations due to the solvent demixing effect and these compounds may occasionally be eluted at some point of the gradient as badly resolved or unresolved narrow peaks. The elution of more strongly retained substances, however, is much less affected by solvent demixing, which can often be neglected or included in the delay of the gradient[4]. Further, this effect is much more significant if the gradient elution is started at zero concentration of the more efficient eluting component in the mobile phase than for the initial concentration of at least a few per cent of this component.

(b) Random or systematic deviations from the pre-set volume ratio of the two components and the flow-rate of the mobile phase (at atmospheric pressure), caused by the imperfect functioning of the mechanical parts of pumps (plungers, valves, seals) or electronic part of the system. In addition, the gradient profile can be influenced by the thermodynamic volume changes connected with the mixing of the two components of the mobile phase. As will be shown later, this effect is negligible with mixtures of organic solvents commonly used in adsorption chromatography, but can cause errors of up to a few per cent in the flow-rate of the mobile phase with solutions of polar organic solvents in water, which are frequently used in reversed-phase chromatography.

(c) The influence of the compressibility of the two components of the mobile phase, which may cause significant deviations from pre-set gradient profile and flow-rate at the operating pressure.

(d) Discrepancies between the actual and expected gradient profiles can be caused by additional mixing of the mobile phase in on- and off-line void spaces between the gradient mixing chamber and the column and subsequently, in the mixing chamber itself.

The instrumental design can influence significantly the errors included in groups (b)–(d). The most frequently used commercial instruments for gradient elution chromatography have recently been reviewed[5–7] with respect to their design and

operational principles. The accuracy and reproducibility of the gradient profile and flow-rate have also been discussed in detail[5–7].

Gradient devices are usually classified into two types: instruments in which the solvents are mixed in the low-pressure part and mixed solvent is pumped through the column, and those in which the solvents are mixed at high pressure before being delivered to the column[6,7]. Instruments of the latter type may be subdivided according to the type of pumps used (the hydraulic part of the system) and according to the way in which the gradient is controlled by the electronic part of the instrument. As the errors in the formation of a gradient usually originate in the hydraulic part of the device, the classification according to the pumps used is more meaningful for our present purpose. At this point, it would be useful to recall briefly possible sources of instrumental errors connected with different types of devices forming gradients from two solvents. (Two-solvent gradients are by far the most frequently used in practice and very few separation problems, if any, can be expected to require gradients composed of more than two solvents[7].) In systems in which pneumatic or hydraulic amplifier pumps deliver two solvents into a mixing chamber of small volume connected to the column, the flow-rate varies with time because of changing viscosity and compressibility of the mobile phase during the gradient run. These devices cannot accurately form the gradient required unless precise feedback control of the flow-rate is employed. The systems based on two large-volume syringe pumps are strongly influenced by compressibility effects. The differences in the compressibilities of the organic solvents or water, usually used as the two components of the mobile phase, can lead to profiles completely different from the theoretically expected gradients, which leads to irreproducibility of retention times[2,6–9]. These effects can be suppressed by operating the two pumps at an equal and constant pressure, higher then the column operation pressure. A constant back-pressure valve can be used for this purpose[2].

The instruments using two reciprocating pumps without a flow-feedback control cannot reproduce accurately the gradient profile in the initial and final part owing to the limited speed range of the driving stepping motors[6–8].

A major part of the drawbacks of the above systems is overcome in a new generation of gradient elution systems based on the use of one reciprocating flow-feedback pump, usually controlled by a microprocessor. The solvents (two or three) are introduced directly into the pump via time-proportioning electrovalves and mixed in the pump plunger chamber and in the lines between the pump and the column, *i.e.*, essentially in the high-pressure part of the instrument. Devices of this type can, in principle, provide accurately and reproducibly the gradient required[7].

The instruments forming the gradient in the low-pressure part mix the solvents before they reach the inlet port of a high-pressure reciprocating pump. The low-pressure gradient mixing units of simple design, utilizing gravity as the driving force, which were used in classical column chromatography have been reviewed by Snyder[10]. Because of poor accuracy and reliability of performance, devices of this type can be hardly used for precise gradient formation as the low-pressure part of a gradient system. Rather, the solvents fed to the high-pressure pump should be controlled by time-proportioning electrovalves or via auxiliary low-pressure precision pump(s).

These gradient systems are little influenced by compressibility effects and can

completely eliminate errors connected with thermodynamic volume changes due to mixing of the solvents. For several years we have been using such a low-pressure system, forming the gradient in a low-pressure reciprocating pump.

In this work, the performance of this system has been tested with respect to the accuracy and precision of the gradient profile and flow-rate.

DESCRIPTION OF THE SYSTEM

The equipment for gradient elution is shown schematically in Fig. 1. Components A and B of the mobile phase are stored in glass reservoirs (erlenmeyer flasks, 500 or 1000 ml) (2), which can be heated and agitated (1). They are pumped by a gradient-generating low-pressure device (3) (PPM-68005, Workshops of the Czechoslovak Academy of Sciences, Prague), which is the reciprocating pump with two plunger blocks operating out-of-phase with a programmed stroke ratio and a constant total flow-rate. The total flow-rate is fixed by adjusting the plunter stroke frequency by means of a gear system. The ratio of the strokes in each plunger block delivering one solvent is continuously adjusted by a servo-motor, controlled by a photoelectric element, which follows the gradient drawn as a broad black trace on a sheet of paper fastened on a slowly rotating drum. Thus, an infinite number of gradients can be formed and reproduced well, as the sheets with drawn gradients can be kept. The pump has been slightly adapted in order to minimize the volume of solvents delivered in each stroke cycle (the total volume of the two solvents delivered in one stroke cycle is 19 μl; this means, for example, a frequency of 62 strokes/min represents a

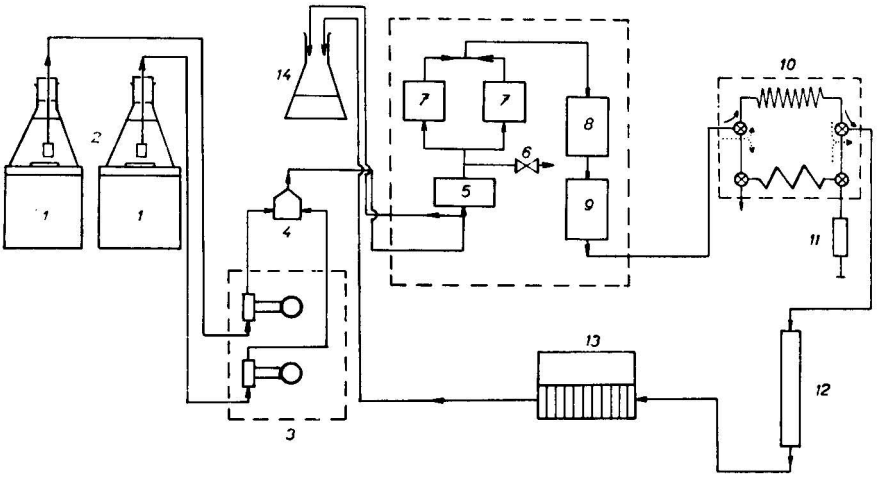

Fig. 1. Gradient-elution equipment with gradient generation in the low-pressure part, using the PPM 68005 gradient-generating device in series with the Waters Assoc. M6000 high-pressure pump. 1 = Electromagnetic stirrers and heaters; 2 = glass reservoirs (erlenmeyer flasks, 500 or 1000 ml); 3 = PPM 68005 two-plunger block gradient-generating device with programmed stroke ratio; 4 = gradient mixing chamber; 5–9 = M6000 high-pressure pump (Waters Assoc.); 5 = adapted inlet port; 6 = flushing vent; 7 = plunger heads; 8 = flow-through pulse damper; 9 = flow-through pressure sensor; 10 = U6K injector (Waters Assoc.); 11 = syringe septumless injection; 12 = column, reversed-phase C_{18} on LiChrosorb Si-100 (10 μm), 300 × 4.2 mm; 13 = detector (UV, 254 nm, in gradient-elution operation; RI in performance tests; both Waters Assoc.); 14 = waste reservoir.

flow-rate of 1.18 ml/min). For further details on the performance of this pump, see ref. 11.

From the mixing chamber (4), the mixed liquid is delivered to a Waters Assoc. M6000 pump (reciprocating, stepping motor driven) with an adapted inlet port (5), enters the two plunger heads (7) of the pump, passes through a flow-through pulse damper (8) and pressure sensor (9) of the pump and is delivered through a sample injector (10) (Waters Assoc. U6K, but septum injectors can also be used) on to the column (12), flows through the detector (13) (UV, 254 nm, Waters) into the waste reservoir (14).

For accurate functioning of the equipment, it is essential to set the total flow-rate of the gradient-forming device (3) approximately 10–20% higher than the flow-rate of the high-pressure pump. The overflowing liquid is by-passed to the waste reservoir (14), which must be placed higher than the pump inlet (5).

The inlet port (5) of the high-pressure pump was adapted by inserting a small-bore Teflon cylinder with a disc frit, in order to minimize the void volume in this part.

TESTS OF THE PERFORMANCE OF GRADIENT ELUTION EQUIPMENT

The gradient-generating pump is capable of reproducing any gradient profile according to the selected mathematical function drawn on a sheet of paper fastened to the rotating drum of the photoelectric curve-follower. To investigate the performance of the system, the flow-rates of components A and B of the gradient delivered by the individual plunger blocks were compared with the expected values at different pre-set volume ratios of B to A, the agreement of the flow-rate at the outlet of the mixing chamber with the sum of the individual flow-rates of A and B was tested and the experimental and required gradient profiles were compared, especially in the initial and final parts of the gradient. The tests were performed for different instrumental arrangements, to determine the influence of the individual parts of the system on the experimental errors. These arrangements included: (a) PPM 68005 and M6000 pumps in series, with the refractive index (RI) detector connected to the outlet of the M6000 pump; (b) the M6000 pump was connected to the column and RI detector; (c) the sample injector (U6K, Waters Assoc.) in the "LOAD" position was connected between the M6000 pump and the column; and (d) the arrangement as (c), but with the injector in the "INJECT" position. A reversed-phase column (C_{18}, 10 μm), 300 $\times$ 4.2 mm, was used in the tests of the system performance.

The results are shown in Tables I–III and Figs. 2–11. As shown in Table I, the flow-rates of the individual components of the organic (*n*-heptane–*n*-propanol) and aqueous (water–methanol) mobile phases delivered by plunger blocks of a PPM 68005 gradient-generating device correspond to the expected values with a standard deviation of *ca.* 0.5%, which is comparable to or better than in the commercial Waters Assoc. equipment (M6000 + M6000A pumps + M660 solvent programmer). The total flow-rate of the mobile phase at the outlet from the mixing chamber of the gradient-generating device (PPM 68005) is independent of the volume ratio of A and B, with a standard deviation of less than 1% for the *n*-heptane–*n*-propanol system, which is comparable to the gradient instrumentation from Waters Assoc. With the water–methanol system, however, the deviations of the total flow-rate from the expected values are systematic and reach maximal values of *ca.* 4–5%

TABLE I

COMPARISON OF THE FLOW-RATE OF THE LIQUID DELIVERED BY THE INDIVIDUAL PLUNGER BLOCKS (PUMPS) (F_A, F_B) AND THE TOTAL FLOW-RATE OF THE MIXED LIQUID (F_C) AT DIFFERENT SETTINGS OF THE VOLUME OF SOLVENT B FOR TWO TYPES OF GRADIENT ELUTION EQUIPMENT BASED ON TWO RECIPROCATING PLUNGER PUMPS

Type I, programmed stroke-ratio gradient-generation equipment, PPM 68005; II, programmed stepping motor speed equipment (M6000 + M6000A pumps controlled by M660 solvent programmer, Waters Assoc.). F_A, F_B and F_C are in ml/min; $\Delta = (F_A + F_B) - F_C$, as % of $F_A + F_B$; a and b are the parameters of the regression lines $F = a + bc$ (c = pre-set % volume of B) and s is the corresponding standard deviation of F values, evaluated by regression analysis; F(mean) represents the arithmetic mean of the corresponding values F for different c.

Instrument	*B (%)*	*A = n-heptane, B = n-propanol*					*A = water, B = methanol*					
		F_A	F_B	$F_A + F_B$	F_C	Δ (%)	F_A	F_B	$F_A + F_B$	F_C	Δ (%)	Δ (theoretical) (%)
I	0	1.220	0	1.220	1.220	0	1.200	0	1.200	1.200	0	0
	10	1.110	0.115	1.226	1.224	+0.16	1.070	0.142	1.211	1.199	+0.79	+0.70
	20	0.992	0.238	1.230	1.230	0	0.961	0.252	1.213	1.189	+1.85	+1.49
	30	0.873	0.358	1.231	1.224	+0.49	0.835	0.375	1.210	1.173	+3.08	+2.26
	40	0.750	0.478	1.228	1.223	+0.43	0.719	0.497	1.216	1.158	+4.21	+2.90
	50	0.620	0.600	1.219	1.221	−0.17	0.601	0.618	1.219	1.152	+4.71	+3.35
	60	0.513	0.723	1.236	1.220	+1.38	0.474	0.732	1.206	1.157	+4.18	+3.55
	70	0.378	0.842	1.220	1.212	+0.65	0.359	0.850	1.209	1.174	+2.98	+3.43
	80	0.250	0.960	1.210	1.210	+0.01	0.238	0.970	1.207	1.190	+1.77	+2.91
	90	0.132	1.085	1.217	1.210	+0.62	0.116	1.087	1.203	1.202	+0.74	+1.88
	100	0	1.210	1.210	1.210	0	0	1.209	1.209	1.209	0	0
	a	1.236	−0.006	1.230	1.227		1.198	0.002	1.210	1.179		
	b	−0.0123	0.0121	−0.00015	−0.00018		−0.0120	0.0120	−0.00002	0.000055		
	s	$7.3 \cdot 10^{-3}$	$2.0 \cdot 10^{-3}$	$8.7 \cdot 10^{-3}$	$8.3 \cdot 10^{-3}$		$4.5 \cdot 10^{-3}$	$6.7 \cdot 10^{-3}$	$8.4 \cdot 10^{-3}$	$2.13 \cdot 10^{-2}$		
	F(mean)	—	—	1.222	1.218		—	—	1.209	1.182		

II	0	0	1.041	1.041	1.041	0	0	1.064	1.064	1.064	0	0
	10	0.080	0.915	0.995	1.008	−1.33	0.070	0.950	1.020	1.003	+1.7	+0.70
	20	0.184	0.817	1.002	1.015	−1.34	0.165	0.837	1.002	0.997	+0.5	+1.49
	30	0.306	0.706	1.011	1.005	+0.61	0.263	0.725	0.988	0.982	+0.6	+2.26
	40	0.401	0.614	1.015	1.009	+0.60	0.374	0.630	1.004	0.968	+3.4	+2.90
	50	0.498	0.508	1.007	1.009	−0.26	0.476	0.521	0.997	0.952	+4.5	+3.35
	60	0.608	0.410	1.017	1.007	+0.97	0.566	0.420	0.986	0.951	+3.6	+3.55
	70	0.684	0.307	0.991	1.005	−1.39	0.669	0.314	0.983	0.950	+3.3	+3.43
	80	0.806	0.205	1.011	1.008	+0.27	0.765	0.223	0.988	0.964	+2.4	+2.91
	90	0.921	0.100	1.021	0.998	+2.28	0.862	0.112	0.974	0.963	+1.0	+1.88
	100	1.018	0	1.018	1.018	0	0.966	0	0.966	0.966	0	0
	a	−0.013	1.018	1.016	1.007		−0.020	1.052	1.031	1.016		
	b	0.0103	−0.0102	−0.00017	0.00002		0.00982	−0.0105	−0.00068	−0.00075		
	s	$7.0 \cdot 10^{-3}$	$4.4 \cdot 10^{-3}$	$10 \cdot 10^{-3}$	$5.4 \cdot 10^{-3}$		$9.4 \cdot 10^{-3}$	$7.6 \cdot 10^{-3}$	$1.50 \cdot 10^{-2}$	$2.35 \cdot 10^{-2}$		
	F(mean)	—	—	1.009	1.008		—	—	0.997	0.978		

TABLE II

ELIMINATION OF THE VOLUME CONTRACTIONS IN THE SYSTEM USING A PPM 68005 DEVICE FOR THE GENERATION OF CONCENTRATION GRADIENTS IN THE LOW-PRESSURE PART, PRIOR TO THE INLET OF THE M6000 HIGH-PRESSURE PUMP (FIG. 1)

F_c = flow-rate at the outlet from the column, ml/min; $\Delta = 100[F_c - F(\text{mean})/F(\text{mean})]$, % (rel.); I, component A = water, component B = methanol; II, component A = *n*-heptane, component B = *n*-propanol. Other symbols as in Table I.

B (%)	*System I*		*System II*	
	F_c	Δ	F_c	Δ
0	0.971	−0.4	0.988	+0.1
10	0.980	+0.5	0.986	−0.1
20	0.973	−0.1	0.989	+0.2
30	0.980	+0.6	0.986	−0.1
40	0.976	+0.1	0.984	−0.3
50	0.976	+0.1	0.987	0
60	0.973	−0.1	0.988	−0.1
70	0.973	−0.1	0.984	−0.3
80	0.978	+0.3	0.986	−0.1
90	0.971	−0.4	0.987	0
100	0.971	−0.4	0.992	+0.5
a	0.976		0.987	
b	−0.00004		−0.000004	
s	$3.4 \cdot 10^{-3}$		$2.2 \cdot 10^{-3}$	
F(mean)	0.975		0.987	

TABLE III

DEVIATIONS OF THE EXPERIMENTAL GRADIENT PROFILES FROM THE PRE-SET VALUES FOR DIFFERENT INSTRUMENTAL ARRANGEMENTS USING AN M6000 PUMP WITH A PPM 68005 LOW-PRESSURE GRADIENT-GENERATING DEVICE

Arrangements: (a) PPM 68005–RI detector; (b) PPM 68005–M6000–RI detector; (c) PPM 68005–M6000–column–RI detector; (d) PPM 68005–M6000–U6K injector in "LOAD" position–column–RI detector; (e) PPM 68005–M6000–U6K injector in "INJECT" position–column–RI detector; column: reversed-phase C_{18} on LiChrosorb Si-100 (10 μm), 300 × 4.2 mm; void volume 3.2 ml. Gradient components: A = methanol; B = 0.3% nitromethane in methanol. B = slope of the gradient function $c = BV$ (c = volume ratio of B; V ml = volume of the eluate); V_z = volume between the mixing chamber of PPM 68005 and the detector; Δ_0, Δ_{100} = experimental deviations from the expected content of component B at the pre-set values 0% and 100% B, respectively (in %B). Flow-rates: (a) 1.18 ml/min; (b–e) 0.97 ml/min.

Instrumental arrangement	*B (theoretical)*	*B (experimental)*	V_z *(ml)*	Δ_0	Δ_{100}
a	0.0035	0.0035	0.18	–	–
	0.0565	0.0564		0	0
b	0.0043	0.0043	3.08	–	–
	0.0687	0.0687		+1.53	−1.47
c	0.0086	0.0086	6.31	–	–
	0.0687	0.0686		+1.19	−1.56
d	0.0086	0.0086	6.49	–	–
	0.0687	0.0681		+1.72	−1.33
e	0.0086	0.0087	9.09	–	–
	0.0687	0.0684		+3.41	−2.87

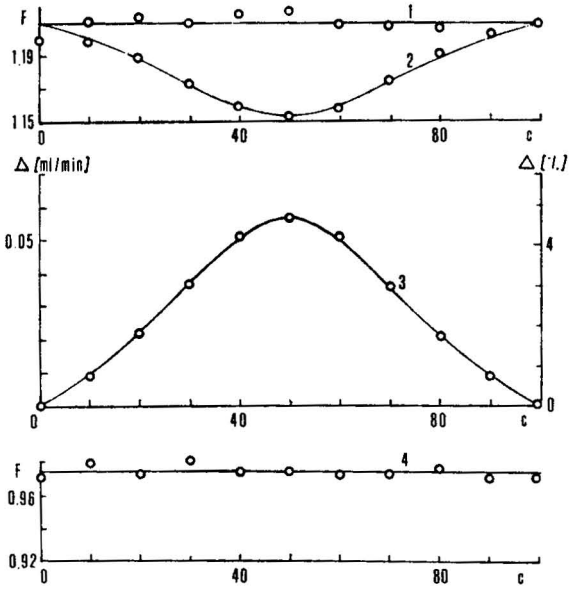

Fig. 2. Dependence of the flow-rate (F) on the pre-set composition of the mobile phase (c, in % of component B) in the system water (component A)–methanol (component B), using the PPM 68005 gradient-generating device (curves 1–3) and the device shown in Fig. 1 (curve 4). Curves: 1 = $F_A + F_B$ *versus* c; 2 = F_c versus c; 3 = $\Delta = F_A + F_B - F_c$, in ml and % (rel.) of $F_A + F_B$, *versus* c; curve 4 = F_c *versus* c. F_A and F_B = flow-rates at the outlet of the individual blocks delivering components A and B, respectively; F_c = total flow-rate at the outlet from the mixing chamber of PPM 68005 (curve 2) and at the outlet from the column in the system shown in Fig. 1 (curve 4).

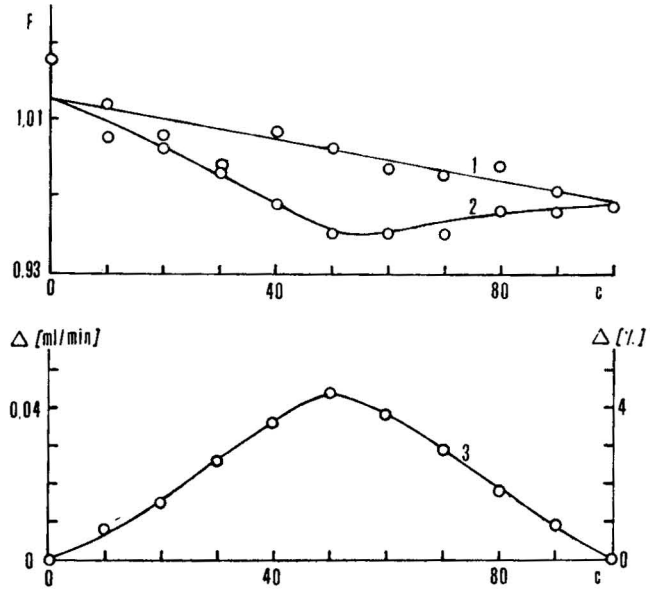

Fig. 3. Dependence of the flow-rate (F) on the pre-set composition of the mobile phase (c, in % of component B) in the system water (component A)–methanol (component B), using the Waters Assoc. gradient-elution system (pumps M6000 + M6000A + M600 solvent programmer). Curves: 1 = $F_A + F_B$ *versus* c; 2 = F_c *versus* c; 3 = Δ *versus* c. Symbols as in Fig. 2.

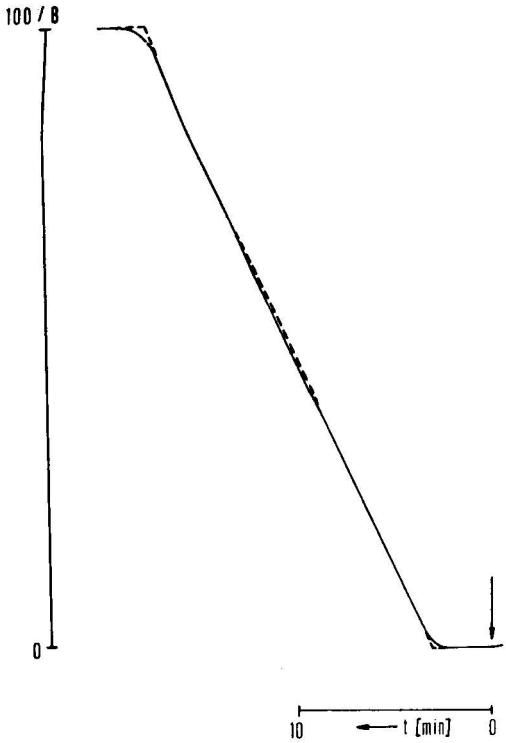

Fig. 4. Comparison of the experimental (full line) and expected (broken line) gradient profiles at the outlet of the M6000 pump connected in series to a PPM 68005 gradient-generating device. Component A = methanol; component B = 0.3% (v/v) solution of nitromethane in methanol. Gradient: $c = 0.06872V$, where c represents the volume ratio of B to A; V ml = volume of the mobile phase delivered from the mixing chamber. The experimental profile is measured as the signal of the R-401 RI detector (Waters Assoc., sensitivity 32).

in 40–60% methanol–water with both PPM 68005 and Waters Assoc. gradient equipment, as illustrated by Figs. 2 and 3. This is in approximate agreement with theoretically expected volume contractions due to the mixing of methanol with water (Table I).

This effect is eliminated in the gradient-generation system using a PPM 68005 gradient device in series with an M6000 high-pressure pump. As shown in Table II, the experimental values of the flow-rate at different settings of %B do not show any systematic decline as in the two above systems and the random errors are approximately the same in the water–methanol and *n*-heptane–*n*-propanol systems, with standard deviation of less than 0.5% of the total flow-rate in both systems. This precision is superior to that achieved with PPM 68005 or Waters Assoc. equipment (see Table I for a comparison). The elimination of the volume contractions in this system is illustrated in Figs. 2 and 3. It is further important that the flow-rates of the two plunger blocks (on pumps) be properly adjusted to achieve equal flow-rates at 0 and 100% B, as shown in Fig. 2, otherwise systematic shifts in flow-rate can be superimposed on to the other effects (Fig. 3, Waters Assoc. system incorrectly adjusted).

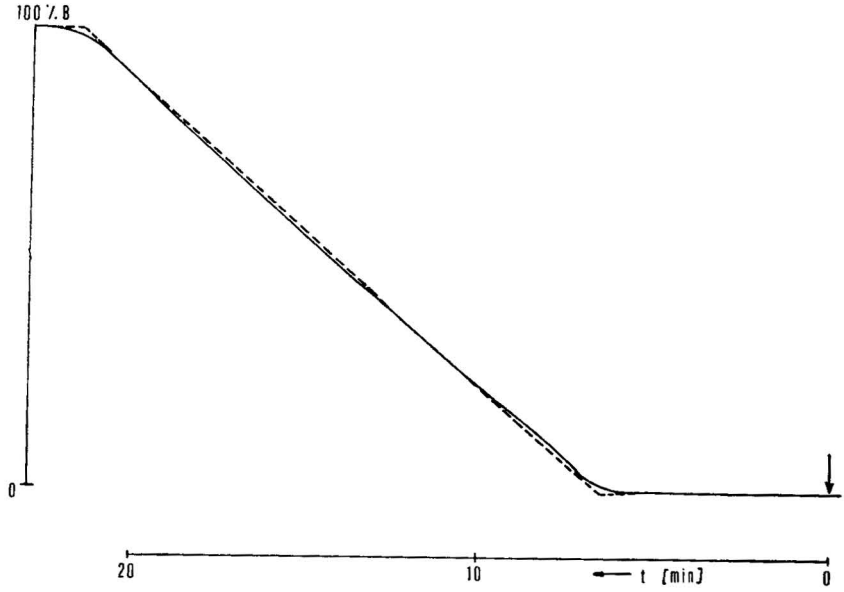

Fig. 5. Comparison of the experimental (full line) and expected (broken line) gradient profiles at the outlet of the column connected in the arrangement PPM 68005–M6000–column (reversed-phase C_{18}, 10 μm, 300 × 4.2 mm). Conditions and symbols as in Fig. 4.

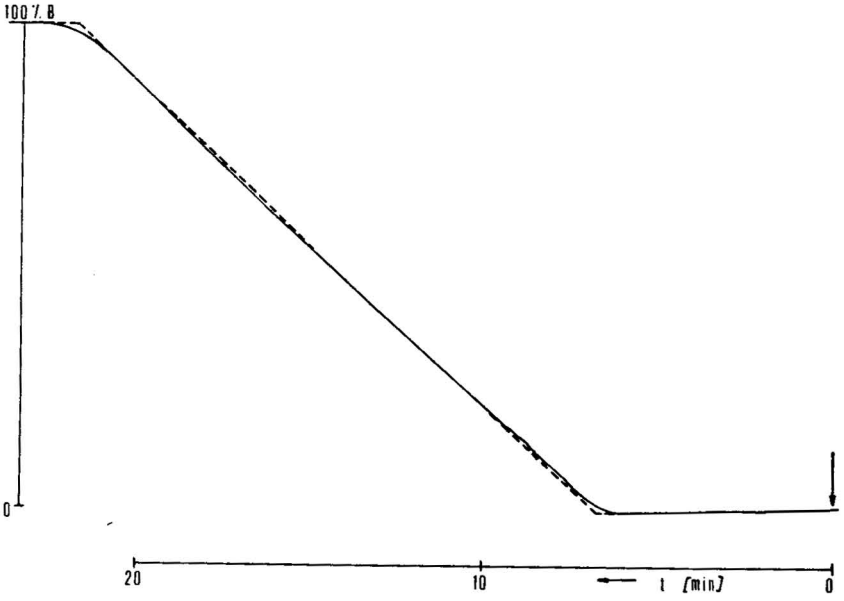

Fig. 6. Comparison of the experimental (full line) and expected (broken line) gradient profiles at the outlet of the column connected in the arrangement PPM 68005–M6000–U6K injector (in the "LOAD" position)–column. Conditions and symbols as in Fig. 4.

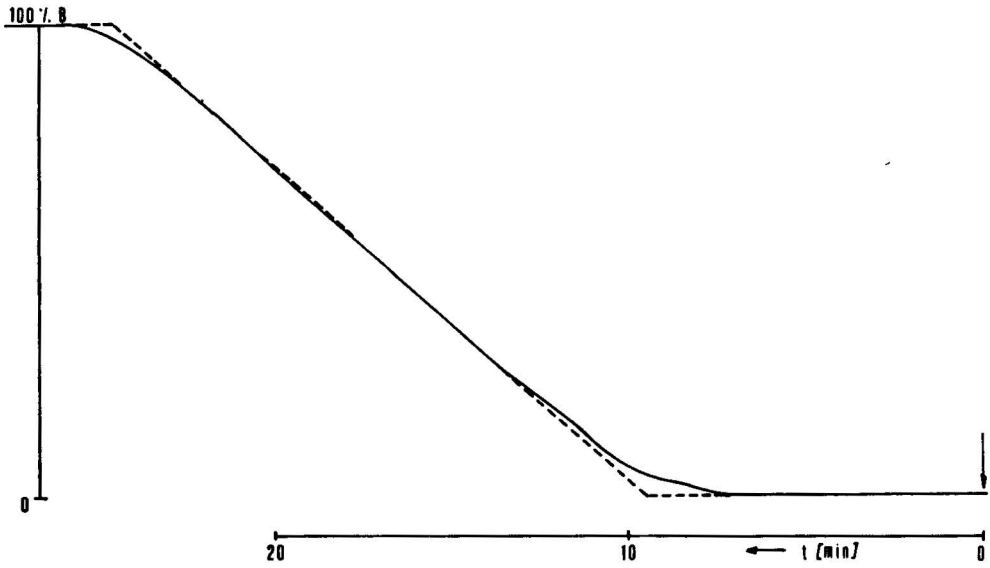

Fig. 7. Comparison of the experimental (full line) and expected (broken line) gradient profiles at the outlet of the column connected in the arrangement PPM 68005–M6000–U6K injector (in the "INJECT" position)–column. Conditions and symbols as in Fig. 4.

The equipments generating gradients in the low-pressure part inevitably contain void spaces between the mixing chamber at the inlet and the outlet of the high-pressure pump, which are given by the volumes of the plunger blocks, valve systems and the necessary connecting tubing. These void volumes, if incorrectly designed, can lead to deviations from the expected gradient profile. In any case, a corresponding volume delay must be considered before the gradient is operative in the column. Table III gives experimental values of this delay (V_z) for the PPM 68005 pump alone (0.18 ml), for the low-pressure and high-pressure pumps PPM 68005 and M6000 in series (3.08 ml) and the contribution of the U6K injector (0.18 ml in the "LOAD" position and 2.78 ml in the "INJECT" position). Thus, in the system shown in Fig. 1, the volume delay is 3.26 ml if the injector is switched to the "LOAD" position at the time corresponding to less than 3 ml of the mobile phase. This delay volume is not much larger than those in most commercial liquid chromatographs, where it is usually 1–2 ml.

Figs. 4–7 show experimental (full lines) and expected (broken lines) gradient profiles in gradient elution equipment with and without the column and U6K injector. As is further demonstrated in Table III, the gradient slope (B in Table III) is reproduced with a precision of better than 1 % (relative). The expected and the experimental gradient profiles at the outlet from the PPM 68005 device cannot be distinguished and the discrepancies are less than 1 % of B for other instrumental arrangements tested, with the exception of the initial and final part of the gradient, where it is *ca.* 1.5 % for *ca.* 0.5 ml of the mobile phase (Figs. 8–11). These systematic errors in the gradient profile are relatively insignificant and approximately equal, regardless of whether the column and U6K injector (in the "LOAD" position) are connected to the M6000 pump or not. However, the deviations are significantly larger (1–3 % of B)

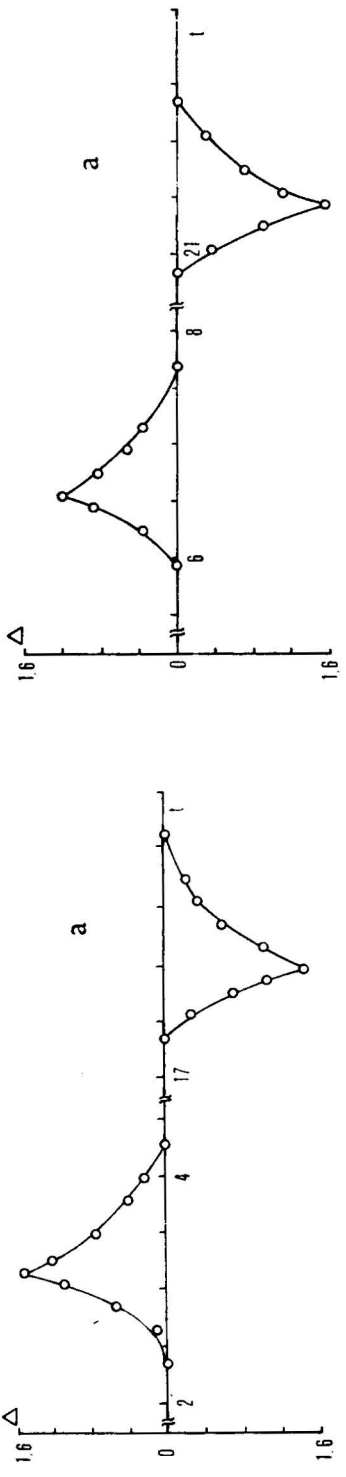

Fig. 8. Deviations of the experimental from the expected gradient profile (Δ) in the initial and final parts of the gradient in the arrangement PPM 68005–M6000 pump. Δ = % of component B. (a) Gradient $c = 0.00687V$ (15 min); (b) gradient $c = 1.6628V$ (0.6 min). Symbols and conditions as in Fig. 4.

Fig. 9. Deviations of the experimental from the expected gradient profile (Δ) in the initial and final parts of the gradient in the arrangement PPM 68005–M6000–column. Conditions and symbols as in Figs. 4 and 8.

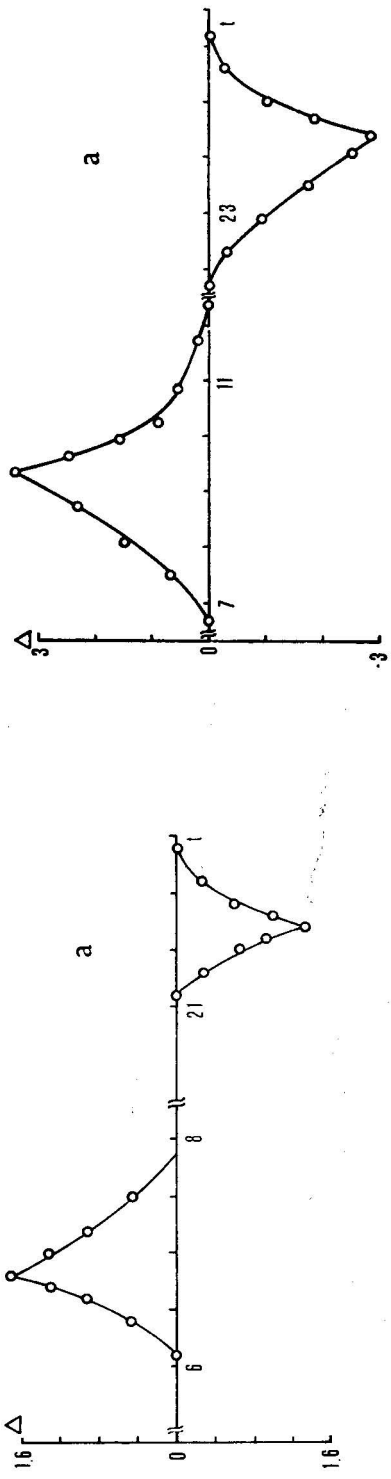

Fig. 10. Deviations of the experimental from the expected gradient profile (Δ) in the initial and final parts of the gradient in the arrangement PPM 68005–M6000–U6K injector (in the "LOAD" position)–column. Conditions and symbols as in Figs. 4 and 8.

Fig. 11. Deviations of the experimental from the expected gradient profile (Δ) in the initial and final parts of the gradient in the arrangement PPM 68005–M6000–U6K injector (in the "INJECT" position)–column. Conditions and symbols as in Figs. 4 and 8.

for a considerably longer part of the gradient (*ca.* 2 ml) if the injector is operated in the "INJECT" position, with a large-volume inner coil contributing to the instrumental void volume. Errors of this magnitude can be expected under the usual conditions of gradient elution operation (15-min gradient, 1 ml/min), but they increase with increasing slope of the gradient and can be considerably larger at extremely short gradients such as those shown in Figs. 8b–11b, which are, however, not used in practice.

CONCLUSIONS

The tests of the performance of the gradient elution device described here demonstrate the utility of this equipment for gradient elution operations, where both good reproducibility and good agreement between the experimental and pre-set gradient profiles and flow-rates of the mobile phase are required. The equipment, if operated with a U6K injector in the aLOAD" position, is able to reproduce accurately the required gradient profile with an error of less than 1% of solvent B during the gradient run, with the exception of a small part (*ca.* 0.5 ml) at the beginning and the end of the gradient, where the deviations are *ca.* 1.5%. The discrepancies between the pre-set and the experimental gradient profiles increase to some extent with increasing slope of the gradient, but this influence is relatively insignificant under the operating conditions usually used in gradient elution chromatography. A random error in the flow-rate of the mobile phase of *ca.* 0.5% (relative) can be expected and the total flow-rate does not depend on the ratio of solvents A and B being mixed. Eventual volume contractions due to the mixing of two liquids, such as a polar organic solvent with water, are eliminated with the system described. The performance of the gradient equipment was further demonstrated by the agreement between the experimental and calculated values of retention volumes in the gradient elution reversed-phase chromatography of various compounds in the water–methanol system, which was better than 5% (relative)[12].

The volume delay of the gradient in the equipment has to be considered and corrected for mathematically in calculations of retention volumes[13], or it can be compensated for by delaying the sample injection with respect to the start of the gradient at the time calculated from the known volume delay and the flow-rate of the mobile phase.

REFERENCES

1 S. R. Bakalyar and R. A. Henry, *J. Chromatogr.*, 126 (1976) 327.
2 S. R. Abbott, J. R. Berg, P. Achener and R. L. Stevenson, *J. Chromatogr.*, 126 (1976) 421.
3 L. R. Snyder and J. J. Kirkland, *Introduction to Modern Liquid Chromatography*, Wiley-Interscience, New York, 1974, Ch. 8.
4 P. Jandera, M. Janderová and J. Churáček, *J. Chromatogr.*, 115 (1975) 9.
5 H. Veening, *J. Chem. Educ.*, 50 (1973) 429.
6 M. Martin and G. Guiochon, in J. F. K. Huber (Editor), *Instrumentation for High-Performance Liquid Chromatography*, Elsevier, Amsterdam, 1978, Ch. 3.
7 L. R. Snyder, in Cs. Horváth (Editor), *Liquid Chromatography*, Academic Press, New York, London, in press.
8 *Characteristics of Gradient Elution Liquid Chromatography*, DuPont, Wilmington, Del., 1976.
9 M. Martin and G. Guiochon, *J. Chromatogr.*, 151 (1978) 267.
10 L. R. Snyder, *Chromatogr. Rev.*, 7 (1965) 1.
11 P. Jandera and J. Churáček, *J. Chromatogr.*, 93 (1974) 17.
12 P. Jandera, J. Churáček and L. Svoboda, *J. Chromatogr.*, 174 (1979) 35.
13 P. Jandera and J. Churáček, *J. Chromatogr.*, 91 (1974) 223.

Journal of Chromatography, 192 (1980) 53–74

CHROM. 12,579

ÉTUDE DE L'ÉLUTION NON-LINÉAIRE EN CHROMATOGRAPHIE EN PHASE LIQUIDE PRÉPARATIVE*

P. GAREIL

Laboratoire de Chimie Analytique des Processus Industriels, École de Physique et de Chimie de Paris, 10 Rue Vauquelin, 75231 Paris Cédex 05 (France)

L. PERSONNAZ

Laboratoire d'Electronique et d'Automatique, École de Physique et de Chimie de Paris, 10 Rue Vauquelin, 75231 Paris Cédex 05 (France) et Laboratoire des Signaux et Systèmes, C.N.R.S.-E.S.E., 91190 Gif-sur-Yvette (France)

et

J. P. FERAUD et M. CAUDE

Laboratoire de Chimie Analytique des Processus Industriels, École de Physique et de Chimie de Paris, 10 Rue Vauquelin, 75231 Paris Cédex 05 (France)

(Reçu le 7 mai 1979; manuscrit modifié reçu le 28 novembre 1979)

SUMMARY

Study of non-linear elution in preparative liquid chromatography

In most papers dealing with preparative elution chromatography the process behaviour is assumed to be linear, but in practice such an assumption may not be valid, since usually large volumes and high concentrations are injected. Thus a study of the non-linear behaviour of the chromatographic process seems highly desirable for better use of the column potential.

First of all, some properties of linear systems which should be useful for preparative chromatography are recalled. Then, the shape of elution profiles of a single solute is systematically studied in terms of the injected volume and concentration. These profiles are described by means of their first few moments. The moment method is convenient since it makes the test of linearity of the column behaviour easier when a large volume is injected. The test is based on a comparison between the first two moments of the analytical profile and those of the output profile under consideration.

The strongly non-linear behaviour of the process is studied in detail, and a set of characteristic properties are derived through experiments in ion-exchange chromatography. In particular, if the concentration profiles are plotted with respect to a common origin coinciding with the end of the pulse injections, they show a quasi-exponential envelope curve; the parameter defining the curve is related to the standard

* Présenté au *4th International Symposium on Column Liquid Chromatography, Boston, Mass., 7–10 mai 1979*. La plupart des communications présentées à ce symposium ont été publiées dans *J. Chromatogr.*, Vol. 185 (1979).

deviation of the analytical chromatogram and the mobile phase flow-rate only. A model, based on this set of properties, is presented and its validity discussed. This model should be of great interest for the optimal control of the column in non-linear preparative chromatography. An example is presented illustrating the experimental determination of the best injection characteristics for the separation of two compounds using the above model.

INTRODUCTION

La technique chromatographique du développement par élution a connu d'abord le succès dans le domaine analytique. Depuis quelques années, cette technique est également utilisée pour la préparation de produits purifiés (chromatographie préparative[1–10]). Cette nouvelle utilisation est caractérisée par des conditions d'injection et de distribution du soluté entre les deux phases différentes de celles de la chromatographie analytique.

Pour l'utilisation analytique le profil d'injection est perçu comme une impulsion par la colonne. La distribution du soluté entre les deux phases peut être considérée comme linéaire. Pour l'utilisation préparative le profil d'injection n'est plus perçu comme une impulsion mais peut être assimilé à un créneau. La distribution du soluté entre les phases peut être linéaire ou non-linéaire selon les concentrations injectées.

Nous commencerons par rappeler des résultats de chromatographie linéaire indispensables pour aborder une étude de la chromatographie préparative. Il est à noter que les procédures proposées dans la littérature supposent le plus souvent, explicitement ou non, la linéarité du système chromatographique. Pourtant, la contrainte d'un fonctionnement linéaire est très restrictive du point de vue de l'optimisation de la commande car il est difficile de savoir a priori dans quel domaine se situent les meilleures conditions préparatives. C'est pourquoi nous étudierons expérimentalement la déformation des profils d'élution dans les domaines linéaire et non-linéaire en vue d'optimiser les conditions d'injection (volume et concentration injectés, périodicité) pour un système chromatographique donné.

Nous avons entrepris cette étude en chromatographie d'échange d'ions car les supports échangeurs d'ions possèdent la propriété d'avoir des capacités parfaitement définies (capacités d'échange). Cette propriété permet de bien apprécier les quantités injectées sur une colonne par rapport à sa capacité.

PARTIE THÉORIQUE

Chromatographie linéaire

Systèmes linéaires. Les propriétés des systèmes linéaires peuvent être utilisées pour l'étude des processus chromatographiques en considérant le profil d'injection comme l'entrée du processus et le chromatogramme obtenu comme sortie[11,12]. De ce point de vue, ce que le chromatographiste nomme couramment "chromatogramme analytique" est la réponse impulsionnelle du processus. Sa connaissance permet de prédire la réponse à toute injection de profil donné. La Fig. 1 montre comment la réponse à une injection en créneau est déduite de la réponse impulsionnelle

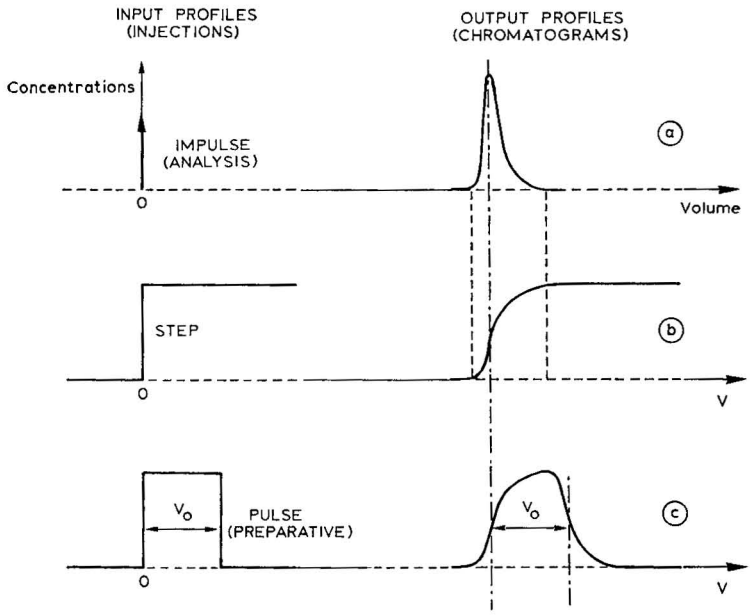

Fig. 1. Application du principe de superposition à la prévision de profils d'élution (comportement linéaire). (a) Réponse impulsionnelle; (b) réponse à un échelon; (c) réponse à un créneau.

en appliquant le principe de superposition. La fonction "échelon" étant l'intégrale de l'impulsion de Dirac, la réponse à un échelon est l'intégrale de la réponse impulsionnelle. Plus généralement, la réponse $y(V)$ est le produit de convolution de l'entrée $x(V)$ par la réponse impulsionnelle $h(V)$:

$$y(V) = \int_0^\infty h(V - w) \cdot x(w) \cdot \mathrm{d}w \tag{1}$$

Représentation mathématique des profils. Moments. Dans l'étude qui suit, nous allons étudier différents types de profils que nous représenterons par leurs moments dont nous rappelons les définitions.

Si $c(V)$ est le profil de concentration en fonction du volume d'élution V, le moment d'ordre zéro est la quantité injectée Q_0:

$$\mathrm{M0} = \int_0^\infty c(V) \cdot \mathrm{d}V = Q_0$$

Le moment normalisé d'ordre 1 est défini par:

$$\mathrm{M1} = \frac{1}{\mathrm{M0}} \int_0^\infty c(V) \cdot V \cdot \mathrm{d}V$$

Le $i$ème moment normalisé et centré est:

$$\mathrm{M}i = \frac{1}{\mathrm{M0}} \int_0^\infty c(V) \cdot (V - \mathrm{M1})^i \cdot \mathrm{d}V \qquad i \geqslant 2$$

A partir de ces moments sont définis les coefficients adimensionnels suivants:

$$\text{coefficient d'asymétrie: } S = \frac{\mathrm{M3}}{(\mathrm{M2})^{1.5}}$$

$$\text{coefficient d'aplatissement: } E = \frac{\mathrm{M4}}{(\mathrm{M2})^2} - 3$$

Une injection impulsionnelle sera donc représentée par:

$$\mathrm{M0} = \mathrm{Q_0}$$
$$\mathrm{M1} = \mathrm{M2} = \ldots = \mathrm{M}i = \ldots = 0$$

Une injection en créneau (V_0, C_0) par:

$$\mathrm{M0} = V_0 \cdot C_0 = Q_0; \quad \mathrm{M1} = \frac{V_0}{2}; \quad \mathrm{M2} = \frac{V_0^2}{12}; \quad \mathrm{M3} = 0; \quad \mathrm{M4} = -\frac{V_0^4}{120}$$

Les profils de sortie seront généralement représentés par leurs quatre premiers moments. Toutefois, dans le cas d'une réponse impulsionnelle symétrique ou si une approximation suffit, les chromatographistes se limitent généralement aux grandeurs suivantes:

$Q_0 = \mathrm{M0}$: quantité injectée

$V_R = \mathrm{M1}$: volume de rétention

$N = \dfrac{(\mathrm{M1})^2}{\mathrm{M2}} = \dfrac{V_R^2}{\sigma^2}$: nombre de plateaux théoriques

Si la fonction de Gauss est utilisée pour représenter le profil, son expression en fonction des paramètres précédents est la suivante:

$$h(V) = \frac{\mathrm{Q_0}}{\sigma\sqrt{2\pi}} \cdot \exp\left(-\frac{(V - V_R)^2}{2\sigma^2}\right)$$

Estimation des moments des profils de sortie. L'utilisation des moments pour représenter les profils permet de traduire très simplement l'intégrale de convolution[13,14]: les moments du profil de sortie notés $\mathrm{M}i_y$ s'expriment en fonction de ceux du profil d'injection noté $\mathrm{M}i_x$ et de ceux de la réponse impulsionnelle notés $\mathrm{M}i_h$ par les relations simples:

$$\mathrm{M}i_y = \mathrm{M}i_x + \mathrm{M}i_h \qquad i = 1,2,3 \tag{2}$$
$$\mathrm{M4}_y - 3(\mathrm{M2}_y)^2 = (\mathrm{M4}_x - 3(\mathrm{M2}_x)^2) + (\mathrm{M4}_h - 3(\mathrm{M2}_h)^2)$$

Ainsi, tant que le comportement est linéaire, il est possible de calculer les moments du profil de sortie à partir de ceux du profil d'injection et de ceux de la réponse impulsionnelle.

La Fig. 2 montre comment utiliser pratiquement ces résultats en chromatographie préparative linéaire à partir du chromatogramme analytique. Dans le cas

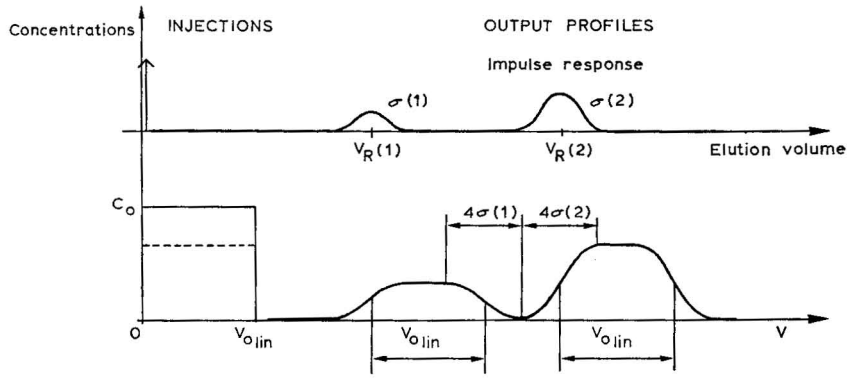

Fig. 2. Chromatographie préparative linéaire. Mélange de deux composés. Réponses impulsionnelles gaussiennes. $V_{0_{lin}} = V_R(2) - V_R(1) - 2[\sigma(1) + \sigma(2)]$; période d'injection: $\theta = 2[V_R(2) - V_R(1)]/D$ (D = débit; V_R = volume de rétention analytique; σ = écart-type analytique).

d'un mélange binaire et si les pics analytiques sont gaussiens, le volume maximum injectable conservant une séparation complète des deux composés est donné par l'expression connue:

$$V_0 = V_R(2) - V_R(1) - 2(\sigma(1) + \sigma(2)) \tag{3}$$

où $V_R(1)$, $\sigma(1)$ et $V_R(2)$, $\sigma(2)$ représentent les réponses analytiques de ces deux composés.

Chromatographie non-linéaire

Test de linéarité. La non-linéarité du comportement du processus peut être due à la distribution du composé entre les deux phases (courbure de l'isotherme) ou à des phénomènes d'écoulement ou de mélange défectueux des composés.

Lors de la mise au point des meilleures conditions d'injections préparatives, il est important de tester la linéarité du comportement. Un test simple peut être déduit des relations (2). Il consiste à comparer les moments invariants de la réponse impulsionnelle Mi_h, calculés auparavant, à la différence: ($Mi_y - Mi_x$) correspondant aux conditions d'injection pour lesquelles on désire savoir si le comportement est linéaire ou non. Si ($Mi_y - Mi_x$) est significativement différent de Mi_h, le comportement est non linéaire.

Modèles non-linéaires. Si le comportement du processus n'est plus linéaire, les profils de sortie ne peuvent plus être déduits de l'intégrale de convolution. Un modèle non-linéaire doit nécessairement prendre en compte dans sa structure le volume et la concentration injectés. Pour élaborer un tel modèle, deux approches sont possibles:

(a) L'approche physico-chimique est utilisée lorsqu'on désire élaborer un modèle de représentation interne du processus. Quelques auteurs ont étudié les solutions mathématiques des équations physico-chimiques dans le cas de profils d'injection ayant la forme d'un créneau ou d'une gaussienne[15]. Leurs résultats ne sont valables que pour de faibles écarts par rapport au comportement linéaire.

D'autres auteurs, se plaçant du point de vue de la conception de systèmes préparatifs, ont étudié les facteurs physico-chimiques intervenant dans la surcharge des colonnes. De telles études ont été faites aussi bien en chromatographie en phase liquide[16] qu'en chromatographie en phase gazeuse[17].

(b) La seconde approche consiste à faire appel à un modèle de représentation externe du processus. Un modèle physico-chimique n'est pas nécessaire si le but poursuivi est de déterminer les meilleures conditions d'injection pour un système donné et une séparation donnée en chromatographie préparative. Un modèle, linéaire ou non-linéaire, permettant de prédire la forme du profil de sortie pour une injection donnée est suffisant dans ce cas. Un tel modèle —dit de représentation externe— peut être élaboré à partir d'une étude expérimentale sans faire fondamentalement appel à des considérations physico-chimiques.

Le but principal de ce travail est de décrire l'élaboration d'un tel modèle non-linéaire qui demande la réalisation d'un plus grand nombre d'expériences qu'un modèle linéaire.

PARTIE EXPÉRIMENTALE

Appareillage

Nous avons utilisé un chromatographe construit par nos soins équipé d'une pompe pneumatique Haskel (Burbank, Calif., U.S.A.) spéciale pour chromatographie.

Les injections de volumes inférieurs à 4 ml sont réalisées par l'intermédiaire de boucles d'échantillonnage et d'une vanne à 6 voies, construites par nos soins. Pour les injections de volumes supérieurs à 4 ml, nous avons utilisé une pompe seringue Varian type 8510 (Varian, Palo, Alto Calif., U.S.A.).

La colonne est constituée d'un tube inox 316, de diamètre intérieur 1.05 cm (diamètre extérieur 1/2 in.), de longueur 47 cm et de volume 40.7 ml. Les extrémités de ce tube sont équipées de raccords réducteurs Swagelok 1/2–1/16 in. de façon à limiter les volumes morts dans les connexions.

La détection est effectuée par absorptiométrie dans l'ultra-violet à l'aide d'un spectrophotomètre Varian Variscan. Nous avons travaillé sur la sensibilité 0.5 D.O. de l'appareil de façon à rester dans le domaine linéaire de la loi de Lambert–Beer. La longueur d'onde est choisie de façon à pouvoir utiliser cette sensibilité à n'importe quelle concentration. Le signal de détection est mesuré par un millivoltmètre numérique Schlumberger 7144 (Paris, France) puis traité sur calculateur Hewlett-Packard 9825 (Palo Alto, Calif., U.S.A.).

Les moments du profil de sortie sont calculés par la méthode d'intégration de Simpson. Les données sont traitées de la façon suivante: La période d'échantillonnage est de 15 sec ($\sqrt{M2_n}/8$); la ligne de base est estimée avant et après le pic par la moyenne sur 40 points expérimentaux; les bornes d'intégration t_0 et t_m sont déterminés par le seuil $c(t_0) = c(t_m) = 1/100\, c(t_{max.})$. (Le rapport signal sur bruit étant voisin de 100.)

Produits

La phase stationnaire est une résine échangeuse d'anions du type base forte triméthylammonium de granulométrie inférieure à 65 μm (résine Dowex AG 1-X8

minus 400 mesh, granulométrie humide 230 mesh; Bio-Rad Labs., Richmond, Calif., U.S.A.). La phase mobile est une solution aqueuse molaire d'acétate d'ammonium de qualité R. P. no. 2120029 (Prolabo, Paris, France), tamponnée à pH 9 avec une solution d'ammoniaque à 25% de qualité Merck no. 5432.

Nous avons choisi comme soluté le maléate d'ammonium, d'une part parce que son comportement chromatographique a déjà été étudié dans notre laboratoire[18], d'autre part à cause de sa grande solubilité dans l'eau, ce qui permet de faire varier dans un large domaine la concentration des solutions injectées. De plus, la faible valeur de son coefficient d'extinction moléculaire permet un dosage en continu par absorptiométrie dans l'ultra violet. Nous avons mis en solution, dans la phase mobile, de l'acide maléique de qualité Merck no. 800380 (Merck, Darmstadt, R.F.A.).

Caractéristiques chromatographiques

La colonne chromatographique a été remplie sous 80 atm avec une suspension de la résine dans la phase mobile afin d'éviter tout échange ionique. Elle renferme 19 g de résine sèche et sa capacité d'échange est de 72 milliéquivalents (mequiv.) Le volume mort, déterminé en mesurant la rétention de Co^{2+} et de $Cu(NH_3)^{2+}$ est de 12 ml.

Dans le but de tester les propriétés chromatographiques de la colonne préparative (que nous noterons "colonne P"), nous avons comparé, sur la séparation du maléate et du fumarate, ses performances à celles d'une colonne analytique de diamètre intérieur 2.1 mm, de même longueur, remplie avec la même résine (colonne A). Le Tableau I montre que l'efficacité de la colonne P est supérieure à celle de la colonne A. Ceci peut s'expliquer par un meilleur remplissage de la colonne P et par l'élimination de l'influence de la paroi; la condition de diamètre infini de Knox et Parcher[19]:

$$d_C > (2.4\, L \cdot d_p)^{1/2}$$

se trouve en effet satisfaite. De plus, à vitesse linéaire égale, on observe une pression d'entrée supérieure sur la colonne P, ce qui confirme un meilleur remplissage de celle-ci et une perméabilité plus homogène[20,21]. A première vue, la valeur de la hauteur equivalente à un plateau théorique (HEPT) réduite h calculée pour le fumarate sur la colonne P parait élevée si l'on se réfère à l'équation de Bristow et Knox[22], puisqu'ici:

$$d_p = 60\ \mu\text{m et } h = \frac{H}{d_p} = 55$$

TABLEAU I

COMPARAISON DES EFFICACITÉS D'UNE COLONNE ANALYTIQUE ET D'UNE COLONNE PRÉPARATIVE DE MÊME LONGUEUR (L = 50 cm)

Phase stationnaire: Dowex AG1-X8 minus 400 mesh. Phase mobile: acétate d'ammonium 1 M, pH 9. Vitesse linéaire: 1.1 cm/sec.

	Colonne analytique (A)	*Colonne préparative (P)*
Diamètre intérieur (mm)	2.1 (1/8 in.)	10.5 (1/2 in.)
Perte de charge (atm)	10	25
Maléate HEPT (mm)	11.5	5.3
Fumarate HEPT (mm)	4.8	3.2

Cette valeur s'explique compte-tenu de la valeur élevée de la vitesse réduite de la phase mobile v. En effet:

avec: $D_m = 1.2 \times 10^{-5}$ cm²/sec (évalué par la relation de Wilke et Chang[23])

on obtient: $v = \dfrac{ud_p}{D_m} = 550$

RÉSULTATS ET DISCUSSION

Dans tout ce qui suit, nous assimilerons les profils d'injection à des créneaux (V_0, C_0). Nous avons étudié l'influence respective du volume V_0 et de la concentration C_0 du soluté injecté sur la forme du profil de sortie. Si ces injections sont représentées sur un diagramme volume–concentration injectés, les courbes "iso-quantité" sont des hyperboles (Fig. 3): $Q_0 = V_0 \cdot C_0$. La capacité d'échange de la colonne est représentée par une hyperbole de quantité 72 mequiv. ($m \cdot C_E = Q_E$) m étant la masse de résine dans la colonne et C_E sa capacité d'échange exprimée en mequiv./g.

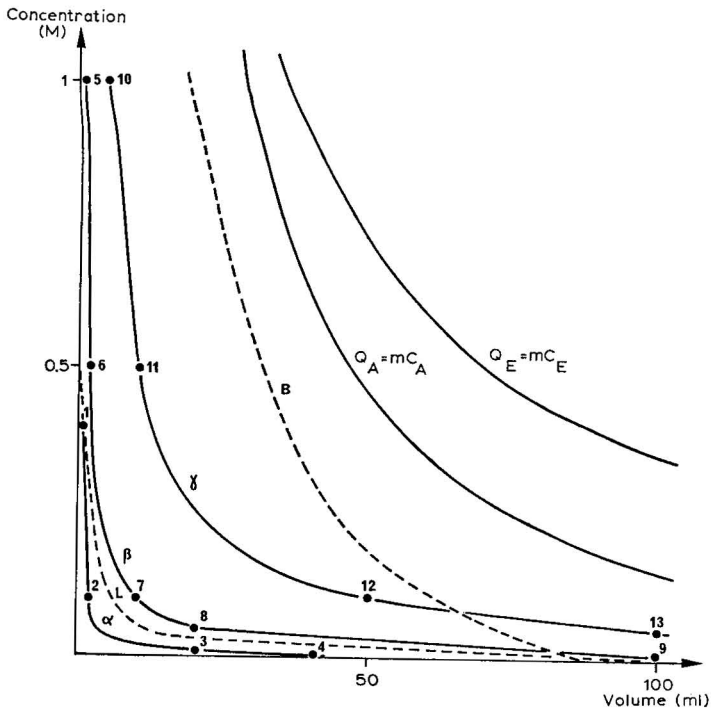

Fig. 3. Diagramme des volumes et concentrations injectés. α: quantité injectée: $Q_0 = 0.4$ mequiv.; β: $Q_0 = 2$ mequiv.; γ: $Q_0 = 10$ mequiv.; $Q_A = m \cdot C_A$: capacité disponible de la colonne; $Q_E = m \cdot C_E$: capacité d'échange de la colonne. B: Frontière entre les injections (V_0, C_0) donnant un profil avec palier et celles donnant un profil sans palier; L: frontière entre les comportements linéaire et non-linéaire.

Étude des profils obtenus en chromatographie analytique (Comportement linéaire)

Dans cette partie, nous avons injecté des quantités "analytiques", au plus égales à 0.1 % de la capacité totale de la colonne. Etant données les faibles valeurs de

V_0, la déconvolution des moments des profils de sortie n'entraîne ici que des corrections inférieures à 1% sur les paramètres: M1, N, S et E.

Le Tableau II montre que le volume d'élution au maximum du pic ($V_{max.}$), qui est couramment utilisé pour mesurer le volume de rétention V_R, est systématiquement inférieur d'environ 2% au moment d'ordre 1 du profil (M1). Ces 2 grandeurs diminuent légèrement avec la quantité injectée, ce qui s'explique par la convexité de l'isotherme, même pour ces faibles concentrations[24,25]. Dans tout ce domaine, le nombre de plateaux théoriques N est sensiblement égal à 88. La dispersion sur le calcul de M2 ($\pm$ 6%) ne laisse pas apparaître une variation significative de N en fonction de la quantité injectée.

TABLEAU II

CARACTÉRISTIQUES DES PROFILS OBTENUS À PARTIR DES INJECTIONS ANALYTIQUES

Q_0 = quantité de soluté injecté; V_0 = volume de soluté injecté; $V_{max.}$ = volume d'élution au maximum du pic; M1 = moment d'ordre 1; C_0 = concentration du soluté injecté; $C_{max.}$ = concentration du soluté au maximum du pic.

Q_0 (mequiv.)	V_0 (ml)	$V_{max.}$ (ml)	M1 (ml)	$Q_0/C_{max.}$ (ml)	$C_0/C_{max.}$
10^{-2}	0.5			94.8	174
	1	325 $\pm$ 1	331 $\pm$ 1	82.1	74
	2			91.8	45
$4 \cdot 10^{-2}$	0.5			85	156
	1	320 $\pm$ 1	326 $\pm$ 1	85.5	77
	2			85.7	42
$8 \cdot 10^{-2}$	0.5			83.9	154
	1	317 $\pm$ 1	320 $\pm$ 1	87.7	79
	2			87.7	43

La valeur positive du coefficient d'asymétrie S voisine de 0.3, est due à la trainée arrière du profil. Le coefficient d'aplatissement E reste pratiquement nul.

Le rapport $C_0/C_{max.}$ (Tableau II), qui définit la dilution du soluté au maximum du pic d'élution ne dépend que du volume injecté. Il revient au même de dire que la concentration au maximum du pic $C_{max.}$ est proportionnelle à la quantité injectée Q_0 et reste indépendante de C_0 et V_0 pris individuellement. Cela signifie que le fonctionnement de la colonne est linéaire, qu'elle perçoit les injections analytiques de ce type comme des impulsions de Dirac et non comme des créneaux de concentration et de volume finis. Augmenter le volume injecté constitue donc un bon moyen pour obtenir une dilution minimale en sortie de colonne. Il ne sert à rien, de ce point de vue, de concentrer le produit avant son injection.

Il est à remarquer que la valeur constante de $Q_0/C_{max.}$ est proche de celle qu'on obtiendrait avec la fonction de Gauss. En effet, dans ce cas:

$$\frac{Q_0}{C_{max.}} = \sigma \cdot \sqrt{2\pi}$$

Pour nos profils: $\sigma = 35 \pm 1$ ml

$$\sigma\sqrt{2\pi} = 88 \pm 3 \text{ ml}$$

Cette valeur est bien en accord avec les valeurs de $Q_0/C_{max.}$ données dans le Tableau II. Ce résultat est dû à la forme quasi-gaussienne des réponses analytiques enregistrées.

Étude des profils obtenus en chromatographie préparative (Comportement non-linéaire)

Nous avons ensuite étudié le comportement du processus chromatographique dans le domaine préparatif, c'est-à-dire pour des injections variant de 0.2 à 10 mequiv., soit respectivement 0.3 et 14% de la capacité totale. Dans ce domaine de charge l'effet de la non-linéarité est significatif. Nous avons utilisé systématiquement le test de linéarité présenté plus haut de façon à préciser les limites des fonctionnements linéaire et non-linéaire. Cette frontière est représentée sur la Fig. 3. Le test a porté sur les deux premiers moments.

Malgré l'importance de l'effet non-linéaire, les paramètres "déconvolués" restent intéressants pour accéder à l'effet de la colonne seule et comprendre son fonctionnement dans ce domaine. Bien entendu, si l'on ne se place plus du point de vue de la compréhension des phénomènes mais de celui —pratique— de la séparation des composés, les paramètres à considérer sont les paramètres non déconvolués.

Les résultats obtenus rassemblés dans le Tableau III entrainent les remarques suivantes:

TABLEAU III

CARACTÉRISTIQUES DES PROFILS D'ÉLUTION À PARTIR D'INJECTIONS PRÉPARATIVES

No. = numéro du point expérimental sur la Fig. 3; Q_0 = quantité de soluté injectée (meq.); V_0 = volume de soluté injecté (ml); $V_{max.}$, $C_{max.}$ = volume d'élution et concentration du soluté au maximum du pic; M1 = moment d'ordre 1 (volume de rétention en ml); N = nombre de plateaux; S = coefficient d'asymétrie; E = coefficient d'excès; ^{0} = paramètre "non-déconvolué"; $'$ = paramètre "déconvolué".

No.	Q_0 *(mequiv.)*	V_0 *(ml)*	$Q_0/C_{max.}$ *(ml)*	$C_0/C_{max.}$	$V_{max.}$ *(ml)*	$M1^0$ *(ml)*	$M1'$ *(ml)*	N^0	N'	S^0	E^0
1	0.4	0.5	85	156	294	306	306	88	88	0.89	0.79
2		2	84.2	41.3	299	310	309	75	75	0.48	0.22
3		20	82	4.1	315	327	317	91	88	0.42	0.20
4		40	89.2	2.2	334	343	323	86	84	0.44	0.11
5	2	1	91	82	235	265	265	39	39	0.90	0.65
6		2	86.5	42.4	242	271	270	44	44	0.91	0.73
7		10	82.7	8.2	249	275	270	51	50	0.86	0.52
8		20	87	4.3	261	288	278	52	50	0.85	0.55
9		100	120	1.2	318	339	289	60	84	0.61	0.07
10	10	5	98.5	19.7	146	194	192	14	13	1.02	0.59
11		10	93.5	9.3	150	198	193	14	13	1.10	0.91
12		50	91	1.8	181	231	206	18	15	1.04	0.64
13		100	132	1.3	223	274	224	25	24	0.93	0.44
Réponse impulsionnelle			87				330		88	0.3	0

(a) Le volume d'effluent $V_{max.}$ mesuré au sommet du pic d'élution et le moment d'ordre 1 déconvolué noté M1′ diminuent quand la quantité injectée augmente, à cause de la non linéarité de l'isotherme. L'écart entre $V_{max.}$ et M1′ augmente avec la charge puisque le chromatogramme se déforme de plus en plus.

A charge constante, les variations de $V_{max.}$ et du moment d'ordre 1 non déconvolué $M1^0$ dues à cette non-linéarité sont masquées par le volume injecté V_0. La non-linéarité est plus clairement mise en évidence par la variation du moment d'ordre 1 déconvolué (M1'), qui est toujours inférieur au volume de rétention analytique (330 ml), et qui décroit quand la concentration injectée C_0 augmente.

(b) Le nombre de plateaux non déconvolué N^0 diminue quand la quantité injectée augmente. A partir d'une quantité injectée de 2 mequiv., qui représente 2.8% de la capacité totale de la colonne, on observe une diminution très importante de N^0.

L'effet du volume injecté sur le nombre de plateaux (effet qui est appelé "surcharge en volume" dans certains articles) peut être supprimé en calculant ce paramètre à partir des moments déconvolués:

$$N' = \frac{(M1')^2}{M2'}$$

La diminution de N' par rapport à la valeur analytique $N = 88$ n'est alors due qu'à la non-linéarité, c'est-à-dire à une modification du fonctionnement de la colonne. A ce sujet, il est intéressant de faire la distinction entre l'efficacité d'un processus définie à partir de sa réponse impulsionnelle par:

$$N = \frac{(M1_h)^2}{M2_h}$$ et la valeur N^0 qui, elle, dépend du volume injecté V_0 (pour un

comportement linéaire: $N' = N$).

(c) A charge constante, N' est d'autant plus grand que le soluté injecté est plus dilué. Ce résultat est en accord avec ceux obtenus par De Stefano et Beachell[21] et par Done[27] en chromatographie d'adsorption.

(d) Les coefficients d'asymétrie S^0 et d'aplatissement E^0 du profil de sortie augmentent avec la quantité injectée. Pour une quantité constante, ces deux coefficients diminuent lorsque V_0 augmente. Cela s'explique par le fait que pour les grands volumes, le profil de sortie garde globalement l'allure symétrique du profil d'injection en créneau. Un résultat analogue a déjà été mis en évidence en chromatographie en phase gazeuse[28].

Pour tous les points expérimentaux reportés dans le Tableau III, sauf pour les plus grands volumes injectés (points 9 et 13), le rapport $Q_0/C_{max.}$ conserve une valeur I indépendante de Q_0, V_0 et C_0. Ici I vaut 88 ml. Cette invariance est remarquable lorsque le comportement est fortement non-linéaire. La dilution $Q_0/C_{max.}$ reste indépendante de la quantité injectée et est uniquement liée, comme dans le cas des injections impulsionnelles, au volume injecté.

A titre d'exemple, l'injection de 10 meq sous la forme de 50 ml d'une solution 0.1 M ou sous la forme de 5 ml d'une solution molaire conduit à la même concentration, $C_{max.}$, au sommet du profil d'élution soit environ $5 \cdot 10^{-2}$ M. Il est donc inutile de concentrer au préalable la solution à injecter dans le but de recueillir un effluent plus concentré en soluté. De plus, d'autres propriétés apparaissent en représentant les profils d'élution en prenant la fin des injections comme origine des abscisses.

(e) Les profils d'élution obtenus pour une même quantité injectée $Q_0 = V_0 \cdot C_0$

mais avec des couples (V_0, C_0) différents sont pratiquement superposables. Les fronts avant des profils sont d'autant plus raides que la quantité injectée est grande.

(f) A partir de leur sommet les profils se raccordent à une courbe enveloppe $C(V)$ qui est quasi-exponentielle. La constante de cette exponentielle est égale à l'invariant I mentionné précédemment:

$$C(V) = C_m \cdot \exp\left(-\frac{(V - V_m)}{I}\right)$$

V_m est le volume mort de la colonne et C_m un paramètre du processus qui peut être déterminé en ajustant l'exponentielle aux valeurs expérimentales (Fig. 4).

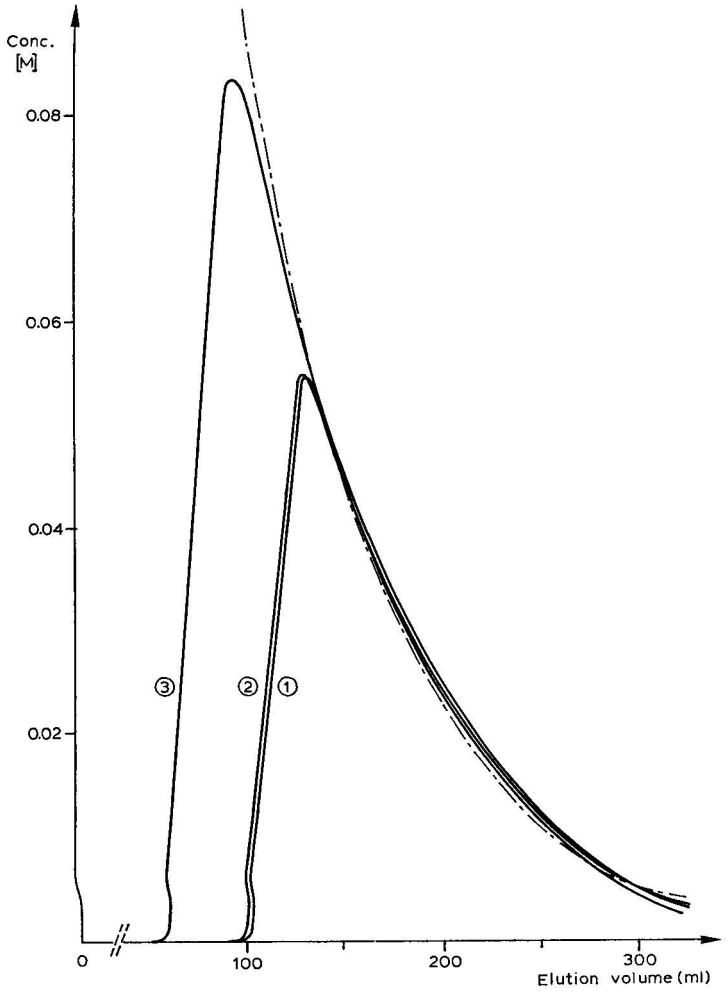

Fig. 4. Enveloppe exponentielle de la partie arrière des profils fortement non-linéaires. Origine des abscisses: fin des injections. 1: $V_0 = 10$ ml; $C_0 = 0.5$ M; $Q_0 = 10$ mequiv. 2: $V_0 = 50$ ml; $C_0 = 0.1$ M; $Q_0 = 10$ mequiv. 3: $V_0 = 10$ ml; $C_0 = 0.75$ M; $Q_0 = 15$ mequiv. —.—, Enveloppe exponentielle obtenue par les moindres carrés.

Ces deux propriétés sont liées au fait que la quantité $Q_0 = C_{max.} \cdot I$ est égale à l'aire comprise sous l'exponentielle limitée à l'abscisse $V_{max.}$.

Les limites de validité de ce comportement dans le diagramme des injections (V_0, C_0) (Fig. 3) sont explicitées au p. 69.

Nous avons également étudié le raccordement du profil d'élution à la ligne de base. Pour cela, nous avons mesuré la concentration C_F correspondant au volume $V_F = V_R + 2\sigma$ avec $V_R = M1_h$ et $\sigma = \sqrt{M2_h}$

En chromatographie analytique, il est généralement admis que V_F correspond à la quasi-totalité de l'élution du composé (97.8% pour une réponse analytique gaussienne). Pour tous les points expérimentaux de la Fig. 3 les valeurs de C_F restent comprises entre 2 et 4% de $C_{max.}$. Ce résultat montre que la notion d'enveloppe pour la trainée arrière de tous les profils n'est plus valable autour de $V_R + 2\sigma$. Néanmoins, la quantité restant à éluer à partir de ce volume est de l'ordre de 2 à 4% de la quantité totale injectée, ce qui ne justifie pas une remise en cause du modèle exponentiel proposé.

D'autres résultats obtenus avec des phases mobiles et des solutés différents mais avec la même vitesse de phase mobile donnent des valeurs de I proportionnelles à l'écart-type analytique $\sigma = \sqrt{M2_h}$. Nous avons également constaté que pour une phase mobile et un soluté donnés, I ne dépend pas de la vitesse de la phase mobile du moins pour des vitesses comprises entre 0.15 et 1.5 cm/sec. Le développement de cette propriété a l'avantage de relier les comportements linéaire et non-linéaire du processus.

Étude des profils obtenus avec saturation de la phase stationnaire de la colonne

Cette étude permet de visualiser qualitativement le processus de dessaturation d'une bande de soluté au cours de son élution à l'intérieur d'une colonne, donc d'interpréter physiquement les résultats précédents. Elle nous permet également de tracer l'isotherme de distribution à saturation, c'est-à-dire de déterminer la capacité disponible, paramètre important du point de vue préparatif. Comme le soluté est mis en solution dans la phase mobile, il existe en effet pour les groupements échangeurs une réaction de compétition entre les ions du soluté et les ions éluants. La capacité de la colonne, disponible pour le soluté, n'est donc plus égale à la capacité d'échange de la phase stationnaire.

Nous avons injecté sur la colonne un créneau de concentration C_0 et de volume V_0 suffisamment grand pour que la concentration du soluté en sortie de colonne atteigne C_0. Il est clair que cette façon de procéder n'est jamais utilisée dans la pratique mais elle permet d'appréhender le développement en tête de colonne lors de l'injection d'un créneau de concentration de grand volume.

A titre d'exemple la Fig. 5 représente le profil d'élution obtenu après une injection jusqu'à saturation de la capacité disponible Q_A de la colonne. Ce profil, qui présente deux paliers est le cas extrême observable en développement par élution. L'aire hachurée mesure la capacité disponible de la colonne Q_A relative à la concentration injectée C_0. L'isotherme de distribution à saturation (isotherme statique) représentée en trait plein sur la Fig. 6 a été déterminée point par point en fonction de C_0.

Le palier de concentration C_0 se termine au volume $V_0 + V_m$, V_m étant le volume mort de la colonne. La concentration du second palier C_p dépend de C_0

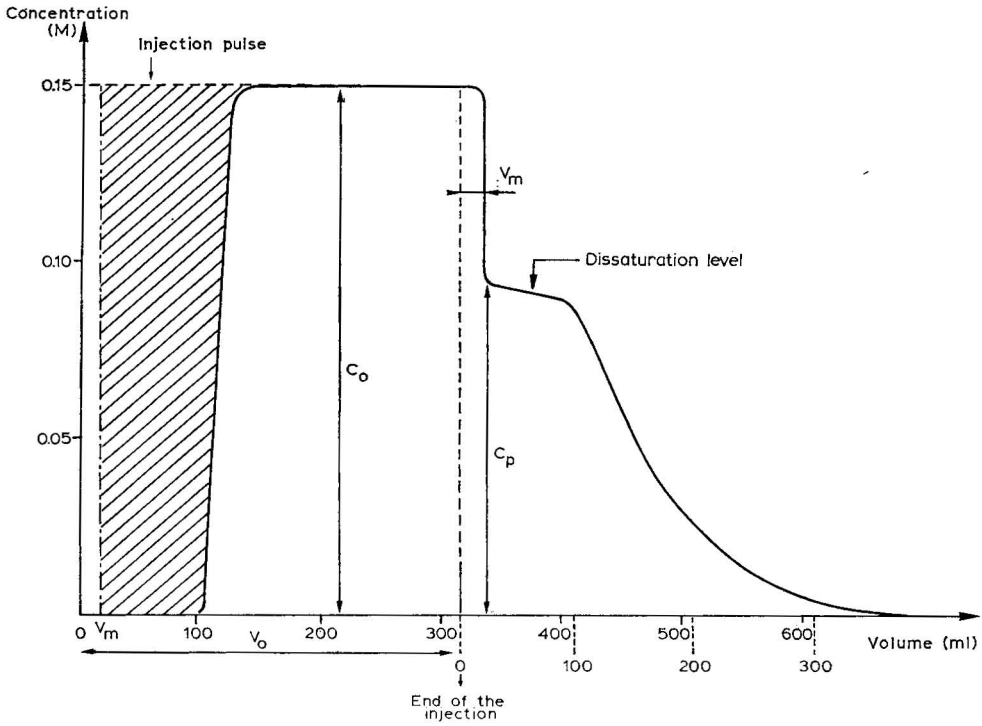

Fig. 5. Profil d'élution de la colonne saturée. L'aire hachurée représente la capacité disponible Q_A de la colonne.

comme le montre la Fig. 7. C_p est voisin de C_0 lorsque C_0 est faible et tend vers la valeur $C_m = 0.23\ M$ pour de très grandes valeurs de C_0 (environ 2 M).

Nous avons simulé ce comportement à l'aide d'un modèle des plateaux non-linéaire dont on trouvera les hypothèses et l'algorithme en annexe. La Fig. 8 représente les variations de la quantité de soluté dans la phase mobile du $p$ième plateau à un instant donné. $Q_m(p)$ est un profil isochrone. T est le nombre de transferts du modèle. L'amplitude du palier qui apparait sur l'isochrone $T = 35$ est la somme des termes d'une progression géométrique. Cette somme converge assez rapidement. Les quantités $Q_m(p)$ contenues dans la phase mobile de deux plateaux consécutifs ne différant que d'un seul terme sont pratiquement égales, d'où l'existence d'un palier de concentration qui correspond à la concentration limite de saturation C_p dans la phase mobile (voir Fig. 6, isothermes en tiretés):

$$Q_m(p) = \left(\frac{1}{1+k} + \frac{1}{(1+k)^2} + \text{---------} + \frac{1}{(1+k)^n}\right)\Delta m \cdot C_A = \frac{1}{k}\Delta m \cdot C_A = \frac{m \cdot C_A}{N \cdot k}$$

m est la masse de résine contenue dans la colonne, Δm la masse de résine par plateau, C_A la capacité disponible rapportée à l'unité de masse de phase stationnaire

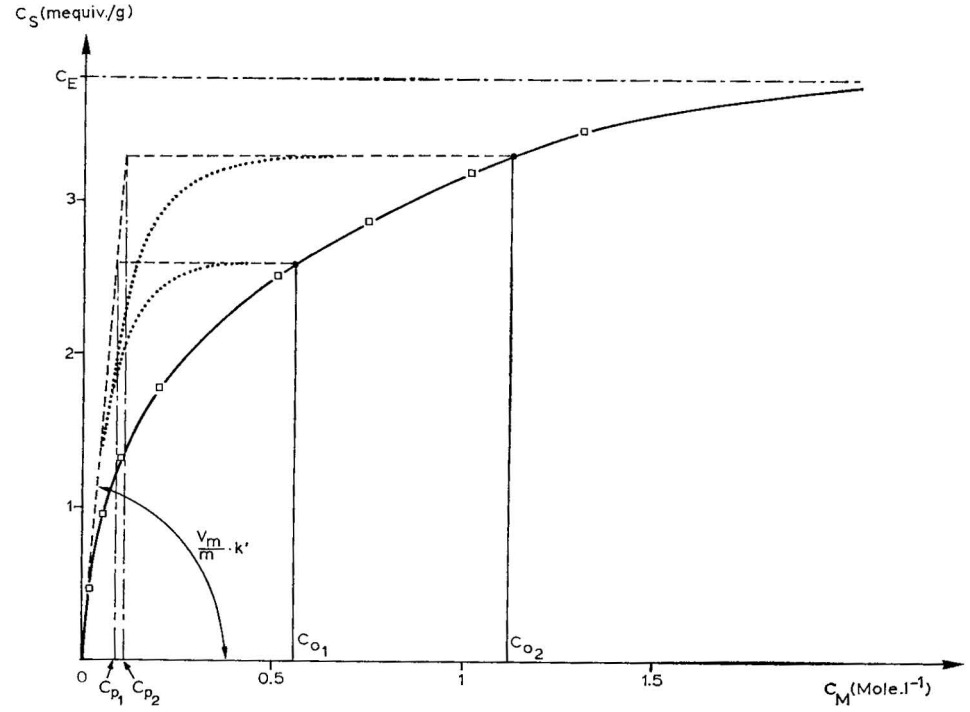

Fig. 6. Isothermes de distribution. Trait plein: isotherme expérimentale de l'anion maléate déterminée par saturation (isotherme statique). Tiretés: isothermes du modèle des plateaux décrit en annexe relatives aux concentrations injectées C_{0_1} et C_{0_2} (isothermes dynamiques). Pointillés: isothermes dynamiques, convexes avant saturation.

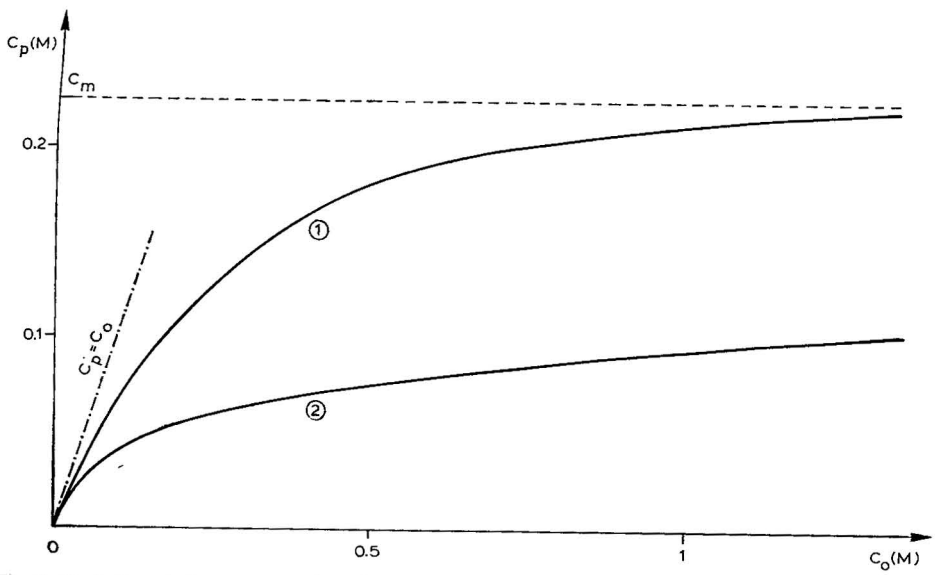

Fig. 7. Variation de la concentration C_p du palier de dessaturation en fonction de la concentration injectée C_0. 1: Courbe expérimentale; 2: $m \cdot C_A / V_m \cdot k' = f(C_0)$.

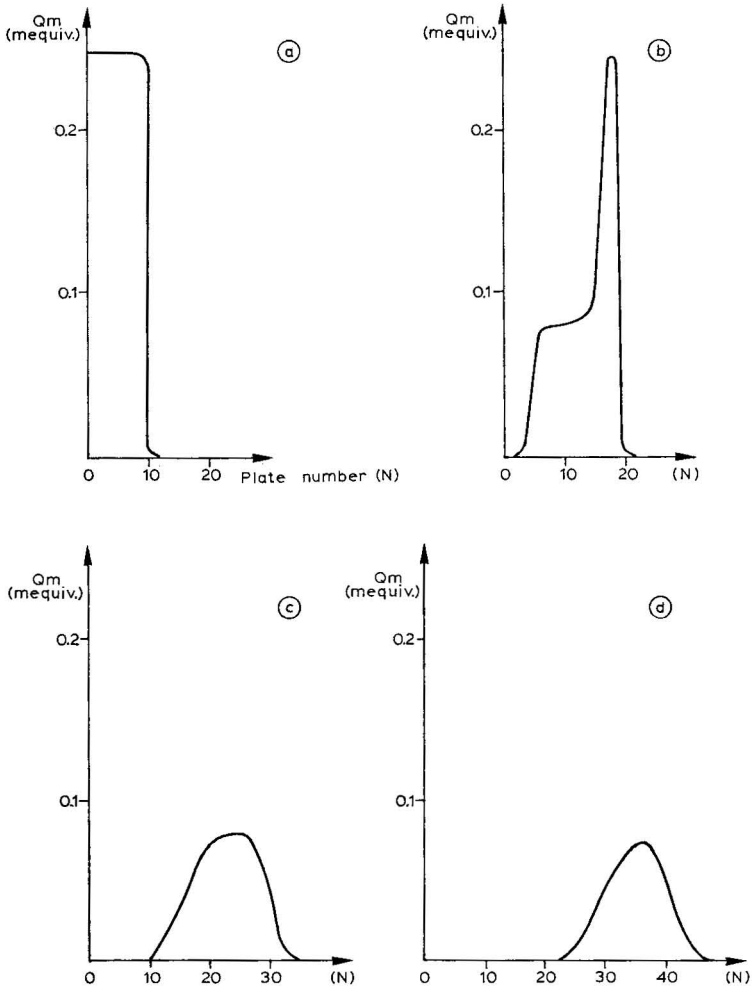

Fig. 8. Variation de la distribution du soluté à l'intérieur de la colonne au cours de son élution (courbes isochrones). a: $T = 20$; b: $T = 35$; c: $T = 100$; d: $T = 200$. T: nombre de transferts; Q_m: quantité de soluté dans la phase mobile; nombre de plateaux: $N = 60$; capacité d'échange de la colonne $Q_E = 19.2$ mequiv. $k' = 4$, $Q_0 = 5$ mequiv., $J = 20$.

et k le facteur de capacité qui varie au cours de la progression de la bande dans la colonne chromatographique. On a alors:

$$C_p = \frac{N}{V_m} Q_m(p) = \frac{m \cdot C_A}{V_m \cdot k}$$

Nous avons représenté sur la Fig. 7, en fonction de C_0, les valeurs de

$$C_p = \frac{m \cdot C_A}{V_m \cdot k}$$

calculées en prenant pour C_A les valeurs de l'isotherme statique de la Fig. 6 et pour k la valeur analytique k' du facteur de capacité. Ces calculs supposent que pour

chaque concentration injectée C_0, la distribution entre les deux phases s'effectue selon une isotherme dynamique particulière du type de celles représentées en tiretés sur la Fig. 6. La concentration calculée s'accorde bien à la concentration expérimentale jusqu'à un C_0 de 10^{-2} M. Jusqu'à cette valeur, l'isotherme est pratiquement linéaire avant la saturation et k est bien égal à k'. Au-delà, la concentration C_p calculée par le modèle est inférieure à la valeur expérimentale.

Un modèle plus adéquat consisterait à disposer d'isothermes dynamiques convexes avant la saturation, du type de celles représentées en pointillés sur la Fig. 6.

La Fig. 9 représente l'évolution des profils expérimentaux obtenus depuis l'injection analytique jusqu'à la saturation correspondant à la capacité disponible de la colonne. Concernant le comportement non-linéaire, trois types de profils sont possibles que l'on peut caractériser par le nombre de paliers qu'ils présentent: 2, 1 ou 0. Les parties arrières de tous ces profils de raccordent sur l'exponentielle déjà mentionnée.

Limite de validité du modèle. La connaissance du comportement à saturation nous permet maintenant de préciser les couples limites (V_0*, C_0*) du domaine d'injection (V_0, C_0) donnant à la sortie un profil sans palier. L'invariance de $Q_0/C_{max.}$ cesse en effet d'être vérifiée quand apparaît le palier de dessaturation C_p. Dans ce cas, $C_{max.}$ devient égal à C_p.

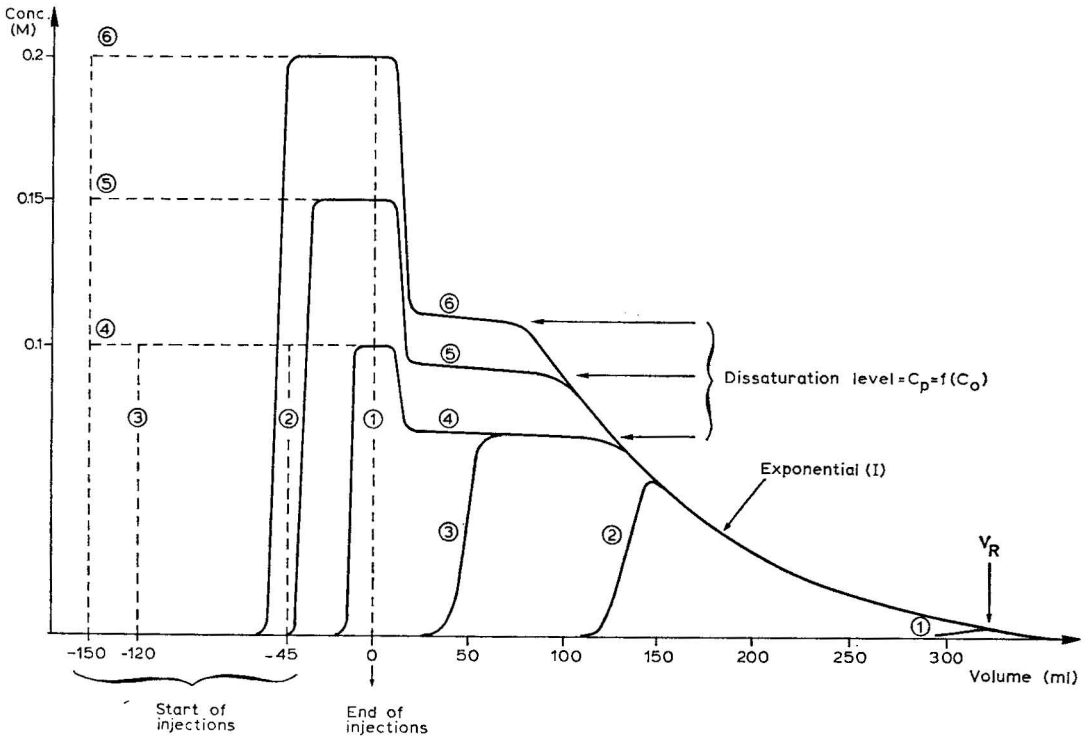

Fig. 9. Evolution expérimentale des profils d'élution non-linéaires. Tiretés: créneaux d'injection. Traits pleins: profils de sortie de colonne. 1: Injection impulsionnelle: $V_0 = 1$ ml; $C_0 = 0.1$ M. 2: $V_0 = 45$ ml; $C_0 = 0.1$ M. 3: $V_0 = 120$ ml; $C_0 = 0.1$ M. 4: $V_0 = 150$ ml; $C_0 = 0.1$ M. 5: $V_0 = 150$ ml; $C_0 = 0.15$ M. 6: $V_0 = 150$ ml; $C_0 = 0.2$ M.

Il est à noter que pour toute quantité donnée Q_0 les trois types de profils signalés plus haut sont possibles suivant les valeurs de V_0 et C_0.

Les résultats précédents permettent de déterminer les conditions à satisfaire pour le couple (V_0, C_0) de façon que le profil de sortie ne présente pas de palier.

Pour Q_0 donné: $C_0 > C_0{}^*$ (ou $V_0 < V_0{}^*$), la recherche des couples limites se fait à l'aide du schéma suivant:

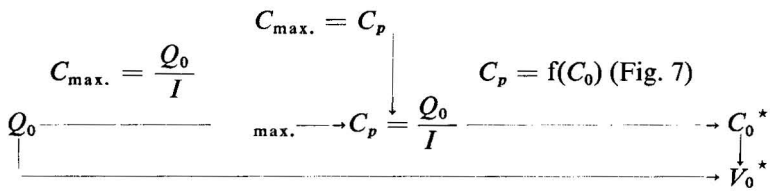

Sur le diagramme "volume–concentration injectés" (Fig. 3), l'ensemble des couples ($V_0{}^*$, $C_0{}^*$) définit la courbe B. Il est à noter que le volume $V_0{}^*$ reste inférieur à I vers lequel il tend pour les faibles concentrations injectées ($C_0 < 10^{-2}$ M). Dans ce cas en effet, $C_p \approx C_0$ et $C_{max.}$ atteint C_0 pour $V_0 = I$.

Pour un volume V_0 supérieur à I, par exemple pour les points expérimentaux no. 9 et 13 où $V_0 = 100$ ml, le palier C_p existe toujours et $Q_0/C_{max.} > I$.

Enfin, $C_{max.}$ ne peut pas dépasser la limite supérieure C_m vers laquelle tend C_p quant C_0 augmente. Les mesures à saturation (Fig. 7) donnent la valeur $C_m = 0.23$ M, en bon accord avec celle obtenue au paragraphe *Étude des profils obtenus en chromatographie préparative (Comportement non-linéaire)* à partir de l'extrapolation de l'exponentielle ajustée.

Application du modèle à la chromatographie préparative. Séparation des anions maléate et fumarate

Les résultats que nous venons de présenter sont d'une grande importance en chromatographie préparative. De ce point de vue, le profil le plus intéressant est celui qui s'étale le moins, c'est-à-dire celui qui ne présente pas de palier. Pour une séparation donnée, le schéma précédent permet de trouver la meilleure injection ($V_0{}^*$, $C_0{}^*$) relativement au compromis quantité–résolution et à la dilution apportée par la colonne chromatographique. Nous présentons ci-dessous un exemple de séparation de deux composés tel que le taux de récupération soit de 1 (résolution totale); le processus relatif au composé le moins retenu noté (1) soit linéaire; le processus relatif au composé le plus retenu (2) soit non-linéaire.

Ce cas de figure est assez fréquent. Il peut être dû aux propriétés chromatographiques des deux composés ou bien à la prédominance du composé (2) dans le mélange. De plus, nous avons noté que le seuil de non-linéarité apparaît pour une quantité injectée d'autant plus faible que le composé est plus retenu.

La Fig. 10 schématise la mise en oeuvre de la procédure que nous proposons pour un cas de séparation des acides maléique et fumarique[29]. La Fig. 10a représente le chromatogramme analytique c'est-à-dire les réponses impulsionnelles de (1) et (2). La Fig. 10b représente la séparation obtenue avec un comportement linéaire pour les deux composés lorsqu'on injecte le volume maximum $V_{0_{lin}}$ donné par l'expression (3). Notons que le modèle linéaire ne fournit aucune indication concernant la concentration maximum injectable. Celle-ci doit être déterminée expérimentalement.

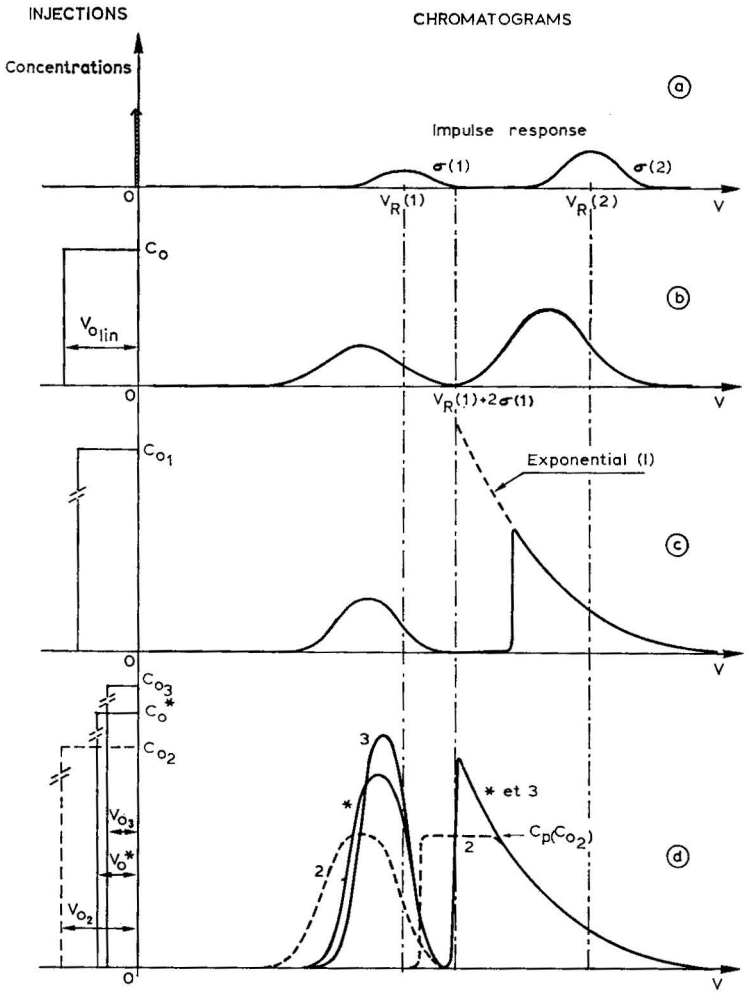

Fig. 10. Détermination de la meilleure injection pour un système préparatif donné. a: Chromatogramme analytique; b: injection optimum avec la contrainte d'un comportement linéaire; c: augmentation de la quantité injectée: comportement fortement non-linéaire du composé (2) (traînée exponentielle); d: quantité injectée $Q_0 = Q_0^*$; $C_{0_2} < C_0^*$: apparition d'un palier C_p; $C_{0_3} > C_0^*$: pas de palier. Profil (2) invariant.

Sur la Fig. 10c, le comportement non-linéaire de (2) apparaît alors que celui de (1) est toujours linéaire. Le front avant de (2) se rapproche de l'origine (fin des injections) alors que la traînée arrière reste fixe.

La quantité maximum injectable Q_0^* est définie par la contrainte du taux de recouvrement (résolution). Elle est égale à l'aire sous la traînée exponentielle de (2), limitée au point d'abscisse $V_R(1) + 2\sigma(1)$. Sur la Fig. 10d nous avons représenté les chromatogrammes obtenus avec la quantité maximum injectable Q_0^* mais avec des couples (V_0, C_0) différents. Lorsque la concentration injectée est supérieure à la valeur C_0^* précédemment définie, nous obtenons toujours sensiblement le même profil

pour le composé (2) (Fig. 10d, cas no. 3). Lorsque C_0 est inférieur à C_0*, il y a apparition du palier qui provoque un décalage important du front avant, ce qui fait chuter la résolution. La condition: $C_0 > C_0$* est donc nécessaire pour obtenir une séparation optimale.

En résumé, le profil de sortie du composé (1) est prévisible en utilisant le principe de superposition puisque le comportement est linéaire. Le profil du composé (2) se déduit d'une ou deux expériences telles que celles schématisées sur la Fig. 10c.

D'autre part, l'étude du raccordement des profils arrières sur la ligne de base que nous avons présentée plus haut permet de définir la période minimum entre deux injections.

Rappelons qu'en chromatographie préparative linéaire, cette période minimum θ est donnée par l'expression:

$$\theta = \frac{V_R(2) - V_R(1) + V_0 + 2[\sigma(1) + \sigma(2)]}{D}$$

où D est le débit constant de la phase mobile. L'indice 1 est relatif au composé le moins retenu et l'indice 2 au composé le plus retenu.

Dans le cas de la séparation non-linéaire que nous présentons, les propriétés relevées à propos du raccordement des profils non-linéaires montrent que l'expression précédente reste valable. Ainsi, la période des injections ne se trouve pas augmentée par le comportement non-linéaire du composé (2).

CONCLUSION

L'influence de la quantité injectée sur la forme des profils d'élution a été étudiée systématiquement et particulièrement dans le domaine de comportement non-linéaire du processus chromatographique. Les propriétés mises en évidence ont permis l'élaboration d'un modèle simple de représentation externe non-linéaire. Pour un processus donné, l'estimation des deux paramètres définissant le modèle nécessite peu d'expériences. Ce modèle rend possible l'optimisation d'une séparation préparative lorsque le chromatographiste désire s'affranchir des limitations imposées par un comportement linéaire.

Il serait évidemment intéressant de transposer les résultats de cet article, obtenus en échange d'ions, aux autres types de chromatographie et en particulier aux chromatographies d'adsorption et de partage, ce que nous sommes en train de réaliser.

ANNEXE

Détermination des profils d'élution par simulation numérique

Le modèle théorique choisi suppose que le fonctionnement de la colonne est identique à celui d'une colonne fictive à plateaux. L'isotherme de distribution est linéaire jusqu'à la saturation de la capacité disponible $C_A = Q_A/m$ (en mequiv./g) de la phase stationnaire (voir Fig. 6). Celle-ci est atteinte pour une concentration C_p dans la phase mobile.

Soient $Q(p,T)$ la quantité totale de soluté dans le plateau p après T transferts, m et s les indices désignant les phases mobile et stationnaire et k le facteur de

capacité du soluté. S'il n'y a pas saturation, le calcul de la répartition du soluté dans chaque plateau et pour chaque transfert se fait par l'algorithme suivant:

$$Q_m(p,T) = Q_m(p-1, T-1) + Q_s(p, T-1)$$

$$Q_m(p,T) = \frac{1}{1+k} Q(p,T)$$

$$Q_s(p,T) = \frac{k}{1+k} Q(p,T)$$

S'il y a saturation, la répartition se fait ainsi:

$$Q_s(p,T) = \Delta m \cdot C_A$$
$$Q_m(p,T) = Q(p,T) - \Delta m \cdot C_A$$

Δm est la masse de résine par plateau. La quantité injectée Q_0 est introduite sur le premier plateau de façon discontinue en J fractions q_0, pendant les $J-1$ premiers transferts.

Ainsi, les paramètres du modèle sont la capacité disponible C_A et le facteur de capacité k.

RÉSUMÉ

Certaines propriétés des systèmes linéaires, utiles en chromatographie préparative, sont présentées. La déformation des profils d'élution d'un soluté unique a été étudiée systématiquement en fonction du volume et de la concentration injectés. Ces profils sont représentés par leurs premiers moments. Cette représentation a l'avantage de faciliter le contrôle de la linéarité du comportement du processus chromatographique. A cet effet, un test fondé sur la déconvolution est proposé.

Une attention particulière est ensuite accordée au comportement fortement non-linéaire du processus. Des propriétés remarquables ont été mises en évidence à partir d'expériences systématiques en échange d'ions. Ces propriétés ont permis l'élaboration d'un modèle dont le domaine de validité est discuté. Ce modèle est d'un grand intérêt pour la commande automatique en chromatographie préparative non-linéaire. Un exemple est présenté dans le cas particulier de la séparation de deux composés.

REMERCIEMENTS

Les auteurs remercient MM. les professeurs R. Rosset et G. Fournet, de l'École Supérieure de Physique et Chimie Industrielles de la ville de Paris, ainsi que M. le professeur G. Guiochon, de l'École Polytechnique et M. P. Bertrand, Maitre de Recherches au C.N.R.S. pour les utiles discussions qu'ils ont eues avec eux.

BIBLIOGRAPHIE

1 F. E. Rickett, *J. Chromatogr.*, 66 (1972) 356–360.
2 D. W. Lamson, A. F. W. Coulson et T. Yonetani, *Anal. Chem.*, 45 (1973) 2273–2276.
3 M. T. Jackson, *Chromatogr. Reviews (Spectra-Physics)*, 1 (1975) 2.

4 C. R. Scholfield, *Anal. Chem.*, 47 (1975) 1417–1420.
5 T. F. Gabriel, J. Michalewsky et J. Meienhofer, *J. Chromatogr.*, 129 (1976) 287–293.
6 J. D. Warthen Jr., *J. Chromatogr. Sci.*, 14 (1976) 513–515.
7 J. C. Suatoni et R. E. Swab, *J. Chromatogr. Sci.*, 14 (1976) 525–537.
8 D. Maysinger, C. S. Marcus, W. Wolf, M. Tarle et J. Casanova, *J. Chromatogr.*, 130 (1977) 129–138.
9 R. G. Berg et H. M. McNair, *J. Chromatogr.*, 131 (1977) 185–190.
10 R. R. Heath, J. H. Tumlinson, E. E. Doolittle, *J. Chromatogr. Sci.*, 15 (1977) 10–13.
11 J. W. Ashley Jr., C. N. Reilly et G. P. Hildebrand, *Anal. Chem.*, 34 (1962) 1198–1213.
12 J. W. Ashley Jr., G. P. Hildebrand et C. N. Reilly, *Anal. Chem.*, 36 (1964) 1369–1371.
13 J. C. Sternberg, *Advan. Chromatogr.*, 2 (1966) 205–270.
14 K. Yamaoka et T. Nakagawa, *Anal. Chem.*, 47 (1975) 2050–2053.
15 K. de Clerk et T. S. Buys, *J. Chromatogr.*, 63 (1971) 193–202.
16 A. I. Kalinichev, A. Pronin, P. P. Zolotarev, N. A. Goryacheva, K. V. Chmutov and V. Ya. Filimonov, *J. Chromatogr.*, 120 (1976) 249–256.
17 B. Roz, R. Bonmati, G. Hagenbach, P. Valentin et G. Guiochon, *J. Chromatogr. Sci.*, 14 (1976) 367–380.
18 J. P. Lefevre, *Thèse*, Paris, 1974.
19 J. H. Knox et J. F. Parcher, *Anal. Chem.*, 41 (1969) 1599–1606.
20 H. C. Beachell et J. J. de Stefano, *J. Chromatogr. Sci.*, 10 (1972) 481–486.
21 J. J. de Stefano et H. C. Beachell, *J. Chromatogr. Sci.*, 10 (1972) 654–662.
22 P. A. Bristow et J. H. Knox, *Chromatographia*, 10 (1977) 279–289.
23 C. R. Wilke et P. Chang, *Amer. Inst. Chem. Engr. J.*, 1 (1955) 264.
24 L. R. Snyder, *Anal. Chem.*, 39 (1967) 698–704.
25 K. Yamaoka et T. Nakagawa, *J. Phys. Chem.*, 79 (1975) 522–525.
26 B. L. Karger, M. Martin et G. Guiochon, *Anal. Chem.*, 46 (1974) 1640–1647.
27 J. N. Done, *J. Chromatogr.*, 125 (1976) 43–57.
28 H. M. McNair et W. M. Cooke, *J. Chromatogr. Sci.*, 10 (1972) 27–30.
29 P. Gareil, L. Personnaz et M. Caude, *Analusis*, 7 (1979) 401–407.

Journal of Chromatography, 192 (1980) 75–87

CHROM. 12,589

TOROIDAL COIL PLANET CENTRIFUGE FOR COUNTER-CURRENT CHROMATOGRAPHY

YOICHIRO ITO

Laboratory of Technical Development, National Heart, Lung and Blood Institute, Bethesda, Md. 20205 (U.S.A.)

(Received November 1st, 1979)

SUMMARY

A simple tabletop model of a versatile counter-current chromatographic system is introduced. The apparatus compactly holds a long coiled column around a drum-shaped holder. The acceleration produced by the synchronous planetary motion of the holder enables stable retention of the stationary phase in each helical turn of the coil while the mobile phase is continuously eluted through the column. The capability of the method was demonstrated on separations of DNP amino acids and oligopeptides using typical two-phase solvent systems. The present method will provide a universal application of solvent systems including aqueous–aqueous polymer phase systems used for partition of cell particles and macromolecules.

INTRODUCTION

The toroidal coil planet centrifuge[1] is one of a family of synchronous coil planet centrifuges that provide a particular mode of planetary motion to a coiled tube for performing counter-current chromatography. The greatest advantage of this present scheme over other counter-current chromatographic schemes[2–4] is that it has the capability of producing a strong centrifugal force field which provides a stable retention of the stationary phase for various two-phase solvent systems in a narrow-bore coiled tube. The apparatus holds a long narrow-bore coiled tube around its large diameter drum-shaped column holder in a coiled helix configuration. The holder undergoes a synchronous planetary motion of one rotation (around its own axis) during one revolution (around the central axis of the centrifuge) in the same directions. This planetary motion allows continuous elution of the solvent through the coiled separation column without the use of rotating seals[3]. Analysis of the acceleration field acting on the column shows that the acceleration vector is always directed inwardly from the periphery of the column holder to retain one of the phases stationary in each turn of the coil while the other phase is continuously eluted through the column. The acceleration vector also undulates in both magnitude and direction during each revolutional cycle to provide efficient mixing of the two phases. Consequently, solutes locally introduced at the inlet of the column are

subjected to an efficient partition process in each turn of the coil and are eluted out according to their partition coefficients as in liquid chromatography but in the absence of solid supports.

A brief introduction of the toroidal coil planet centrifuge has been given earlier[1]. In the present paper the principle of the method is elucidated by the aid of the analysis of acceleration and the performance characteristics of the apparatus is demonstrated by separations of dinitrophenyl (DNP) amino acids and oligopeptides using conventional two-phase solvent systems.

PRINCIPLE AND ANALYSIS OF ACCELERATION FIELD

Fig. 1A schematically illustrates the principle of the toroidal coil planet centrifuge. A large cylindrical coil holder is connected to the planetary gear which rolls around an identical stationary sun gear (shaded) mounted on the central axis of the centrifuge. With this gear arrangement the holder revolves around the central axis (axis of revolution) of the apparatus and simultaneously rotates about its own axis (axis of rotation) at the same angular velocity in the same direction. A pair of flow tubes from the coiled column first exits the holder at the axis of rotation, forms a loop to reach the axis of revolution, and then passes through the center of the stationary sun gear as illustrated in the figure. These tubes are tightly supported at the center of the sun gear. As reported earlier[3], the rolling action of the planetary gear around the stationary sun gear cancels out any revolutional effect, therefore the flow tubes are free of twisting at any arbitrary revolutional rate.

In order to comprehend the acceleration field produced in the present scheme, it is necessary to review the analysis previously made on the horizontal flow-through coil planet centrifuge[3,5]. This has a long, thin column holder but with the identical mode of planetary motion. For an analysis of acceleration, Fig. 1A may be reduced to a simple coordinate system shown in Fig. 1B where the axis of revolution is located at point 0. For the convenience of analysis, the coordinate system is selected in such a way that both the axis of rotation (Q_0) and the arbitrary point (P_0) on the holder start on the x-axis as illustrated. After time t, the location of the arbitrary point, P (x,y), is expressed by

$$x = R\cos\theta + r\cos 2\theta \tag{1}$$

$$y = R\sin\theta + r\sin 2\theta \tag{2}$$

where $R = \overline{Q_0}$, the radius of revolution; $r = \overline{PQ}$, the radius of rotation; $\theta = \omega t$; ω denotes the angular velocity of revolution. The magnitude of acceleration, α, is derived from these equations as

$$\alpha = \{(d^2x/dt^2)^2 + (d^2y/dt^2)^2\}^{\frac{1}{2}} = R\omega^2(1 + 16\beta^2 + 8\beta\cos\theta)^{\frac{1}{2}} \tag{3}$$

acting at the angle, γ_x, relative to the x-axis, *i.e.*,

$$\gamma_x = \pi + \tan^{-1}\{(d^2y/dt^2)/(d^2x/dt^2)\} = \pi + \tan^{-1}\frac{\sin\theta + 4\beta\sin 2\theta}{\cos\theta + 4\beta\cos 2\theta} \tag{4}$$

where $\beta = r/R$ provided $R \neq 0$.

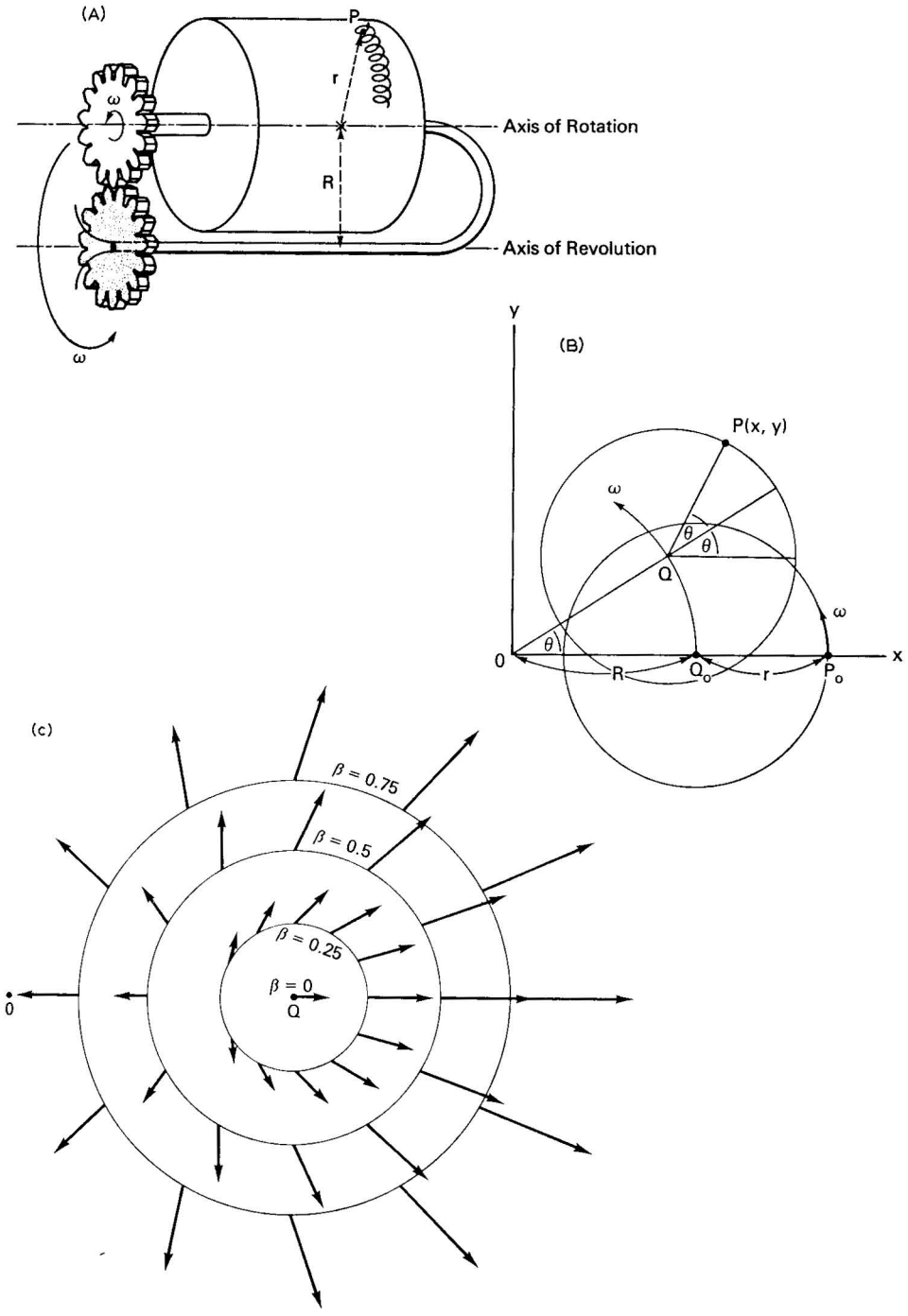

Fig. 1. (A), Principle of the toroidal coil planet centrifuge. (B), Coordinate system for analysis of acceleration. (C), Distribution pattern of the relative centrifugal force vector at various locations of the holder.

For ease of visualizing and further analyzing this undulating acceleration vector, the acting angle may be more conveniently expressed with respect to the rotating holder. Thus, the angle, γ, formed at the arbitrary point P relative to the rotational radius, PQ, is computed from eqn. 4 as

$$\gamma = \gamma_x - 2\theta - \pi = \tan^{-1}\{(-\sin\theta)/(4\beta + \cos\theta)\} \quad (5)$$

Using eqns. 3 and 5, the relative centrifugal vectors acting at various locations on the holder can be obtained and expressed as sets of arrows as shown in Fig. 1C.

Three circles centered at Q correspond to β values of 0.25, 0.5 and 0.75 as labelled while point Q, the center of rotation, is at $\beta = 0$. A set of arrows around each circle indicates the distribution pattern of the centrifugal force field at a given moment. It is important to note that the arbitrary point on the holder experiences these vectors in sequence during each revolutional cycle.

As clearly shown in the figure, when $\beta > 0.25$, the vector is always directed outwardly from the circle. The vector also undulates in its relative magnitude and direction according to the location on the holder at given β values. As the β value increases, the magnitude of the relative centrifugal force vector becomes greater while the amplitude of angular oscillation around the axis of rotation is reduced. This distribution pattern of the force vector provides a great advantage when the scheme is used for performing counter-current chromatography.

When a coiled tube is mounted around the holder, each helical turn of the column is exposed to the above centrifugal force field which separates two liquid phases in such a way that the heavier phase occupies the outer half and the lighter phase, the inner half of each coil unit. Angular undulation of the force vector efficiently mixes the interface and the two phases in each turn of the coil to reduce the mass transfer resistance. Consequently, solutes introduced locally at the inlet of the column are subjected to an efficient partition process and separated according to their relative partition coefficients as in liquid partition chromatography but without the use of solid supports.

The results of these analysis disclose a versatile feature of the present scheme. The use of two-phase solvent systems having extremely low interfacial tension requires a strong centrifugal force field combined with a small amplitude of angular oscillation to provide satisfactory retention of the stationary phase. Elution with a high interfacial tension phase system through a small-bore column also necessitates application of a strong centrifugal force field to overcome the tendency of plug flow which would cause carryover of the stationary phase. The operational conditions to meet such requirements can be attained in the present scheme simply by increasing the β value of the holder. Thus the present scheme permits universal application of the two-phase solvent systems including aqueous–aqueous polymer phase systems used for partition of macromolecules and cell particles[6].

The present scheme provides an additional advantage in its mechanical design. Because the large drum-shaped holder compactly holds a long coiled column, the length of the column holder shaft can be reduced so that the distortion of the shaft under a strong centrifugal force field is minimized. This allows operation at a high revolutional speed without imposing an excessive strain on the bearings supporting the column holder shaft. Furthermore, the effective force field acting on

the column mounted at the periphery of the holder is far greater than the force acting at the axis of the holder as illustrated in Fig. 1C. Thus, the present design is capable of producing a centrifugal force field of several hundred g which can retain even small cell particles suspended in a saline solution within the column.

Design of the apparatus

Fig. 2A shows a photograph of our prototype. The rotary frame consists of a pair of circular aluminum plates rigidly bridged with multiple aluminum links and is driven by a motor (ElectroCraft) around the stationary pipe mounted on the central axis of the centrifuge. The rotary frame holds a pair of cylindrical holders symmetrically spaced at a distance of 10 cm from the central axis of the apparatus. The holder having the coiled column is 15 cm in diameter ($\beta = 0.75$) while the other holder with a counterweight, 10 cm in diameter ($\beta = 0.5$). Each coil holder is equipped with a plastic gear (Winfred M. Berg, Inc.) which is engaged to an identical stationary gear mounted on the central stationary pipe. With this gear arrangement, each holder undergoes the desired planetary motion illustrated in Fig. 1A, *i.e.*, revolution around the central axis of the apparatus and rotation about its own axis at the same angular velocity in the same direction. In order to mechanically stabilize the centrifuge system, a short coupling pipe is coaxially mounted on the free end (right side) of the rotary frame while the other end of the coupling pipe is supported by the wall of the outside enclosure of the apparatus through a ball bearing.

The coiled separation column is prepared by winding PTFE tubing (Zeus Industrial Products, Raritan, N.J., U.S.A.) onto a flexible core which is again coiled around the holder to form a coiled helix configuration as shown in Fig. 2B. A counterweight is applied to the other holder to balance the centrifuge. The flow tubes from the separation column are first passed through the center hole of the column holder shaft and then led into the coupling pipe through a side hole to enter the opening of the stationary pipe. The flow tubes pass through the central stationary pipe and emerge at the left side of the centrifuge enclosure. These flow tubes are thoroughly lubricated with silicone grease and also protected with a piece of plastic tubing at each supported portion to prevent direct contact against metal parts. When this protection is provided, the flow tubes can maintain their function almost permanently. The revolutional speed of the prototype is continuously adjustable up to 1000 rpm (450 *g*) with a Motomatic speed control unit (ElectroCraft).

A Chromatronix Cheminert metering pump was used for elution of the solvent and an LKB Uvicord III for monitoring the absorbance at 280 nm.

Studies on partition capabilities of the apparatus

As in other counter-current chromatographic schemes, the performance of the present apparatus relies upon retention of the stationary phase and efficiency of solute partitioning between the two solvent phases in the coiled column. In order to determine the optimum operational conditions, a series of experiments were performed to study the degree of stationary phase retention and partition efficiency in short coiled columns under various revolutional speeds and flow-rates.

Two types of coiled columns were prepared each from a 7 m long, 0.55 mm I.D. PTFE tube by winding it onto a flexible nylon core of different diameters. One

Fig. 2. (A), Overall view of the apparatus. (B), Coiled separation column mounted on the holder.

column had a core diameter of 5 mm and the other column, 1.5 mm. In both columns, the total capacity measured was approximately 2 ml. These columns were mounted on the column holder having β value of 0.75.

In the present study, two typical phase systems were selected, chloroform–acetic acid–0.1 *N* hydrochloric acid (2:2:1) for partition of DNP-amino acids and *n*-butanol–acetic acid–water (4:1:5) for partition of oligopeptides (figures in the parentheses indicate the volume ratios of the solvents). For each phase system a pair of samples with suitable partition coefficients were selected: N-DNP-L-glutamic acid and N-DNP-L-alanine for the chloroform phase system; L-valyl-L-tyrosine and L-tryptophyl-L-tyrosine for the *n*-butanol phase system. The DNP-amino acid sample mixture was prepared by dissolving each component in the aqueous phase at 0.5 g% and 10 μl of this solution was charged in each separation. The dipeptide sample mixture was similarly prepared to make final concentration of 1 g% for L-valyl-L-tyrosine and 0.3 g% for L-tryptophyl-L-tyrosine and 20 μl was applied in each run.

In each separation the column was first filled with the stationary phase followed by sample injection through the sample port. Then the column was eluted with the mobile phase while the apparatus was run at the desired revolutional speed. The eluate was continuously monitored through an LKB Uvicord III at 280 nm and then collected into a graduated cylinder to measure the volume of the stationary phase eluted from the column. The percentage retention of the stationary phase relative to the total column capacity can be obtained from the eluted stationary phase volume, V_s, the total column capacity, V_c, and the free space in the flow path, V_f, by

$$\text{Retention}\,(\%) = 100\,(V_c + V_f - V_s)/V_c \tag{6}$$

Figs. 3A and B summarize the data for retention of the stationary phase under various operational conditions. In each diagram, the retention is plotted against the applied revolutional speed at two different flow-rates. The retention of near 50% is ideal but that over 30% is considered to be satisfactory if the inclination of the curve is relatively small. Operation at the near horizontal portion of the curve insures minimum carryover of the stationary phase even if there are shifts of revolutional speed. The overall results indicate that the satisfactory level of retention is obtained over a wide range of revolutional speeds and flow-rates for both solvent systems. The 5-mm core column gives a slightly higher level of retention than the 1.5-mm core column. Because of the solvent–wall interaction in a narrow-bore tube, the non-aqueous phase having an affinity to the PTFE tube gives substantially higher level of retention than the aqueous phase under a given set of operational conditions. The retention levels of the *n*-butanol phase system (Fig. 3B) is generally lower than those of chloroform phase system (Fig. 3A) due to its higher viscosity and the smaller difference in density between the two phases. Satisfactory retention levels obtained from these typical phase systems with contrasting physical properties suggest that the present method permits universal application of the two-phase solvent systems.

Fig. 4A summarizes the results of DNP-amino acid separations with both 5-mm and 1.5-mm core columns performed at revolutional speeds ranging between

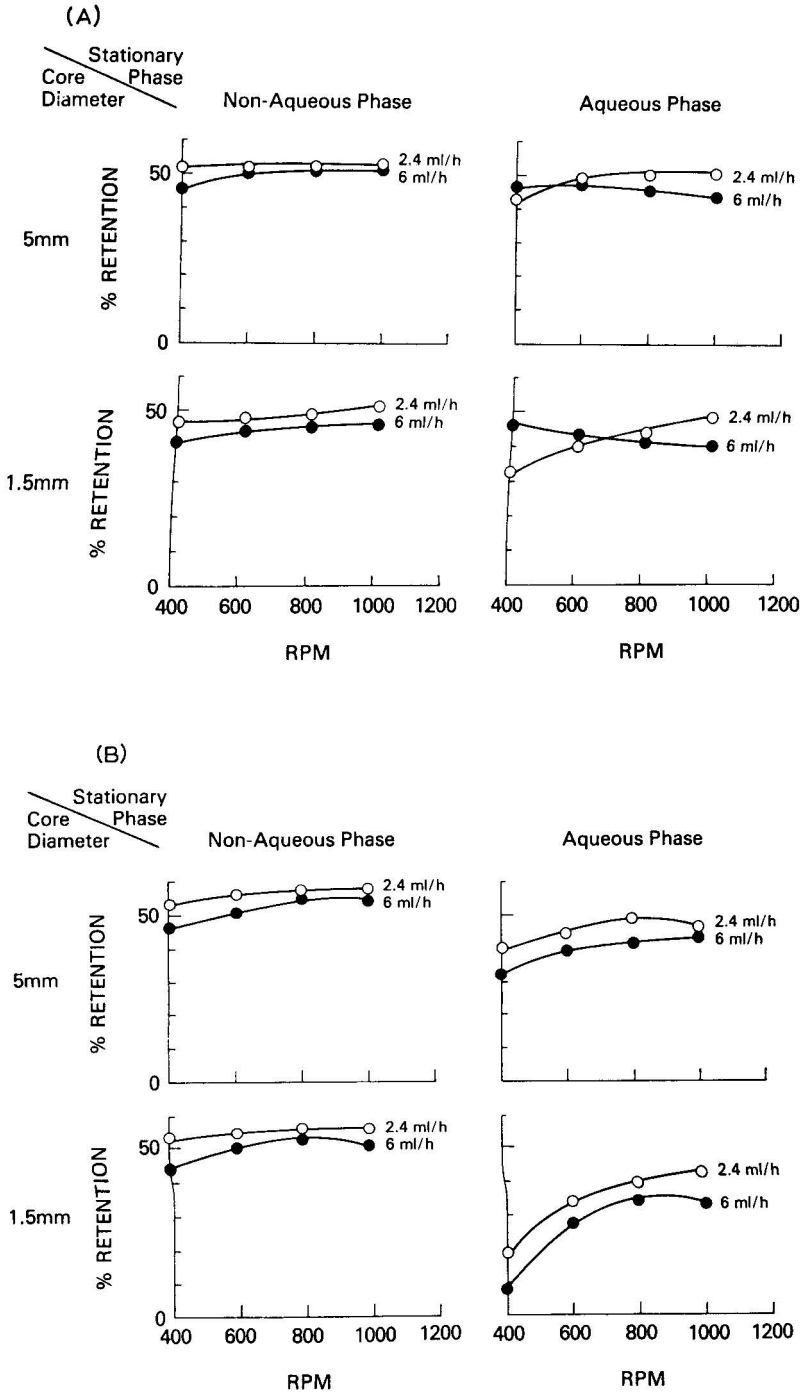

Fig. 3. (A), Retention of the stationary phase of the chloroform phase system in both 5-mm and 1.5-mm core columns. (B), Retention of the stationary phase of the *n*-butanol phase system in both 5-mm and 1.5-mm core columns.

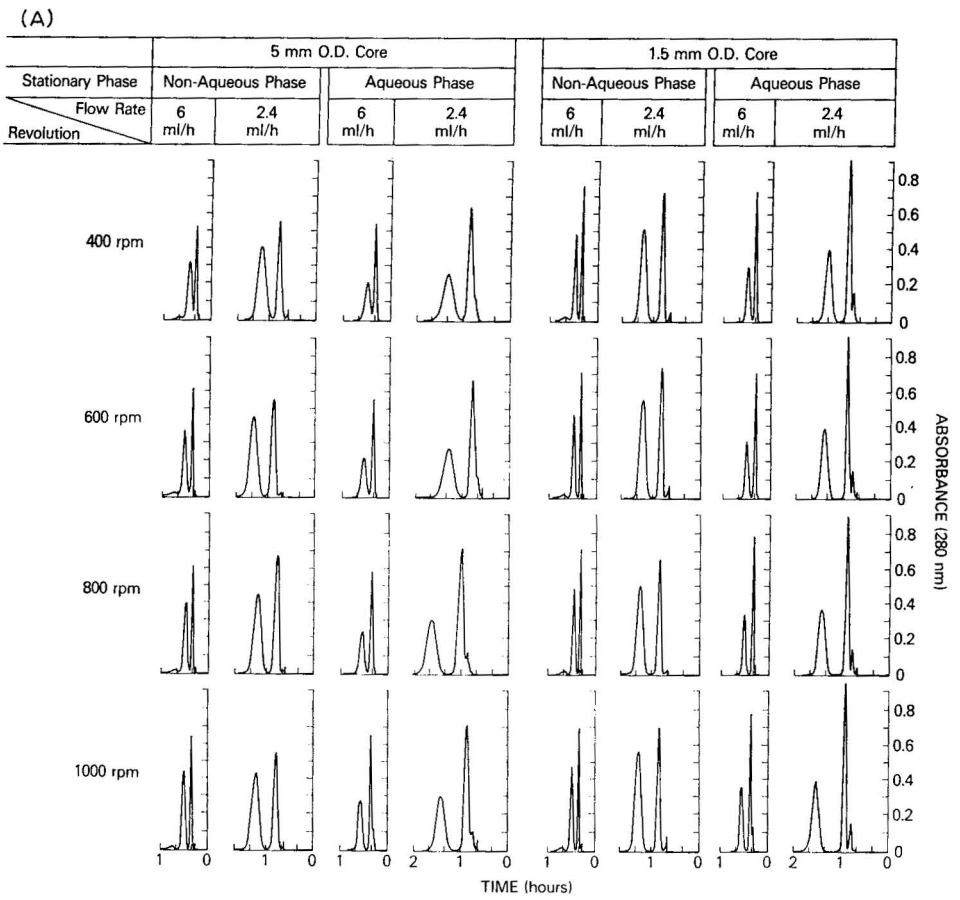

Fig. 4.

(Continued on p. 84)

400 and 1000 rpm. Flow-rates of 6 and 2.4 ml/h were applied using both non-aqueous and aqueous phases as the stationary phase. In each chromatogram, partition efficiency can be easily estimated by observing the degree of peak resolution and, if desired, expressed in terms of the number of theoretical plates using the conventional equation

$$N = (4R/w)^2 \tag{7}$$

where R denotes the retention time and w the peak width.

Overall results indicate that the 1.5-mm core column yields higher peak resolution than the 5-mm core column. Although good peak resolutions are given at 6 ml/h flow-rate in short periods of time, the highest partition efficiency is obtained at 2.4 ml/h flow-rate under revolutional speeds of 600 to 1000 rpm.

Fig. 4B similarly summarizes the results of the oligopeptide separation. Here again the peak resolution obtained by the 1.5-mm core column generally exceeds that obtained by the 5-mm core column. Poor peak resolution observed at 6 ml/h under

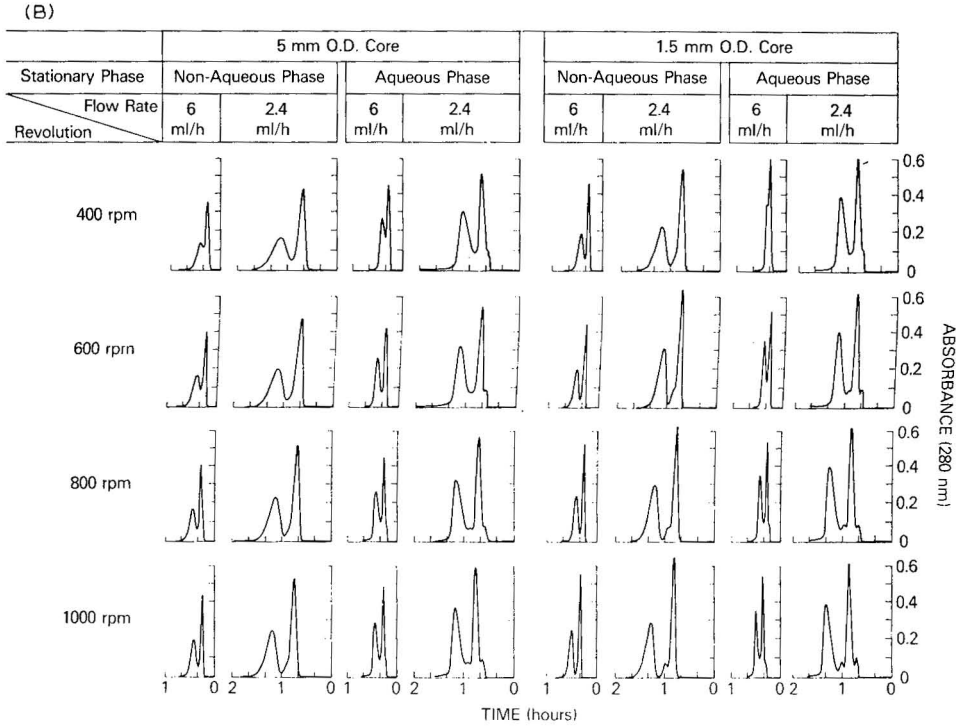

Fig. 4. (A), Effects of the revolutional speeds and flow-rates on the separations of DNP-amino acids with the chloroform phase system. (B), Effects of the revolutional speeds and flow-rates on the separations of dipeptides with the *n*-butanol phase system.

400 rpm was apparently caused by a low retention level of the stationary phase as seen in Fig. 3B. The best results are obtained by the 1.5-mm core column at 2.4 ml/h under 800 to 1000 rpm, where impurities present in the sample solution are partly resolved from the major peaks.

Separation of DNP-amino acids and peptides with a long column

The present method was applied for separation of DNP-amino acids and oligopeptides using a long coiled column. The separation column was prepared from a 50 m × 0.55 mm I.D. PTFE tube by winding it onto a 13 m × 1.5 mm O.D. nylon pipe to make approximately 8500 helical turns with a total capacity of about 18 ml. The column was mounted on the column holder with $\beta = 0.75$.

Suitable sets of samples were selected each from DNP-amino acids (Sigma, St. Louis, Mo., U.S.A.) and oligopeptides (Sigma) for separation with the two-phase solvent systems used in the previous experiments. The DNP-amino acid mixture was prepared by dissolving a set of samples in the aqueous phase to make a concentration of each component at 0.1 to 0.4 g%. The oligopeptide sample mixture was similarly prepared to bring the final concentration of each component at 0.05 to 0.6 g%.

In each separation, the column was first filled with the stationary phase and

50 μl of the above sample solution was injected through the sample port. Then the mobile phase was pumped into the column at a flow-rate of 2.4 ml/h while the apparatus was run at revolutional speeds ranging between 400 and 600 rpm. The eluate was continuously monitored with an LKB Uvicord III at 280 nm.

Fig. 5A shows a chromatogram obtained from a set of DNP amino acids by eluting with the aqueous phase under a revolutional speed of 400 rpm. All components were well resolved as symmetrical peaks and eluted out in 18 h. Fig. 5B shows a similar chromatogram obtained by elution with the non-aqueous phase. Partition efficiencies of these separations estimated from eqn. 7 range between 6000 and 2000 theoretical plates. Fig. 6A shows a chromatogram of oligopeptides obtained by eluting with the aqueous phase. Because of the non-linear distribution isotherm of

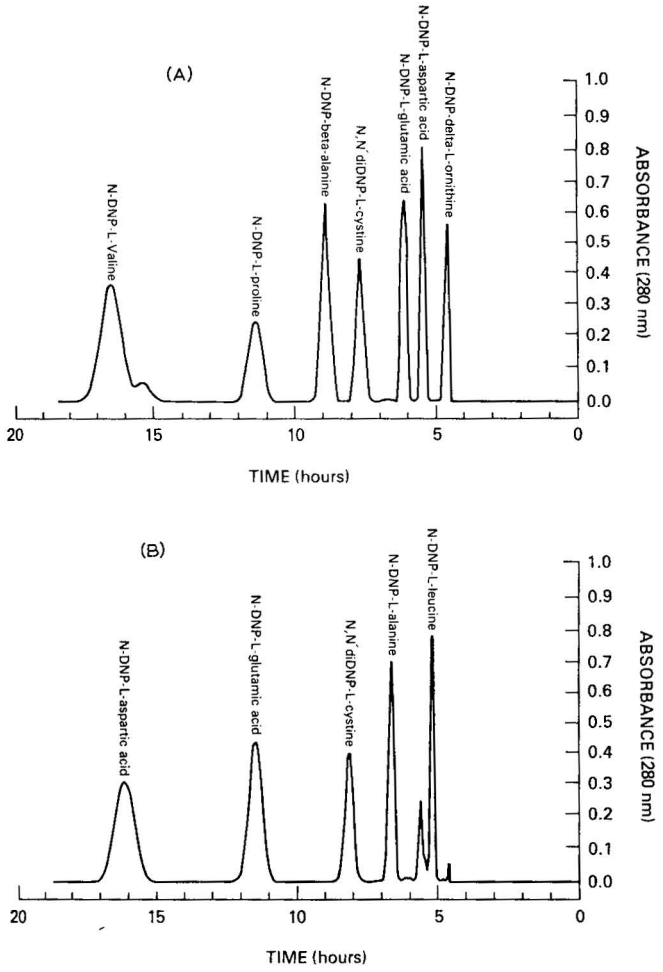

Fig. 5. Separations of DNP-amino acids with a long coiled column. Column: 0.55 mm I.D., 18 ml capacity, $\beta = 0.75$; solvent system: chloroform–acetic acid–0.1 N hydrochloric acid (2:2:1); sample volume: 50 μl; revolution: 400 rpm; flow-rate: 2.4 ml/h. (A), Chromatogram obtained by eluting with the aqueous phase. (B), Chromatogram obtained by eluting with the non-aqueous phase.

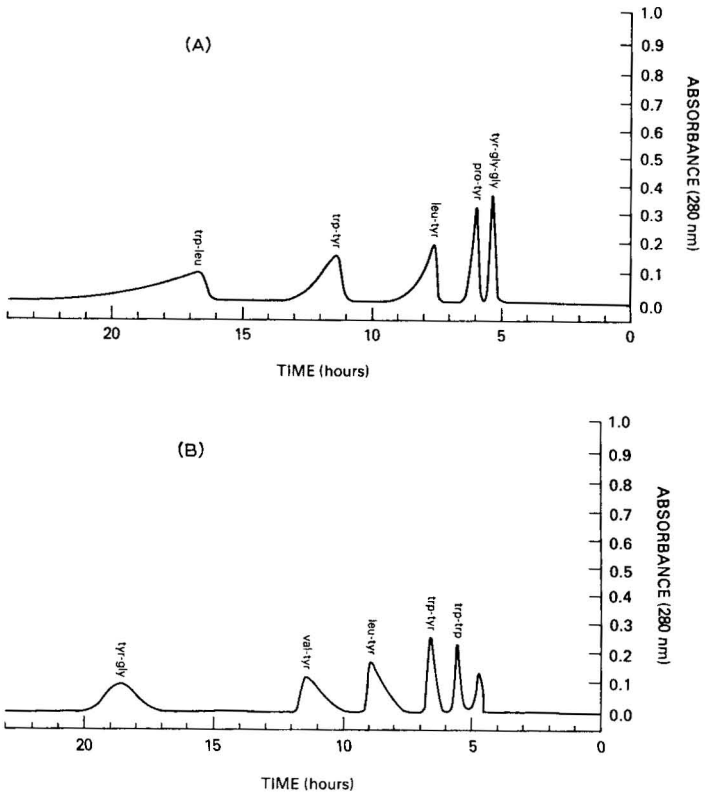

Fig. 6. Separations of oligopeptides with a long coiled column. Solvent system: *n*-butanol–acetic acid–water (4:1:5); revolution: 600 rpm; other conditions as in Fig. 5. (A), Chromatogram obtained by eluting with the aqueous phase. (B), Chromatogram obtained by eluting with the non-aqueous phase.

the samples in the *n*-butanol phase system, peaks show intensive skewing. The shape of this skewing is reversed when the samples are eluted with the non-aqueous phase as shown in Fig. 6B. The degree of skewing will be decreased as the sample concentration is reduced. As expected from the results of the previous studies, partition efficiency of the oligopeptide separation is lower than that in the DNP-amino acid separation mainly due to the higher viscosity of the normal butanol phase system. Partition efficiencies of these oligopeptide separations range between 3000 and 300 theoretical plates.

These chromatograms were obtained under the revolutional speeds considerably below the optimum ranges determined by the previous studies. The use of a long coiled column causes a pressure build-up in the column which could exceed the maximum capacity of the Chromatronix pump rated at 500 p.s.i. This limited the operation from 400 to 600 rpm to maintain a safety pressure range below 400 p.s.i. However, the PTFE tube used in the column can hold much higher pressures and, therefore, the use of a metering pump with a higher pressure capacity would yield substantially better resolution by allowing higher revolutional speeds.

CONCLUSIONS

The toroidal coil planet centrifuge is a compact tabletop model suitable for laboratory use. Because of the use of the unique pattern of the centrifugal force field together with the stable mechanical design, the method allows universal applications of two-phase solvent systems to yield highly efficient chromatographic separations of solutes which are comparable to those obtainable by a refined liquid chromatography. The method offers a great advantage over liquid chromatography in that the separation is performed under the absence of solid support, hence eliminates all complications caused by the adsorption effects such as a sample loss, contamination and tailing of the solute peaks.

The capability of the present method will be extended to partition of macromolecules and cells on aqueous–aqueous polymer phase systems[6] and also to the elutriation of cell particles with a physiological solution.

ACKNOWLEDGEMENT

The author is deeply indebted to Mr. Howard Chapman for fabrication of the instrument.

REFERENCES

1 Y. Ito, *Anal. Biochem.*, in press.
2 Y. Ito, R. E. Hurst, R. L. Bowman and E. K. Achter, *Separ. Purif. Methods*, 3 (1974) 133.
3 Y. Ito and R. L. Bowman, *J. Chromatogr.*, 147 (1978) 221.
4 Y. Ito, *Anal. Biochem.*, 100 (1979) 271.
5 Y. Ito, *J. Chromatogr.*, 188 (1980) 33.
6 P. Å. Albertsson, *Partition of Cell Particles and Macromolecules*, Almqvist & Wiksell, Stockholm and Wiley, New York, 1971.

Journal of Chromatography, 192 (1980) 89–96

CHROM. 12,585

LIQUID CRYSTALS AS THE STATIONARY PHASE IN GAS CHROMATOGRAPHY

ADSORPTION PHENOMENA CAUSED BY AN ELECTRIC FIELD APPLIED ACROSS THE COLUMN

KATSUNORI WATABE and SHIGETAKA SUZUKI

Department of Industrial Chemistry, Faculty of Technology, Tokyo Metropolitan University, Fukasawa, Setagaya-ku, Tokyo 158 (Japan)

and

SHUN ARAKI

Laboratory of Industrial Analytical Chemistry, Faculty of Technology, Yokohama National University, Tokiwadai, Hodogaya-ku, Yokohama 240 (Japan)

(First received October 29th, 1979; revised manuscript received December 4th, 1979)

SUMMARY

An investigation of the direct current electric field effect on capillary column gas chromatography, in which liquid crystals were used as the stationary phase, is described. When the electric field was applied across the column axis, the peak size was reduced, to an extent that depended on the configuration of the solute molecule, the field strength and the stationary phase employed. When the field strength was increased the amount adsorbed also increased. At every injection, the amount of sample adsorbed was constant, *i.e.* independent of sample size. This phenomenon was successfully exploited in qualitative and quantitative experiments.

INTRODUCTION

Liquid crystals have the mobility of ordinary liquids and the anisotropic properties of solid crystals. In other words, the liquid crystalline state has more order in the arrangement of its molecules than the liquid state, but less than solid state. Their interesting properties have been extensively investigated, and electro-optical, thermographic, structural and other properties are being used in various fields, such as display devices, temperature indicators, solvents, etc.

In gas chromatography (GC), the use of liquid crystals as the stationary phase was first reported by Kelker[1] and Dewar and Schroeder[2]. They showed that many disubstituted benzenes (or isomers of disubstituted benzenes) could be separated much better by nematic liquid crystals than with conventional column packing materials. Thereafter, many types of liquid crystals were introduced for the separation of various kinds of compounds[3–5].

Generally, the molecular arrangement of liquid crystals is significantly affected by the conditions. An electric field may promote the molecular arrangement and/or may give rise to the molecular rearrangement. Such liquid crystals are called field effect type liquid crystals.

Rogers *et al.*[6] investigated a field effect type liquid crystal, Vali Light A, as a liquid phase for GC: the retention behaviour and column efficiency for several kinds of organic compounds were examined in the presence of alternating current (a.c.) and direct current (d.c.) electric fields. They reported that application of the electric field increased retention values and sharpened peaks. They also studied a cholesteric liquid crystal capillary column with an applied electric field[7,8]. The apparent capacity ratio of the liquid crystal stationary phase was increased, and the peak fronting phenomenon was a function of both the dielectric constant of carrier gas and the strength of the field.

There have been, however, no detailed investigations on the strength of the electric field. In the course of our experiments, using a d.c. electric field, we discovered that some solutes were extensively retained in the column. This "adsorption" phenomenon, which results in the reduction of peak size on application of the electric field, increased with increasing field strength. Further, we found that the peak of *o*-dichlorobenzene did not elute from a cholesteryl palmitate column, when a field of 500 V was applied across the column. This adsorption phenomenon may lead to a new identification technique in GC.

EXPERIMENTAL

Materials

All reagents used were analytical grade, and each sample injected into the gas chromatograph was dissolved in *n*-hexane (2000 ppm). Cholesteryl palmitate (cholesteric mesophase in temperature, 80–146°) and *p*-dianisal-3,3′-dichlorobenzidine (nematic mesophase, 144–330° dec.) were obtained from Tokyo Chemical Industry (Tokyo, Japan), and *p*-azoxydianisol (nematic mesophase, 116–136°) and OV-17 from Nishio Industry (Tokyo, Japan). Liquid crystals were used without further purification. Fine metal wires (0.150 mm diameter) made of stainless steel or nickel were obtained from Nishio Industry and Nippon Denkyu (Tokyo, Japan), respectively. Sealbest P-246, an electroconductive resin, which is composed of fine carbon and silver suspended in the dispersoid solvent, was obtained from Tokuriki Kagaku Institute (Kanagawa, Japan).

d.c. generator

A laboratory-made d.c. generator was used (capacity, 5 kV × 10 mA).

Gas chromatography

An F & M Model 810 gas chromatograph equipped with a flame ionization detector was modified so that a glass capillary column of special conformation could be connected.

The GC conditions were as follows: injection temperature, 200°; detector temperature, 230°; column temperature, mesomorphic temperature; carrier gas, high-purity nitrogen; flow-rate, 0.5–1.5 ml/min; sample size, 1 μl; split ratio, 1:20.

Preparation of column

Coiled glass capillaries were made by drawing Pyrex glass tube (2.0 mm I.D. and 9.0 mm O.D.) with a Shimadzu Model GDM-1 glass drawing machine (Shimadzu Seisakusho, Kyoto, Japan). A fine metal wire for an internal electrode was inserted into the Pyrex tube during the drawing. The capillaries were washed with acetone and dried with nitrogen, then coated with a liquid crystal by passing 1–5% benzene or chloroform with a Shimadzu Model MCT-1 microcolumn treating machine. The outer surface of the capillary was painted with an electroconductive resin, Sealbest P-246, for an external electrode. The cross-section of the column is ideally as shown in Fig. 1, but it is most likely that the wire rests on the inside of the capillary. Table I lists the columns used.

Each column was conditioned for two days at 5–10° above the upper limit of the mesomorphic temperature. The sample injection was started after the field had been applied for 4–5 h.

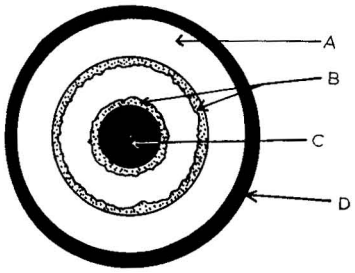

Fig. 1. Cross-section of column. A = Glass capillary; B = liquid crystal; C = metal wire electrode; D = electroconductive resin electrode.

TABLE I

LIST OF COLUMNS

	Cholesteryl palmitate	*p-Azoxy-dianisol*	*p-Dianisal-3,3'-dichloro-benzidine*
Length (m)	20	20	30
Diameter (mm)	0.25 I.D. 0.75 O.D.	0.30 I.D. 0.80 O.D.	0.20 I.D. 0.80 O.D.
Wire electrode	stainless steel 0.150 mm dia.	stainless steel 0.150 mm dia.	nickel 0.125 mm dia.
Column temperature	100°	120°	150°

RESULTS AND DISCUSSION

We examined the effect of changing the strength of the electric field from 0 to 500 V, and the adsorption of *o*-dichlorobenzene on four stationary phases, OV-17, cholesteryl palmitate, *p*-azoxydianisol and *p*-dianisal-3,3'-dichlorobenzidine. The adsorption phenomenon was not observed on the OV-17 column, but *o*-dichlorobenzene was completely adsorbed on the other three columns at field strengths greater than 300 V.

We then investigated the d.c. field effect on the adsorption of halogenated aromatic hydrocarbons, *o*-, *m*- and *p*-methoxytoluene, *m*- and *p*-diisopropylbenzene and tridecane, using a cholesteryl palmitate column at 100°. The relationship between the amount adsorbed and the field strength is shown in Fig. 2. The adsorption of the chlorinated aromatic hydrocarbons increased with increasing field strength, and each compound was adsorbed in different extent. Hydrocarbons were not adsorbed at all, whereas dichlorobenzene and dibromobenzene were strongly adsorbed. Methoxytoluene was weakly adsorbed, and chlorotoluene moderately so. It seems that the *o*-isomers were more strongly adsorbed than the other two positional isomers.

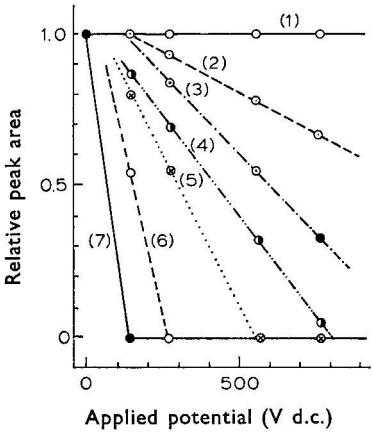

Fig. 2. Relationship between field strength and relative peak area. 1 = *n*-Tridecane and diisopropylbenzene; 2 = *p*-methoxytoluene; 3 = *o*- and *p*-methoxytoluene; 4 = *o*-chlorotoluene; 5 = *o*-dichlorobenzene; 6 = *m*-dibromobenzene; 7 = *o*-dibromobenzene. Cholesteryl palmitate column, at 100°.

The adsorption on the other two liquid crystalline phases, *p*-azoxydianisol and *p*-dianisal-3,3′-dichlorobenzidine, was also investigated, and similar relationships to that on cholesteryl palmitate were obtained.

The amounts of compounds adsorbed on these three liquid crystal columns were compared at the same field strength. The result was that the extent of adsorption depended on the liquid crystals, *i.e.* *o*-dichlorobenzene was adsorbed by 80% on *p*-dianisal-3,3′-dichlorobenzidine, 70% on *p*-azoxydianisol and only a little on cholesteryl palmitate. On the whole, cholesteryl palmitate was found to adsorb less strongly than the other two. Table II lists the critical values of electric field strength at which peaks disappeared from the chromatograms. It can be concluded from these data that cholesteryl palmitate requires a stronger field than the other two for complete adsorption.

The retention times and column efficiences were determined with electric fields of 0 and 200 V. Table III summarized the results for cholesteryl palmitate at 100°. In the presence of a field, the retention times of halogenated aromatic compounds, except *o*-dichlorobenzene and *p*-bromotoluene, were generally decreased. But the variation was always less than 15% and mostly negligibly small. The peaks were sharpened by the field and the height equivalent to a theoretical plate (HETP) values were lower in the presence of the field.

TABLE II

POTENTIALS (V) AT WHICH PEAKS DISAPPEARED ON CHROMATOGRAMS

Sample, chloroform solution, 1 μl.

Compound	*Stationary phase*		
	p-Azoxydianisol	*p-Dianisal-3,3'-dichloro-benzidine*	*Cholesteryl palmitate*
m-Chlorotoluene	76	56	400
o-Dichlorobenzene	70	56	270
o-Methoxytoluene	120	92	over 600
o-Dibromobenzene	28	28	150
m-Dibromobenzene	56	44	200
p-Dibromobenzene	120	92	over 600

TABLE III

EFFECT OF APPLIED POTENTIAL ON RETENTION TIME (min) AND HETP (cm)

Cholesteryl palmitate column, column temperature, 100°.

Compound	*Retention time*		*HETP*	
	0 V	*200 V*	*0 V*	*200 V*
p-Chlorotoluene	2.14	1.80	0.655	0.608
o-Dichlorobenzene	4.90	4.96	1.00	0.478
p-Bromotoluene	5.12	5.15	1.13	0.735
p-Methoxytoluene	3.70	3.57	1.09	0.924
m-Diisopropylbenzene	9.20	8.83	1.67	1.48

Fig. 3 shows the relationship between the amount adsorbed and sample size. The solid line was obtained without a field, and the broken line with a field of 14 V. From 30 to 660 nmol the lines are linear and parallel, which suggests that the amount adsorbed was independent of the sample size.

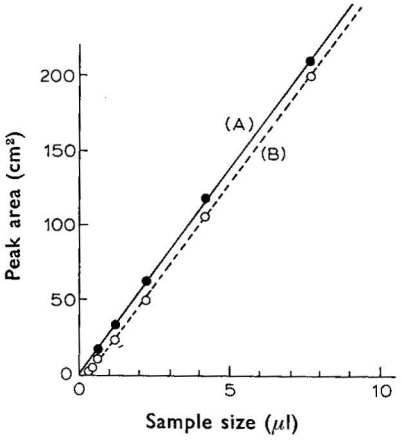

Fig. 3. Effect of sample size on adsorption. A, Without electric field; B, with d.c. electric field (14 V). Sample, methanol ($8.24 \cdot 10^2$ nmol/μl). Column *p*-azoxydianisol, at 120°.

The time-course of the adsorption was also investigated on *p*-azoxydianisol at 118° under a constant field of 14 V (Fig. 4). Steady adsorption was observed over 50 h, although the amount adsorbed did not settle down until 5 h after starting. The reproducibility of this phenomenon was confirmed by exactly the same experiment.

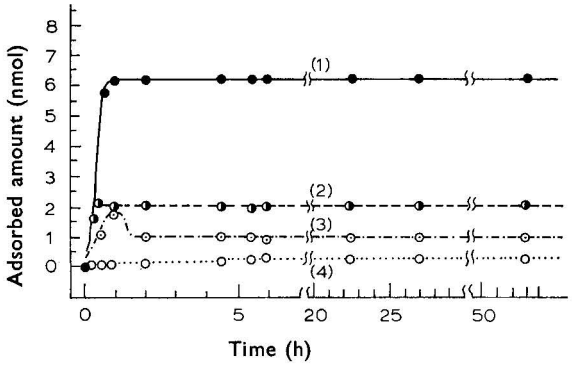

Fig. 4. Variation with time of amount adsorbed. 1 = α,3,4-Trichlorotoluene; 2 = 1,2,4-trichlorobenzene; 3 = 3,4-dichlorotoluene; 4 = *o*-dichlorobenzene. *p*-Azoxydianisol column, at 118°, under 14 V d.c.

No solvent effect on the adsorption was observed. However, as shown in Fig. 5, a portion of the amount previously adsorbed comes out of the column. This is thought to be caused by the displacement of the adsorbed compound by a polar solvent, such as methanol, ethanol, chloroform, 1,2-dichloroethane, acetone and so on. This phenomenon was not observed when non-polar solvents were used for the preparation of the sample.

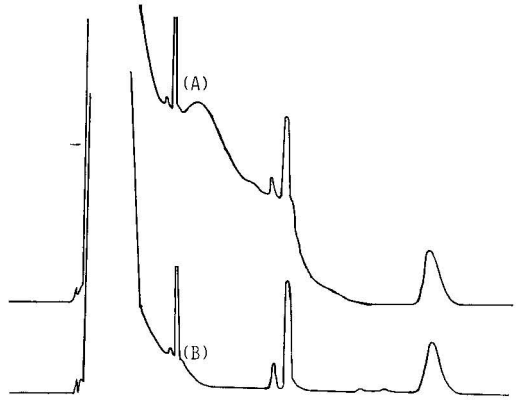

Fig. 5. Solvent effect on elution. (A), Chromatogram after over 20 injections; (B), chromatogram at an early time. Solvent, methanol; sample size, 1 μl; cholestryl palmitate column, at 114°, 200 V d.c.

Additionally, when the electric field was turned off, the adsorption gradually diminished and finally became undetectable. Though the low-level bleeding of the adsorbed compounds was predicted, no appreciable change of the base line could be observed on the chromatogram.

The features discussed above were used in the separation of multi-component samples, particularly those with overlapping peaks. Fig. 6a and b shows that application of the field results in selective adsorption and the identification of each peak. Furthermore, it is of importance that the adsorption behaviour is not affected by the coexisting compound.

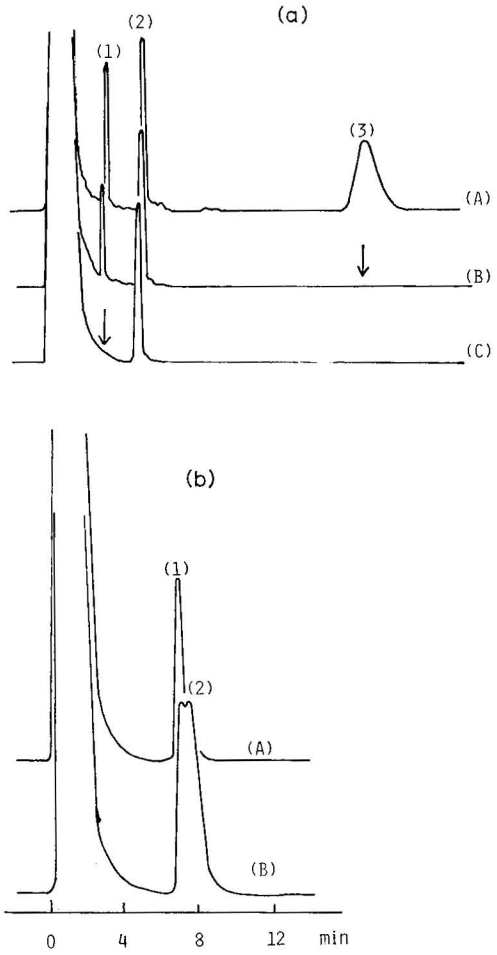

Fig. 6.(a), Chromatograms of aromatic compounds. 1 = *m*-Chlorotoluene; 2 = *m*-methoxytoluene; 3 = *m*-dibromobenzene. A, Without electric field; B, at 250 V d.c.; C, at 500 V d.c. Cholesteryl palmitate column, at 100°. Sample size 1 μl. (b) Chromatograms of *p*-methoxytoluene (1) and *o*-dichlorobenzene (2). A, with electric field (400 V d.c.); B, without electric field.

CONCLUSIONS

The adsorption phenomena were found only with the liquid crystal columns, and not with the ordinary liquid phase OV-17.

The amount adsorbed increased with increasing electric field strength.

The amount adsorbed was dependent on the sort of solute injected. Hydrocarbons were not adsorbed, methoxytoluene was weakly adsorbed, chlorotoluene slightly, and dichlorobenzene and dibromobenzene strongly.

Steady and constant adsorption could be maintained, reproducibly, for 50 h.

The amount adsorbed was independent of the sample size.

These adsorption phenomena are thought to be worth studying for the development of a new gas chromatographic technique, and further investigation is under way in our laboratory.

ACKNOWLEDGEMENTS

We are grateful to Dr. G. Nakayama (Tokyo Chemical Industry Co. Ltd.) for his gift of the liquid crystals. We also thank Dr. T. Hobo and Dr. M. Yamada for their valuable suggestions and reviewing of this report.

REFERENCES

1 H. Kelker, *Ber. Bunsenges. Phys. Chem.*, 67 (1963) 698.
2 M. J. S. Dewar and J. P. Schroeder, *J. Amer. Chem. Soc.*, 86 (1964) 5235.
3 H. Kelker and A. Verhelst, *J. Chromatogr. Sci.*, 7 (1969) 79.
4 D. G. Willey and G. H. Brown, *J. Phys. Chem.*, 76 (1972) 99.
5 P. J. Porcaro and P. Shubiak, *J. Chromatogr. Sci.*, 9 (1971) 690.
6 P. J. Taylor, R. A. Culp, C. H. Lochmuller, L. B. Rogers and E. M. Barall, II, *Separ. Sci.*, 6 (1971) 841.
7 R. B. Westerberg, F. J. Van Lenten and L. B. Rogers, *Separ. Sci.*, 10 (1975) 593.
8 J. E. Conaway and L. B. Rogers, *Separ. Sci.*, 13 (1978) 303.

Journal of Chromatography, 192 (1980) 97–106

CHROM. 12,559

LÖSEVERHALTEN KRISTALLIN-FLÜSSIGER PHASEN IN DER KAPILLARGASCHROMATOGRAPHIE

II. LÖSEEIGENSCHAFTEN SMEKTISCHER A-, B- UND C-MODIFIKATIONEN

KARLHEINZ SEIFERT

Institut für Biochemie der Pflanzen der Akademie der Wissenschaften der D.D.R., 402 Halle/Saale (D.D.R.)

und

GÜNTER KRAUS*

Martin-Luther-Universität Halle-Wittenberg, Sektion Chemie, 402 Halle/Saale (D.D.R.)

(Eingegangen am 15. August 1979; geänderte Fassung eingegangen am 21. November 1979)

SUMMARY

Solution behaviour of liquid crystal phases in capillary gas chromatography. II. Solution properties of smectic A-, B- and C-modifications

The solution behaviour of smectic A-, B- and C-modifications has been investigated by capillary gas chromatography. When the crystalline liquid order of the phases smectic B, C and A decreases the solubilities increase. At the transition temperatures the partial molar free excess enthalpy differences can be correlated to the heats of transition. The thermodynamic data determined by gas chromatography confirm the system of thermotropic liquid crystal phases.

EINLEITUNG

Die Verwendung kristallin-flüssiger Schmelzen als Solvenzien in der Gaschromatographie beschränkte sich vorwiegend auf nematische Flüssigkristalle[1]. Aufgrund des hohen Ordnungsgrades der smektischen Modifikationen erscheinen Übergänge zwischen nematisch und smektisch sowie die smektischen Bereiche selbst besonders interessant.

Nach Untersuchungen an nematischen Verbindungen[2] wurde das Löseverhalten der Modifikationen smektisch A, B und C untersucht.

* Korrespondenz autor.

THEORIE

Smektische Modifikationen werden vorwiegend durch eine Schichtstruktur bestimmt, die aus parallel zueinander gelagerten Molekülachsen und aus der Bindung der Molekülschwerpunkte an bestimmte Ebenen resultiert. Eine Klassifikation des smektischen Zustandes konnte mit Hilfe von Röntgenbeugungsanalysen, der Bestimmung von Mischbarkeitsbeziehungen in binären Systemen, mikroskopischen Texturbetrachtungen und durch Untersuchung des Temperaturganges der Umwandlung an homologen Reihen erreicht werden.

Nach Sackmann und Demus[3] kennt man die smektischen Zustände A, B, C, D, E, F und G, bei denen die Tieftemperaturmodifikationen (E, F und G) gegenüber den Hochtemperaturmodifikationen eine höhere Ordnung aufweisen[4]. Die smektische A-Modifikation besitzt eine Ordnung der Moleküle in Schichten, in denen sie statistisch verteilt sind. Smektische C-Modifikationen lassen im Röntgendiagramm keine Unterschiede zu smektisch A erkennen. Während der Neigungswinkel der Moleküle im smektischen A-Gebiet mit 0° angegeben wird, werden für smektisch C Winkel von 30–45° angegeben[5–7]. Die smektische B-Modifikation unterscheidet sich jedoch wesentlich von A und C. Die Moleküle haben in den Schichten eine hexagonale Anordnung[8].

Die Umwandlungsenthalpien für den Übergang smektisch B–smektisch C liegen in einem Bereich von 1–2 kcal/mol, für die Umwandlung smektisch C–smektisch A zwischen 0.02 und 0.2 kcal/mol.

Partielle molare Lösungsenthalpien ($\Delta\bar{H}_2$) werden aus dem Anstieg der Geraden $\ln V_g^0$ gegen $1/T$

$$\frac{\mathrm{d} \ln V_g^0}{\mathrm{d}\, 1/T} = \frac{\Delta\bar{H}_2}{R}$$

berechnet.

Für die partielle molare freie Exzessenthalpie ($\bar{G}_2^E$) bei der Temperatur T gilt:

$$\bar{G}_2^E = RT \ln f_2.$$

Aktivitätskoeffizienten bei unendlicher Verdünnung (f_2) sind mit dem spezifischen Retentionsvolumen V_g^0 durch

$$f_2 = \frac{1.704 \cdot 10^7}{M_1 p_2^0 V_g^0}$$

verknüpft, wobei M_1 die Molmasse der Trennflüssigkeit und p_2^0 der Sättigungsdampfdruck des Substrates in Torr bei der Trennsäulentemperatur sind.

Mit Hilfe der statistischen Thermodynamik ist eine molekulare Interpretation der Aktivitätskoeffizienten und der partiellen molaren Lösungsenthalpien möglich. Bei einer grossen Änderung der Translationsenergie beim Lösevorgang verkleinert sich der Aktivitätskoeffizient und vergrössert sich die Löslichkeit, ein grosser Rotations-Schwingungsenergieverlust bewirkt einen hohen Aktivitätskoeffizienten und eine geringere Löslichkeit.

EXPERIMENTELLES

Solvenzien

Das Löseverhalten wurde an folgenden Verbindungen untersucht:
4-(4-Dodecyloxy-benzylidenamino)-zimtsäure-*n*-amylester (DOBAZA)

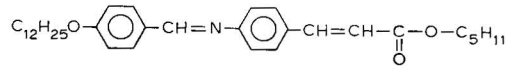

73.9 – sm B – 95 – sm C – 106.7 – sm A – 134.3 – I
ΔHu 6.68 1.31 0.14 2.01

5-*n*-Octyl-2-(4-*n*-hexyloxy-phenyl)-pyrimidin (OHOPP)

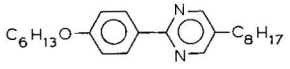

27.5 – sm C – 44.5 – sm A – 57.2 – N – 65 – I
ΔHu 6.88 0.09 0.43

4,4′-Bis-*n*-heptyloxy-azoxybenzol (BHOAB)

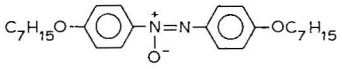

74.4 – sm C – 95.4 – N – 124.2 – I
ΔHu 9.77 0.38 0.24
(Temperaturangaben in °C und Umwandlungsenthalpien in kcal/mol).

Die Phasen wurden in Glaskapillaren von 0.3 mm Durchmesser und Längen von 8–12 m vermessen. Eine gleichmässige Belegung konnte durch eine Epoxidharzvorbehandlung[9] der Kapillaren erreicht werden.

Substrate

Die spezifischen Retentionsvolumina folgender Verbindungen wurden gemessen: *o*-, *m*- und *p*-Isomere von Xylol, Chlortoluol, Bromtoluol und Dichlorbenzol, von Toluol, Äthylbenzol, Cumol und Benzaldehyd, von *n*-Hexanol, Cyclohexanol, Cyclohexanon und von *n*-Octan, *n*-Nonan, *n*-Decan, *n*-Dodecan.

Apparatives

Die Untersuchungen wurden mit einem modifizierten Gaschromatographen GCHF 18.3 des VEB Chromatron Berlin mit Flammenionisationsdetektor (FID) und Argon als Trägergas durchgeführt. Die Säulentemperatur wurde mit einem Eisen-Konstantan-Thermoelement mit einer Genauigkeit von $\pm$ 0.2° gemessen.

ERGEBNISSE UND DISKUSSION

Sowohl in den Bereichen smektisch A, B, C und nematisch als auch den isotropen Bereichen der Solvenzien wurden von 23 Substraten bei verschiedenen Tem-

peraturen spezifische Retentionsvolumina bestimmt, aus denen Aktivitätskoeffizienten, partielle molare Lösungsenthalpien, Exzessenthalpien, partielle molare Lösungsentropien und Exzessentropien berechnet wurden.

Die diskontinuierlichen Änderungen der Aktivitätskoeffizienten bei dem Umwandlungstemperaturen smektisch B–smektisch C, smektisch C–smektisch A, smektisch A–nematisch und nematisch–isotrop spiegeln die diskontinuierlichen Veränderungen der Wechselwirkungen zwischen Substrat und Solvens wider. In den Tabellen I–III sind die Differenzen der partiellen molaren freien Exzessenthalpien ($\Delta\bar{G}_2^E$) einiger Substrate bei den Umwandlungstemperaturen für DOBAZA, OHOPP und BHOAB angegeben.

TABELLE I

DIFFERENZEN DER PARTIELLEN MOLAREN FREIEN EXZESSENTHALPIEN BEI DEN UMWANDLUNGSTEMPERATUREN AN DOBAZA IN cal/mol

Substrat	$\Delta\bar{G}_2$, *sm. C–sm. B*	$\Delta\bar{G}_2$, *sm. A–sm. C*	$\Delta\bar{G}_2$, *is.–sm. A*
o-Xylol	−309	+30	−592
m-Xylol	−316	+38	−585
p-Xylol	−367	+30	−525
o-Chlortoluol	−331	+14	−600
m-Chlortoluol	−331	+15	−624
p-Chlortoluol	−338	+23	−537
p-Bromtoluol	−434	± 0	−515
o-Dichlorbenzol	−353	+23	−595
m-Dichlorbenzol	−353	+30	−602
p-Dichlorbenzol	−426	+ 7	−512
n-Nonan	−301	+45	−505
n-Dodecan	−397	± 0	−554
Durchschnittswert	−355	+21	−561

TABELLE II

DIFFERENZEN DER PARTIELLEN MOLAREN FREIEN EXZESSENTHALPIEN BEI DEN UMWANDLUNGSTEMPERATUREN AN OHOPP IN cal/mol

Substrat	$\Delta\bar{G}_2$, *sm. A–sm. C*	$\Delta\bar{G}_2$, *is.–sm. A*
o-Xylol	± 0	−375
m-Xylol	+12	−390
p-Xylol	+ 6	−328
o-Chlortoluol	−13	−443
m-Chlortoluol	± 0	−430
p-Chlortoluol	± 0	−370
o-Bromtoluol	+19	−430
p-Bromtoluol	+13	−396
o-Dichlorbenzol	+19	−409
m-Dichlorbenzol	+13	−443
p-Dichlorbenzol	+25	−382
n-Decan	± 0	−563
Durchschnittswert	+10	−412

TABELLE III

DIFFERENZEN DER PARTIELLEN MOLAREN FREIEN EXZESSENTHALPIEN BEI DEN UMWANDLUNGSTEMPERATUREN AN BHOAB IN cal/mol

Substrat	$\Delta\bar{G}_2$, *nem.–sm. C*	$\Delta\bar{G}_2$, *is.–nem.*
o-Xylol	−154	−134
m-Xylol	−146	−174
p-Xylol	−161	−135
o-Chlortoluol	−161	−139
o-Bromtoluol	−154	−126
p-Bromtoluol	−183	−110
o-Dichlorbenzol	−161	−102
m-Dichlorbenzol	−168	− 63
p-Dichlorbenzol	−198	−126
n-Nonan	−139	−150
n-Decan	−168	−134
n-Dodecan	−205	−150
Durchschnittswert	−166	−129

Wie aus Tabelle I und Fig. 1 hervorgeht, entspricht der grossen Umwandlungsenthalpie smektisch B–smektisch C von 1.31 kcal/mol bei DOBAZA die relativ

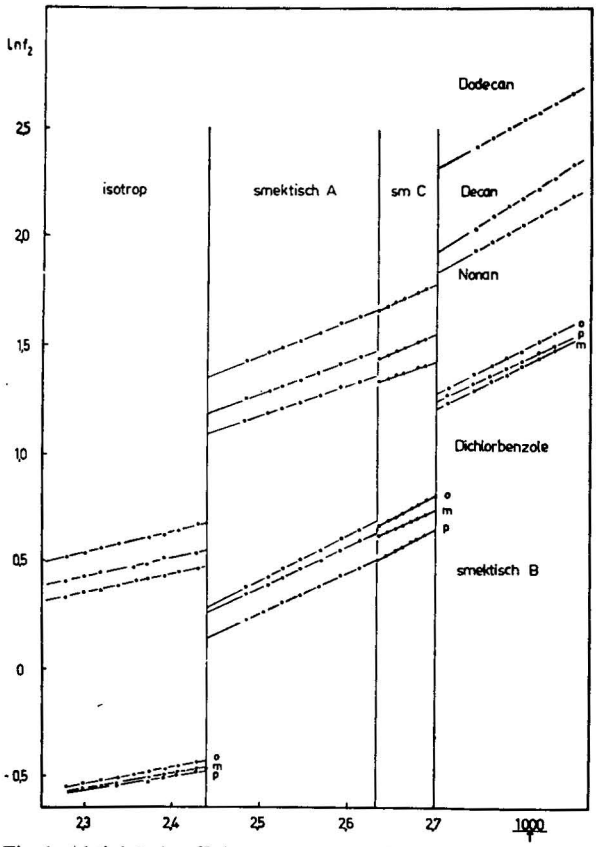

Fig. 1. Aktivitätskoeffizienten von *n*-Alkanen und der Dichlorbenzol-Isomere gegen $1000/T$ an DOBAZA.

grossen Änderungen der partiellen molaren freien Exzessenthalpien. Die Übergänge smektisch C–smektisch A und smektisch A–isotrop werden von einer Umwandlungsenthalpie von 0.14 kcal/mol bzw. 2.01 kcal/mol begleitet. Analog dazu verhalten sich die Differenzen der partiellen molaren freien Exzessenthalpien.

Die für DOBAZA angestellten Betrachtungen gelten in gleicher Weise für OHOPP und BHOAB, wie den Tabellen II und III und den Fig. 2 und 3 zu entnehmen ist.

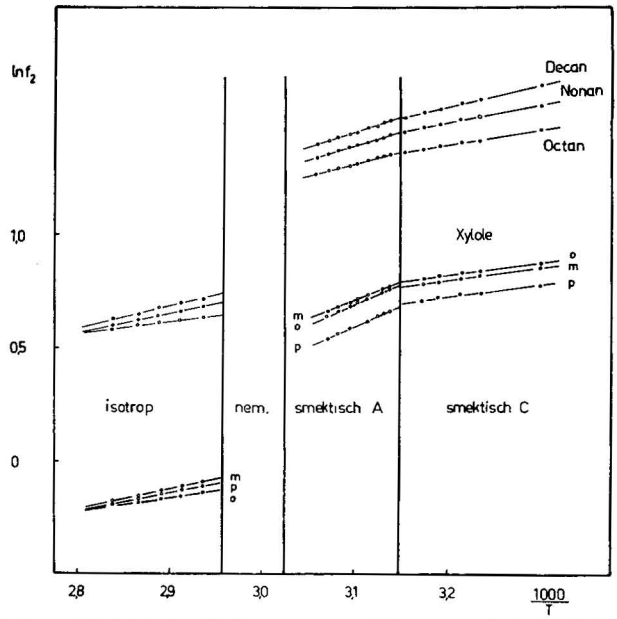

Fig. 2. Aktivitätskoeffizienten von *n*-Alkanen und der Xylol-Isomere gegen $1000/T$ an OHOPP.

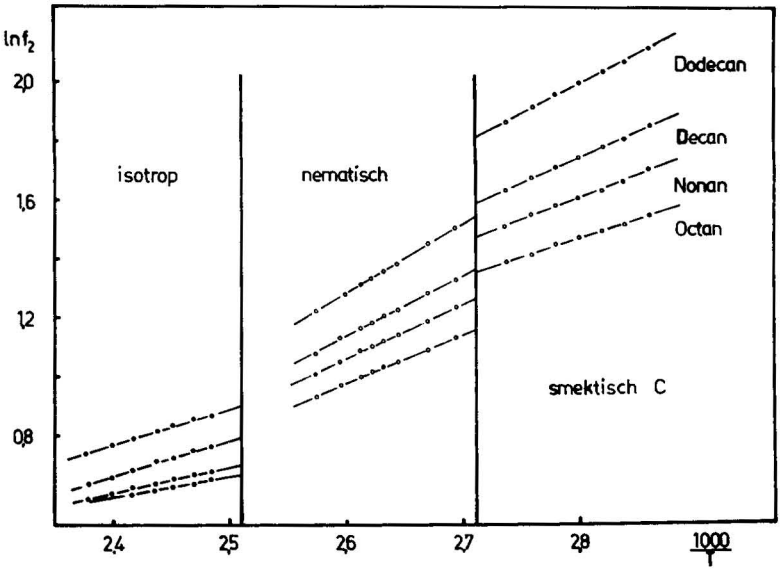

Fig. 3. Aktivitätskoeffizienten von *n*-Alkanen gegen $1000/T$ an BHOAB.

Übereinstimmend mit anderen Eigenschaftswerten wie Umwandlungsenthalpien oder Dichteänderungen sind die Änderungen der partiellen molaren freien Exzessenthalpien sehr klein bei der Übergangstemperatur smektisch C–smektisch A. Das ist verständlich, weil sich nur der Neigungswinkel der Moleküle in den beiden smektischen Schichten unterscheidet.

Wird die Anordnung der Lösungsmittelmoleküle in Schichten aufgehoben und bleibt die Parallellagerung einziges Ordnungsmerkmal, so kommt es zu einer Erhöhung der Löslichkeit, wie am Übergang smektisch C–nematisch von BHOAB zu erkennen ist.

Eine starke Vergrösserung der Löslichkeit wird auch bei den Übergängen smektisch–isotrop oder nematisch–isotrop beobachtet.

Von smektisch B über smektisch C, smektisch A und nematisch findet ein stufenweiser Ordnungsabbau bis schliesslich zum isotropen Zustand statt. Da sich die nicht-mesomorphen Substrate besser in isotropen als in anisotropen Flüssigkeiten lösen, wird die Zunahme der Löslichkeit bei einem Ordnungsabbau mit steigender Temperatur verständlich.

Die gaschromatographischen Daten bestätigen die durch Mischbarkeitsbeziehungen gefundene Systematik der kristallin-flüssigen Zustände.

Die Unterschiede der partiellen molaren Lösungsenthalpien eines Substrates an smektisch B, C und A von DOBAZA sind gering (Tabelle IV), was auf die grosse

TABELLE IV

PARTIELLE MOLARE LÖSUNGSENTHALPIEN UND LÖSUNGSENTROPIEN AN DOBAZA

$\Delta\bar{H}_2$-Werte in kcal/mol; $\Delta\bar{S}_2$-Werte in cal/mol·°K.

Substrat	*Smektisch B (bei 76 °C)*		*Smektisch C (bei 100 °C)*		*Smektisch A (bei 126 °C)*		*Isotrop (bei 140 °C)*	
	$\Delta\bar{H}_2$	$\Delta\bar{S}_2$	$\Delta\bar{H}_2$	$\Delta\bar{S}_2$	$\Delta\bar{H}_2$	$\Delta\bar{S}_2$	$\Delta\bar{H}_2$	$\Delta\bar{S}_2$
o-Xylol	−5.12	−18.00	−5.65	−16.35	−5.74	−14.56	− 8.06	−18.17
m-Xylol	−5.00	−17.65	−5.70	−16.42	−5.73	−14.43	− 7.95	−17.89
p-Xylol	−5.95	−20.03	−5.65	−16.22	−5.77	−14.41	− 7.96	−17.81
o-Chlortoluol	−6.64	−22.15	−6.32	−18.33	−6.42	−17.14	− 8.09	−19.87
m-Chlortoluol	−6.58	−22.65	−6.09	−18.50	−6.34	−17.31	− 8.48	−19.96
p-Chlortoluol	−6.52	−23.00	−5.83	−17.00	−6.45	−17.28	− 8.55	−20.12
o-Bromtoluol	−7.15	−24.00	−6.74	−19.97	−6.60	−17.18	− 9.00	−20.11
m-Bromtoluol	−7.37	−24.60	−6.50	−20.30	−6.48	−17.32	− 9.05	−21.15
p-Bromtoluol	−7.23	−24.05	−6.39	−18.70	−6.87	−17.62	− 9.05	−21.32
o-Dichlorbenzol	−6.89	−23.15	−6.30	−18.40	−6.52	−16.57	− 9.03	−20.61
m-Dichlorbenzol	−6.74	−22.63	−6.66	−19.26	−6.54	−16.57	− 8.75	−19.95
p-Dichlorbenzol	−7.03	−23.40	−6.08	−17.40	−6.60	−16.52	− 8.91	−20.24
Toluol	−4.62	−15.96	−5.07	−14.78	−5.18	−13.64	− 6.51	−14.71
Äthylbenzol	−4.75	−16.90	−5.57	−16.59	−5.57	−15.40	− 7.31	−17.25
Cumol	−4.90	−18.00	−6.86	−20.42	−6.32	−16.83	− 7.67	−18.19
Benzaldehyd	−6.70	−19.70	−5.38	−16.80	−5.65	−14.91	− 8.52	−19.52
n-Octam	−4.58	−17.35	−6.80	−20.70	−6.61	−17.20	− 7.60	−18.03
n-Nonan	−5.71	−20.93	−7.03	−21.02	−6.93	−18.52	− 7.88	−18.84
n-Decan	−6.59	−23.83	−7.50	−23.30	−7.84	−21.39	− 8.82	−21.83
n-Dodecan	−8.97	−31.22	−9.31	−28.66	−9.62	−26.31	−10.40	−26.53
n-Hexanol	−7.34	−25.20	−6.36	−20.40	−6.66	−18.20	− 8.21	−19.45
Cyclohexanon	−4.70	−18.70	−5.42	−17.20	−4.87	−13.41	− 8.08	−18.72
Cyclohexanol	−5.24	−21.60	−6.27	−20.92	−5.98	−16.91	− 8.15	−19.62

Ähnlichkeit der seitlichen Anordnung der Moleküle in den smektischen Ebenen der 3 Modifikationen zurückgeführt werden kann.

Bemerkenswert sind jedoch die verschiedenen Trends der $\Delta\bar{H}_2$-Werte von disubstituierten Benzolisomeren an smektisch C und A und der daraus resultierende kleinere Rotations-Schwingungsenergieverlust des *p*-Isomeren gegenüber *o*- und *m*-Isomeren im smektischen C-Bereich.

Bei der Phase OHOPP waren die partiellen molaren Lösungsenthalpen der Substrate (Tabelle V) bei smektisch C grösser als bei smektisch A. Danach müssten die Verluste an Rotationen und Schwingungen eines Substrates beim Übergang aus der idealen Gasphase in die smektische C-Phase grösser sein als beim Übergang in die smektische A-Phase.

TABELLE V

PARTIELLE MOLARE LÖSUNGSENTHALPIEN UND LÖSUNGSENTROPIEN AN OHOPP
$\Delta\bar{H}_2$-Werte in kcal/mol; $\Delta\bar{S}_2$-Werte in cal/mol·°K.

Substrat	*Smektisch C (bei 40 °C)*		*Smektisch A (bei 50 °C)*		*Isotrop (bei 76 °C)*	
	$\Delta\bar{H}_2$	$\Delta\bar{S}_2$	$\Delta\bar{H}_2$	$\Delta\bar{S}_2$	$\Delta\bar{H}_2$	$\Delta\bar{S}_2$
o-Xylol	−8.83	−29.18	−6.40	−20.91	− 8.63	−24.18
m-Xylol	−8.63	−28.80	−6.94	−22.51	− 8.11	−22.83
p-Xylol	−8.38	−27.44	−6.59	−21.12	− 8.05	−22.47
o-Chlortoluol	−8.82	−29.31	−7.67	−24.77	− 9.24	−25.74
m-Chlortoluol	−8.82	−30.30	−7.36	−24.20	− 9.03	−25.35
p-Chlortoluol	−8.54	−29.10	−7.23	−23.72	− 9.31	−26.14
o-Bromtoluol	−9.18	−30.02	−7.59	−24.61	− 9.98	−27.96
m-Bromtoluol	−9.11	−30.77	−7.62	−25.40	− 9.81	−27.62
p-Bromtoluol	−8.51	−27.33	−8.34	−26.72	−10.16	−28.36
o-Dichlorbenzol	−8.41	−27.40	−7.77	−24.90	− 9.98	−27.77
m-Dichlorbenzol	−7.91	−26.15	−7.59	−24.50	− 9.71	−26.09
p-Dichlorbenzol	−7.51	−24.90	−7.28	−23.71	− 9.89	−27.34
Toluol	−6.81	−22.50	−6.19	−20.03	− 7.25	−20.16
Äthylbenzol	−8.39	−27.66	−6.90	−22.55	− 7.91	−22.23
Cumol	−8.75	−29.10	−7.54	−24.75	− 8.23	−23.42
Benzaldehyd	−8.23	−27.00	−6.85	−21.30	− 9.31	−23.73
n-Octan	−8.32	−28.61	−7.61	−25.78	− 8.18	−24.42
n-Nonan	−9.36	−32.12	−8.31	−28.18	− 8.82	−26.38
n-Decan	−9.55	−32.60	−9.27	−31.25	− 9.58	−28.37
n-Hexanol	−9.30	−33.60	−8.27	−29.72	−10.37	−29.97
Cyclohexanon	−7.13	−25.07	−5.43	−19.42	− 7.68	−21.35
Cyclohexanol	−8.85	−33.55	−6.46	−22.61	− 9.03	−25.95

Ein analoges Verhalten wird bei smektisch C und nematisch von BHOAB beobachtet (Tabelle VI).

Beim Übergang aus der idealen Gasphase in eine smektische C-Phase müsste ein Substratmolekül einen höheren Rotations-Schwingungsenergieverlust haben als beim Übergang in eine nematische Flüssigkeit, worauf die höheren partiellen molaren

TABELLE VI

PARTIELLE MOLARE LÖSUNGSENTHALPIEN UND LÖSUNGSENTROPIEN AN BHOAB

$\Delta\bar{H}_2$-Werte in kcal/mol; $\Delta\bar{S}_2$-Werte in cal/mol·°K.

Substrat	*Smektisch C (bei 80 °C)*		*Nematisch (bei 100 °C)*		*Isotrop (bei 126 °C)*	
	$\Delta\bar{H}_2$	$\Delta\bar{S}_2$	$\Delta\bar{H}_2$	$\Delta\bar{S}_2$	$\Delta\bar{H}_2$	$\Delta\bar{S}_2$
o-Xylol	−6.97	−21.36	−5.37	−15.10	− 7.24	−17.62
m-Xylol	−6.93	−21.25	−5.41	−15.25	− 7.11	−17.34
p-Xylol	−6.67	−20.30	−5.57	−15.50	− 7.19	−17.40
o-Chlortoluol	−7.52	−22.67	−5.80	−16.30	− 7.93	−20.09
m-Chlortoluol	−7.44	−23.70	−5.67	−16.60	− 7.96	−20.11
p-Chlortoluol	−7.11	−22.69	−5.88	−16.40	− 8.10	−21.24
o-Bromtoluol	−8.17	−24.70	−6.07	−17.50	− 8.32	−20.35
m-Bromtoluol	−7.99	−24.37	−6.02	−17.71	− 8.63	−21.36
p-Bromtoluol	−7.73	−23.40	−6.29	−17.80	− 8.87	−21.97
o-Dichlorbenzol	−8.05	−24.25	−6.22	−17.41	− 8.73	−21.38
m-Dichlorbenzol	−7.81	−23.37	−5.76	−16.30	− 8.31	−20.29
p-Dichlorbenzol	−7.41	−21.83	−5.82	−16.30	− 8.43	−20.55
Toluol	−6.17	−18.76	−4.70	−13.27	− 6.88	−17.08
Äthylbenzol	−6.88	−20.96	−5.30	−15.37	− 7.47	−18.64
Cumol	−7.27	−22.64	−5.60	−16.50	− 7.53	−19.02
Benzaldehyd	−7.30	−19.42	−5.36	−16.00	− 8.19	−20.00
n-Octan	−6.31	−21.39	−5.26	−16.25	− 6.89	−18.40
n-Nonan	−7.22	−23.72	−6.01	−18.35	− 7.32	−19.42
n-Decan	−7.91	−25.79	−6.88	−21.18	− 8.60	−22.85
n-Dodecan	−9.45	−30.65	−8.41	−25.86	−10.22	−27.35
n-Hexanol	−7.53	−24.32	−5.38	−17.50	− 8.07	−20.71
Cyclohexanon	−6.13	−20.85	−4.45	−13.71	− 7.32	−18.06
Cyclohexanol	−7.15	−25.37	−4.74	−15.72	− 7.37	−19.27

Lösungsenthalpien und die grösseren Aktivitätskoeffizienten im smektischen C-Bereich hinweisen.

Nach den Reihenfolgen der partiellen molaren Lösungsenthalpien (Tabellen IV–VI) haben in den smektischen C-Bereichen der untersuchten Phasen die *p*-Isomeren stets die kleinsten partiellen molaren Lösungsenthalpien gegenüber *o*- und *m*-Isomeren. Aufgrund der ebenfalls meist kleineren Aktivitätskoeffizienten der *p*-Isomeren sollte ihr Rotations-Schwingungsverlust kleiner sein als der von *o*- und *m*-Isomeren. Die smektischen A-Phasen werden nicht durch eine so strenge Reihenfolge der $\Delta\bar{H}_2$-Werte von disubstituierten Benzolisomeren charakterisiert wie smektisch C, wobei die Aktivitätskoeffizienten der *p*-Isomeren auch häufig den kleinsten Wert haben. In seinen Löseeigenschaften liegt smektisch A zwischen smektisch C und nematisch, wobei eine grosse Ähnlichkeit zwischen smektisch A und nematisch zu erkennen ist.

SCHLUSSFOLGERUNGEN

Zwischen den einzelnen smektischen Modifikationen ergaben sich deutliche Unterschiede im Löseverhalten. Die Umwandlung smektisch B–smektisch C ist mit

einer starken Zunahme der Löslichkeit verbunden. Der höhere Ordnungsgrad von smektisch B ("hexagonales Gitter") bewirkt eine geringere Löslichkeit. Die sich nur durch den Neigungswinkel der Moleküle in den smektischen Schichten unterscheidenden Strukturen von smektisch C und A zeigen nur geringe Unterscheide im Löseverhalten. Der Übergang von smektisch C zur nematischen Struktur ist durch die Aufhebung der Anordnung der Moleküle in Schichten wiederum mit einer grossen Zunahme der Löslichkeit verbunden.

ZUSAMMENFASSUNG

Das Löseverhalten von smektisch A, B und C-Modifikationen wurde unter Verwendung von Glaskapillaren gas chromatographisch untersucht. Entsprechend dem Ordnungsabbau von smektisch B über smektisch C zu smektisch A wurde eine Zunahme der Löslichkeit beobachtet. Die Differenzen der partiellen molaren freien Exzessenthalpien bei den Umwandlungstemperaturen verlaufen parallel zu den Umwandlungsenthalpien. Die mit Hilfe der Gaschromatographie bestimmten thermodynamischen Daten bestätigen die durch Mischbarkeitsbeziehungen gefundene Systematik der kristallin-flüssigen Zustände.

LITERATUR

1 H. Kelker, *Advan. Liquid Cryst.*, 3 (1978) 237.
2 G. Kraus, K. Seifert und H. Schubert, *J. Chromatogr.*, 100 (1974) 101.
3 H. Sackmann und D. Demus, *Mol. Cryst. Liq. Cryst.*, 21 (1973) 293.
4 D. Demus und L. Richter, *Textures of Liquid Crystals*, Verl. für Grundstoffind., Leipzig, 1978.
5 T. R. Taylor, S. L. Arora und J. L. Fergason, *Phys. Rev. Lett.*, 25 (1970) 722.
6 T. R. Taylor, J. L. Fergason und S. L. Arora, *Phys. Rev. Lett.*, 24 (1970) 359.
7 E. Gelerinter und G. C. Fryburg, *Appl. Phys. Lett.*, 18 (1971) 84.
8 A. M. Levelut und M. Lambert, *Compt. Rend.*, 272 (B) (1971) 1018.
9 E. Liebnitz und G. Struppe, *Handbuch der Gaschromatographie*, Akademische Verlagsgesellschaft Geest & Portig, Leipzig, 2. Aufl., 1970, S. 581.

Journal of Chromatography, 192 (1980) 107–116

CHROM. 12,584

DIFFERENT BASES FOR THE GAS CHROMATOGRAPHIC RETENTION INDEX SYSTEM

U. HELDT and H. J. K. KÖSER

Institut für Chemische Technologie und Brennstofftechnik der TU, Erzstr. 18, D-3392 Clausthal-Zellerfeld (G.F.R.)

(First received September 12th, 1979; revised manuscript received November 9th, 1979)

SUMMARY

The concept of a generalized retention index is discussed. The potential usefulness of nine homologous series as a reference for a retention index system is investigated. The functional constants —the additive terms for interconversion between systems— are given, together with their confidence intervals. *n*-Alkanes are not suitable reference compounds for high polarity stationary phases. Compounds of medium polarity, such as the *n*-aldehydes, give more precise values for stationary phases of low and high polarity. A polarity scale may be based on these more reproducible indices. This is shown by comparing *n*-alkane with *n*-aldehyde polarities. A polarity scale based on the variance of the retention indices can compare indices referred to different homologues.

INTRODUCTION

The Kovats' retention index system[1] has been widely accepted in the chromatographic literature as a means of comparing retention data and characterizing stationary phases. Kovats' index compares the retention behaviour of a compound with that of *n*-alkanes measured under identical conditions. The retention index is approximately independent of the gas flow-rate. The temperature dependence of the retention index is usually less than 1 index unit per degree[2]. If adsorption effects are negligible, *i.e.* the support surface is deactivated and Gibbs adsorption is of minor importance because the polarity difference between solutes and stationary phase is small, then the Kovats' index is also independent of the liquid phase loading[3]. Under high resolution conditions the reproducibility from laboratory to laboratory is about 1 index unit[4] for low polarity stationary phases. For high polarity columns the capacity ratio of the *n*-alkanes is very sensitive to impurities, ageing, solute concentration and the surface to volume ratio of the stationary phase. In these cases the reproducibility of the classical Kovats' retention index leaves much to be desired, and from a practical point of view it is inconvenient to inject solutes together with their reference *n*-alkanes having a boiling point of 150° or higher[5]. To remedy these deficiencies it has frequently been suggested that a more polar homologous series than the *n*-alkanes be employed[5–7]

as reference series. Primary alcohols[5,8,9], methyl-*n*-alkyl ketones[6,8], *n*-alkyl esters[2,7,8,10], *n*-alkylbenzenes[11] and *n*-alkyl iodides[12] have been suggested for this purpose. Lipid chemists are using the ECL (equivalent chain length) system and the CN (carbon number) system, where the methyl esters of linear saturated acids are performing the same function as the *n*-alkanes in the Kovats' retention index system. Generally speaking, it is desirable to use reference compounds that are chemically similar to those under analysis.

This paper is an application of the generalized retention index system of Novák and Ružičková[8]. Nine homologous series of reference compounds on four stationary phases of widely different polarities are compared.

EXPERIMENTAL

Measurements were made using an F & M 810 gas chromatograph (F & M, Avondale, Pa., U.S.A.) equipped with a flame ionization detector. Retention times were obtained using a D26 computing integrator (Bodenseewerk Perkin-Elmer, Überlingen, G.F.R.) measuring to 0.01 min. The column temperature was kept at $100 \pm 0.2°$. The columns (2.5 mm I.D.) contained 4–8% of stationary phase on a Chromosorb G AW DMCS (80–100 mesh) support. The stationary phases were (1) squalane (Applied Science, State College, Pa., U.S.A.), (2) di(2-ethylhexyl)sebacate (DOS) (Heyden, München, G.F.R.), (3) Carbowax 20M (Regis, Chicago, Ill., U.S.A.), (4) 1,2,3-tris(2-cyanoethoxy)propane (TCEP) (Merck, Darmstadt, G.F.R.).

The flow-rate of the nitrogen carrier gas was 30 ml/min. The column length was varied between 2 and 5 m to keep the retention times above 1 min. The dead time was determined by injecting methane[13], as the iterative procedure using data of homologous series[14] can be subject to larger errors. The injected sample sizes were kept as small as possible, usually under 0.02 μl. At least three columns were prepared of each stationary phase.

The retention times for each solute investigated were determined on each column at least three times. The 30 substances suggested by Rohrschneider[15] and members of the following homologous series were selected as solutes: (1) *n*-alkane, (2) *n*-alk-1-ene, (3) 1-chloro-*n*-alkane, (4) *n*-aldehyde, (5) *n*-alkan-2-ol, (6) *n*-alkan-1-ol, (7) 1-amino-*n*-alkane, (8) *n*-alkylbenzene, (9) *n*-alkylcyclohexane.

THEORY

The generalized retention index $I_y^x(i)$ of a substance i on the stationary phase x refers to the retention of the homologous series y[8]:

$$I_y^x(i) = 100 \frac{\log V_N^x(i) - \log V_N^x(yn)}{\log V_N^x(yn+\alpha) - \log V_N^x(yn)} + 100n + K_y \qquad (1)$$

where $V_N^x(yn)$ is the net retention volume on the stationary phase x of the reference compound with n methylene groups, $V_N^x(yn+\alpha)$ is the net retention volume of the reference compound with $n+\alpha$ methylene groups, and K_y is a constant, chosen to avoid negative indices (for y = *n*-alkane, $K_y = 0$).

When y is the *n*-alkane series, the Kovats' retention index is a special case.

If the slope of log $V_N^x(yn)$ over $I_y^x(yn)$ is the same for all reference series, the difference between all retention indices measured in the index system $y1$ and the one measured in the index system $y2$ reduces to a constant[8]. In a computationally appropriate form one can write:

$$I_{y1}^x(i) - I_{y2}^x(i) = A_{y2}^x/B_{y2}^x - A_{y1}^x/B_{y1}^x = FU_{y1,y2}^x \quad (2)$$

where B_y^x is the slope of log $V_N^x(yn)$ over $I_y^x(yn)$, and A_y^x is the ordinate intercept of line log $V_n^x(yn)$ over $I_y^x(yn)$. In this case the difference for all substances is equal to the functional constant $FU_{y1,y2}^x$ which depends on the reference compounds $y1$ and $y2$ and the stationary phase x.

The differences between Kovats' indices of certain standard substances on the phase in question and on squalane are used as a polarity measure of the stationary phase[16]. If one employs the generalized retention index system in the same way, the difference between the two polarity scales thus obtained is of interest. This difference between the indices referred to as $y1$ and measured on the stationary phases $x1$ and $x2$ and the indices referred to as $y2$ is, if the slopes are the same for each column, given by:

$$[I_{y1}^{x1}(i) - I_{y1}^{x2}(i)] - [I_{y2}^{x1}(i) - I_{y2}^{x2}(i)] = ([A_{y1}^{x2} - A_{y2}^{x2}]/B_{y1}^{x2}) + ([A_{y2}^{x1} - A_{y1}^{x1}]/B_{y1}^{x1}) \quad (3)$$

The polarity values will differ by a constant factor. Their difference will be a function of the retention volumes if the assumption about the slopes does not hold.

The slopes B_y^x are equal if log $V_N^x(yn+1)/V_N^x(yn)$ is the same for the higher members of all homologous groups. In terms of an additivity model for the free energy of retention[8], this means that the molar Gibbs free energy of the methylene group on a given stationary phase is the same for all homologues.

RESULTS AND DISCUSSION

Table I lists the mean value of the measured *n*-aldehyde retention indices for the four columns investigated. The retention indices of the references have assigned values. The indices in the respective index systems have been chosen in such a way that the following substances have index values of 1000:

(1) *n*-Decane; (2) Hept-1-ene; (3) 1-Chlorohexane; (4) Hexylaldehyde; (5) Octan-2-ol; (6) Hexan-1-ol; (7) 1-Aminohexane; (8) Methylbenzene; (9) Methylcyclohexane. This means that, for example, in the aldehyde index system an index of 1150 signifies a substance eluting between *n*-heptyl and *n*-octyl aldehyde, whereas the same index in the alkylbenzene system denotes a substance between ethylbenzene and *n*-propylbenzene. This choice avoids negative retention indices.

The gas hold-up time has been experimentally determined. Assuming a linear relationship between the adjusted retention times and the carbon number of the reference series, one linear least square fit was calculated using all reference points. In this way the measured indices of the references differ by up to four retention index units from their assigned values, since the relationship is in fact not strictly linear (compare Table I). One can force the experimental values to coincide with their assigned values by fitting piecewise or using a non-linear relationship. However, we consider these latter methods less accurate in cases where one has to extrapolate.

TABLE I

MEASURED *n*-ALDEHYDE RETENTION INDICES

Substances	*Stationary phase*			
	Squalane	*DOS*	*Carbowax 20M*	*TCEP*
n-Aldehyde				
C_3H_7CHO	–	700	704	701
C_4H_9CHO	790	797	794	793
$C_5H_{11}CHO$	897	901	899	901
$C_6H_{13}CHO$	1000	1003	1001	1004
$C_7H_{15}CHO$	1103	1101	1102	1104
$C_8H_{17}CHO$	1202	1197	1201	1201
$C_9H_{19}CHO$	1301	–	1300	1299
$C_{10}H_{21}CHO$	1397	–	1399	1397
Rohrschneider substances				
Ethanol	604	701	818	793
$CH_3COC_2H_5$	781	800	820	864
Nitromethane	698	833	1064	1160
Pyridine	952	976	1100	1174
2,4-Dimethylpentane	880	789	512	211
2-Ethylhex-1-ene	1031	953	752	507
Cyclohexane	923	836	650	399
Benzene	900	878	870	794
Toluene	1010	982	970	902
Styrene	1127	1118	1176	1158
Acetone	658	698	721	781
Crotonaldehyde	834	876	962	1041
t-Butanol	713	772	776	730
Chloroform	836	872	927	775
Thiophene	905	898	949	885
n-Butylacetate	1002	991	986	958
Allylalcohol	713	822	1004	1002
Dioxane	906	914	986	1063
Acetonitrile	615	735	921	1021
Nitroethane	811	904	1073	1187
Methyl iodide	763	742	730	600
n-Butylether	1113	1042	879	690
Ethyl bromide	743	724	672	454
CCl_4	905	859	796	574
Propan-2-ol	671	742	806	768
Phenylacetylene	1089	1114	1270	1234
$1,1\text{-}C_2F_2Cl_4$	715	880	790	559
Cyclopentanol	987	1048	1206	1221
n-Alkane				
C_5H_{12}	736	–	–	–
C_6H_{14}	852	–	–	–
C_7H_{16}	953	856	–	–
C_8H_{18}	1054	954	–	–
C_9H_{20}	1154	1052	815	–
$C_{10}H_{22}$	1252	1149	912	–
$C_{11}H_{24}$	1351	1245	1011	–
$C_{12}H_{26}$	1449	1340	1109	–
$C_{13}H_{28}$	–	–	1206	–
$C_{14}H_{30}$	–	–	1303	–
$C_{15}H_{32}$	–	–	1402	–

TABLE I *(continued)*

Substances	*Stationary phase*			
	Squalane	*DOS*	*Carbowax 20M*	*TCEP*
n-Alkan-1-ol				
C_3H_7OH	–	814	927	897
C_4H_9OH	–	919	1037	1007
$C_5H_{11}OH$	–	1023	1143	1113
$C_6H_{13}OH$	–	1124	1247	1216
$C_7H_{15}OH$	–	1222	1347	1315
$C_8H_{17}OH$	–	1320	1448	1413
$C_9H_{19}OH$	–	–	–	1513
$C_{10}H_{21}OH$	–	–	–	1608
n-Alkan-2-ol				
$CH_3CH_2OHCH_3$	681	743	812	762
$C_2H_5CH_2OHCH_2$	799	851	913	864
$C_3H_7CH_2OHCH_3$	901	950	1010	958
$C_4H_9CH_2OHCH_3$	1003	1049	1113	1061
$C_5H_{11}CH_2OHCH_3$	1104	1147	1214	1161
$C_6H_{13}CH_2OHCH_3$	1204	1245	1314	1260
$C_7H_{15}CH_2OHCH_3$	1303	1340	1408	1358
1-Amino-n-alkane				
$C_4H_9NH_2$	–	–	804	–
$C_5H_{11}NH_2$	–	–	911	–
$C_6H_{13}NH_2$	–	–	1010	–
$C_7H_{15}NH_2$	–	–	1114	–
$C_8H_{17}NH_2$	–	–	1214	–
$C_9H_{19}NH_2$	–	–	1312	–
$C_{10}H_{21}NH_2$	–	–	1411	–
1-Chloro-n-alkane				
C_3H_7Cl	776	744	–	–
C_4H_9Cl	881	847	761	–
$C_5H_{11}Cl$	987	948	866	–
$C_6H_{13}Cl$	1087	1047	966	–
$C_7H_{15}Cl$	1187	1145	1066	–
$C_8H_{17}Cl$	1287	1243	1166	–
n-Alkylbenzene				
$C_2H_5C_6H_5$	1102	1067	–	–
$C_3H_7C_6H_5$	1191	1152	1135	1058
$C_4H_9C_6H_5$	1290	1249	1232	1155
$C_5H_{11}C_6H_5$	1384	1341	1327	1251
$C_6H_{13}C_6H_5$	–	–	1421	1346
$C_7H_{15}C_6H_5$	–	–	1517	1447
n-Alk-1-ene				
$C_3H_7CHCH_2$	727	654	–	–
$C_4H_9CHCH_2$	834	757	–	–
$C_5H_{11}CHCH_2$	936	858	655	–
$C_6H_{13}CHCH_2$	1036	956	755	–
$C_7H_{15}CHCH_2$	1136	1054	856	–
$C_8H_{17}CHCH_2$	1235	1150	955	–
n-Alkylcyclohexane				
$C_2H_5C_6H_{11}$	1101	1006	826	–
$C_3H_7C_6H_{11}$	1192	1096	915	–
$C_4H_9C_6H_{11}$	1288	1190	1013	–
$C_5H_{11}C_6H_{11}$	1386	1286	1110	–

TABLE II

95% CONFIDENCE INTERVAL OF THE MEAN RETENTION INDICES

Column	*Reference*								
	n-Alkane	*n-Alk-1-ene*	*1-Chloro-n-alkane*	*n-Aldehyde*	*n-Alkan-2-ol*	*n-Alkan-1-ol*	*1-Amino-alkane*	*n-Alkyl-benzene*	*n-Alkyl-cyclohexane*
Squalane	3.2	1.7	3.5	3.1	3.7			3.2	4.1
DOS	2.2	2.6	2.0	2.6	2.4	3.2		3.1	4.1
Carbowax 20M	3.8	4.4	3.4	3.2	3.7	3.2	5.3	3.4	4.1
TCEP				4.9	7.1	5.8		8.2	

Table II gives the confidence intervals of the mean retention data. These values are high compared with what can be achieved in terms of reproducibility on high resolution capillary columns[4]. However, in our experience reproducibility is appreciably better only if data obtained on the same column are compared or in cases where the polarity difference between solutes and stationary phase is small. In the present study the polarity of the solutes ranged from the *n*-alkanes to the *n*-alkanols. In these cases one can get more precise data only by measuring the retention at equal concentrations[17] and not simply via the maximum of the elution peak, as is common practice.

The polar columns in particular show marked ageing effects[4]. Because the retention ratio of two successive homologues decreases as the polarity of the stationary phase increases, the precision of the retention indices on polar columns will be inherently smaller than on non-polar columns. The retention on polar columns is also more sensitive to small amounts of impurities[18]. The listed confidence intervals are fairly typical for retention indices determined for solutes covering a wide range of polarities on more than one packed column prepared from the stationary phase.

The precision depends also on the reference compounds used. The confidence interval of the classical Kovats' indices on TCEP was as high as 20 index units, whereas the *n*-alkan-1-ol indices on these columns could be reproduced within 6 index units. For squalane the opposite holds true. The *n*-aldehydes (reference compounds of a median polarity) show a fair precision on all columns investigated.

Table III compares the measured Kovats' indices with published data. The agreement for squalane is fair. For the more polar Carbowax 20M a systematic error, well beyond the limits of experimental error, is observed.

TABLE III

COMPARISON OF MEASURED WITH PUBLISHED KOVATS' RETENTION INDICES FOR *n*-ALKYLBENZENES AT 100°

Reference compound	*Squalane*				*Carbowax 20M*		
	Measured	*Ref. 22*	*Ref. 4*	*Ref. 15*	*Measured*	*Ref. 22*	*Ref. 15*
Benzene	647	650	649	649	956	947	971
Methylbenzene	757	760	757	757	1059	1043	1066
Ethylbenzene	850	850	847		1147	1127	
n-Propylbenzene	939	938	936		1227	1205	
n-Butylbenzene	1038	1037	1035		1327	1302	
n-Pentylbenzene	1133	1133	1134		1424	1394	
n-Hexylbenzene		1231			1519	1489	

Table IV shows the relationship between Kovats' indices and the other retention indices. The latter can be transformed into Kovats' indices by adding a constant factor, the functional constant *FU*. These factors and the standard deviation between the thus obtained and the measured Kovats' indices are shown in Table IV. Usually the standard deviation is smaller than the combined confidence intervals. The assumptions underlying eqns 2 and 3 hold within the experimental error. Only the slopes of the *n*-alkan-1-ols and the *n*-alkylbenzenes differ more than allowed for by the experimental uncertainties.

TABLE IV

RELATIONSHIP BETWEEN KOVATS' INDICES AND ALTERNATIVE RETENTION INDICES. THE FUNCTIONAL CONSTANT $FU_{y1,y2}$

a = functional constant $FU_{y1,y2}$; b = standard deviation between Kovats' indices calculated via the functional constant and determined directly; c = combined confidences intervals of the means on a level of significance of 95%.

Column		*Reference: 1*		*2*						
		n-Alkane	*n-Alk-1-ene*	*1-Chloro-n-alkane*	*n-Aldehyde*	*n-Alkan-2-ol*	*n-Alkan-1-ol*	*1-Amino-alkane*	*n-Alkyl-benzene*	*n-Alkyl-cyclohexane*
Squalane	a	0	−319	−170	−253	−51			−247	−248
	b	0	4	1	1	3			12	10
	c	(4)	(4)	(6)	(6)	(6)			(6)	(6)
DOS	a	0	−299	−107	−153	96	− 34		−181	−246
	b	0	5	5	5	2	8		10	7
	c	(3)	(4)	(4)	(4)	(4)	(5)		(5)	(6)
Carbowax 20M	a	0	−255	56	90	401	325	100	41	−197
	b	0	5	7	5	5	13	7	12	6
	c	(4)	(7)	(6)	(6)	(7)	(6)	(8)	(6)	(7)

Comparing the merits of the other retention index systems, it is evident that *n*-alkylbenzenes and *n*-alkylcyclohexanes are not very practical for low-molecular-weight substances. The lowest applicable members, ethylbenzene and ethylcyclohexane, have retention times at least as high as that of octane. For high-temperature chromatography, however, they might have advantages over homologues with a low-molecular-weight functional group. The *n*-alkanes are not to be recommended for highly polar phases, whereas the *n*-alkan-1-ols are unsuitable for non-polar phases. The *n*-alk-1-enes show similar behaviour to the *n*-alkanes. The first member of the *n*-alkan-2-ols showing a linear methylene increment is *n*-butan-2-ol. Ketones, which have been suggested as reference compounds[6,8], should show a similar behaviour.

Neither of the series is a practical reference for solutes with volatilities comparable to hexane or less. The 1-aminoalkanes are not to be recommended as references for an index system. The 1-chloro-*n*-alkanes may be used except for high polarity phases. The aldehydes give reproducible data on all phases. They are superior in this respect to the *n*-alkanes. Even propionaldehyde shows, with the exception of squalane, a constant methylene increment. The odour and the instability of aldehydes towards oxygen are not serious problems if aldehydes are kept in appropriate vials[7]. The data show that within a confidence interval of 2 index units the difference between even and odd members of the homologous series can be neglected[19].

Polarity values based on Kovats' indices and the aldehyde indices are compared in Table V. The aldehyde polarities do not increase as much as the *n*-alkane polarities. The aldehyde polarity of benzene decreases with increasing polarity of the stationary phase. The aldehydes make the effect of phase polarity on relative retention more obvious[16]. Their values for highly polar phases are more accurate than those based on *n*-alkanes.

TABLE V

POLARITY SCALE BASED ON KOVATS' (1) AND THE ALDEHYDE RETENTION INDICES (4)

(1) $= I^{x}_{\text{alkane}} - I^{\text{squalane}}_{\text{alkane}}$; (4) $= I^{x}_{\text{aldehyde}} - I^{\text{squalane}}_{\text{aldehyde}}$.

Probe (x)	*Squalane*		*DOS*		*Carbowax 20M*		*TCEP*	
	(1)	*(4)*	*(1)*	*(4)*	*(1)*	*(4)*	*(1)*	*(4)*
Benzene	0	0	74	−22	309	−30	491	−106
Ethanol	0	0	190	97	554	214	782	189
Butan-2-one	0	0	115	19	379	39	665	64
Nitromethane	0	0	232	135	711	366	988	462
Pyridine	0	0	123	24	492	148	747	222
Total	0	0	734	253	2445	737	3673	831

If aldehydes are not available or precluded from use for other reasons, one should quote retention data by referring to homologous which are similar to the solutes of interest. These data are on the whole proportional to Kovats' indices. However, in using the latter for polar stationary phases, one of the main advantages of retention indices is lost, namely reproducibility and insensitivity towards experimental parameters. This is especially important for analytical work.

Polarity scales using the index differences of certain probes on two phases have to be based on the same reference. If one employs a polarity scale based on the variance of a set of standard solutes, as has been proposed[18], one may compare retention indices referred to different reference systems. The variance is not effected by the choice of reference provided eqns. 2 and 3 hold. Attempts to analyse retention indices for the basics of the retention mechanism by means of factor analysis or pattern recognition[20,21] are also independent of the reference chosen.

ACKNOWLEDGEMENTS

The authors thank H. H. Oelert for helpful discussions and J. Stremmler for his support in carrying out the experiments.

REFERENCES

1 E. sz. Kovats, *Advan. Chromatogr.*, 1 (1965) 229.
2 G. Schomburg and G. Dielmann, *J. Chromatogr. Sci.*, 11 (1973) 151.
3 G. Dahlmann, H. J. K. Köser and H. H. Oelert, *J. Chromatogr.*, 171 (1979) 398.
4 L. Sojak and J. A. Rijks, *J. Chromatogr.*, 119 (1976) 505.
5 A. Gröbler, *J. Chromatogr. Sci.*, 10 (1972) 128.
6 R. G. Ackman, *J. Chromatogr. Sci.*, 10 (1972) 535.
7 S. J. Hawkes, *J. Chromatogr. Sci.*, 10 (1972) 536.
8 J. Novák and J. Ružičková, *J. Chromatogr.*, 91 (1974) 79.
9 G. Castello and G. D'Amato, *J. Chromatogr.*, 131 (1977) 41.
10 J. R. Ashes and J. K. Haken, *J. Chromatogr.*, 101 (1974) 103.
11 L. Mathiasson, J. A. Jönsson, A. M. Olsson and L. Haraldson, *J. Chromatogr.*, 152 (1978) 11.
12 G. Castello, G. D'Amato and E. Biagini, *J. Chromatogr.*, 41 (1969) 313.
13 W. E. Sharples and F. Vernon, *J. Chromatogr.*, 161 (1978) 83.
14 J. R. Ashes, S. C. Mills and J. K. Haken, *J. Chromatogr.*, 166 (1978) 391.
15 L. Rohrschneider, *J. Chromatogr.*, 22 (1976) 6.
16 W. A. Aue and V. Paramasigamani, *J. Chromatogr.*, 166 (1978) 253.
17 J. R. Conder, *J. Chromatogr.*, 39 (1969) 273.
18 G. Dahlmann, H. J. K. Köser and H. H. Oelert, *J. Chromatogr. Sci.*, 17 (1979) 307.
19 M. S. Vigdergauz and V. I. Seomkin, *J. Chromatogr.*, 158 (1978) 57.
20 P. H. Weiner and J. F. Parcher, *Anal. Chem.*, 45 (1973) 302.
21 S. Wold and K. Andersson, *J. Chromatogr.*, 80 (1973) 43.
22 W. Engewald and L. Wennrich, *Chromatographia*, 9 (1976) 540.

Journal of Chromatography, 192 (1980) 117–125

CHROM. 12,616

NON-LINEAR RESPONSES OF THE ELECTRON-CAPTURE DETECTOR TO ALKYL MONOCHLORIDES

E. P. GRIMSRUD and D. A. MILLER
Department of Chemistry, Montana State University, Bozeman, Mont. 59717 (U.S.A.)
(First received October 30th, 1979; revised manuscript received December 7th, 1979)

SUMMARY

Calibration curves for the response of a constant-current electron-capture detector with a ^{63}Ni ionization cell to methyl and ethyl chloride are reported to be non-linear. The molar response to low-concentration samples is shown to be very much greater than to high-concentration samples. Oxygen contamination of the carrier gas is investigated as a likely cause of the low-concentration, increased responses, but this possibility is not supported by the experiments reported here. Other possible causes are discussed. Superior calibration curves for alkyl monochlorides are obtained by the use of intentionally oxygen-doped carrier gas.

INTRODUCTION

One of the most significant improvements made in the pulsed electron-capture detector (ECD) for gas chromatography (GC) occurred with the introduction of the constant-current or frequency-modulated mode of signal processing[1]. While possessing the high sensitivity and specificity characteristic of all ECD configurations, this mode of operation greatly extended the linear dynamic range of response of the pulsed ECD from two to four or five orders of magnitude change in the sample concentration. This wide range of linear response has been demonstrated for many electron-attaching molecules (ref. 2, for example). Some exceptions to linearity have been observed for the cases where the sample molecule attaches electrons so rapidly that its concentration within the cell is altered by the electron-capture process itself. Lovelock and Watson[3] recently described and explained this anomaly of the constant-current ECD for the case of CCl_3F. For most molecules, however, for which the electron attachment rates are not ultra fast, linear responses have come to be expected when using the constant-current ECD.

In this paper the responses of a constant-current ECD to simple alkyl chlorides are described, and are shown to be non-linear under all of the conditions examined here. While the ECD is used most frequently for polychlorinated molecules, to which it responds extremely sensitively, the ECD is also used for the analysis of many other classes of compounds, such as mono- and dichlorinated hydrocarbons, to which it may respond three to five orders of magnitude less sensitively. The analysis of methyl

chloride in air, for example, has been performed using the ECD[4–6], undoubtedly because of its lack of response to potentially interfering hydrocarbons. For these compounds linear responses might have been expected since their electron attachment rates are relatively slow. The intention of this article is to characterize and discuss the non-linear responses observed for alkyl chlorides so that improved accuracies in the analysis of these compounds by the ECD might result.

This study is also motivated by a recently discovered application of the ECD —the use of oxygen doping of the carrier gas for obtaining improved responses to alkyl chlorides[7–9]. In addition to providing greater sensitivity, another potential application of oxygen doping is the use of "response enhancement" values which might facilitate the identification of unknown sample components. A response enhancement value for a given compound is the ratio of its ECD responses with and without oxygen added to the carrier gas. This application of the ECD, however, requires that the normal response, as well as the oxygen-caused responses, be well understood.

EXPERIMENTAL

All halocarbons studied were reagent-grade obtained from commercial suppliers. Standards of methyl and ethyl chloride were prepared by the successive dilution of the pure compound into nitrogen gas using airtight glass flasks and carboys. Standards for 1,4-dichlorobutane and tetrachloroethylene were prepared by dilution into hexane.

The gas chromatograph used for most of these studies is a Varian 3700 Aerograph with constant-current, pulse-modulated operation of a ^{63}Ni detector. A 10 ft. × 1/8 in. stainless-steel column packed with 10% SF-96 on Chromosorb W was used at oven temperatures of 30 to 60°. The GC flow-rate was 30 ml/min. The detector temperature was 300°. Gaseous samples were introduced to the gas chromatograph using a 2-ml volume sample loop (Carle 8030). Liquid samples were introduced with a 10-μl syringe and the normal injection port.

RESULTS AND DISCUSSION

In Fig. 1 are shown the ECD responses measured as peak heights in units of kHz (ref. 2) to methyl and ethyl chloride in the small sample concentration range where the sample size is increased to about 500 times the detection limit. It is seen in each case that only a narrow range of approximate linearity exists prior to the onset of curvature and diminished molar response. For more strongly electron capturing molecules, the instrument used here has been shown in our laboratory and elsewhere[2] to provide linear responses up to peak heights correspondnig to pulse frequencies of 100 kHz. For the molecules examined here the range of initial linearity extends only to considerably less than 1 kHz of frequency increase above the baseline frequency of 2 kHz. In Fig. 2 the responses to larger sample sizes of methyl and ethyl chloride are shown. It is seen that a wide, linear plateau of response is observed after the region of curvature. The sensitivity of response in this region is very much less than in the small sample region, especially for the case of ethyl chloride.

We have recently demonstrated that the response of the ECD to mono-

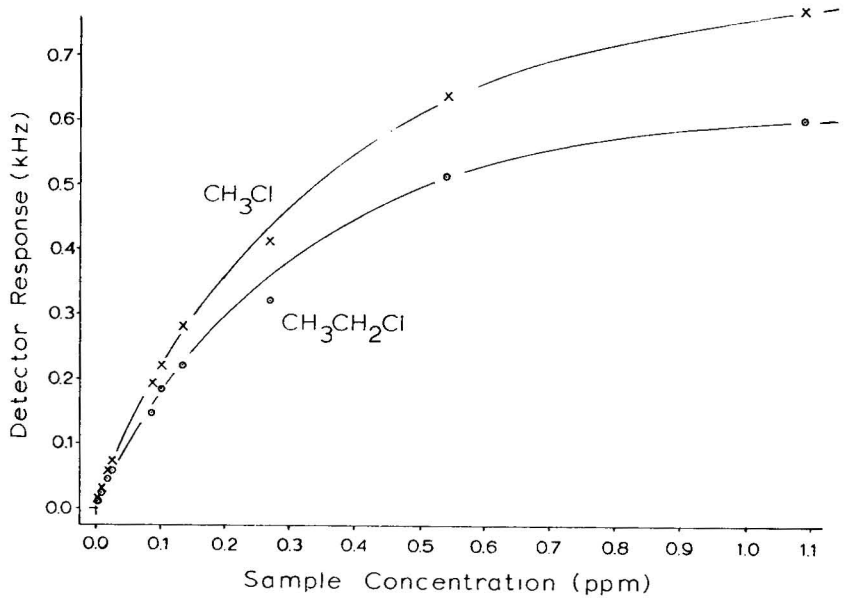

Fig. 1. ECD response to standards in the low-concentration range. Units of sample concentration are molar ratio (ppm) of gaseous sample in nitrogen. Detector temperature 300°.

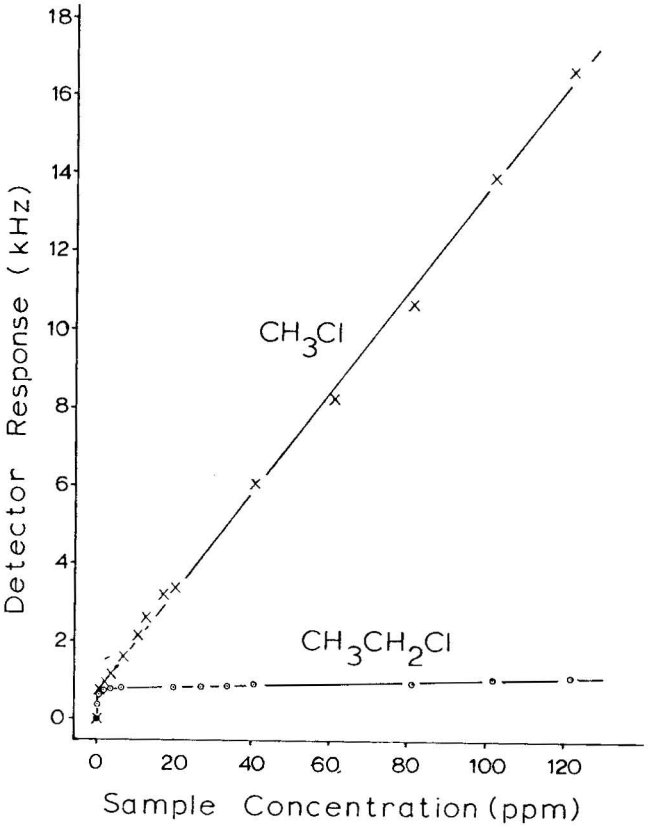

Fig. 2. ECD response to standards throughout wide range of concentration.

chlorinated aliphatic hydrocarbons can be greatly increased by the intentional addition of oxygen to the carrier gas[7–9]. For this reason it was initially suspected that the effects shown in Figs. 1 and 2 may be due to traces of oxygen frequently present in sources of nitrogen carrier gas. Considering this possibility for the moment, at very small sample sizes, reaction 1

$$O_2^- + RCl \rightarrow Cl^- + \text{neutrals} \tag{1}$$

may provide the fastest means of sample ionization, as long as the sample size is small. If reaction 1 occurs, the negative charge is then irreversibly held by Cl^-, rather than O_2^- which would rapidly release the electron. The steady-state electron density of the ECD plasma would be thereby reduced, causing a response. This mechanism is discussed in detail in previous studies of oxygen's effects[9,10]. At higher sample sizes, the steady-state O_2^- negative ion concentration may be depleted by reaction 1, and the slower electron-capture reaction 2,

$$e^- + RCl \rightarrow Cl^- + \text{neutrals} \tag{2}$$

must provide any further increase in response as the sample size is increased. The observation that the slope of the high-concentration plateau for methyl chloride in Fig. 2 is significantly larger than that for ethyl chloride would be taken to indicate that its electron capture rate is greater. A portion of the difference in these slopes, however, will also be attributed to a dilution effect of the solute in the carrier gas where the larger compound's retention time and longitudinal spreading within the column is greater.

We have conducted several experiments designed to test whether or not the initial portion of the calibration curves are being determined by the trace presence of oxygen. We have added oxygen scrubbers to the carrier system which are reported to remove trace oxygen to less than 1 ppm. The normal carrier gas was ultra high purity nitrogen guaranteed to contain less than 10 ppm oxygen. The addition of the oxygen scrubber had only small effects (less than 10% reduction of responses) on the calibration curves of Figs. 1 and 2. Calibration curves were also obtained with oxygen intentionally added to the carrier gas. These are shown in Fig. 3 for methyl chloride with 30 ppm oxygen added to the carrier gas. It is seen in Fig. 3 that the addition of oxygen does amplify the initial portion of the calibration curves somewhat. However, if the initial responses for the case where no oxygen has been added are assumed to be proportional to trace oxygen, Fig. 3 would imply that the oxygen concentration of the undoped carrier is roughly 100 ppm, much higher than is expected of our carrier gas.

It is always possible that the oxygen content of a carrier gas is much higher in the detector than in the purified carrier further upstream, due to leaks in the flow system. This is especially true if leaks occur at the column–detector interface where the system pressure is only slightly above atmospheric pressure. For this reason we performed another experiment by which it appears a very large fraction of any trace oxygen entering the detector can be removed. This is done by a procedure which was discovered accidentally while cleaning our detector with hydrogen as recommended by the instrument manufacturer. For a period of time of about one hour after flowing

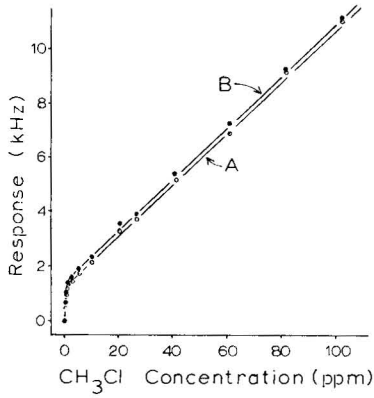

Fig. 3. ECD response to methyl chloride standards using (A) high purity nitrogen carrier gas and (B) nitrogen carrier gas doped with 30 ppm oxygen.

hydrogen gas at high temperature through the detector and the transfer line leading to it, the transfer line apparently becomes activated by the hydrogen and then has the capacity for removing oxygen in the carrier stream. Evidence for this effect is shown in Fig. 4, where chromatograms of the same standard containing ethyl chloride in utility-grade nitrogen are shown. In Fig. 4A a peak due to oxygen in this contaminated nitrogen source, as well as one due to added ethyl chloride, is observed. Following treatment of the detector with hydrogen at high temperature, a repeated analysis is shown in Fig. 4B. The peak due to oxygen is now absent. Upon repeated analyses, the oxygen peak begins to reappear in about one hour and increases steadily until the original peak height is reestablished. It appears that this effect is due to a surface reaction removing trace oxygen probably within the transfer line. That it is not due to a gas-phase reaction involving small amounts of hydrogen within the ECD cell itself, was indicated by our observation that the suppression of the oxygen peak is not caused by doping the carrier gas with small amounts of hydrogen.

The chromatograms in Fig. 4 indicate that with the transfer line so activated, remaining traces of oxygen in the carrier gas should be further reduced to a small

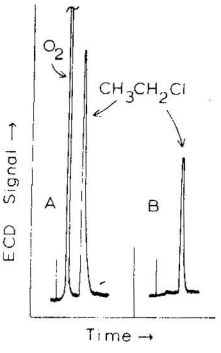

Fig. 4. Chromatograms of a standard containing 0.68 ppm ethyl chloride in nitrogen which is also contaminated with oxygen, (A) prior to hydrogen cleaning and (B) immediately following hydrogen cleaning of the detector.

fraction of the concentration present in the already purified carrier. Thus, analyses performed under this condition might be assumed to be uncommonly free of oxygen contamination. Calibration curves for ethyl chloride obtained before and after hydrogen activation of the detector transfer lines are shown in Fig. 5. It is seen that with this procedure the magnitude of the initial response region has been reduced, but only to about one-half of its original level. If oxygen had been the only cause of non-linearity, a much greater reduction of response might have been anticipated. It appears from this test, also, that something other than trace oxygen is a major cause of the high responses toward these compounds at low concentrations.

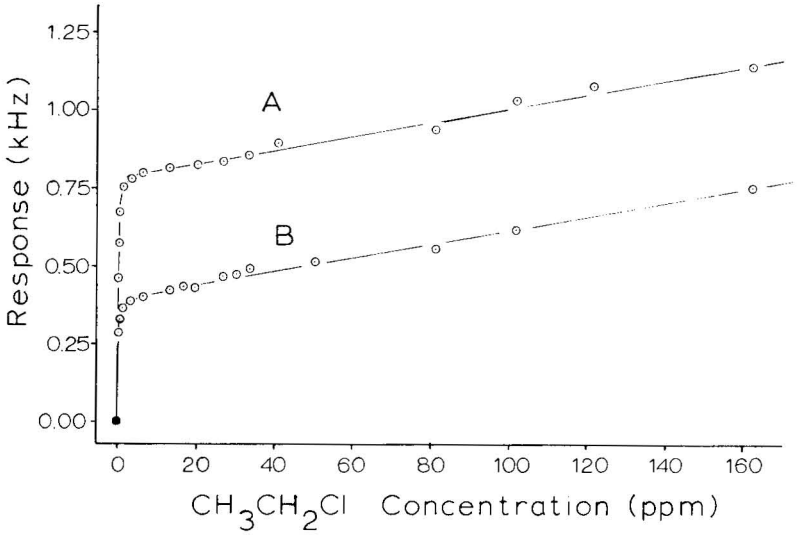

Fig. 5. ECD response to ethyl chloride standards (A) prior to hydrogen cleaning and (B) immediately following hydrogen cleaning of the detector.

At this time we can only speculate as to the basis of the unusual responses observed for monochloroalkanes (we have observed these effects for *n*-propyl and *n*-butyl chloride also). One possibility is that the carrier gas contains an impurity other than oxygen which causes this effect. Perhaps the partial removal of this unknown substance caused the decreased signals observed in Fig. 5 following treatment of the detector with hydrogen. The use of several different sources of carrier gas, however, has produced similar results. The possibility that column bleed provides this unknown impurity was not supported in an experiment where the peak areas of several small-concentration samples were found to be independent of changes in the temperature of the column. The responses of completely different instruments using various columns, carrier gases, detectors and signal processing methods were compared using a sample containing 1,4-dichlorobutane in hexane. These results are shown in Table I. Instrument A is the Varian 3700 used for all the experiments described above. Instrument B is another Varian 3700 with a similar ECD. This instrument is used daily for routine environmental analyses in another laboratory on our campus. Its response is also derived by the constant-current method. Its carrier

TABLE I

RESPONSES OF VARIOUS ^{63}Ni ECD GAS CHROMATOGRAPHS TO 1,4-DICHLOROBUTANE AND TETRACHLOROETHYLENE

Responses are determined from peak heights and have been converted to the functions indicated. The function $(I_0-I)/I$ is explained in the text. Responses relative to that of the lowest concentration sample in each case are shown in parentheses. Instruments A, B and C are described in the text. Instrument C was used with nitrogen and argon–10% methane carrier gases.

*Relative concentration**	*Intrument*							
	A, *kHz*		*B*, *kHz*		*C* (N_2), $(I_0-I)/I$		*C* $(Ar-CH_4)$, $(I_0-I)/I$	
1,4-Dichlorobutane								
1	0.12	(1)	0.030	(1)	0.065	(1)	0.036	(1)
5	0.41	(3.4)	0.089	(3.0)	0.20	(3.1)	0.141	(3.8)
50	0.88	(7.1)	0.18	(6.0)	0.43	(6.6)	0.21	(5.8)
500	3.2	(23)	0.85	(28)	0.70	(10.8)	0.28	(7.8)
Tetrachloroethylene								
1	0.56	(1)			0.024	(1)		
2.5	1.20	(2.2)			0.055	(2.3)		
12.5	6.8	(12.2)			0.25	(10.2)		
25	14.8	(26)			0.51	(22)		
100	63.2	(105)			2.1	(90)		

* The concentrations of the smallest samples of 1,4-dichloroethylene and tetrachlorobutane in the 2 μl of hexane injected were $5.0 \cdot 10^{-10}$ g/μl and $1.3 \cdot 10^{-12}$ g/μl, respectively.

gas is nitrogen with a Varian oxygen trap. Its column is glass packed with a 6% QF-1 + 4% SE-30 stationary phase. Instrument C is a home-built gas chromatograph–ECD incorporating ^{63}Ni ionization detector of 1 ml volume. A 1/16 in. anode pin extends the length of its cylindrical geometry. This signal from this instrument was processed as the function $(I_0-I)/I$ where I_0 is the standing current obtained with 50 V pulses of 1.5 μsec duration and a period between pulses of 350 μsec, and I is the ECD current remaining at the point of maximum response to the sample. This function has been shown to provide the greatest range of linear response for the fixed frequency, pulsed ECD[11]. Instrument C contained a column packed with SF-96, and both nitrogen and argon–10% methane carrier gases were used with oxygen removing traps. It is seen in Table I that all instruments respond to 1,4-dichlorobutane, also, in a pronounced non-linear manner. Furthermore, instrument C responds non-linearly whether the carrier gas is nitrogen or argon–methane. To demonstrate that these instruments are, indeed, capable of responding linearly to more strongly electron-attaching compounds, the response of instruments A and C to tetrachloroethylene is also shown in Table I.

Another potential explanation for the responses observed of a completely different nature may be worthy of consideration. If the set of electrons within the ECD do not all have precisely the same energy, the possibility exists that the initially greater response to small samples of the alkyl chlorides is due to the faster electron attachment reactions of a fraction of the total electron population, which possesses greater than average energy. It has been shown[12] that the rates of electron attachments to 1,2-dichloroethane, for example, increases rapidly with small increases in the

electron energy above thermal energy. Electrons within the ECD have been produced initially at higher-than-thermal energies by ^{63}Ni β-radiation of the carrier gas. These electrons are generally thought to be thermalized rapidly by inelastic collisions in nitrogen or argon–methane carrier gas so that all electrons can be assumed to have the same energy determined simply by the temperature of the gas[13]. As this assumption has not yet been examined in great detail, however, it remains possible that small, but significant differences in the energies of the electrons exist, and that for some weakly electron attaching molecules some dependence of reactivity on these energy differences may be observable under conditions of the ECD. While this possibility has little precedence in the ECD literature, it is being investigated further in our laboratory.

We have recently described an improved analysis procedure for alkyl chlorides which results when relatively large amounts of oxygen are added to the carrier gas of a constant-current ECD. In Fig. 6 the calibration curve for methyl chloride is shown where the nitrogen carrier gas also contains 2000 ppm added oxygen. In comparing this with the calibration curve for CH_3Cl obtained under normal conditions shown in Fig. 1, the use of the oxygen-doped carrier is clearly recommended. Not only is the detector response to a given quantity of sample much greater with the oxygen-doped carrier, but also a linear calibration curve is obtained which passes through the origin and, as has been shown elsewhere[8], extends the full linear dynamic range (to 100 kHz) expected for this instrument.

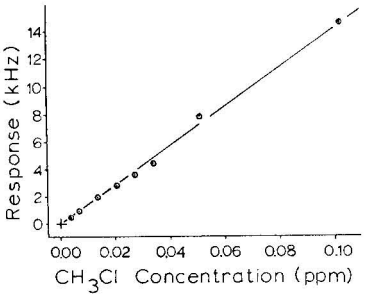

Fig. 6. ECD response to methyl chloride samples using nitrogen carrier gas doped with 2.0 parts per thousand oxygen. Detector temperature 300°.

In the use of oxygen-doping for the determination of response enhancements[7–9], however, caution is necessary because of the non-linearity of the normal response shown in Fig. 1. Our response enhancement measurements for methyl chloride will be reasonably constant only in the concentration range 0.0–0.1 ppm, where the calibration curve in Fig. 1 is reasonably constant. With higher concentrations of methyl chloride, the measured response enhancement caused by oxygen doping will increase continuously with increased sample size. In the use of response enhancement measurements for compound identification, therefore, it is recommended that the range of linear response of the instrument to each sample component be established under the normal oxygen-free carrier gas condition, and that response enhancement values then be used only for sample sizes within this range.

CONCLUSIONS

Regardless of the cause of the non-linearity of response of the ^{63}Ni ECDs to alkyl chlorides, which as been characterized here but not identified, it seems likely that this may constitute a common source of error wherever the ECD is used for the analysis of simple alkyl chlorides. Although we have altered our experimental conditions in many ways, we have as yet been unable to obtain linear responses to these compounds using the normal ECD carrier gases. If calibration curves are unwittingly prepared for alkyl monochlorides from the measured responses of a few high concentration standards (which is often the easiest procedure) and by forcing the calibration line to pass through zero response at zero sample concentration, very large errors in subsequent analyses of small sample sizes will result. In spite of the wide linear dynamic range commonly associated with the constant-current ECD, it remains necessary to carefully check the response of the instrument over the entire concentration range to be used for each type of compound analyzed. The basis of the non-linear calibration curves described here is under continued investigation in hopes that this GC detector might be more completely understood and controlled. The use of oxygen-doped carrier gas is strongly recommended in the analysis of alkyl monochlorides by the ECD as higher sensitivity and a linear calibration curve are thereby enjoyed.

ACKNOWLEDGEMENT

This material is based upon work supported by the National Science Foundation under Grant CHE-7824515.

REFERENCES

1 R. J. Maggs, P. L. Joynes, A. J. Davies and J. E. Lovelock, *Anal. Chem.*, 43 (1971) 1966.
2 P. L. Patterson, *J. Chromatogr.*, 134 (1977) 25.
3 J. E. Lovelock and A. J. Watson, *J. Chromatogr.*, 158 (1978) 123.
4 J. E. Lovelock, *Nature (London)*, 256 (1975) 193.
5 R. A. Cox, R. G. Derwent, A. E. J. Eggleton and J. E. Lovelock, *Atmos. Environ.*, 10 (1976) 305.
6 H. B. Singh, L. Salas and A. Crawford, *Atmos. Environ.*, 11 (1977) 819.
7 E. P. Grimsrud and D. A. Miller, *Anal. Chem.*, 50 (1978) 1151.
8 E. P. Grimsrud and D. A. Miller, *Special Publication 519*, National Bureau of Standards, Washington, D.C., April, 1979.
9 D. A. Miller and E. P. Grimsrud, *Anal. Chem.*, 51 (1979) 851.
10 E. P. Grimsrud and R. G. Stebbins, *J. Chromatogr.*, 155 (1978) 19.
11 D. C. Fenimore, A. Zlatkis and W. E. Wentworth, *Anal. Chem.*, 40 (1968) 1594.
12 J. P. Johnson, L. G. Christophorou and J. G. Carter, *J. Chem. Phys.*, 67 (1977) 2196.
13 W. E. Wentworth, E. Chen and J. E. Lovelock, *J. Phys. Chem.*, 70 (1966) 445.

Journal of Chromatography, 192 (1980) 127–134

CHROM. 12,582

STUDIES ON OPEN-TUBULAR MICROCAPILLARY LIQUID CHROMATOGRAPHY

VI. STYRENE–DIVINYLBENZENE COPOLYMER STATIONARY PHASE

TOYOHIDE TAKEUCHI, KIYONARI MATSUOKA, YOICHI WATANABE and DAIDO ISHII

Department of Applied Chemistry, Faculty of Engineering, Nagoya University, Chikusa-ku, Nagoya-shi 464 (Japan)

(Received December 3rd, 1979)

SUMMARY

Styrene–divinylbenzene copolymer is formed on the inner surface of a glass capillary tube of *ca.* 0.05 mm I.D. and *ca.* 5 m in length, by thermal, catalytic and radiation-induced polymerizations. The polymerization conditions that give good results chromatographically are thermal polymerization for 20 h at 100–260°. These polystyrene glass capillary columns can be employed for separations of aromatic hydrocarbons and phthalates in reversed-phase system. No bleeding of the stationary phase from the column is observed when various organic solvents are used.

INTRODUCTION

Recently, interest has developed in liquid chromatography (LC) with the use of microbore capillary columns that give higher efficiencies in terms of theoretical plate numbers than those used in ordinary high-performance liquid chromatography (HPLC). At present, three types of these columns are available: (1) packed microbore columns[1–3]; (2) packed microcapillary columns[4,5]; and (3) open-tubular microcapillary columns[6–12].

Columns of length 10 m and I.D. 1 mm packed with commercially available silica gel are commonly employed for packed microbore columns[1–3], giving 250,000 theoretical plates, the highest of the three types of column, at the dead volume (retention time 4–6 h). Columns of length 10–40 m and I.D. 0.06–0.08 mm packed with alumina (particle diameter 30 μm)[4], sometimes followed by the bonding of various silanes so as to obtain different selectivities[5], have been used for the packed microcapillary columns and 85,000 theoretical plates have been attained for quinoline (retention time 100 min) on a 20 m × 0.075 mm I.D. alumina-packed microcapillary column[4]. About 10,000–20,000 theoretical plates were attained for aromatic amines (retention time 30 min) on 5 m × 0.05 mm I.D. glass open-tubular microcapillary column coated with β,β'-oxydipropionitrile (BOP)[11].

For open-tubular microcapillary columns the theoretical plate number is inversely proportional to the square of the column diameter, and can therefore be increased by using a narrower bore column. A relatively low inlet pressure (less than 300 p.s.i.) is required in order to pass the eluent at 1 cm/min (linear velocity) into a 5 m × 0.05 mm I.D. open-tubular microcapillary column. This suggests that it might be possible to develop longer and/or narrower open-tubular microcapillary columns that have higher efficiencies, if the pumping, sample injection and detection systems could be improved.

We have studied open-tubular microcapillary liquid chromatography (OMCLC) for a few years and have developed several types of columns, such as physically coated[8,11], chemically bonded[9] and support-deposited columns[13]. For the physically coated columns, SE-30[8], BOP[11] and polyethylene glycols (PEG)[11] were coated on the surface of glass capillary after appropriate pre-treatments and, if a mobile phase saturated with each stationary phase was employed, long-term stability of the columns was observed.

Octadecylsilane was examined as the stationary phase for the chemically bonded columns[9] and was found to be more stable than those of physically coated columns.

For the deposited columns, soda-lime glass columns treated with aqueous alkaline solutions were investigated[13]. It was found that silica gel was deposited on the glass surface by treatment with 1 *N* sodium hydroxide solution for 2–6 days at 25–55° and functioned as the adsorbent in a normal-phase system.

In this work, we have examined the formation of polystyrene on the inner surface of a glass capillary and employed it as a stationary phase in a reversed-phase system, while styrene–divinylbenzene copolymer was employed as the packing material for gel permeation and partition chromatography or as the matrix for ion-exchange resins in LC. Thermal, catalytic and radiation-induced polymerizations were tried and polymerization conditions such as temperature, time and proportions of styrene and divinylbenzene were examined, using aromatic hydrocarbons as test samples.

EXPERIMENTAL

All reagents were purchased from Wako (Osaka, Japan). Styrene monomer was of practical grade and the divinylbenzene had a content of about 55%.

The apparatus is the same as that used in previously reported work[8]. A microfeeder and a 100-μl gas-tight syringe were used for the pumping system and a UVIDEC-100 UV spectrometer (with a modified micro flow cell) (Japan Spectroscopic Co., Hachioji-shi, Japan) for the detection system.

Soda-lime glass was selected as the glass material, as pre-treatment with an alkaline solution was effective for surface modification of this glass, as reported earlier[11,13]. Glass capillaries, 0.6–0.7 mm O.D. and 0.05–0.06 mm I.D., were prepared with a GDM 1 glass drawing machine (Shimadzu Seisakusho, Kyoto, Japan), followed by pre-treatment with 1 *N* sodium hydroxide solution for 2 days at 25–50°.

Subsequent to the pre-treatment, the glass capillary was washed with methanol until the eluent became neutral and then with dichloromethane. A mixture of 10% (v/v) of styrene monomer and 0.1–4% (v/v) of divinylbenzene in dichloromethane (with benzoyl peroxide as a catalyst for catalytic polymerization) was coated on the

inner surface of the glass capillary by dynamic coating and dried in a stream of nitrogen for 30 min at room temperature (25–30°). Then both ends of the glass capillary were closed and polymerization was promoted. For the thermal and catalytic polymerizations, coated glass capillaries were placed in an oven and heated to the reaction temperature at the rate of 4°/min and kept at that temperature for 2–20 h. For the radiation-induced polymerization, the glass capillaries were placed 10 cm from the γ-ray source (^{60}Co), where the absorbed dose was $3.4 \cdot 10^5$ rad/h and the temperature was about 25°. With irradiation for *ca.* 23 h, the total absorbed dose was *ca.* 8 Mrad.

Finally, each polymerized column was washed with mobile phase (acetonitrile–water), acetonitrile, dichloromethane, tetrahydrofuran, acetonitrile and mobile phase (*ca.* 100 μl of each).

RESULTS AND DISCUSSION

Effect of pre-treatment with alkaline solution

It was observed previously[11] that polar liquid phases such as BOP and PEG were well dispersed on the inner surface of a soda-lime glass capillary treated with 1 *N* sodium hydroxide solution, owing to the deposition of silica gel by that treatment[13]. Therefore, good dispersion of styrene and divinylbenzene on surfaces treated with alkaline solution was expected.

After pre-treatment with 1 *N* sodium hydroxide solution at different temperatures had been carried out, thermal polymerization was promoted. Subsequently, mobile phase was passed into the column. After the baseline had stabilized, the samples were injected and the k' values were measured.

The k' values of biphenyl on columns treated at different temperatures are listed in Table I, including that for a column without pre-treatment. Whereas the k' value without pre-treatment is zero, the higher temperature treatment gives a larger

TABLE I

EFFECT OF PRE-TREATMENT TEMPERATURE ON RETENTION

Pre-treatment: column filled with 1 *N* sodium hydroxide solution for 2 days at different temperatures. Polymerization conditions: thermally polymerized for *ca.* 20 h at 200°. Mobile phase: acetonitrile–water (30:70). Sample: biphenyl.

Treatment temperature (°C)	*k' value*
No treatment	0
27	0.3
40	1.2
50	1.3

k' value. This suggests that styrene and divinylbenzene are well dispersed on the treated surface. Pre-treatments at temperatures higher than 60° were not examined as no useful results were obtained at these temperatures in the previous work[13].

As treatments at 40° and 50° gave nearly same results, soda-lime glass capillaries were treated at 40–50° in all subsequent examinations.

Effect of concentration of divinylbenzene in styrene

A dichloromethane solution of styrene containing 0–18% (mole/mole) of divinylbenzene was coated on the column, dried in a stream of nitrogen and thermally polymerized for 20 h at 200°.

The relationship between the retention of a sample and the concentration of divinylbenzene is shown in Fig. 1. As the concentration of divinylbenzene increases, the k' value of biphenyl increases when thermal polymerization is used. In the absence of divinylbenzene, polystyrene was dissolved in the mobile phase and the retention of the sample decreased during a chromatographic run, whereas with polystyrene in the presence of divinylbenzene there was no decrease in retention. In the latter instance, the retention increased after the passage of organic solvents such as acetonitrile, dichloromethane and tetrahydrofuran, which probably resulted from the increase in surface area of the stationary phase due to the elution of unreacted monomers or homopolymers from the column.

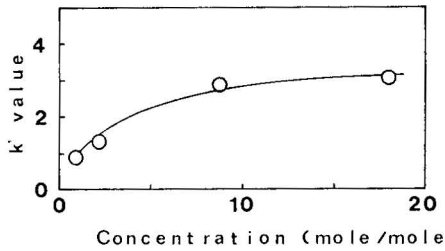

Fig. 1. Effect of concentration of divinylbenzene on retention. Polymerization conditions: thermal polymerization for 20 h at 200°. Mobile phase: acetonitrile–water (30:70). Sample: biphenyl.

Dependence of HETP on concentration of divinylbenzene is shown in Fig. 2. A low HETP value is obtained between 2 and 10% of divinylbenzene. At a concentration of 18%, the peak shape of the largely retained sample ($k' > 1$) was skewed. It is considered that the desirable concentration range of divinylbenzene in styrene is 2–10% (mole/mole).

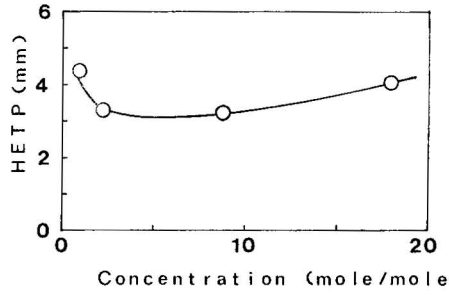

Fig. 2. Effect of concentration of divinylbenzene on HETP. Polymerization conditions as in Fig. 1. Linear velocity: *ca.* 1 cm/min. Sample: biphenyl ($k' = 1$).

Effect of thermal polymerization temperature

A styrene solution containing 8.8% of divinylbenzene was polymerized between 50° and 260° and k' values of the samples were measured. The results are shown in Fig. 3. Nearly same retentions are observed for columns polymerized at 100–260°, whereas biphenyl is not retained on columns polymerized at less than 80° by the use of 30% (v/v) acetonitrile in water as the mobile phase; nor are samples retained in the latter instance by the use of 20% (v/v) acetonitrile in water as the mobile phase, which indicates that the thermal polymerization has hardly been promoted.

The relationship between column efficiency and thermal polymerization temperature is shown in Fig. 4. Nearly the same HETP values are obtained in the region between 100° and 260°.

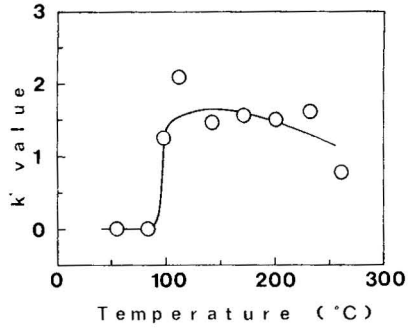

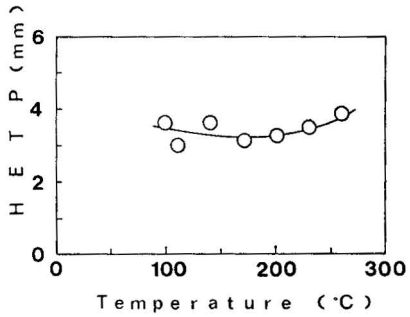

Fig. 3. Effect of polymerization temperature on retention. Polymerization conditions: thermal polymerization for 20 h. Concentration of divinylbenzene: 8.8%. Mobile phase: acetonitrile–water (35:65). Sample: biphenyl.

Fig. 4. Effect of polymerization temperature on HETP. Polymerization conditions as in Fig. 3. Flow-rate: 1.7 μl/min. Sample: biphenyl ($k' = 1$).

Influence of polymerization time

The influence of polymerization time on the retention of samples was examined for thermal and catalytic polymerization. Divinylbenzene (8.8%, mole/mole) was added to styrene for both polymerizations, and 1% (w/v) of benzoyl peroxide was included for the catalytic polymerization. A temperature of 110° was adopted for the thermal polymerization and 80° for the catalytic polymerization. The relationship between the retention of the sample and the polymerization time is shown in Fig. 5. In both instances, as the polymerization time increases the k' values of biphenyl increase. A larger k' value is obtained for the thermal polymerization than for the catalytic polymerization. In addition, it can be concluded that the catalytic polymerization is predominantly promoted in the latter instance as the thermal polymerization is hardly promoted at 80°, as discussed in the preceding section.

Comparison of polymerization methods

At present, the best columns can be obtained by thermal polymerization. The k' values of samples for catalytic and radiation-induced polymerization are lower than that for thermal polymerization, as shown in Table II. It is considered that

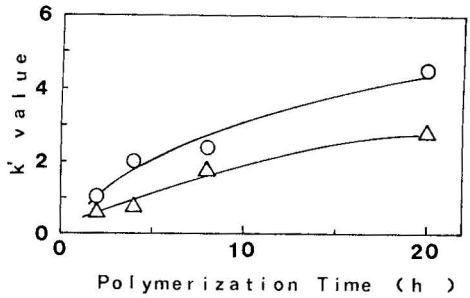

Fig. 5. Relationship between retention of sample and polymerization time. Thermal polymerization at 110° (○); catalytic polymerization at 80° (△). Mobile phase: acetonitrile–water (30:70). Sample: biphenyl.

the polymerization reactions are not adequately promoted in the catalytic and radiation-induced polymerization under the conditions used. Sometimes clogging was caused on passing water into the column, especially when using catalytic and radiation-induced polymerizations.

TABLE II

COMPARISON OF k' VALUES ON COLUMNS PREPARED BY DIFFERENT METHODS

Mobile phase: acetonitrile–water (30:70). Sample: biphenyl.

Polymerization conditions			*Concentration of divinylbenzene (%)*	*k' value*
Method	*Temperature (°C)*	*Time (h)*		
Thermal	110	20	8.8	4.5
Catalytic	80	20	8.8	2.8
Radiation-induced	25	23 (7.8 Mrad)	18	0.2

Effect of amount of sample injected

The effect of amount of sample injected on column efficiency is shown in Fig. 6. An increase in HETP is observed when amounts larger than 10 ng are used.

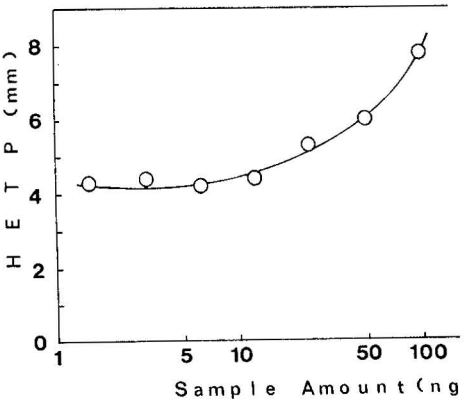

Fig. 6. Effect of amount of sample injected on HETP. Column: 5.4 m × 58 μm I.D. glass capillary. Stationary phase: styrene–divinylbenzene copolymer thermally polymerized for 20 h at 200°. Mobile phase: acetonitrile–water (40:60). Flow-rate: 2.2 μl/min. Sample: biphenyl.

Also, as the amount of sample injected increases, a decrease in k' values is observed. Although the capacity of this polystyrene column is lower than those of SE-30[8] and ODS column[9], the column efficiencies are comparable.

Typical separations of aromatic hydrocarbons and phthalates are shown in Figs. 7 and 8, respectively.

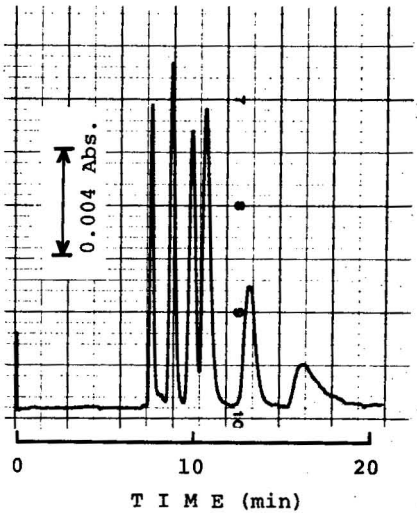

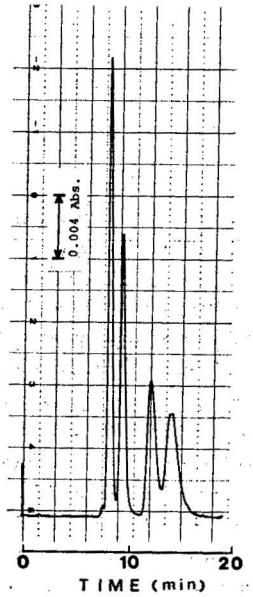

Fig. 7. Separation of aromatic hydrocarbons. Column: 5.4 m × 52 μm I.D. glass capillary. Stationary phase: styrene–8.8% divinylbenzene copolymer thermally polymerized for 20 h at 110°. Mobile phase: acetonitrile–water (50:50). Flow-rate: 1.7 μl/min. Sample: acetonitrile solution containing 180 ng of benzene, 17 ng of naphthalene, 3 ng of biphenyl, 5 ng of fluorene, 0.5 ng of anthracene and 4 ng of pyrene, eluted in that order. Wavelength of detection: 254 nm (UV).

Fig. 8. Separation of phthalates. Column: 5.4 m × 53 μm I.D. glass capillary. Stationary phase: styrene–8.8% divinylbenzene copolymer thermally polymerized for 20 h at 170°. Mobile phase: acetonitrile–water (32:68). Flow-rate: 1.7 μl/min. Sample: acetonitrile solution containing 21 ng of dimethyl, 21 ng of diethyl, 21 ng of diisopropyl and 19 ng of di-*n*-propyl phthalate, eluted in that order. Wavelength of detection: 235 nm (UV).

CONCLUSION

Styrene–divinylbenzene copolymer polymerized on the surface of a soda-lime glass capillary treated with 1 *N* sodium hydroxide solution can be employed as the stationary phase in a reversed-phase system. The optimal polymerization conditions are thermal polymerization for 20 h at 100–260° in the presence of 2–10% of divinylbenzene as the cross-linking material. This stationary phase is useful for the separation of aromatic hydrocarbons and phthalates, and is stable towards organic solvents. It is expected to be possible to introduce ion-exchange groups into this copolymer.

REFERENCES

1 R. P. W. Scott and P. Kucera, *J. Chromatogr.*, 125 (1976) 251.
2 R. P. W. Scott, *Analyst (London)*, 103 (1978) 37.
3 R. P. W. Scott and P. Kucera, *J. Chromatogr.*, 169 (1979) 51.
4 T. Tsuda and M. Novotny, *Anal. Chem.*, 50 (1978) 271.
5 Y. Hirata, M. Novotny, T. Tsuda and D. Ishii, *Anal. Chem.*, 51 (1979) 1807.
6 T. Tsuda and M. Novotny, *Anal. Chem.*, 50 (1978) 632.
7 G. Nota, G. Marino, V. Buonocore and A. Ballio, *J. Chromatogr.*, 46 (1970) 103.
8 K. Hibi, D. Ishii, I. Fujishima, T. Takeuchi and T. Nakanishi, *J. High Resolut. Chromatogr. Chromatogr. Commun.*, 1 (1978) 21.
9 T. Tsuda, K. Hibi, T. Nakanishi, T. Takeuchi and D. Ishii, *J. Chromatogr.*, 158 (1978) 227.
10 R. Tijssen, *13th International Symposium Advances in Chromatography, October 16–19th, 1978, St. Louis, Mo., U.S.A.*
11 K. Hibi, T. Tsuda, T. Takeuchi, T. Nakanishi and D. Ishii, *J. Chromatogr.*, 175 (1979) 105.
12 D. Ishii, T. Tsuda, K. Hibi, T. Takeuchi and T. Nakanishi, *J. High Resolut. Chromatogr. Chromatogr. Commun.*, 2 (1979) 371.
13 D. Ishii, T. Tsuda and T. Takeuchi, *J. Chromatogr.*, 185 (1979) 73.

Journal of Chromatography, 192 (1980) 135–141

CHROM. 12,580

ELECTROCHEMICAL DETECTOR FOR HIGH-PERFORMANCE LIQUID CHROMATOGRAPHY

KAREL ŠTULÍK and VĚRA PACÁKOVÁ

Department of Analytical Chemistry, Faculty of Sciences, Charles University, Albertov 2030, 128 40 Prague 2 (Czechoslovakia)

(First received October 1st, 1979; revised manuscript received November 28th, 1979)

SUMMARY

A voltammetric detector has been developed for high-performance liquid chromatography, based on a three-electrode system with a platinum tubular working electrode. The detector has a small volume (about 1 μl) and has been used in the d.c. and differential pulse polarographic (DPP) modes. Its function was tested using various organic compounds, *e.g.*, phenol, ascorbic acid and uric acid. The detection limit is about 0.5 ng, the linear dynamic range is at least five orders of magnitude of concentration and the measurements exhibit good reproducibility. The d.c. and DPP methods of detection were about equally sensitive and the reproducibilities of the peak areas were similar, but the d.c. peak height exhibited better reproducibility than that of the DPP peaks.

The detector was used in the separation of the catecholamines adrenaline, noradrenaline, dopamine and L-dopa in a reversed-phase system. It was found that nanogram amounts can be detected, with narrow and symmetrical peaks.

INTRODUCTION

The development of high-performance liquid chromatography (HPLC) has necessitated the construction of various types of detectors, as a completely universal detector is not available. Therefore, specific detectors have great importance. In addition to common spectrophotometric, refractometric and fluorescence detectors, electrochemical detectors have received a great deal of attention, because they are sensitive, have a broad linear dynamic range, exhibit good reproducibility and are selective (except for conductimetric and high-frequency detectors), so that they do not place great demands on the purity of the samples.

Among electrochemical detectors[1], those based on the voltammetric principle have the broadest application range. Most of them use either the dropping mercury electrode, the disadvantages of which are the limited anodic potential range and difficulty of attaining a small dead volume, or planar solid electrodes in thin-layer (*e.g.*, refs. 2–4), or the "wall-jet" (*e.g.*, ref. 5) hydrodynamic systems.

Cells with tubular electrodes have rarely been used[6–8], although they are

hydrodynamically advantageous. In this work a cell with a platinum tubular working electrode and a small dead volume was constructed and tested.

EXPERIMENTAL

Reagents and apparatus

All chemicals used were of analytical-reagent grade (Lachema, Brnó, Czechoslovakia) and were not further purified. The preparations of the catecholamines were obtained from the Endocrinological Institute, Prague, and the Research Institute for Pharmacy and Biochemistry, Prague, Czechoslovakia. Aqueous stock solutions were prepared at a concentration of 10^{-3} *M* and were appropriately diluted before use. The principal detector parameters were tested by direct injection of solutions into the base electrolyte stream, without a column or with a column containing an inert packing. The response to phenol was tested using 0.1 *M* sulphuric acid as the base electrolyte, and that to other substances (ascorbic acid and uric acid) using a 0.1 *M* phosphate–citrate buffer[9]. The separation and detection of catecholamines were carried out in a reversed-system with μBondapak C_{18} as the stationary phase (10 μm), packed in a 25 cm × 2.2 mm I.D. column, and a 0.1 *M* phosphate–citrate buffer[9] containing lauryl sulphate as the mobile phase (300 ml of 0.1 *M* citric acid, 160 ml of 0.1 *M* disodium hydrogen orthophosphate and 0.02 g of lauryl sulphate).

The mobile phases were freed from dissolved atmospheric oxygen by passing purified nitrogen and then degassed *in vacuo*.

For the detector construction, see Results and Discussion. The measurements were carried out with a Varian Model 8500 liquid chromatograph, LP-9 d.c. and differential pulse polarographs (DPP) (Laboratorní Přístroje, Prague, Czechoslovakia) and Varian A-25-1 and EZ-2 (Laboratorní Přístroje) line recorders. The electrochemical detection was compared with UV photometric detection using a Pye Unicam LC 3 UV detector. Small volumes of sample solutions were injected into the measuring system with microsyringes (Hamilton Micromesure, The Hague, The Netherlands). All of the measurements were performed at laboratory temperature.

RESULTS AND DISCUSSION

Detector construction

The construction of the detector was based on the following general requirements: (a) simplicity of design; (b) easy access to the working electrode to allow its mechanical polishing; (c) as small a dead volume as possible; (d) a three-electrode system that would allow work in mobile phases of low conductivity and application of measuring techniques other than d.c. voltammetry.

The basic concept of the detector is based on a cell, described earlier[8], which contained a tubular electrode system but had a large dead volume, as it was constructed for continuous monitoring in flowing systems rather than for HPLC.

The present detector is depicted in Fig. 1. It consists of two cylindrical PTFE parts. The outer part contains an inlet from the column (a steel capillary sealed in place with a piece of PTFE tubing), a depression in which the working electrode is placed and which is provided with a hole for an outlet tube. The inner part is screwed into the outer part and keeps the working electrode in place. The platinum cylindrical

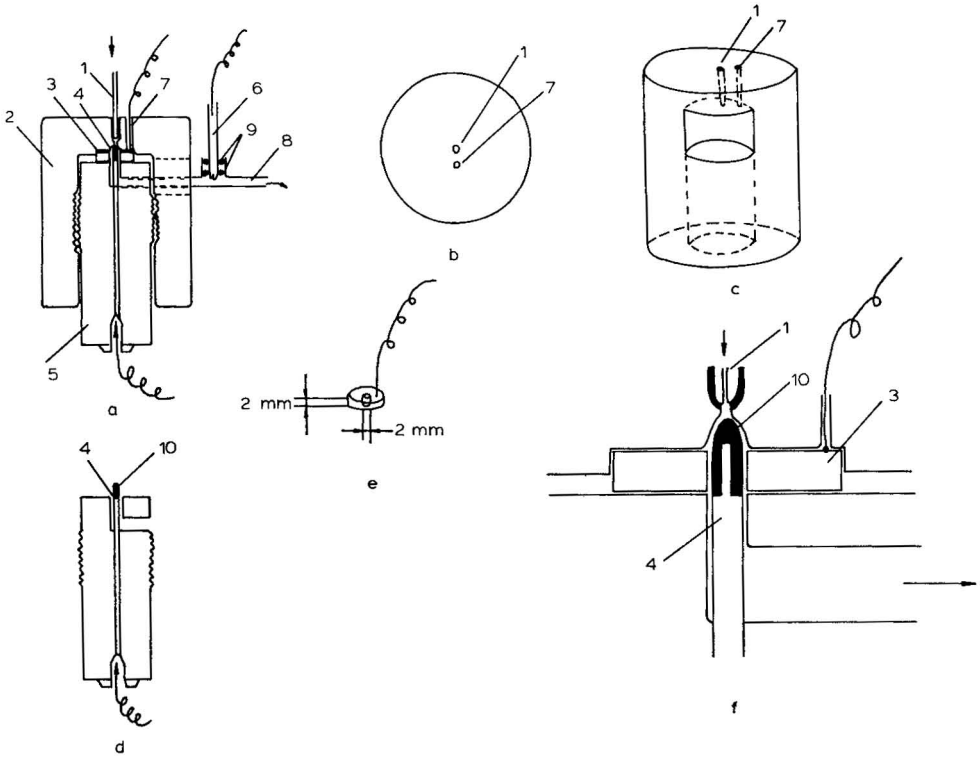

Fig. 1. The voltammetric detector. a, Cross-section through the assembled detector; b, top view; c, side view of the outer part; d, the inner part; e, working platinum tubular electrode; f, expanded view of the working–auxiliary electrode system. 1 = Inlet from the column (stainless-steel capillary, 0.23 mm I.D.); 2 = PTFE body, outer part; 3 = tubular platinum working electrode; 4 = platinum cylindrical auxiliary electrode; 5 = PTFE internal part of the detector; 6 = reference electrode (S.C.E.); 7 = channel for the lead from the working electrode; 8 = glass tube to waste; 9 = PTFE rings; 10 = PTFE insulating cap.

auxiliary electrode is placed in the channel in this inner part and reaches through the hole in the working electrode. It is equipped with a PTFE insulating cap to prevent short-circuiting of the electrodes and electrochemical interferences from the products of the reaction on the auxiliary electrode. The mobile phase thus passes through the narrow gap between the working and auxiliary electrodes (about 0.1 mm), which ensures that the dead volume of the cell is about 1 μl. The mobile phase leaves the detector through the side channel, where a glass tube is fixed with PTFE tubing and contains the reference electrode sealed by two PTFE rings. The working electrode is easily removed for mechanical polishing with metallographic papers.

Principal operating parameters of the detector

The performance of the detector was tested by injecting phenol, ascorbic acid and uric acid in a stream of base electrolyte either into a 10 cm × 1.2 mm I.D. column containing an inert packing of glass beads or directly into the detector through a short capillary. The injection of phenol into a short inert column sometimes led to peak tailing, whereas direct injection into the detector produced narrow and symmetri-

cal peaks (see Fig. 2). The limit of detection, the linear dynamic range, the reproducibility of the peak height and area and the dependence of the detector response on the mobile phase flow-rate were determined.

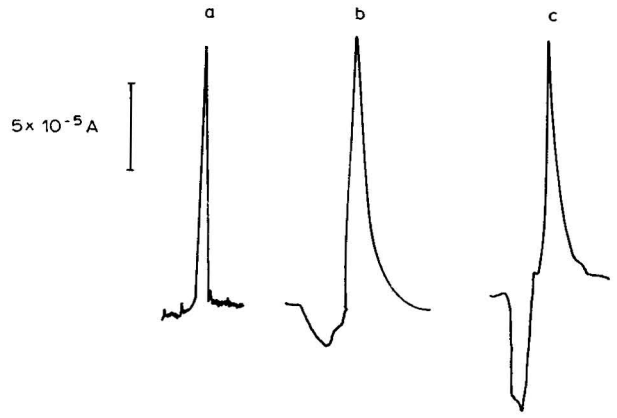

Fig. 2. d.c. and DPP detector responses to phenol. $2.7 \cdot 10^{-4}$ M aqueous phenol solution; 4 µl injected; 0.1 M H_2SO_4 mobile phase, flow-rate 130 ml/h; working electrode potential, +0.8 V (vs. S.C.E.); pulse height, 50 mV; pulse frequency, 1 sec. a = d.c. peak (direct injection to the detector); b = d.c. peak (injection through an inert column); c = DPP peak (injection through an inert column).

The detection limit as the peak height corresponding to twice the standard deviation of the noise, was determined by injecting 10^{-4} M aqueous solutions of phenol, ascorbic acid and adrenaline. The value found was approximately 0.5 ng in all instances.

The dependence of the detector response on the concentration of the test substances (the linear dynamic range) was studied using aqueous solutions of phenol. Amounts of $0.5–5 \cdot 10^4$ ng of phenol were injected and both the peak height and peak area were measured. It was found that the detector response is linear at least over the whole concentration range studied (five orders of magnitude).

The reproducibility of the detector response was found for phenol in the d.c. and DPP modes. Amounts of 4 µl of a 10^{-4} M solution were injected and the peak heights and areas measured. The results are given in Table I.

TABLE I

REPRODUCIBILITY OF THE DETECTOR RESPONSE

An amount of 4 µl of a 10^{-4} M aqueous phenol solution injected; 0.1 M H_2SO_4 mobile phase; flow-rate, 150 ml/h; working electrode potential, +0.8 V (vs. S.C.E.); pulse height, 50 mV; pulse frequency, 1 sec. Average values determined from ten measurements, 95% probability level; C.V. = coefficient of variation (%).

Detection	*Peak height (mm)*	*C.V. (%)*	*Peak area (arbitrary units)*	*C.V. (%)*	*Peak half-width (mm)*	*C.V. (%)*
d.c.	143.0	2.8	56.0	4.6	3.0	5.0
DPP	50.7	13.6	20.2	4.1	2.3	5.8

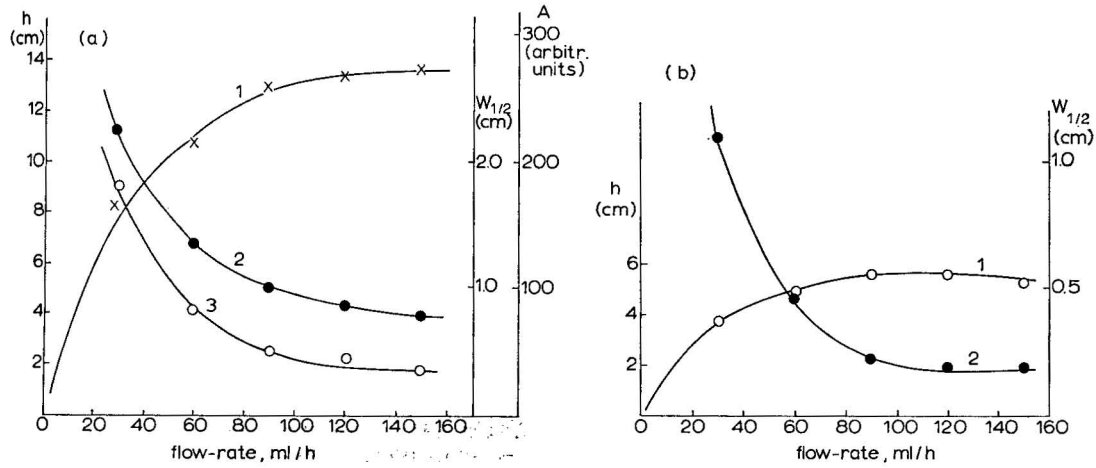

Fig. 3. Dependence of detector response on the flow-rate of mobile phase. (a) d.c. measurement: $2.7 \cdot 10^{-4}$ *M* aqueous phenol solution, 4 μl injected; 0.1 *M* H_2SO_4 mobile phase; working electrode potential, +0.8 V (*vs.* S.C.E.). Curve 1, peak height, *h* (cm); curve 2, peak area, *A* (arbitrary units); curve 3, peak half-width, $w_{1/2}$ (cm). (b) DPP measurements: $9.5 \cdot 10^{-4}$ *M* aqueous uric acid solution, 6 μl injected; 0.1 *M* H_2SO_4 mobile phase; working electrode potential, +0.8 V (*vs.* S.C.E.); pulse height, 50 mV; pulse frequency, 1 sec. Curve 1, peak height, *h* (cm); curve 2, peak half-width, $w_{1/2}$ (cm).

The dependence of the detector response on the mobile phase flow-rate was determined for phenol (d.c. measurement) and uric acid (DPP measurement). The results are summarized in Fig. 3.

The DPP detector response also depends on the pulse height, as shown in Fig. 4.

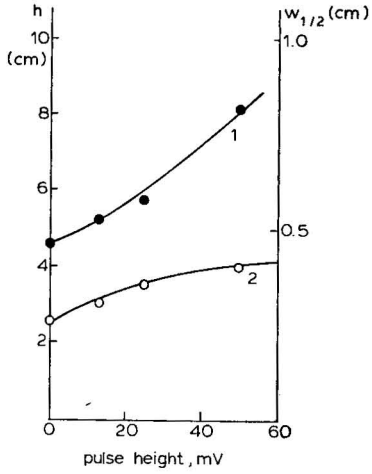

Fig. 4. Dependence of DPP detector response on pulse height. $9.5 \cdot 10^{-4}$ *M* aqueous uric acid solution, 10 μl injected; 0.1 *M* H_2SO_4 mobile phase, flow-rate 60 ml/h; working electrode potential, +0.8 V (*vs.* S.C.E.), pulse frequency, 1 sec. Curve 1, peak height, *h* (cm); curve 2, peak half-width, $w_{1/2}$ (cm).

It follows from the results obtained that the measurements in both the d.c. and DPP systems are sufficiently sensitive and reproducible and the linear dynamic range is broad. There is virtually no difference in the sensitivities of the d.c. and DPP measurements. The reproducibility of the peak areas is similar in both instances, whereas the peak height is more reproducible in the d.c. measurement.

The d.c. and DPP responses exhibit dependences on the experimental conditions that would be expected from electrochemical theory. It is sometimes claimed that the DPP measurement is less sensitive to changes in the mobile phase flow-rate, as could be expected from the fact that the diffusion layer at the electrode is thinner in non-stationary measurements. However, our measurements showed little differences in this respect between the d.c. and DPP measurements. Moreover, the DPP measurement is more sensitive to the presence of surfactants, which alter the capacity of the electric double layer, and suffers from a larger background current. For these reasons, the d.c. measurements seem more advantageous, also in view of the simpler measuring circuit.

The main problem in the use of the detector is the magnitude of the background current, and it is therefore important that the mobile phase is perfectly free of dissolved oxygen and of electroactive impurities. In our measurements, the currents corresponding to the solutes studied were relatively large (of the order of 10^{-7} A at the lowest concentrations), but were superimposed on a background current more than one order of magnitude higher. It can therefore be expected that careful purification of the mobile phase will lead to a considerable decrease in the background current and consequently to a futher decrease in the detection limit. Even under the present conditions the detection limit is the same as that of UV detection at the highest detector sensitivity, as was found by comparing the responses of the electrochemical detector and a UV detector to phenol and ascorbic acid at 240 nm.

The electrode activity did not change, even during prolonged measurements, and the background current did not exhibit the drift that is sometimes reported for electrochemical detectors[10].

Measurements with a wall-jet detector showed that the proposed detector is more sensitive. Its performance is similar to that of thin-layer detectors with planar electrodes, but from the constructional point of view it is easier to attain a small dead

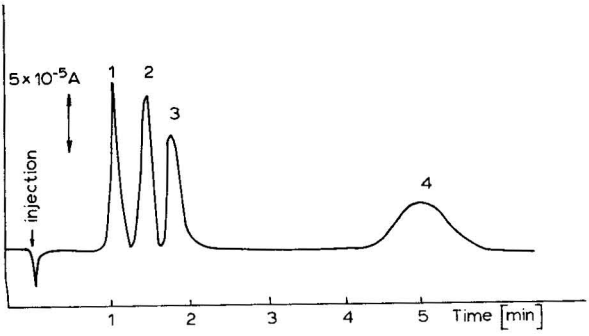

Fig. 5. Separation of catecholamines. 1 = Noradrenaline; 2 = L-dopa; 3 = adrenaline; 4 = dopamine. Flow-rate, 60 ml/h; injected amounts, 20 ng of each compound. d.c. detection, working electrode potential +0.75 V (*vs.* S.C.E.).

volume. As shown by calculations of the theoretical currents for tubular and planar systems (for the appropriate equations, see refs. 11 and 12), this system behaves similarly to detectors with planar electrodes. This could be expected as the curvature of the electrode surface can be neglected in view of the very narrow gap between the working and auxiliary electrodes.

Separation and electrochemical detection of catecholamines

Practical use of the detector described is demonstrated with the analysis of catecholamines. Fig. 5 shows a chromatogram of a mixture of adrenaline, noradrenaline, L-dopa and dopamine on a column packed with μBondapak C_{18} chemically bonded phase, using a citrate–phosphate buffer containing lauryl sulphate as the mobile phase. Good separation was attained, with narrow and symmetrical peaks for catecholamines. It can be seen that the detector can be used successfully for the detection of catecholamines in nanogram and sub-nanogram amounts.

REFERENCES

1 K. Štulík and V. Pacáková, *Chem. Listy*, 73 (1979) 795.
2 D. C. Schwartzfager, *Anal. Chem.*, 48 (1976) 2189.
3 P. T. Kissinger, C. J. Felice, R. M. Riggin, C. A. Pachla and D. C. Wenke, *Clin. Chem.*, 20 (1974) 992.
4 R. M. Riggin, L.-D. Rau, R. L. Alcorn and P. T. Kissinger, *Anal. Lett.*, 7 (1974) 791.
5 J. Yamada and H. Matsuda, *J. Electroanal. Chem.*, 44 (1973) 189.
6 W. J. Blaedel, C. L. Olson, and R. L. Sharma, *Anal. Chem.*, 35 (1963) 2100.
7 W. J. Blaedel and S. L. Boyer, *Anal. Chem.*, 43 (1971) 1538.
8 K. Štulík and V. Hora, *J. Electroanal. Chem.*, 70 (1976) 253.
9 R. M. Riggin and P. T. Kissinger, *Anal. Chem.*, 49 (1977) 2109.
10 F. Vandemark and T. H. Ryan, *Chromatogr. Newsl.*, 6 (1978) 20.
11 V. G. Levich, *Discuss. Faraday Soc.*, 1 (1947) 37.
12 V. G. Levich, *Physico-Chemical Hydrodynamics*, Prentice-Hall, Englewood Cliffs, N.J., 1962.

Journal of Chromatography, 192 (1980) 143–158

CHROM. 12,558

BROAD SPECTRUM RESOLUTION OF OPTICAL ISOMERS USING CHIRAL HIGH-PERFORMANCE LIQUID CHROMATOGRAPHIC BONDED PHASES*

WILLIAM H. PIRKLE, DAVID W. HOUSE and JOHN M. FINN
School of Chemical Sciences, University of Illinois, Urbana, Ill. 61801 (U.S.A.)
(First received May 4th, 1979; revised manuscript received November 22nd, 1979)

SUMMARY

Using a chiral recognition rationale, a chiral fluoroalcoholic bonded stationary phase has been devised which proves capable of separating the enantiomers of a large number of solutes including sulfoxides, lactones, and derivatives of alcohols, amines, amino acids, hydroxy acids, and mercaptans.

Chiral recognition being a reciprocal event, chiral stationary phases modeled after solutes resolvable upon the fluoroalcoholic columns successfully separate the enantiomers of a number of fluoroalcohols.

INTRODUCTION

The development of chiral stationary phases (CSP) for the direct chromatographic separation of optical isomers is a problem that has been addressed by many researchers. Despite impressive but scattered successes, no CSP has been devised to suffice for the separation of more than a relatively narrow range of structurally related compounds. To date, most liquid chromatographers have confined their efforts to amino acids[1–4], helicenes[5–7], and di- and triphenic acids[8].

In this paper, we set forth a chiral recognition rationale that can be used to design CSP for the chromatographic separation of an assortment of optical isomers. Several successful applications of this rationale are presented.

RATIONALE

It should be generally appreciated that a minimum of three reference points are needed to distinguish the handedness of a chiral object. In molecular terms, this means that a CSP, in order to interact preferentially with one solute enantiomer, must undergo a minimum of three simultaneous interactions with that enantiomer.

* Presented at the *4th International Symposium on Column Liquid Chromatography, Boston, May 7–10, 1979*. The majority of the papers presented at this symposium has been published in *J. Chromatogr.*, Vol. 185 (1979).

Nuclear magnetic resonance (NMR) studies of the interactions of chiral fluoroalcohols such as I with a wide variety of solutes have shown that, whenever possible, the fluoroalcohol employs a two-point chelate-like mode of solvation[9–20]. The principal interaction is hydrogen bonding; the secondary interaction is carbinyl hydrogen bonding[20]. Many commonly occurring structural subunits suffice as interaction sites as indicated in Fig. 1.

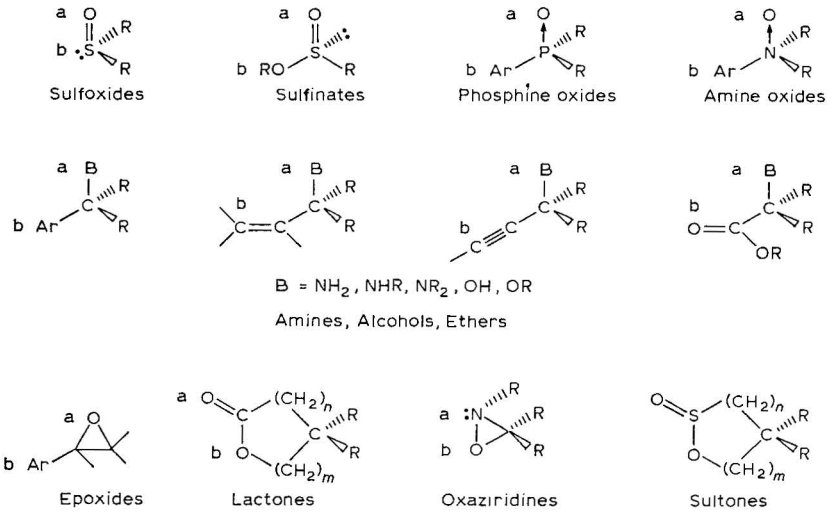

Fig. 1. A representative sampling of solutes known to give chelate-like solvates upon solvation by type I fluoroalcohols. The site of primary hydrogen bonding is designated as a; the site of secondary interaction is designated as b.

Interaction of chiral type I fluoroalcohols with enantiomeric solutes gives rise to diastereomeric solvates, the chelate-like diasteromeric solvates of present interest being represented in a general way as IIa and b. Although diastereomeric, these solvates differ significantly in stability only if the alcohol substituents, R_f and W, interact, either directly or indirectly, with the remaining solute substituents, Y and Z.

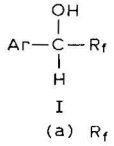

I

(a) $R_f = CF_3$, Ar = 9-(10-methyl)anthryl

(IIa) (IIb)

X = C, N, P, S
B_1 = hydrogen bond receptor
B_2 = less basic (than B_1) site

In order to incorporate the widespread chelating ability of type I fluoroalcohols into a chiral stationary phase that would truly have a greater affinity for one solute enantiomer than the other, it was evident that the alcohol substituents, R_f and W, would have to interact with and distinguish between Z and Y. Since the principal function of the simple perfluoroalkyl substituent, R_f, is to strengthen the primary and secondary interactions by conferring acidity upon the hydroxyl and carbinyl hydrogens, the major role in differentiating between Y and Z was expected to fall to the remaining alcohol substituent W. To differentiate between Y and Z, W must take advantage of some structural difference such as size, charge distribution, additional hydrogen bonding sites, or hydrophobic interactions. Since the ease of enantiomer separation stems from the magnitude of the stability difference of the diastereomeric solvates, the strength of the stereochemically dependent third interaction should be appreciable. (Future chiral stationary phases might contain modified "R_f" substituents so as to lead to a "push-pull" situation involving a fourth stereochemically dependent interaction to further augment chiral recognition.)

In our first chiral stationary phase, we have chosen to use π–π donor–acceptor interactions as the stereochemically dependent third interaction. Prior work[21,22] had shown that the diastereomeric solvates derived from 2,2,2-trifluoro-1-[(10-methyl)-9-anthryl]ethanol, Ia, and the enantiomers of methyl 2,4-dinitrophenyl sulfoxide were of different stability owing to the stereochemical dependence of the interaction between the electron-rich anthryl group and the electron-deficient dinitrophenyl substituent. A general representation of these diastereomers is shown in IIIa and b and provides a basis for anticipating the selective interaction of a CSP derived from Ia with a number of π-acid substituted chelate-forming solutes.

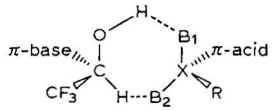

III a

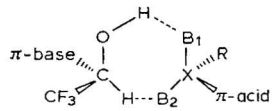

III b

X = C, N, S, P
B_1 = hydrogen bond receptor
B_2 = carbinyl hydrogen bond receptor

EXPERIMENTAL

Chromatography was performed using an Altex 100A pump, a Valco 7000 p.s.i. injector with a 10-μl loop and an Altex Model 152 dual wavelength (254 and 280 nm) detector. Columns were slurry packed using conventional methods. Solutes were available from prior studies, prepared from commercially available materials, or generously provided by colleagues throughout the world.

Fluoroalcoholic stationary phase IV

The preparation of this CSP has been described[23].

Second-generation chiral stationary phases XIII and XIV

Owing to the preliminary nature of this work and the number of bonded phases prepared, we have initially employed an inexpensive silica gel (Ventron 58 μm,

large pore, 600 m^2/g) ball-milled to a powder. While the theoretical plate count of columns so derived is far from "state of the art", these columns adequately serve the intended purpose. More efficient columns based upon 5-μm spherical particles of silica gel will be prepared ultimately.

Aminopropyl functionalized silica. A slurry of 50 g of ball-milled silica in 500 ml of toluene was heated to reflux until water was no longer removed azeotropically (Dean-Stark trap). Thereupon, 100 g of γ-aminopropyltriethoxysilane was added and solvent was slowly and intermittently distilled until the infrared spectrum of the distillate no longer (18–36 h) showed hydroxy adsorption. The silica was isolated by filtration and washed repeatedly with toluene, methanol, ether and finally pentane. After drying, appreciable weight gain (*ca.* 40%) is noted. Anal. found: C, 10.91; H, 2.53; N, 2.78; Si, 39.28%.

3,5-Dinitrobenzoylphenylglycine. A mixture of 50 g of D-(—)-phenylglycine and 72 g of 3,5-dinitrobenzoyl chloride in 600 ml of dry tetrahydrofuran (THF) was stirred for one week at room temperature. The THF was removed under vacuum, the residue was dissolved in 5% aqueous sodium bicarbonate, and this solution was washed with two (100-ml) portions of ether. The aqueous extract was acidified to a pH of 5.3 and continuously extracted with ether until material was no longer being extracted into the ether. The ether extracts were dried over anhydrous $MgSO_4$ and the ether was removed under vacuum to afford 57.72 g of colorless crystalline 3,5-dinitrobenzoylphenylglycine (54%). The enantiomeric purity of this material was determined by chromatography upon CSP IV (Table IV) to be 96%. Recrystallization (methanol)* can be used to increase enantiomeric purity. The enantiomerically pure material has a m.p. of 211–213°.

NMR: (d_6 Acetone) δ 5.81 (d, 1 H), δ 7.30–7.65 (m, 5 H), δ 8.90–9.20 (m, 4 H). Infrared (IR): (KBr disc) 3400–3085, 1733, 1652, 1580, 1345, 1218, 1190, 1080, 920, 732, 722 cm^{-1}. Anal. Calculated for $C_{15}H_{11}N_3O_7$: C, 52.18; H, 3.21; N, 12.17. Found: C, 52.12; H, 3.24; N, 12.20.

Chiral stationary phase XIII. A solution of 10 g of D-3,5-dinitrobenzoylphenylglycine in 200 ml of dry THF was poured over 10 g of dry aminopropyl silica gel and 7.9 g of N-ethoxycarbonyl-2-ethoxy-1,2-dihydroquinoline (EEDQ) was added with swirling. After 8 h at room temperature, the silica was isolated by filtration and washed repeatedly with methanol, acetone and ether. These last washings employed centrifugation–decantation and some fines were thus removed. After drying, *ca.* 12 g of the silica bonded phase was obtained.

Anal. Calculated: 0.51 mmoles/g (based on C). Found: C, 14.64; H, 2.28; N, 3.09; Si, 31.39%.

It is at this last stage that partial racemization might occur. Use of *n*-butylamine as a trapping nucleophile leads to the nonracemized amide. However, racemization and trapping would be competitive reactions and the aminopropyl silica could be less reactive than *n*-butylamine.

After being packed, the column was washed with 10 g of trifluoroacetic acid in 150 ml of methylene chloride to protonate remaining free aminopropyl groups.

N-(3,5-Dinitrobenzoyl)phenylglycinol. To a solution of 16.72 g of D-phenylglycinol (122 mmoles) and 14.50 g of pyridine (183 mmoles) in 250 ml of methylene

* This solvent can lead to esterification upon heating or long standing.

chloride was slowly added 28.10 g of 3,5-dinitrobenzoyl chloride (122 mmoles). The mixture was heated at reflux for 4 h. Acetonitrile ($\approx$ 250 ml) was added to dissolve the solid product and the organic phase was washed with 5% hydrochloric acid (2 $\times$ 100 ml) and 3 *N* sodium hydroxide solution (4 $\times$ 200 ml). After the organic phase was dried over anhydrous $MgSO_4$, the solvents were removed under vacuum to afford 31.67 g (78%) of a pale yellow solid (m.p. 231–234°). The enantiomeric purity of this material can be ascertained by chromatography upon CSP IV.

NMR: (d_6 Acetone) δ 2.8 (s, 1 H), δ 3.8 (d, 2 H), δ 5.2 (t, 1 H), δ 7.1–7.5 (m, 5 H), δ 8.7 (s, 1 H), δ 9.0–9.1 (m, 3 H). IR: (Nujol) 3500, 1660, 1540, 1470, 1350, 1260, 1080, 1020, 920 cm^{-1}.

N-(3,5-Dinitrobenzoyl)phenylglycinol chloroformate. To a solution of phosgene (9.5 g, 96 mmoles) in 150 ml of methylene chloride cooled to $-5°$ was added dropwise a solution of 14.23 g of N-(3,5-dinitrobenzoyl)phenylglycinol (43 mmoles) and 3.4 g of pyridine (43 mmoles) in 300 ml of methylene chloride. After the addition was completed, stirring was continued for 30 min at 0°. The solution was filtered under nitrogen and the solvent was removed under vacuum to give the crude chloroformate as an orange syrup.

NMR: ($CDCl_3$) δ 5.0 (d, 2 H), δ 5.4 (t, 1 H), δ 7.1–7.5 (m, 5 H), δ 8.7 (t, 1 H), δ 9.0–9.1 (m, 3 H).

The crude chloroformate was not otherwise characterized but was used immediately.

Chiral stationary phase XIV. To a stirred mixture of aminopropyl silica (12.45 g) and triethylamine (2.52 g, 25 mmoles) in 50 ml of methylene chloride was added the crude chloroformate from the above reaction. The mixture was stirred at room temperature for two days. The solution was filtered and the silica washed with methylene chloride, methanol, acetone, ether, and pentane.

Anal. Found: C, 14.82%, H, 2.16%, N, 3.73%; Si, 32.67%. Calcd: 0.37 mmoles per g (based on C).

After being packed, the column was treated with 10 g of trifluoroacetic acid in 100 ml of methylene chloride to protonate any residual aminopropyl groups.

RESULTS

Chiral stationary phase IV, derived from R-Ia, has shown an impressive ability to separate the enantiomers of solutes falling into the purview of its chiral recognition scheme*. First, it separates the enantiomers of a wide range of π-acid

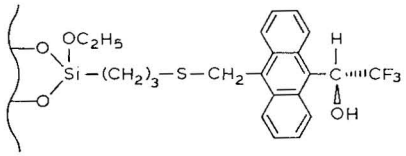

IV

substituted sulfoxides (Fig. 2, Table I). In general, the ability of CSP IV to separate sulfoxide enantiomers correlates with the π-acidity of the sulfoxide substituent and is

* Experimental details for the preparation of IV and a sampling of the enantiomer separations achieved thereon are being reported elsewhere[23].

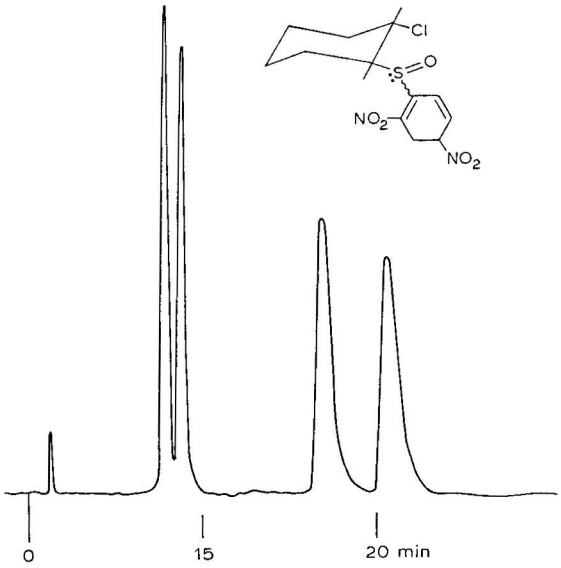

Fig. 2. Separation of the four stereoisomers (two racemic diastereomers) of *trans*-1-chloro-2-(2,4-dinitrophenylsulfinyl)cyclohexane upon chiral stationary phase IV using 5% isopropyl alcohol in hexane.

TABLE I

SEPARATION OF SULFOXIDE ENANTIOMERS UPON CHIRAL STATIONARY PHASE IV

Eluent was 20% isopropyl alcohol in hexane. Stationary phase IV was bonded onto 10 μm Porasil and slurry packed into a 9 × 250 mm column. The absolute configuration of the initially eluted sulfoxide enantiomer is presumed in all cases to be that shown above. The elution orders of the first and twelfth entries in this table are as indicated and C.D. spectroscopy shows the elution order of entries two to six to be the same as that of one. The absolute configurations of the remaining sulfoxides have not been assigned previously.

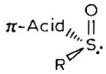

R	*π-Acid*	*α*	k_1'
CH_3	2,4-$(NO_2)_2C_6H_3$	1.12	13.05
n-Butyl	2,4-$(NO_2)_2C_6H_3$	1.19	6.32
n-Octyl	2,4-$(NO_2)_2C_6H_3$	1.24	4.44
n-Dodecyl	2,4-$(NO_2)_2C_6H_3$	1.26	3.33
n-Octadecyl	2,4-$(NO_2)_2C_6H_3$	1.28	2.44
Phenyl	2,4-$(NO_2)_2C_6H_3$	1.23	6.82
Benzyl	2,4-$(NO_2)_2C_6H_3$	1.22	7.70
n-Dodecyl	4-NO_2-C_6H_4	1.09	2.78
Phenyl	4-NO_2-C_6H_4	1.05	6.95
n-Dodecyl	2,4-$(NO_2)_2$-C_6H_3-CH_2	1.38	6.39
n-Dodecyl	C_6F_5	1.09	0.51
n-Dodecyl	4-ClC_6H_4	1.02	1.26
CH_3	C_6Cl_5	1.04	2.51

but slightly dependent upon the remaining "inert" (which means that additional functionality which would interfere with the primary or secondary interactions is lacking) sulfoxide substituent. [It is not yet known whether the observed modest variation in α values stems from variations in chiral recognition (higher order interactions) or contributions from additional retention mechanisms that do not involve chiral recognition. The presence of free silanol groups could well give rise to such additional retention.] Elution orders are those expected from the rationale[23].

Chiral stationary phase IV also separates the enantiomers of the π-acid bearing lactone V (Fig. 3).

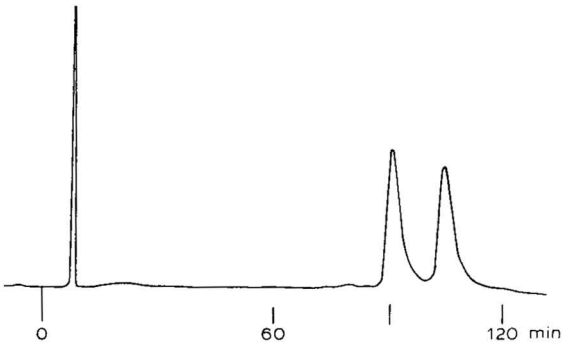

Fig. 3. Separation of the enantiomers of γ-2,4-dinitrophenyl-γ-butyrolactone upon chiral stationary phase IV using 20% isopropyl alcohol in hexane.

Solutes lacking π-acid substituents can often be derivatized to incorporate such functionality so as to markedly increase the scope of CSP IV. Amines, alcohols, and thiols react readily with 2,4-dinitrofluorobenzene or 3,5-dinitrobenzoyl chloride. The latter has proven to be generally useful in leading to derivatives resolvable upon CSP IV. (The 3,5-dinitrobenzoyl moiety is both a π-acid and a basic site suitable for either the primary or secondary interactions. It is also a strongly absorbing ultraviolet chromaphore that facilitates detection. Moreover, this group can generally be removed hydrolytically if the original solute enantiomer is to be recovered after resolution. An additional advantage, shared by all achiral derivatizing agents, is that no optical fractionation occurs during reaction with a solute, the enantiomeric purity of which is to be determined chromatographically after derivatization.)

The 3,5-dinitrobenzoyl (DNB) derivatives of a number of primary amines, alcohols and mercaptans are represented by generalized structures VI–VIII. These derivatives preferentially populate conformations that place the DNB carbonyl oxygen near the methine hydrogen (presumably, for reasons of carbinyl hydrogen bonding)[20]. This conformational preference, greater in amides than in esters, appears to influence the chromatographic behavior of DNB derivatives upon CSP IV. Both the DNB carbonyl oxygen and group B can serve as basic sites to afford transient chelate-like solvates with CSP IV. If the DNB carbonyl oxygen is more basic than group B, the primary and secondary interactions occur as shown in solvate IX. If group B is more basic than the DNB carbonyl oxygen, a solvate such as X is preferentially afforded. The consequence of chelate-like solvation of derivatives VI–VIII by CSP IV is that, for the solvate diastereomers shown in IX–X, the π-acid moiety is,

using the chelate ring for reference, *cis* to the π-acceptor moiety and a π–π tertiary interaction can occur. In the other diastereomers, the π-acid and π-base groups are *trans* to one another, rendering impossible the tertiary interaction. Once again, a stereochemically dependent π–π donor–acceptor interaction leads to enantiomer separation and predictable elution orders so long as one correctly assesses the relative basicities of the DNB carbonyl oxygen and B. Note that a basicity inversion inverts the elution order expected for a given absolute configuration*.

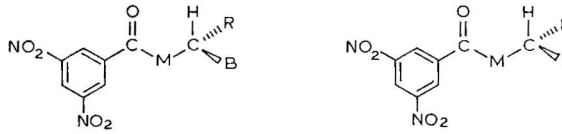

VI M = NH
VII M = O B = basic site
VIII M = S

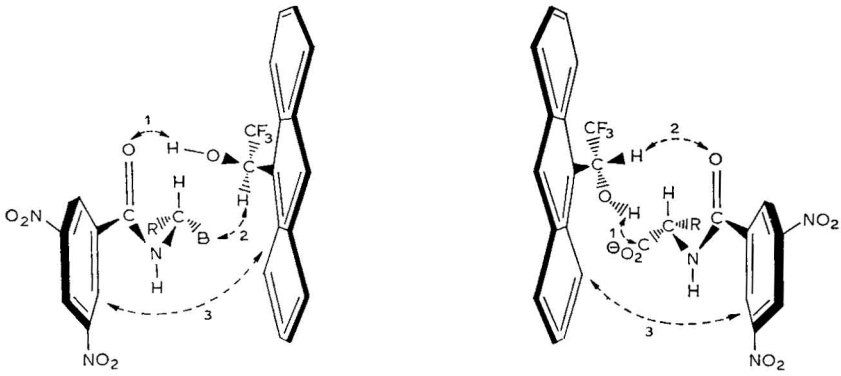

IX X

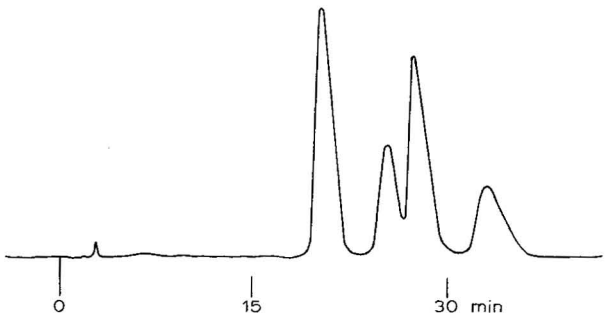

Fig. 4. Separation of the enantiomers of the racemic *trans* and *cis* diastereomers of 2-phenyl-1-aminocyclohexane upon chiral stationary phase IV using 5% isopropyl alcohol in hexane.

* The astute reader will realize that even in situations where there is a clear basicity difference between B_1 and B_2, the least stable solvate (*i.e.*, the one expected to have but two simultaneous interactions) can in principle have three simultaneous interactions by adopting the less favored chelation mode. What is experimentally observed, of course, is a weighted time average of all possible interaction modes.

TABLE II

SEPARATION OF THE ENANTIOMERS OF 3,5-DINITROBENZOYL DERIVATIVES OF AMINES, ALCOHOLS AND THIOLS UPON CHIRAL STATIONARY PHASE IV

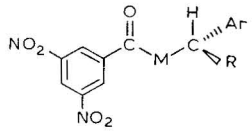

Solvent was 20% isopropyl alcohol in hexane. The elution order of each starred* solute was determined by chromatography of a partially resolved configurationally established sample. In every instance, the configuration of the initially eluted enantiomer proved to be that shown above. The presumption is that the elution orders of the remaining solutes also follow this pattern.

R	*Ar*	*M*	α	k_1'
CH_3	Phenyl	NH	1.19*	3.01
CH_3	*p*-Anisyl	NH	1.18*	5.19
CH_3	*p*-$CF_3C_6H_4$	NH	1.11	2.03
CH_3	α-Thienyl	NH	1.14*	3.04
CH_3	α-Naphthyl	NH	1.10*	3.53
CH_3	*p*-Biphenyl	NH	1.17	3.64
C_2H_5	*p*-Biphenyl	NH	1.21	3.09
C_2H_5	Phenyl	NH	1.29*	2.63
iso-C_3H_7	Phenyl	NH	1.26*	2.29
n-C_3H_7	4-$CH_3OC_6H_4$	NH	1.30	3.49
n-C_3H_7	4-$C_3H_7OC_6H_4$	NH	1.34	2.35
$CH_3O_2C(CH_2)_2$	Phenyl	NH	1.18	6.33
CH_3	Phenyl	O	1.08*	1.56
C_2H_5	Phenyl	O	1.10	1.23
n-C_3H_7	Phenyl	O	1.12	1.09
iso-C_3H_7	Phenyl	O	1.14	0.81
Cyclopropyl	Phenyl	O	1.09	1.32
tert.-C_4H_9	Phenyl	O	1.13	0.81
Cyclobutyl	Phenyl	O	1.12	1.09
Cyclopentyl	Phenyl	O	1.16	0.97
Cyclohexyl	Phenyl	O	1.13	0.93
Benzyl	Phenyl	O	1.03	1.69
CH_3	*p*-ClC_6H_4	O	1.04	1.28
CH_3	α-Naphthyl	O	1.04	2.21
n-C_3H_7	2,5-$(CH_3O)_2C_6H_3$	O	1.09	2.01
CH_3	9-Anthryl	O	1.06	3.49
CF_3	*m*-$NO_2C_6H_4$	O	1.06	3.93
CF_3	α-Naphthyl	O	1.10*	1.76
CF_3	3-Pyrenyl	O	1.10*	3.07
CCl_3	Phenyl	O	1.11	1.21
CBr_3	Phenyl	O	1.10	1.67
iso-C_3H_7	Phenyl	O	1.14	0.81
iso-C_3H_7	Phenyl	S	1.16	1.05
CH_3	Phenyl	S	1.07	1.47

Table II contains data pertinent to the separation of 3,5-DNB derivatized amines, alcohols and thiols in which the B moiety is an aryl system. In all such instances, chromatography of partially resolved configurationally known samples leads to elution orders indicating the DNB carbonyl oxygen to be the site of primary interaction (see IX), a chemically reasonable result. Fig. 4 illustrates such separations.

TABLE III

SEPARATION OF THE ENANTIOMERS OF 3,5-DINITROBENZOYL DERIVATIVES OF AMINO ACIDS, AMINO ALCOHOLS AND HYDROXY ACIDS

Separations were performed using 20% isopropyl alcohol in hexane unless otherwise specified. The elution order of each starred solute was determined by chromatography of a partially resolved configurationally established sample. In every instance, the configuration of the initially eluted enantiomer proved to be that shown above. The presumption is that the elution orders of the remaining solutes also follow this pattern.

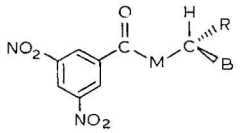

R	*B*	*M*	α	k_1'
CH_3	CO_2CH_3	NH	1.08*	4.16
CH_3	$CO_2C_2H_5$	NH	1.10	3.32
CH_3	CO_2-*i*-C_3H_7	NH	1.14	2.76
iso-C_3H_7	CO_2CH_3	NH	1.05*	2.75
iso-C_4H_9	CO_2CH_3	NH	1.07*	2.00
$CH_3S(CH_2)_2$	CO_2CH_3	NH	1.04*	4.81
Phenyl	CO_2CH_3	NH	1.19*	4.17
Benzyl	CO_2CH_3	NH	1.10*	4.00
CH_3	$CONHC_4H_9$	NH	1.34*	12.24§
iso-C_3H_7	$CONHC_4H_9$	NH	1.33*	0.82
Isobutyl	$CONHC_4H_9$	NH	1.65*	3.76§
$CH_3S(CH_2)_2$–	$CONHC_4H_9$	NH	1.38*	9.93§
Phenyl	$CONHC_4H_9$	NH	1.78*	0.75
Benzyl	$CONHC_4H_9$	NH	1.52*	6.78§
α-Naphthyl	$CONHC_4H_9$	NH	1.65	1.15
Phenyl	CH_2OH	NH	1.38*	2.36
Benzyl	$CH_2O(CH_2)_2OCH_3$	NH	1.18	5.00
Phenyl	$CH_2O_2CCH_3$	NH	1.18	5.30
Phenyl	$C(CH_3)_2OH$	NH	1.35	5.94§§
CH_3	CH_2OH	NH	1.06*	8.40§§
Isopropyl	CH_2OH	NH	1.19*	3.68§§
CH_3	$(CH_2)_2OH$	NH	1.15	4.30§§
CH_3	CO_2CH_3	O	1.05*	3.39
Phenyl	$CONHCH_3$	O	1.12	9.88
CH_3	$CONH_2$	O	1.10	8.90
2,5-$(CH_3)_2C_6H_3$	CO_2CH_3	O	1.05	2.51
CCl_3	$CH_2CO_2CH_3$	O	1.06	1.80
$CH_3O_2CCH_2$	CO_2CH_3	O	1.12	6.95
Phenyl	$PO(OC_2H_5)_2$	NH	1.38	4.75§§
p-Tolyl	$PO(OC_2H_5)_2$	NH	1.40	4.38§§
p-Anisyl	$PO(OC_2H_2)_5$	NH	1.37	7.50§§
p-ClC_6H_4	$PO(OC_2H_5)_2$	NH	1.26	4.38§§
p-BrC_6H_4	$PO(OC_2H_5)_2$	NH	1.25	4.50§§

§ 5% Isopropyl alcohol in hexane.
§§ 10% Isopropyl alcohol in hexane.

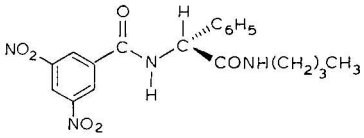

XI

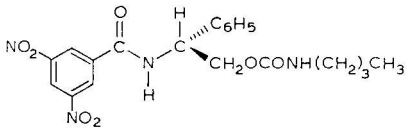

XII

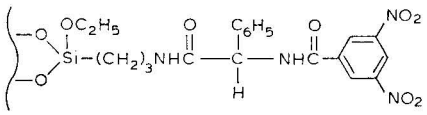

XIII

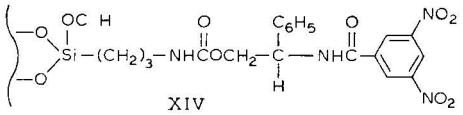

XIV

TABLE IV

DIRECT AND REVERSED-PHASE SEPARATION OF ENANTIOMERS OF 3,5-DINITROBENZOYL DERIVATIVES OF α-AMINO ACIDS UPON CHIRAL STATIONARY PHASE IV

The elution order of each starred solute was determined by chromatography of a partially resolved configurationally established sample. In every instance, the configuration of the initially eluted enantiomer proved to be that shown above. The presumption is that the elution orders of the remaining solutes also follow this pattern.

a = 10% isopropyl alcohol in hexane. b = 80% water, 20% methanol, 0.25% $NaHCO_3$. In this solvent, the carboxyl group is ionized.

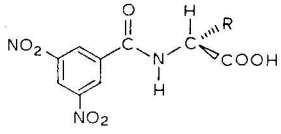

	α a/b	k_1 *a/b*
Alanine	1.17/1.40*	6.05/0.75
Valine	1.14/1.36*	3.76/1.4
Leucine	1.12/1.42*	2.82/2.8
Phenylalanine	1.17/1.40*	4.88/6.0
Methionine	1.12/1.31*	6.10/3.2
Phenylglycine	1.27/1.73*	7.48/3.0
α-Naphthylglycine	1.21/1.74	10.0/15.5
Tyrosine	1.16/1.41*	11.9/2.2
Glutamic acid	1.09/—	10.6/*ca.* 0.0
Isoleucine	1.16/1.50	3.26/2.1

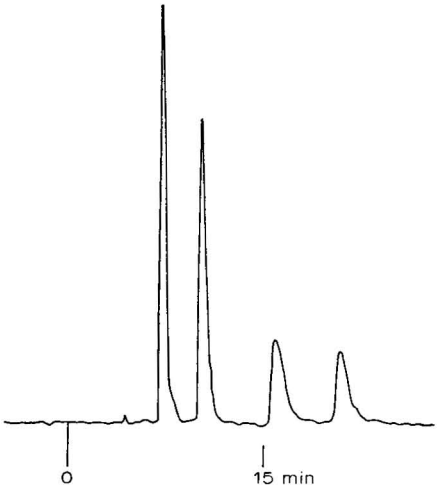

Fig. 5. Separation of the enantiomers of the racemic N-3,5-dinitrobenzoyl derivatives of leucine and alanine *n*-butyl amides upon chiral stationary phase IV using 5% isopropyl alcohol in hexane. The order of elution is D-leu, L-leu, D-ala and L-ala.

Tables III and IV contain data relevant to the separation of enantiomers of 3,5-DNB derivatives of amines and alcohols in which the basic site B is more basic than the DNB carbonyl oxygen. The primary hydrogen bonding interaction now occurs at B and the DNB carbonyl oxygen is the site of the secondary interaction (see X). This role change must be borne in mind when elution orders are correlated with absolute configurations. Fig. 5 illustrates the separation of the enantiomers of two racemic amino acids. Note that, as one increases the basicity difference between B and the DNB carbonyl oxygen, the quality of the chiral recognition (*i.e.*, the magnitude of α) increases. This trend is easily noted for the α-amino acids as one progresses from the acids to esters to the carboxylate anions to the amides. Derivatized amino phosphonic acids have been similarly resolved (Table III) as have (without elaboration at this time) 3,5-DNB derivatized di- and tripeptide enantiomers and diastereomers.

The degree of chiral recognition, as judged by the magnitude of α, is not especially sensitive to the eluent employed; indeed, aqueous solvents have been employed for neutral solutes without substantial alteration of the observed α values. Table IV and Fig. 6 document the separation of a number of α-amino acid enantiomers (as the DNB derivatives) upon CSP phase IV using a water–methanol–sodium bicarbonate eluent. In the latter solvent, the solutes are present as carboxylate anions rather than free acids. Hence, α values do change. To date, solvent changes have never altered elution order of the enantiomers from that expected on the basis of the chiral recognition rationale. Reduction in temperature increases the magnitudes of the α values but concomitant loss in column efficiency (owing to slowed mass transport) tends to offset any gain in resolution ability. Each case should be judged individually, however.

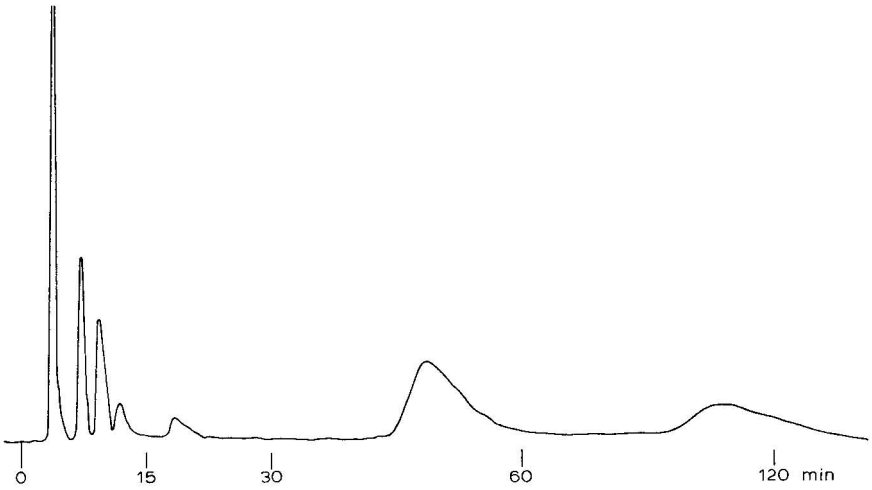

Fig. 6. Reversed-phase separation of the enantiomers of the N-3,5-dinitrobenzoyl derivatives of racemic isoleucine, phenylglycine, and α-naphthyl glycine. In order of elution: 3,5-dinitrobenzoic acid, D-isoleu, L-isoleu, D-phenyl gly, L-phenyl gly, D-α-naphthyl gly and L-α-naphthyl gly. Solvent was 80% water, 20% methanol and 0.25% sodium bicarbonate.

Second-generation chiral stationary phases

If is useful to remember that chiral recognition works in two directions. That is, a "second-generation" stationary phase appropriately* prepared from a single enantiomer of a solute resolvable upon chiral fluoroalcoholic stationary phase IV should, in turn, separate the enantiomers of fluoroalcohol Ia and its analogs. By comparing the quality of the enantiomer separation (*i.e.*, the α value) of Ia with those of its analogs, one can, with rather small racemic samples, quickly ascertain the relative suitabilities of the various fluoroalcohols as chiral stationary phase precursors. Such "iterative" procedures will allow facile optimization of CSP design.

Using CSP IV, the enantiomers of phenylglycine derivative XI and phenylglycinol derivative XII were found to have α values of 1.78 and 1.26, respectively. Using D-phenylglycine, second-generation chiral stationary phases XIII and XIV were prepared and found to separate the enantiomers of a series of fluoroalcohols analogous to Ia. Table V lists representative chromatographic parameters for resolutions of these alcohols upon XIII and XIV. Fig. 7 shows several such resolutions upon XIII. Chromatography of partially resolved configurationally known fluoroalcohols shows that the R-enantiomers are first to be eluted, as expected. (The D-enantiomers of phenylglycine derivatives XI and XII are first to be eluted from R-IV.) As shown in Table V, increasing the size of the R_f group increases the magnitude of the α value while introduction of substituents into the anthryl system can either increase or diminish α, depending upon the electron donating or withdrawing properties of the substituent. The α value can also be diminished if the substituent

* It should be evident that bonding to the solid support must not interfere with the essential chiral recognition interactions.

TABLE V

SEPARATION OF FLUOROALCOHOL ENANTIOMERS UPON SECOND GENERATION CHIRAL STATIONARY PHASES XI AND XII

Unless otherwise specified, solvent was 5% isopropyl alcohol in hexane. The elution order of each starred solute was determined by chromatography of a partially resolved configurationally established sample. In every instance, the configuration of the initially eluted enantiomer proved to be that shown above. The presumption is that the elution orders of the remaining solutes also follow this pattern.

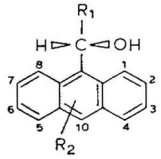

R_1	R_2	α upon		k_1' [§] upon	
		XI	*XII*	*XI*	*XII*
CF_3	H	1.33*	1.13*	4.74	13.0
CF_3	10-CH_3	1.44*	1.22*	6.0	13.3
CF_3	3-CH_3	1.32	1.12	4.36	12.2
CF_3	10-Br	1.34*	1.24*	5.07	9.70
CF_3	4-Cl	1.32	1.15	3.7	8.52
CF_3	10-CN		1.00		4.14
CF_3	10-n-C_4H_9	1.42	1.17	3.13	8.00
CF_3	10-Benzyl	1.30	1.12	2.10[§]	10.4
CF_3	10-CH_3O	1.39	1.52	8.50	9.75
CF_3	10-CH_3S	1.29	1.13*	3.5	9.82
CF_3	10-Phenyl	1.19*		2.4	
CH_3	H	1.28	1.20	7.07	8.21
C_2F_5	H	1.37	1.20	2.43	8.76
C_3F_7	H	1.40*	1.26*	2.14	6.66

[§] 10% Isopropyl alcohol in hexane.

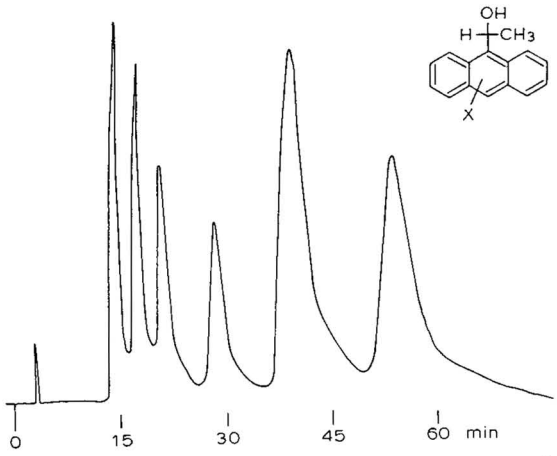

Fig. 7. Separation of the enantiomers of three type I fluoroalcohols upon chiral stationary phase XIII. In order of elution, the chromatographic bands arise from the *R*- and *S*-enantiomers respectively of 2,2,2-trifluoro-1-[(4-chloro)-9-anthryl]ethanol, 2,2,2-trifluoro-1-[(10-methyl)-9-anthryl]-ethanol and 2,2,2-trifluoro-1-[(10-methoxy)-9-anthryl]ethanol. Eluent used was 5% isopropyl alcohol in hexane.

sterically interferes with the close approach (third interaction) of the π-acid moiety. A clear inference is that CSPs derived from carbinols bearing large R_f groups and anthryl (or other polynuclear aromatic) systems bearing small electron donating substituents would outperform our initial CSP IV in terms of scope and quality of chiral recognition. Such CSPs are being prepared. It is interesting to note that replacing the R_f group with a simple alkyl group does not drastically interfere with chiral recognition. Possibly, the diminished acidity of the nonfluorinated carbinols is offset somewhat by unfavorable hydrophobic-like interactions between perfluoroalkyl groups and polar solutes.

It will be noted that the α values realized upon chiral stationary phase XIII, although appreciable, are not as large as the α value shown by phenylglycine derivative XI upon chiral stationary phase IV. These low α values may stem from partial racemization of the phenylglycine during preparation of XIII, insufficient length of the connecting "arm", or residual polar sites on the silica gel that give rise to retention mechanisms other than those responsible for the chiral recognition*. These questions are being studied and will be commented upon at a later date. Similarly, it can be noted that essentially the same α value is noted whether phenylglycinol derivative XII is chromatographed upon IV or whether 2,2,2-trifluoro-1-[9-(10-alkyl)anthryl]-ethanols are chromatographed upon chiral stationary phase XIV. Racemization is known not to have occurred during preparation of XIV; moreover, a longer connecting arm is used.

ACKNOWLEDGEMENT

This work has been supported by the National Science Foundation and by the National Institutes of Health.

REFERENCES

1 R. J. Baczuk, G. K. Landram, R. J. Dubois and H. C. Dehm, *J. Chromatogr.*, 60 (1971) 351.
2 L. R. Sousa, G. D. Y. Sogah, D. H. Hoffman and D. J. Cram, *J. Amer. Chem. Soc.*, 100 (1978) 4569.
3 B. Lefebvre, R. Audeburt and C. Quivovon, *J. Liquid Chrom.*, 1 (1978) 761.
4 J. N. LePage, W. Lindner, G. Davies, D. E. Seitz and B. L. Karger, *Anal. Chem.*, 51 (1979) 433.
5 F. Mikeš, G. Boshart and E. Gil-Av, *Chem. Commun.*, (1976) 99.
6 F. Mikeš, G. Boshart and E. Gil-Av, *J. Chromatogr.*, 122 (1976) 205.
7 C. H. Lochmüller and R. R. Ryall, *J. Chromatogr.*, 150 (1978) 511.
8 H. Hess, G. Burger and H. Musso, *Angew. Chem., Int. Ed. Engl.*, 17 (1978) 612.
9 W. H. Pirkle and R. L. Muntz, *J. Amer. Chem. Soc.*, 93 (1971) 2817.
10 W. H. Pirkle, S. D. Beare and R. L. Muntz, *Tetrahedron Lett.*, (1974) 2295.
11 W. H. Pirkle and T. A. Whitney, *Tetrahedron Lett.*, (1974) 2299.
12 W. H. Pirkle and M. S. Pavlin, *Chem. Commun.*, (1974) 274.
13 W. H. Pirkle and M. S. Hoekstra, *J. Mag. Res.*, 18 (1975) 396.
14 W. H. Pirkle and M. S. Hoekstra, *J. Amer. Chem. Soc.*, 98 (1976) 1832.
15 W. H. Pirkle, D. L. Sikkenga and M. S. Pavlin, *J. Org. Chem.*, 42 (1977) 384.
16 W. H. Pirkle and D. L. Sikkenga, *J. Org. Chem.*, 42 (1977) 1370.

* Additional retention mechanisms attenuate the α value. Hence, stability differences between diastereomeric solvates calculated from observed α values will represent minimum values.

17 W. H. Pirkle and P. L. Rinaldi, *J. Org. Chem.*, 42 (1977) 3217.
18 W. H. Pirkle and C. W. Boeder, *J. Org. Chem.*, 42 (1977) 3697.
19 W. H. Pirkle and P. L. Rinaldi, *J. Org. Chem.*, 43 (1978) 4475.
20 W. H. Pirkle and J. R. Hauske, *J. Org. Chem.*, 41 (1976) 801.
21 W. H. Pirkle and D. L. Sikkenga, *J. Chromatogr.*, 123 (1976) 400.
22 W. H. Pirkle and D. L. Sikkenga, *J. Org. Chem.*, 40 (1975) 3430.
23 W. H. Pirkle and D. W. House, *J. Org. Chem.*, 44 (1979) 1957.

Journal of Chromatography, 192 (1980) 159–172

CHROM. 12,569

ION-EXCHANGE DERIVATIVES OF SPHERON

III. CARBOXYLIC CATION EXCHANGERS*

O. MIKEŠ and P. ŠTROP

Institute of Organic Chemistry and Biochemistry, Czechoslovak Academy of Sciences, 166 10 Prague 6 (Czechoslovakia)

M. SMRŽ

Research Institute of Pure Chemicals, Lachema, 621 33 Brno (Czechoslovakia)

and

J. ČOUPEK

Laboratory Instruments Works, VVCHP, 162 03 Prague 6 (Czechoslovakia)

(Received November 23rd, 1979)

SUMMARY

Weakly acid cation-exchange derivatives of the glycol–methacrylate macroreticular gel Spheron 300 were prepared by carboxymethylation, succinylation and oxidation. The use of the latter method was also attempted in the preparation from the more macroporous Spheron 1000. Carboxymethyl derivatives were prepared with four nominal capacities for small ions: 0.26, 0.50, 1.02 and 2.20 mequiv./g. The ion-exchange samples thus prepared were characterized by the determination of the working volume, the specific non-penetratable volume and the specific weight of non-penetratatable mass in the swollen state, by titration curves and by the determination of the specific inner surface area and the magnitude of sorption for proteins (serum albumin). The samples were tested by chromatographic separation experiments using a natural mixture of egg proteins, a synthetic mixture of serum albumin, chymotrypsinogen and lysozyme; chromatography of some cyanogen bromide fragments of serum albumin was also tested. Equipment used in the medium-pressure chromatography of proteins and a dynamic method for the determination of protein sorption on the chromatographic column are described. The comparatively large differences between the determination of protein capacity using the dynamic and static (batch) methods are explained by means of a hypothesis assuming multiple sorption of proteins in batch experiments. The possibility of applying a high-performance liquid chromatograph in protein analysis is discussed.

* One part of this work was reported at the *6th IUPAC Discussion Conference, Chromatography of Polymers and Polymers in Chromatography, Czechoslovakia, Prague, July 17th–21st, 1978*, Abstract No. C30 (Institute of Macromolecular Chemistry, Czechoslovak Academy of Sciences, Prague, 1978). For Part II, see *J. Chromatogr.*, 180 (1979) 17; for Part I, see *J. Chromatogr.*, 153 (1978) 23.

INTRODUCTION

Macroporous Spheron ion exchangers have been used successfully in the high-performance liquid chromatography (HPLC) of proteins and of their higher molecular weight fragments[1–7] and of oligonucleotides[8], and in the separation of monosaccharides[9] and oligosaccharides[10]. In Parts I and II we described the properties of the polymeric matrix of Spheron[3], and the preparation and properties of the diethylaminoethyl derivative[7]. This paper is concerned with the carboxylic derivatives of Spheron. Hydrophilic macroporous weakly to medium basic anion exchangers and weakly acid cation exchangers have been most frequently used in biochemistry, which is why these derivatives of Spheron were the first to attract our attention.

EXPERIMENTAL

Materials

Spheron 300*, bead size 20–40 μm, was a product of Lachema (Brno, Czechoslovakia); it was extracted before use as described in Part I[3]. Unextracted Spheron 1000, particle size 40–60 μm, was also a Lachema product. Human serum albumin, bovine chymotrypsinogen and chicken lysozyme were of the same origin as earlier[1,3]. Chicken egg proteins were prepared according Rhodes *et al.*[11]. Cyanogen bromide fragments of human serum albumin were obtained by courtesy of Dr. B. Meloun (Institute of Organic Chemistry and Biochemistry, Czechoslovak Academy of Sciences, Prague). All other chemicals (reagent grade) were supplied by Lachema.

Preparation of carboxymethyl-Spheron 300 (CM-Spheron 300) by carboxymethylation

Spheron 300 was mixed in the cold for at least 1 h with an aqueous solution containing a 2-fold weight amount of potassium hydroxide. Then a 2-fold weight amount of potassium iodide and a 1.5-fold weight amount of chloroacetic acid (with respect to the weight of Spheron) were added gradually and with cooling[12]. The temperature was gradually increased to 60°, 15% (w/w) of potassium hydroxide was added, and the mixture was digested at 60° for 15 min. All of the gel was washed with water on a fritted disc.

This substitution procedure was repeated three times, the ion exchanger was decanted in water and cyclized with 2 *M* sodium hydroxide solution and 2 *M* hydrochloric acid, and the H^+ form was then thoroughly washed with water, methanol and acetone, and eventually dried. The dependence of the degree of ionogenic substitution on the number of repetitions of the procedure is shown in Fig. 1.

Preparation of succinyl-Spheron 300 (Suc-Spheron 300) by succinylation

To Spheron 300, pre-swollen in pyridine, the same weight amount of succinic anhydride was added gradually with cooling (18°) and stirring[12]. The suspension was then heated to 60°. On cooling, the gel was washed on a fritted disc with acetone, methanol and water, and dried *in vacuo*. Fig. 2 illustrates the relationship between the

* An analogous series of sorbents based on copolymers of 2-hydroxyethylmethacrylate with ethylenedimethacrylate under the name of Separon H is also produced by Laboratory Instruments Works, Prague, Czechoslovakia.

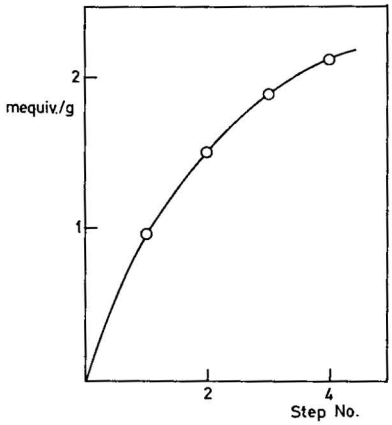

Fig. 1. Dependence of the nominal capacity of CM-Spheron 300 on the number of repetitions of the carboxymethylation process.

time of succinylation of Spheron 300 and the eventual nominal capacity of the cation exchanger thus formed. The substitution of pyridine with dimethylformamide or ethyl acetate with addition of a minor amount of pyridine or triethylamine did not result in any increase in the nominal capacity of the cation exchanger.

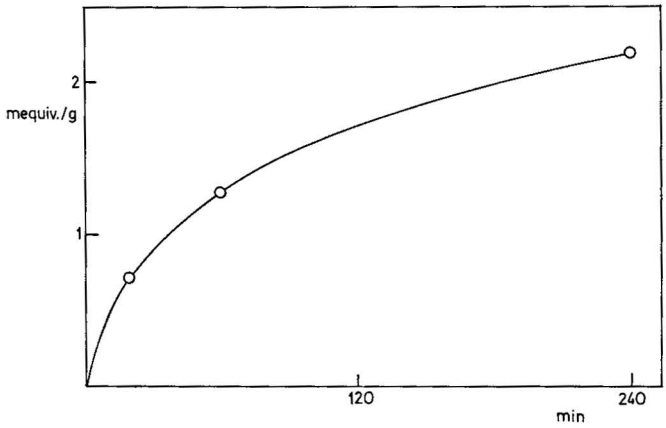

Fig. 2. Dependence of the resulting nominal cation-exchange capacity of Suc-Spheron 300 on the duration of succinylation under conditions described in the text.

Preparation of carboxylic derivatives (C-Spheron 300 and Spheron C 1000) by oxidation

To the suspension of Spheron 300 (or Spheron 1000) pre-swollen in 1 *M* sulphuric acid, a 2.75% solution of potassium permanganate was added with stirring at room temperature[13]. On completion of the reaction, the excess of permanganate was removed with several portions of oxalic acid, the ion exchanger was thoroughly washed with 2 *M* hydrochloric acid (at the beginning with oxalic acid added) and cyclized with 2 *M* sodium hydroxide solution and 2 *M* hydrochloric acid. The ion exchanger in the H^+ form was washed with water, methanol and acetone, and dried

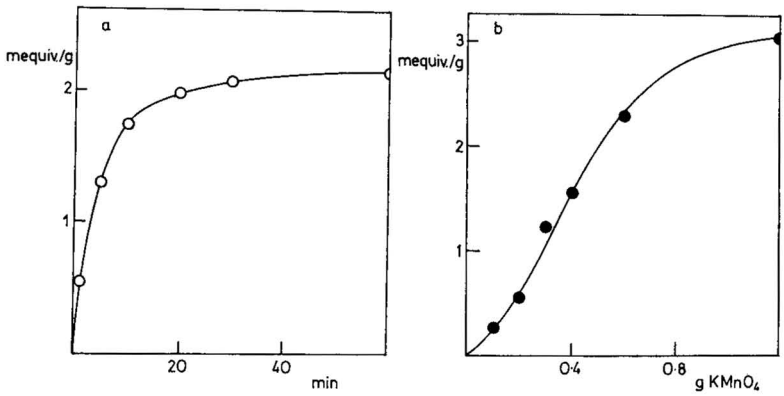

Fig. 3. Effect of time (a) and of the amount of oxidizer (b) on the resulting nominal capacity of Spheron C 1000. Oxidation was performed in acidic solution. (a) 0.55 g of potassium permanganate per gram of Spheron 1000; (b) oxidation lasted for 30 min with the given amount of potassium permanganate per gram of Spheron 1000.

under the vacuum of a water pump. The effect of reaction time and of the amount of oxidizing agent on the resulting capacity is illustrated in Fig. 3.

Equipment for the determination of the capacity of ion exchangers by the dynamic method and for the pressure chromatography of proteins

The equipment is shown in Fig. 4. A Plexiglass GM mixer provided with a side funnel made possible the continuous linking of linear gradients without inter-

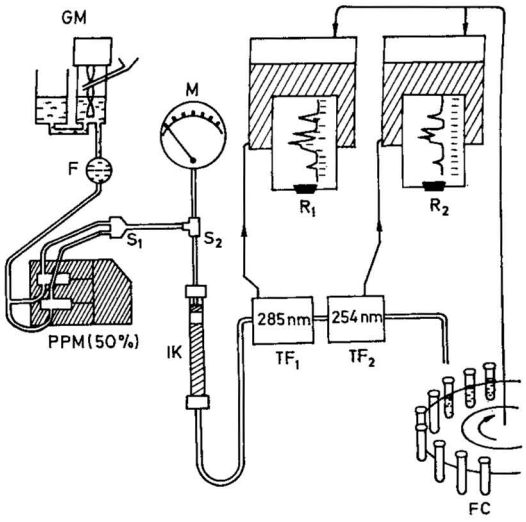

Fig. 4. Chromatographic device used also in the determination of the capacity of ion exchangers for proteins by the dynamic procedure. GM = gradient mixer; F = fritted disc, functioning both as a filter and a bubble collector; PPM = proportional programmable micropump with two reversely operating pistons, adjusted to the same output power for reduction of pulses; $S_{1,2}$ = fitting connections; IK = column with ion-exchanger column, 20 × 0.8 cm; M = manometer, 0–6 MPa (0–60 atm); $TF_{1,2}$ = flow photocells for absorbance measurements at 285 and 254 nm; $R_{1,2}$ = linear recorders; FC = fraction collector yielding recordable pulses.

ruption of the operation; it was built at the Institute of Organic Chemistry and Biochemistry. The proportional pump was manufactured in the Development Works of the Czechoslovak Academy of Sciences (henceforth referred to as Development Works). The ion-exchange column, its fittings and the manometer were those used in amino acid analysers (Development Works and Laboratory Instruments Works). Flow ultraviolet analysers (285 and 254 nm) and the line recorder (R_2) were from the Development Works. The recorder EZ 4 and fraction collector (denoted by FC) were manufactured at the Laboratory Instruments Works, Prague. The equipment was provided with a pulse generator (Institute of Organic Chemistry and Biochemistry), allowing fractions from the collector to be recorded with both recorders. In the collected fractions, pH was measured with a compensation pH meter (Development Works) and the electric conductivity was recorded with an OK-102/1 conductivity meter (Radelkis, Budapest, Hungary). In addition to measurements of capacity, all the pressure chromatographic analyses of proteins were also performed using this equipment.

Determination of the capacity of ion exchangers for proteins by the dynamic method (on a chromatographic column)

The determination was carried out using the equipment described in the preceding section and shown in Fig. 4. The ion exchanger of known volume in the column (IK) was equilibrated with a sorption buffer (of low ionic strength). The buffer was then replaced with a protein solution in the sorption buffer within the whole system including the head of the column.

Sorption. The protein solution was pumped on to the ion exchanger. As soon as breakthrough of the protein was observed, the elution volume was recorded. The protein solution was allowed to pass through the ion exchanger until its concentration in the effluent remained constant.

Washing. Only pure sorption buffer was pumped on to the ion exchanger, until the recorded absorbance line dropped to the baseline.

For desorption of the protein a linear gradient of the desorption buffer was applied (high ionic strength), which was followed by isocratic elution with the absorbance line dropped to the baseline. Then the effluent volume was measured in which the amount of eluted protein was determined spectrophotometrically. This procedure is illustrated in Fig. 5 by the determination of the capacities of four cation exchangers for serum albumin.

Other methods

The ion exchangers prepared in this work were characterized by the determination of the nominal capacity for small ions[3], by titration curves[7], by the non-penetratable volume[3] and by measurements of the specific inner surface area by the one-point method. The capacity for serum albumin was determined by the static (batch) method in a slowly rotating test-tube[7] using buffer A (0.01 *M* ammonia + acetic acid, pH 5.0) for sorption and buffer B (0.1 *M* ammonia + acetic acid, pH 7.0, 2 *M* with respect to sodium chloride) for desorption.

Before the first application and between the particular chromatographic experiments, the ion exchangers were regenerated and cyclized on a fritted disc; the ion exchanger was mixed with an approximately 3-fold volume of the regenerant, the

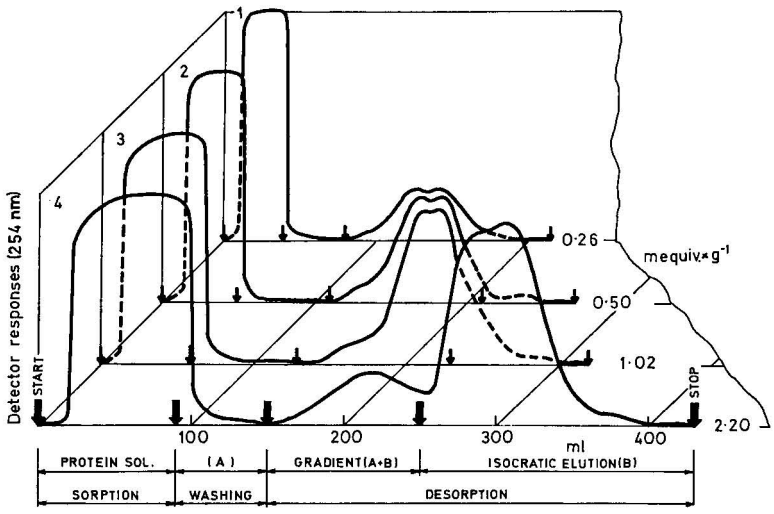

Fig. 5. Determination of the capacities of four samples of CM-Spheron 300 for serum albumin by the dynamic method. Samples of cation exchangers are denoted by numbers on the left (according to Table I), nominal capacities are given on the right. Ion-exchange column IK (*cf.*, Fig. 4) was equilibrated with sorption buffer A having a low ionic strength (0.01 *M* ammonia + acetic acid, pH 5.0). A 5% (w/w) solution of serum albumin in buffer A, centrifuged before use, was pumped on to the column. Pure buffer A was used for washing. Desorption was performed by using buffer B having a high ionic strength (0.1 *M* ammonia + acetic acid, pH 7.0, 2 *M* with respect to sodium chloride). Effluent from the whole desorption (*i.e.*, from gradient elution + isocratic elution) was collected, and the amount of washed-out serum albumin in it was determined and re-calculated to 1 ml of the bed of the ion-exchanger used. Calculated capacities for serum albumin are given in Table I. Minimal respective volumes of effluent needed for complete sorption and desorption depend on the nominal capacity of the cation exchanger and were adjusted in particular cases according to the record of absorbance.

solution was sucked off after 5–10 min, and the procedure was repeated. The regenerant was subsequently washed repeatedly with water in a similar manner. The order of regenerants for cation exchangers was 2 *M* sodium chloride solution, 2 *M* sodium hydroxide solution and 2 *M* hydrochloric acid.

Equilibration. Cation exchanger in the H^+ form was mixed on a fritted disc with the first elution buffer and the decreased pH value, measured by a glass electrode, was balanced using the base of the respective buffer. The ion exchanger was then repeatedly washed on the fritted disc by employing the procedure just described until equilibrium was established between the buffer and effluent (identical pH values, conductivities and absorbances).

RESULTS AND DISCUSSION

Survey of cation exchangers prepared in this work

Weakly acidic cation exchangers of the macroreticular 2-hydroxyethyl methacrylate Spheron[1] can be prepared by direct copolymerization of inogenic components[14] (this procedure has not been examined here), or by additional substitution of

hydrogen atoms on numerous hydroxyl groups of Spheron with a suitable ionogenic group[12]:

a

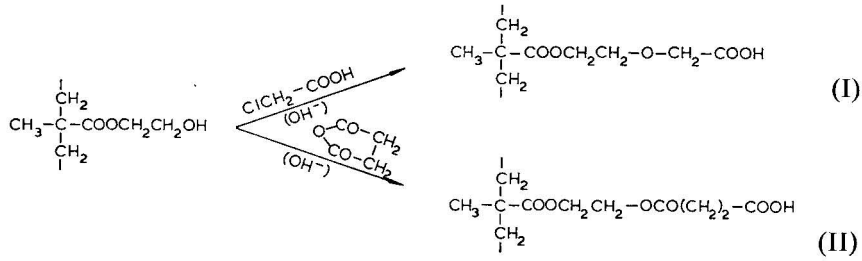

(I)

(II)

Finally, the third method[13] consists in oxidation of the copolymer with a strong oxidation agent:

b

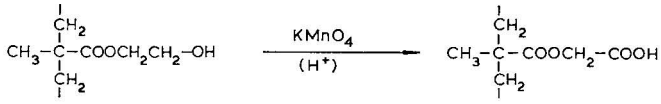

(III)

All of these routes of preparation are possible owing to the extraordinary stability of the ester bond on the trimethylacetate group. The first procedure was employed in the preparation of CM-Spheron (I), the second led to Suc-Spheron (II), and the third yielded the carboxylic derivative with the oxidized matrix (C-Spheron) (III). The ion exchangers thus prepared are summarized in Table I.

There is essentially no difference between the titration curves of CM-Spheron and C-Spheron (Fig. 6). The working volume of cation exchangers decreases with increasing nominal capacity within the whole range (samples 1–4), in both acidic and basic solution. Hence, the same paradox that has already been commented upon for anion-exchange derivatives of DEAE-Spheron with different capacities[7] occurs also in this instance. The specific inner surface area of all of the derivatives of Spheron 300 usually varies between 50 and 100 m^2/g and is considerably dependent on the method of extraction and drying of the samples.

Relationship between the protein sorption values determined by the static and dynamic methods

The capacity values of carboxylic ion exchangers determined by the static (batch) and dynamic (column) methods differed considerably, as shown in Fig. 7. The curve of the dependence of the static sorption of serum albumin on nominal capacity (solid line) has a form very similar so that of the static sorption of proteins on the nominal capacity of DEAE-Spheron (*cf.*, Fig. 4 in ref. 7): there is a steep rise at the beginning, after which the curve remains almost horizontal. The curve determined by the dynamic method is not linear as was the relationship between the capacity for small ions and the degree of ionogenic substitution (*cf.*, Fig. 4 in ref. 7), but approaches this relationship. The difference between the two methods does not lie only in the form of the two dependences. Both methods also differ considerably in

TABLE I

SURVEY AND CHARACTERIZATION OF SPHERON 300 WEAKLY ACIDIC CATION EXCHANGERS PREPARED IN THIS WORK

Property	*Unit*	*Unsubstituted* Spheron 300*	*Sample No.*					
			1	*2*	*3*	*4*	*5*	*6*
Type of ion exchanger**			CM	CM	CM	CM	Suc	C
Nominal capacity	mequiv./g	0.035	0.26	0.50	1.02	2.20	0.51	2.12
Capacity for serum albumin:								
Sorption statically***	mg/g	2–3	88	247	307	305		
Desorption statically***	mg/g		104	256	313	298		
Desorption dynamically	mg/ml		4.5	10.6	15.8	24.9		
	mg/g		17.8	41.6	60.8	85.7		
Specific non-penetratable volume***	ml/g	0.752	0.754	0.731	0.679	0.752		0.746
Specific weight of non-penetratable mass in swollen state***	g/cm^3	1.330	1.326	1.367	1.473	1.330		1.341
Working volume***:								
In 2 *M* sodium hydroxide	ml/g		3.97	3.94	3.92	3.57	3.82	4.02
In 2 *M* hydrochloric acid	ml/g	3.95§	3.92	3.89	3.77	3.32	3.77	3.77
Specific inner surface area (by the Klyachko–Gurvich method)***	m^2/g	55	94	96	75	56		55

* For comparison with samples 1–6 some data[3] are given for unsubstituted Spheron 300, which was the initial raw material used in ionogenic substitutions.

** Types denote derivatives: CM = carboxymethyl; Suc = succinyl; C = carboxyl. In the text these types are denoted as structures I, II and III, respectively.

*** Methods were described in detail or cited in refs. 3 and 7.

§ Holds for distilled water.

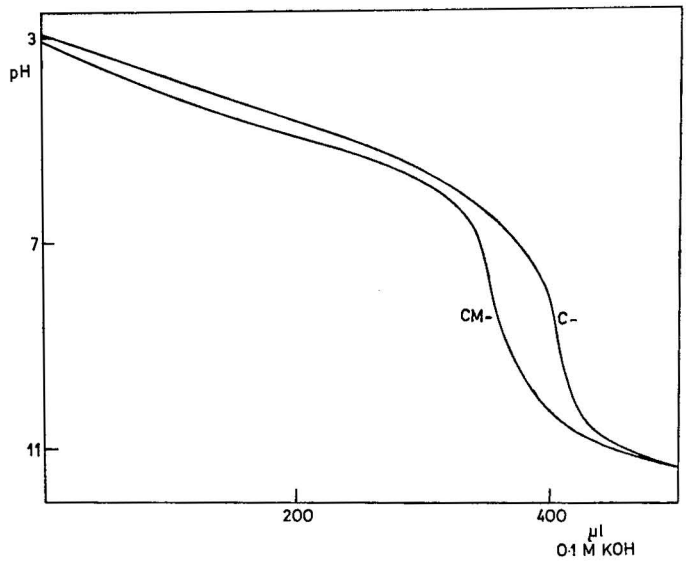

Fig. 6. Titration curves of CM-Spheron 300 with nominal capcity 1.02 mequiv./g and C-Spheron 300 with capacity 2.16 mequiv./g. Titrations performed with autotitrator in 1 *M* potassium chloride solution.

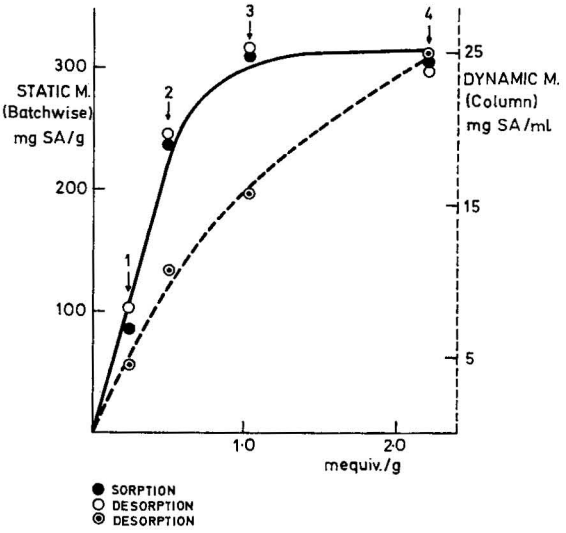

Fig. 7. Relationship between capacities of carboxymethyl derivatives of Spheron 300 for sorption of serum albumin determined by static and dynamic methods. Samples numbered as in Table I. Solid line and left-hand weight scale relate to results of the static method; broken line and right-hand volume scale relate to the dynamic method. Horizontal axis expresses nominal capacities of tested CM-Spherons for small ions (*e.g.*, Na^+).

the absolute values of their results, which becomes evident if they are converted into the same units, *e.g.*, weight units (*cf.*, Table I). The values measured by the static method are three to four times higher.

This may be explained by a hypothesis of multiple sorption under static conditions, as follows. With a protein bound on the ion exchanger its charge distribution is shifted owing to the effect of the functional groups present. For this reason, the layer of sorbed protein behaves as a cation exchanger and may sorb another layer. This effect may be transferred to yet another layer. Multiple sorption, based only on weak interactions, is due to the higher protein concentration in the neighbourhood, and the respective equilibrium needs a long time to be established. This equilibrium mostly does not hold under dynamic conditions, even if the same buffer is used as in the static method. On the outer parts of the beads it is perturbed hydrodynamically, while in the bulk of the macropores it is upset by the rapid change in the protein concentration. In the static method[7] we measure the final equilibrium of sorbed protein towards the protein solution in the mobile phase, while in the dynamic procedure the final equilibrium is evaluated towards the pure sorption buffer. The protein sorption values determined by the dynamic method more adequately describe the possibilities of loading the ion exchanger in chromatography. In contrast values ascertained by the static method give a better picture of the possibility of utilization of the ion exchanger for sorption using the batch method.

Testing of the chromatographic properties of cation exchangers prepared in this work

The chromatographic properties of the ion exchangers were tested by the separation of a natural mixture of egg proteins and of a synthetic artificial mixture of proteins. The dependence of the separation of a natural mixture of proteins on the nominal capacity of CM-Spheron 300 can be seen in Fig. 8. Cation exchangers with low nominal capacity are unable to retain the proteins, and the greatest part of the latter is eluted in a single large peak at the beginning of the chromatogram. With increasing capacity the retention increases, and some peaks are displaced. Similar comparative experiments were performed on the individual ion exchangers with increasing load (*e.g.*, 8, 15 and 30 mg of the protein mixture). At the same time it was observed, as expected, that ion exchangers of higher capacity give adequate separations also at a higher load. Fig. 9 illustrates the separation of 60 mg of egg proteins on a high-capacity cation exchanger. Comparison with the separation on a ion exchanger with the same high capacity, but at a lower load (2.20 mequiv./g, load only 8 mg; Fig. 8) leads to the conclusion that also at higher loads the positions of the peaks in the elution profile remain constant.

Tests with C-Spheron 300 yielded results similar to those with CM-Spheron, if subjected to regeneration (*i.e.*, used repeatedly). The first chromatographic analysis on C-Spheron usually did not proceed in the expected way. In repeated chromatographic analyses of the proteins, C-Spheron differed from CM-Spheron only insignificantly in the displacement of peaks. Both sorbents differed in their nominal capacities and in the length of the spacer carrying the functional group.

Further chromatographic tests on the cation exchangers were performed using a synthetic mixture of serum albumin (SA), chymotrypsinogen (CH) and lysozyme (LZ). An interesting effect of the pH of ammonium acetate buffers on the separation of SA and CH was observed, as illustrated in Fig. 10. The synthetic mixture could be adequately separated on CM-Spheron 300 with a capacity of 2.20 mequiv./g at pH 8 and 7, exhibiting three separate peaks, I, II and III. At pH 5 and 6, on the other hand, only two peaks were revealed by the chromatographic analysis. Tests involving pure

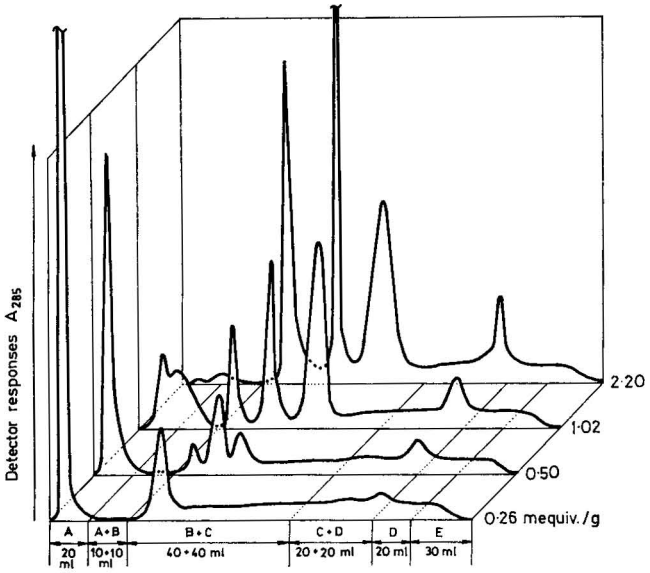

Fig. 8. Effect of nominal capacity of CM-Spheron 300 on separation of egg proteins. Dimensions of column 20 × 0.8 cm, load 8 mg in all instances. Capacities of tested ion exchangers are given on the right. Buffers used: A, 0.05 *M* ammonia + acetic acid, pH 5.0; B, 0.3 *M* Tris + acetic acid, pH 7.5; C, 0.5 *M* Tris + hydrochloric acid, pH 9.5; D, buffer C, 1 *M* with respect to sodium chloride. Short isocratic elution was followed by three linear gradients and by isocratic elution with buffer having a high ionic strength. The column was finally washed with 2 *M* sodium chloride solution (E).

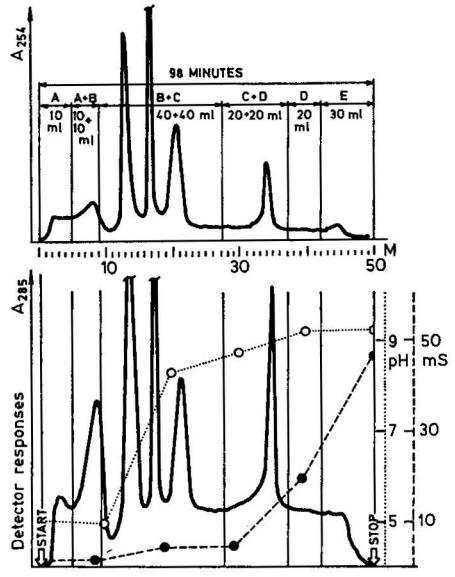

Fig. 9. Chromatographic analysis of 60 mg of a mixture of egg proteins on CM-Spheron 300 (column 20 × 0.8 cm), nominal capacity 2.20 mequiv./g. Detection performed with a tandem system of UV analysers (*cf.*, Fig. 4). Buffers used and the other parameters as in Fig. 8. Fractions 4.2 ml in volume were collected in intervals of 118 sec. M = step-marks of the fraction collector. Right-hand scales: for measurements of pH (open circles) and conductivity (full circles).

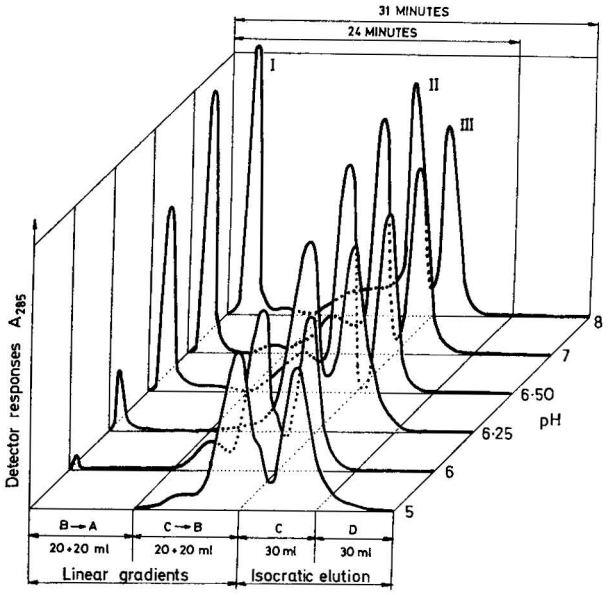

Fig. 10. Diagram illustrating separation of 8 mg of serum albumin (I), 4 mg of chymotrypsinogen (II) and 4 mg of lysozyme (III) on a 20 × 0.8 cm column of CM-Spheron 300, nominal capacity 2.20 mequiv./g, using buffers of different pH. Ion exchanger equilibrated with buffer A. Mixture of proteins was applied in 0.3 ml of buffer A. Arrows indicate mixing of buffers when linear gradients are formed. All buffers were prepared from ammonia solution (the resulting molarity of which is indicated below) acidified with acetic acid to the pH shown. Buffer A was 0.01 *M*, B was 0.1 *M*, C was buffer B which was 1 *M* with respect to sodium chloride, D was 2 *M* sodium chloride solution. Flow-rate, 4.5 ml/min; temperature, 25°; counter pressure, 5–7 atm. Peaks I–III contain the given proteins only at runs at pH 8 and 7. A further decrease in pH led to displacement of serum albumin from peak I to peak II (see text).

proteins alone at pH 5 showed that both SA and CH exhibit, under the conditions used, virtually identical retention volumes, in agreement with the effect of pH on the displacement of the peaks of these proteins. In experiments involving the separation of the above mixture of three proteins in the pH range 6–7, the peak of SA was shifted from position I to II, but not owing to a gradual change in the retention volume. Already at pH 6 traces of SA could be observed at position I, and the amount gradually increased as the pH increased to 6.25 and 6.50, reaching a maximum at pH 7. At the same time, the area of peak II gradually decreased. Similar results were recorded with C-Spheron 300 with a capacity of 2.12 mequiv./g. All of these phenomena can be explained by a hypothesis involving the interaction of both proteins under the experimental conditions, giving rise to a product that is not separated on the carboxylic derivatives of Spheron within the given range of pH.

CM-Spheron was also used in the testing of separations of higher molecular weight fragments of proteins. Fig. 11 illustrates such tests, aimed at establishing conditions for the chromatography of cyanogen bromide fragments of serum albumin[5]. Further chromatographic applications of this cation exchanger were described earlier[2], together with a description of its testing in the reversible sorption of proteolytic enzymes. In earlier work[1], CM-Spheron 300 was compared with CM-

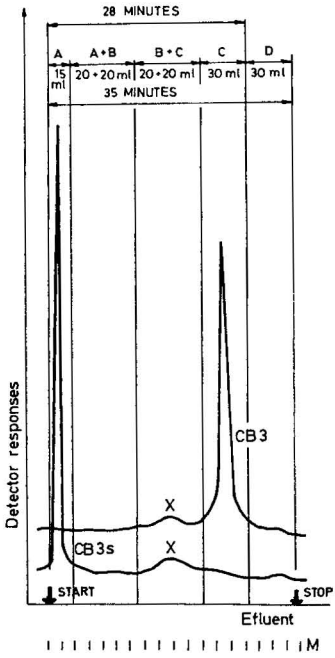

Fig. 11. Chromatographic analysis of cyanogen bromide fragment of serum albumin CB3 and of its succinylated derivative CB3s on a column of CM-Spheron 300, nominal capacity 2.20 mequiv./g. The figure is a superposition of records made with the apparatus shown in Fig. 4. Records at 285 and 254 nm were connected by averaging. Individual chromatograms are arranged one above another with intervals between blank lines. In uniformly performed experiments, 8 mg of fragment was applied each time in 0.2 ml of starting buffer. Short isocratic elution was followed by two linear gradients and by isocratic elution with the last buffer. The flow-rate was 4 ml/min. Fractions denoted by M were collected at 2-min intervals. Buffers used: A = 0.01 *M* ammonia + acetic acid, pH 7.0; B = 0.1 *M* ammonia + acetic acid, pH 7.0; C = 0.5 *M* ammonia + acetic acid, pH 7.0, 1 *M* with respect to sodium chloride. The column was finally washed with 2 *M* sodium chloride solution (D). Cyanogen bromide fragments have been characterized in detail in ref. 15; they contain 175 amino acid residues. X = unidentified peak, probably a residue of pyridine from preceding treatment. At the same time, the figure illustrates the effect of succinylation of polypeptide on the positions in the elution profile.

cellulose, and it was found that it did not exhibit irreversible sorption. The commercially produced weakly acid cation exchanger of type III, the so-called Spheron C 1000 (*cf.*, ref. 16, Table 5.6B, p. 260) yielded good results in a systematic study of the HPLC of pectolytic enzymes, which is now in progress.

CONCLUSIONS

Weakly acid carboxylic hydrophilic and macroporous cation exchangers are in general well suited for the separation of proteins and their higher molecular weight fragments. Samples of CM-Spheron 300 corresponding to this classification have been applied in many chromatographic experiments, in which they exhibited separation properties similar to those observed with carboxymethyl derivatives of cellulose or polydextran. With CM-Spheron or Spheron C, however, higher pressures could

be employed, which considerably accelerated the separation process. Spheron ion exchangers can be subjected to multiple regeneration without any change in their sorption properties.

Chromatographic analyses of various enzymes and other proteins and their fragments may be performed with Spheron derivatives of particle size 20–40 μm within a period of tens of minutes, using a moderate pressure not exceeding 15–20 atm. This makes possible the utilization of glass columns, pumps and connections used in amino acids analysers. Reduced particle size, together with a higher pressure applied in suitable devices equipped for the ion-exchange HPLC of proteins, leads to retention times measurable in minutes. Experiments carried out in this direction may lead to the construction of a high-speed protein analyser, which may be used not only in biochemistry and related fields, but also in fermentation technology (*e.g.*, in the investigation of the formation of bioproducts in large fermentors), in clinical diagnostics (*e.g.*, in the high-speed analysis of plasma proteins), in the production of sera and vaccines, technical enzymes and other proteins, in food technology and in agrochemical research. Spheron ion exchangers appear to be prospective packings for such an HPLC protein analyser.

ACKNOWLEDGEMENTS

The authors are indebted to Dr. B. Meloun for kindly supplying cyanogen bromide fragments of serum albumin and to Mrs. J. Sedláčková for careful technical assistance.

REFERENCES

1 O. Mikeš, P. Štrop, J. Zbrožek and J. Čoupek, *J. Chromatogr.*, 119 (1976) 339.
2 O. Mikeš, P. Štrop and J. Sedláčková, *J. Chromatogr.*, 148 (1978) 237.
3 O. Mikeš, P. Štrop and J. Čoupek, *J. Chromatogr.*, 153 (1978) 23.
4 O. Mikeš, J. Čoupek and J. Sedláčková, *6th IUPAC Discussion Conference, Chromatography of Polymers and Polymers in Chromatography, Prague, Czechoslovakia, July 17–21, 1978*, Abstr. No. C30, Institute of Macromolecular Chemistry, Czechoslovak Academy of Sciences, Prague, 1978.
5 O. Mikeš, *Int. J. Peptide Protein Res.*, 14 (1979) 393.
6 O. Mikeš, J. Šatava and P. Štrop, Summaries of *International 2nd Danube Symposium, Progress in Chromatography, Carlsbad, April 1979*, Czechoslovak Chemical Society, Abstr. No. D 1.5.
7 O. Mikeš, P. Štrop, J. Zbrožek and J. Čoupek, *J. Chromatogr.*, 180 (1979) 17.
8 J. Šatava, O. Mikeš and P. Štrop, *J. Chromatogr.*, 180 (1979) 31.
9 Z. Chytilová, O. Mikeš, J. Farkaš, P. Štrop and P. Vrátný, *J. Chromatogr.*, 153 (1978) 37.
10 P. Vrátný, O. Mikeš, J. Farkaš, P. Štrop, J. Čopíková and K. Nejepínská, *J. Chromatogr.*, 180 (1979) 39.
11 M. B. Rhodes, P. B. Azari and R. E. Feeney, *J. Biol. Chem.*, 230 (1958) 399.
12 P. Štrop, O. Mikeš and J. Čoupek, *Czech. Pat.*, 171,963 (1976).
13 M. Smrž and S. Slováková, *Czech. Pat.*, 169,131 (1976).
14 J. Čoupek, O. Mikeš, P. Štrop and M. Křiváková, *Czech. Pat.*, 171,962 (1976).
15 B. Meloun, L. Morávek and V. Kostka, *FEBS Lett.*, 58 (1975) 135.
16 O. Mikeš (Editor), *Laboratory Handbook of Chromatographic and Allied Methods*, Ellis Horwood, Chicester, 1979.

Journal of Chromatography, 192 (1980) 173–184

CHROM. 12,576

STIMULATED SEQUENTIAL DEHYDROXY-FLUORINATION: A SAFE, CONVENIENT METHOD FOR GAS CHROMATOGRAPHIC ANALYSIS OF PHOSPHATE DIESTERS WITH POSSIBLE APPLICATION TO HYDROLYSATES OF ORGANOPHOSPHORUS PESTICIDES AND NERVE GASES

WAYNE H. GRIEST* and T. W. MARTIN**

Department of Chemistry, Vanderbilt University, Box 1506, Station B, Nashville, Tenn. 37235 (U.S.A.)

(First received September 10th, 1979; revised manuscript received November 26th, 1979)

SUMMARY

Model studies with di-*n*-butylphosphate show that organic triester derivatives chosen to gain increased volatility by simply minimizing total molecular weight are relatively poorer in gas chromatographic properties than the diesterphosphorofluoridate analogue because both the molecular weight and the overall polarity of the derivative are critical factors. We find the substitution of the hydroxyl group by fluorine is the most successful way at present to derivatize phosphate diesters. Fluorine substitution is effective because it reduces the strong phosphoryl dipole, presumably by decreasing the electron density on the oxygen atom via $p\pi$–$d\pi$ backbonding to the phosphorus. Dehydroxy-fluorination is best carried-out by a sequential reagent process starting with dicyclohexylcarbodiimide to stimulate and direct the dehydroxy-step before adding hydrogen fluoride as the active fluorinating agent. This procedure is safe and convenient and is believed applicable to a wide range of hydroxyphosphates including the hydrolysates of many organophosphorus pesticides and nerve gases at minimal sample sizes.

INTRODUCTION

In a previous paper[1], we demonstrated an unavoidable phosphorus–oxygen bond cleavage reaction which renders trimethylsilyl (TMS) derivatization useless for the quantitation by gas chromatography (GC) of condensed polyphosphates and related nucleotides. Although TMS or methyl ester derivatives of phosphoric acid and its mono- or diesters have often been applied to these simpler phosphate substrates[2–11], derivatization and subsequent GC analysis are not easy or dependable procedures. In fact, reliable reports of sensitive and reproducibly precise GC methods

* Present address: Analytical Chemistry Division, Oak Ridge National Laboratory, Oak Ridge, Tenn. 37830, U.S.A.

** To whom correspondence should be addressed.

for phosphates are practically non-existent, and the few available reports[4,12–17] differ in methods, sensitivity, specificity, and precision.

For a number of years we have sought improvements in the derivatization and GC analysis of certain classes of phosphates by assuming the principal difficulties stem from essentially two interrelated and unavoidable factors: (1) the relatively high molecular weights of all phosphate derivatives and (2) the large inherent polarity of the phosphate group, a complicated function of the normally strong phosphoryl dipole mixed with significant dipolar contributions from the other three P–O bonds. Rather than simply trying to reduce molecular weight, we reasoned that if one could modify the phosphate group's structure in such a way as to reduce its overall polar character such a derivative might have improved GC properties. This paper reports the results of a study to test this "polar hypothesis" using di-*n*-butylphosphate (DBP) as a model monohydroxyphosphate. Such dialkylphosphates are common pesticide hydrolysis products and their determination in physiological fluids[12,13] or water[17] is of continuing importance for public health services and in monitoring environmental pollution.

EXPERIMENTAL

Materials

The principal chemicals and other materials used are listed below by chemical name or formula with any useful acronym in parentheses followed by the supplier's name and address and any special information in square brackets: tetrahydrofuran (THF), pyridine and acetonitrile [Fisher Scientific, Pittsburgh, Pa., U.S.A.; each of these solvents was redistilled, reagent-grade and stored over activated molecular sieve, 13X]; methyl iodide, triethylamine, benzene, methylene chloride, dimethoxypropane, diethylether, *n*-butanol, phosphoryltrichloride, potassium fluoride and sodium fluoride [also from Fisher Scientific]; HF and $COCl_2$ [Matheson Gas Products, East Rutherford, N.J., U.S.A.; in lecture bottles]; AgF and BiF_3 [Alfa Division, Ventron, Danvers, Mass., U.S.A.]; 2,4-dinitrofluorobenzene (DNFB) [Aldrich, Milwaukee, Wisc., U.S.A.]; bis(trimethylsilyl)trifluoroacetamide (BSTFA), hexamethyldisilizane (HMDS), trimethylchlorosilane (TMCS) and dicyclohexylcarbodiimide (DCCI) [Pierce, Rockford, Ill., U.S.A.]; 0.3-ml reaction vials [Regis, Morton, Ill., U.S.A.]; all GC stationary phases, solid supports and syringes [Applied Science Labs., State College, Pa., U.S.A.].

Preparation of reagents and substrate

Diazomethane (CH_2N_2). The precursor, N-nitrosomethyl urea, was synthesized by a previous procedure[18]. CH_2N_2 was generated on reaction of the precursor with aqueous sodium hydroxide and was collected by bubbling through diethyl ether in a micro apparatus[19].

DBP. The precursor for this substance, chosen as our model substrate, was dibutylphosphorochloridate (DBPC) which was synthesized from a modification of the published method[20] for the diethyl homologue. In our procedure, a solution of 20 ml of *n*-butanol plus 17.6 ml of pyridine in 80 ml benzene was slowly added over 45 min into a well stirred solution consisting of 10 ml phosphoryl trichloride and 250 ml benzene contained in a 1-l round-bottom flask. The reaction mixture was

stirred 1 h, refluxed 6 h and allowed to stand at room temperature overnight, protected from moisture by a $CaCl_2$-trap, before filtration and vacuum distillation. A 27% yield of DBPC was achieved by this procedure but GC analysis of this product revealed a 10% contamination with tributylphosphate (TBP). However, this impurity was not removed because it served as a convenient internal standard (IS). The DBPC preparation was stored in a round-bottom flask with ground-glass stopper in a desiccator over dry $CaCl_2$. Hydrolysis to DBP was carried out daily on a 3-μl aliquot of a solution containing 120 μl DBPC diluted to 1 ml with THF. This 3-μl aliquot was added to 60 μl of THF and 30 μl of water, and the combined solution was heated at 60 to 90° for 15 min before the solvents were evaporated under a gentle stream of nitrogen. The residue was treated with methylene chloride or dimethoxypropane and re-evaporated to remove traces of water, and was finally redissolved in 250 μl of THF. From this solution, 3-μl aliquots corresponding to 20 nmol of DBP were transferred to reaction vials for derivatization and GC analysis.

HF–THF. Solutions of HF in THF were prepared by bubbling HF from a lecture bottle through dry, redistilled THF contained in a 2-oz. polyethylene jar, using a 0.25-in. O.D. PTFE tube connected to the HF lecture bottle valve. Contact with atmospheric moisture during bubbling was minimized by using a cap on the jar with a hole drilled just large enough to accept the PTFE tubing. This procedure was conducted in a fume hood to avoid exposure to HF. The HF–THF solution was standardized by pipetting a 100-μl aliquot into 15 ml of water, and titrating the HF to the phenolphthalein end point with standard NaOH solution. Generally, HF concentrations of about 1 *M* were prepared, and the tightly capped jar was stored in a desiccator over Drierite for a maximum of two weeks before replacement.

$COCl_2$–THF. A stock solution of $COCl_2$ in THF was prepared by directly bubbling $COCl_2$ into THF contained in a 2-oz. polyethylene jar in a fume hood, similar to the procedure used for preparing the HF–THF solution. The concentration of $COCl_2$ was estimated by pipetting 100 μl of the solution into 15 ml of well-stirred standardized NaOH solution and titrating the excess base with standard HCl solution to the phenolphthalein end point. Generally, a concentration of 0.04 *M* $COCl_2$ was prepared and this $COCl_2$–THF reagent was stored like the HF–THF reagent.

AgF–CH_3CN. Powdered AgF was slowly stirred into CH_3CN at a ratio of 3 mg AgF per ml CH_3CN. The mixture was warmed slightly (30–35°). After cooling the solution, the excess AgF was removed by centrifugation for 3–5 min using a bench-top clinical centrifuge. Gravimetric analysis of the residue obtained from evaporating aliquots of the solution indicated an AgF concentration of 23.0 ± 0.6 m*M*.

Derivatization reactions

Safety precautions. It is to be emphasized that the ability of some dialkylphosphorofluoridates (such as diisopropylphosphorofluoridate) to inhibit neural cholinesterase[21] makes fluorinated DBP derivatives potentially quite hazardous, and extreme care must be exercised in their generation and handling. However, generation and sampling under sealed containment can be accomplished conveniently by the use of 0.3-ml reaction vials with PTFE-lined septum caps. The DBP substrate in these derivatizations was pipetted into the vials, the vials then sealed, and the dehydroxy–fluorination reagents were introduced through the septum with graduated 100-μl Hamilton syringes. Heating was conducted in a metal heating block as previously

described[1]. Samples for GC analysis were withdrawn directly through the septum with a 10-μl Hamilton syringe. After GC analysis of the derivatives, the vials were cleaned and the contents were destroyed by soaking in chromic acid.

The following are the derivatization reactions conducted upon DBP. All but the first three produce a potentially hazardous phosphorofluoridate.

TMS derivatization. A 20-nmol aliquot of DBP was reacted with a 100-fold molar excess of either BSTFA or HMDS (either reagent in a solution containing 1% of TMCS (v/v) and 100 μl of CH_3CN). The sealed reaction vial was heated at 80° for 15 min, and after cooling was sampled for GC analysis.

Methylation with CH_2N_2. In a fume hood, diazomethane in diethyl ether was added dropwise to 20 nmol of DBP in 100 μl of methanol until a stable yellow color remained. The vial was then sealed and the solution allowed to react at room temperature for 5 min. After this, the top was loosened and excess CH_2N_2 and diethyl ether flushed out by bubbling with a stream of dry nitrogen for a few minutes. Then the remaining methanol solution was sampled for analysis.

Methylation with AgF–CH_3I. A 20-nmol aliquot of DBP was reacted with a 3-fold molar excess of AgF in CH_3CN to precipitate the Ag salt of DBP. The CH_3CN was evaporated with a stream of dry nitrogen, and 100-fold molar excess of CH_3I was added. The sealed vial was heated at 80° for 15 min, and allowed to cool before sampling.

Fluorination with DCCI–HF. A 2.0-μmol aliquot (100-fold molar excess) of DCCI in 100 μl THF was added to 20 nmol of DBP, and the mixture was allowed to react in a sealed vial at room temperature for 2–3 min. A 1000-fold molar excess of HF in 20 μl THF was then added, and the sealed vial was allowed to stand at room temperature for 45 min before sampling.

Fluorination with DCCI–AgF. This derivatization reaction was conducted as described above for the DCCI–HF reagents, except that 26 μl of CH_3CN containing a 300-fold molar excess of AgF was substituted for HF–THF.

Fluorination with DCCI–KF or DCCI–NaF. This derivatization was conducted as described above for the DCCI–HF reagents, except that 2–3 mg of powdered KF or NaF was added instead of HF–THF.

Fluorination with $COCl_2$–AgF. To a 17-nmol aliquot of DBP in 20 μl THF was added a 2000-fold molar excess of $COCl_2$ in 100 μl THF and 2–3 mg powdered AgF. The reaction was allowed to proceed at room temperature for 24 h in a sealed vial before sampling.

Fluorination with HF. A 1000-fold molar excess of HF in 20 μl of THF was added to 20 nmol of DBP in 100 μl of THF and the reaction vial sealed. The reaction was carried out at room temperature for 5 h before analysis.

Fluorination with DNFB. To 20 nmol of DBP in 100 μl THF was added a 1000-fold molar excess of DNFB and a 2700-fold molar excess of triethylamine. The vial was sealed, heated at 95° for 15 min, and cooled before a sample was withdrawn for analysis.

Fluorination with BiF_3. Two to three mg of BiF_3 were added to a 20-nmol aliquot of DBP in 100 μl of THF. The vial was sealed and heated at 40° for 1 h. After the vial was cooled a sample was taken for analysis.

GC analysis

A 2-μl volume of a reaction mixture was withdrawn from the reaction vial through the septum cap using a 10-μl Model 701 Hamilton syringe. This sample was injected into a Hewlett-Packard Model 5750 gas chromatograph. The column used was a 6 ft. $\times$ 0.125 in. O.D. stainless steel coil packed with 10% (w/w) OV-61 coated on 80–100 mesh, acid-washed, dimethyldichlorosilane-treated Chromosorb W prepared by the evaporative method[22]. The column oven temperature was maintained isothermally at 183°, and the injector and detectors were held at 195 and 190°, respectively. Helium carrier gas was flow-regulated at 25 cm^3/min. The stainless steel injection port was lined with PTFE by simply inserting a 6 in. $\times$ 0.0625 in. O.D. PTFE tubing into the injector liner.

TMS derivatives were analyzed with the conventional flame ionization detector (FID), and all others (except methyl esters, when compared with TMS derivatives) were analyzed with the alkali flame ionization detector (AFID), which was installed and adjusted according to factory instructions[23].

Quantitative comparison of DBP derivatives was accomplished conveniently by the method of internal standards[24], letting the unavoidable TBP contamination in the DPBC precursor to the DBP substrate serve as a convenient internal standard (IS).

RESULTS AND DISCUSSION

Our contention that simply increasing the volatility of an organic phosphate triester by minimizing molecular weight alone is not sufficient to produce a superior derivative for GC analysis is supported by a comparison of the properties of trimethylsilyl dibutylphosphate (TMS-DBP) and methyl dibutylphosphate (CH_3-DBP) prepared by the TMS derivatization and the methyl esterification methods described above. Using the FID technique because the AFID loses sensitivity when exposed to TMS compounds[25], we found that the response of the TMS-DBP produced with the BSTFA reagent was approximately the same as that of the CH_3-DBP produced with either CH_2N_2 or AgF–CH_3I. However, the response of TMS-DBP produced with the HMDS reagent was approximately 8% less than that produced with the BSTFA reagent, consistent with our previous observations[1] of their relative potencies as TMS-donors. Although CH_3-DBP was somewhat more volatile than TMS-DBP (GC retention times of 3.5 and 3.7 min, respectively), the chromatographic peaks of both derivatives exhibited noticeable tailing, suggesting that the column and/or packing material were not sufficiently inert toward these derivatives. Hence, we believe only a reduction in the net polarity of the phosphate group will improve the GC response of these compounds.

The obvious means of diminishing the phosphate group polarity is by a reduction of the phosphoryl dipole strength, which entails either a chemical reduction of the formal oxidation state of the phosphorus atom (such as from 5+ in phosphate to 3+ in phosphite) or by replacement of the hydroxyl group with a more electronegative substituent such as flourine. The lack of literature precedent, plus the many difficulties we experienced[26] in attempting to carry-out controlled chemical reduction of phosphate to a stable lower oxidation state, forced us to discard actual chemical reduction as a possible route to improved GC derivatives. In contrast, the general stability of P–F bonds[27,28] and the many experimental successes for the chlorination

of phosphates by $COCl_2$ [29–31], the fluorination of organic compounds by COF_2 [32], and the fluorination of phosphates by HF[33,34] or by DNFB[35] convinced us that a systematic study of the fluorination of DBP as a model diester might be a promising way to test whether decreasing the relative polarity of the phosphate moiety by dehydroxy-fluorination might yield a better derivative in support of our introductory "polar hypothesis".

Initial investigation revealed that a number of reagents can be employed to convert DBP to dibutylphosphorofluoridate (DBPF). Normalized DBPF yields for the reagents studied are listed in Table I. The $COCl_2$–AgF reagent combination was unsatisfactory because it produced mixed products of both DBPF and DBPC. Also, it is seen in Table I that most reagents gave relatively low DBPF yields except for the DCCI–HF sequential method which is so unique that it deserves more extensive discussion.

TABLE I

RELATIVE YIELDS OF DBPF IN THE DEHYDROXY-FLUORINATION OF DBP

Reagents	*Relative yield (%)*
DCCI–HF	100*
$COCl_2$–AgF	35
DCCI–AgF	25
HF	23
DNFB–$(C_2H_5)_3N$	17
BiF_3	3.0
DCCI–KF or DCCI–NaF	1.0

* Assumed to be quantitative.

We are convinced that the DCCI–HF sequential system is the best known method for carrying-out the dehydroxy-fluorination of phosphate diesters. A comprehensive review[36] indicates the few methods available for the direct conversion of a dialkyl phosphate to a dialkylphosphorofluoridate. Judging from the relative yields of DBPF from the DCCI–HF sequential combination as compared to that achieved by HF alone, there can be no question that DCCI stimulates the dehydroxy-fluorination process in a remarkably way. Since DCCI has been used for years to promote the synthesis of pyrophosphates[37–40], presumably by activating one phosphate for nucleophilic attack by another, we envision by analogy in Scheme I a reasonable mechanism for converting DBP to DBPF in accord with our results and which explains the possible role of DCCI in the dehydroxy-fluorination process.

Reaction 1 can be viewed as a rather fast acid–base addition reaction between DBP and DCCI. The result is intermediate complex I which is the first necessary stage for stimulated dehydroxylation and a directed activation of the phosphate group. Reaction 2 completes the dehydroxy-fluorination process by a double attack of both the proton electrophile and the fluoride nucleophile. We have no information to decide whether reactions 1 and 2 proceed in time as distinguishable steps or in a more concerted or simultaneous fashion; but the sequential use of DCCI and HF is crucial to maximize yields of DBPF, so we postulate that there are at least two stages in the process along the lines suggested by reactions 1 and 2.

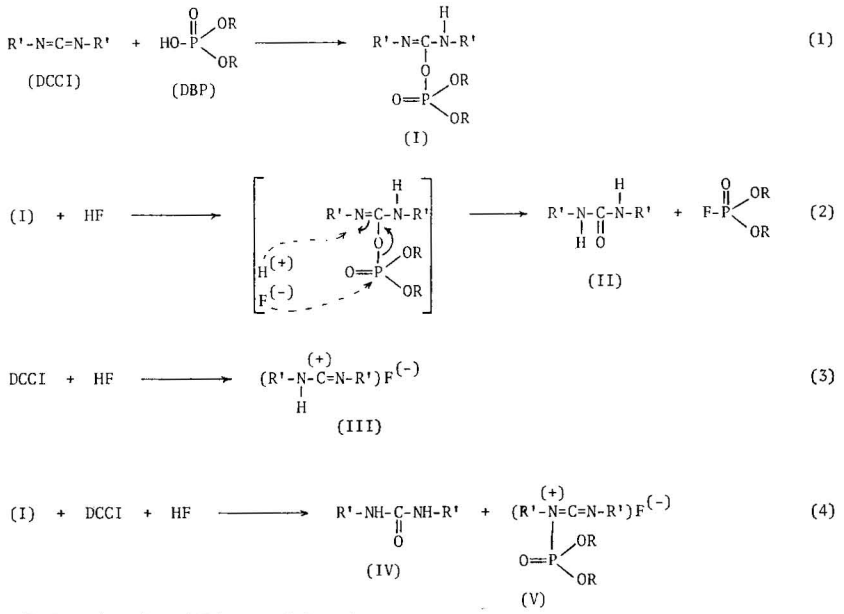

Scheme I. R = butyl and R′ = cyclohexyl.

The time course for DBPF production, determined with a 100-fold molar excess of DCCI followed by a 1000-fold molar excess of HF is shown in Fig. 1A. Fluorination proceeds rapidly at room temperature and appears to reach a maximum after 30–40 min. Thus, a reaction period of at least 45 min was chosen as standard protocol. The 100-fold molar excess of DCCI forces a close to quantitative yield of intermediate complex I and inhibits possible pyrophosphate formation. The latter process is possible whenever phosphate anions are free to complete as nucleophiles in this system.

To find the optimum ratio of HF–DCCI, we fixed one reagent while the other was systematically varied. The results of these experiments are shown in Fig. 1B and C. The optimum level of DCCI appeared to be about a 100-fold molar excess relative to DBP. We interpret the gradual decline in DBPF yield above this level as evidence for possible competing side reactions induced by excess DCCI which either inhibit the attack by HF or catalyze the rearrangement of intermediate complex I. Reactions 3 and 4 are reasonable examples of such competing processes. Product III ties up HF in an ionic salt-like complex, reducing its activity as a fluorinating agent. Reaction 4 is a suggested HF catalyzed rearrangement of intermediate I to a stable urea derivative (IV) and a quarternary salt (V). Somewhat analogous rearrangements have been observed between 2′- and 3′-nucleotides and DCCI[37,38]. It is reasonable that a stable quarternary salt such as V might not be as susceptible to nucleophilic attack by F^- as I, explaining how the yield of DBPF could fall off as observed.

Extending the pre-incubation of DCCI with DBP to 16 h before adding HF decreased the yield of DBPF to 86%. This also is evidence for a possible rearrangement process such as reaction 4. Interestingly, an even lesser yield of DBPF (49%) was achieved by premixing the HF and DCCI before adding DBP. This effect may

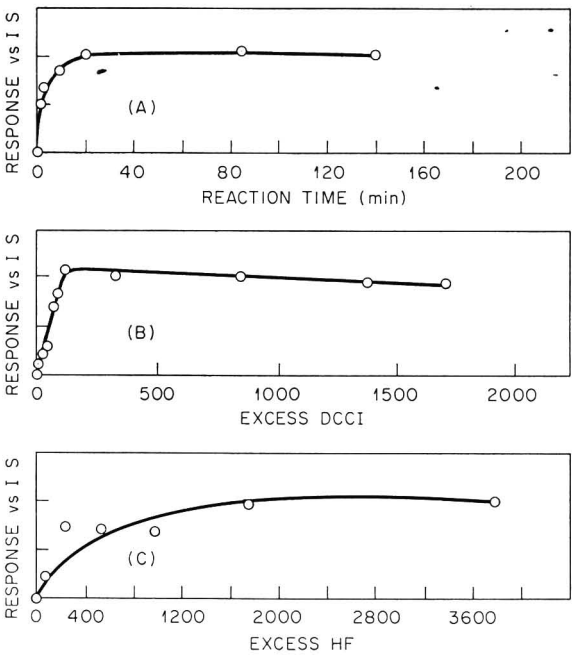

Fig. 1. Effects of (A), reaction time at room temperature; (B), concentration of DCCI and (C), concentration of HF on DBPF yield.

have resulted from the formation of a salt-like addition compound III via reaction 3, but it demonstrates dramatically why our reagent sequence method is a necessary protocol for maximizing DBPF yields.

The effect of HF on DBPF yield was more scattered at lower concentrations but became steady and optimal at about 1000-fold mol excess of substrate. Replacement of HF with AgF decreased the DBPF yield to about 25%; substituting solid NaF or KF for HF likewise in each trial gave poorer yields. A summary of the various methods and relative yields is found in Table I. It is clear that our sequential dehydroxy-fluorination method with DCCI–HF (see recommended procedure in Experimental) is by far the best reagent system tried.

A derivatization reaction must also be quantitative to be of value in an analytical method. Because no authenic DBPF standards were available commercially, we resorted to two independent, indirect procedures for evidence of the completeness of the sequential DCCI–HF dehydroxy-fluorination reaction. The first procedure consisted of a comparison of GC responses of DBPF and CH_3-DBP. Comparison of the GC peaks for DBPF produced from our sequential DCCI–HF system on DBP, and for CH_3-DBP from the reaction of CH_2N_2 on the same amount of DBP, showed a 47% greater GC response (peak area relative to TBP as the IS) for DBPF. Although this result suggests a significantly greater derivatization yield of DBPF *versus* CH_3-DBP, we note that it may also indicate a substantial enhancement of the AFID response to phosphorus compounds by F-substitution. It is reported[41] that halogens can enhance the AFID response to some phosphorus compounds; hence, it is not unreasonable to suppose that direct fluorine to phosphorus bonding

can explain most of the increased response of DBPF *versus* CH_3-DBP. The possibility that the TBP impurity (used as IS) might react with HF, as reported for triphenylphosphate[42], and thus be a second source of DBPF increasing its relative response is discounted because TBP is too inert and too dilute to account for the DBPF enhancement observed.

More convincing indirect evidence for the completeness of the sequential process was obtained by a post-fluorination derivatization of the DCCI–HF–DBP reaction solution. We found that subsequent treatment of this mixture with a gross excess of CH_2N_2 produced no detectable CH_3-DBP, proving conclusively that no free DBP was present. In a previous experiment using this technique, we did recover some CH_3-DBP from aged HF–THF–DBP reaction mixtures. This demonstrated that unreacted DBP could be derivatized and detected by this post-fluorination technique. Therefore, we are confident that the sequential DCCI–HF reaction is capable of quantitative conversion of DBP to DBPF when fresh reagents are employed.

The general GC properties of the fluorinated phosphate derivative in comparison to other derivatives are illustrated by the chromatogram shown in Fig. 2. The relative retention data in Table II indicate the relative volatilities of these species. Not only is the fluoride species much more volatile, but it also exhibits considerably less GC peak tailing than the other ester derivatives. We were pleasantly surprised to note that DBPF is even more volatile than dibutyl phosphite, an ester with phosphorus in the 3+ oxidation state. This greater volatility of DBPF, despite the greater molecular weight of F- *versus* H-substitution, is convincing evidence in support of our "polar hypothesis" proving that substitution of hydroxyl by a more electronegative group, such as fluorine, can reduce the net polar character of the phosphate moiety and give a better GC derivative. We interpret the greater volatility and sharper peak shape of DBPF over triesters to be due primarily to an inductive effect of the very electronegative fluorine substituent on the phosphorus atom. This induction forces an increased $p\pi$–$d\pi$ back-bonding from the phosphoryl oxygen and a general shifting of electron density from all oxygens toward the central phosphorus. This shift of electron density strengthens the phosphorus to oxygen bonds and decreases the magnitude of the P–O dipoles, especially that of the phosphoryl dipole. This general interpretation is corroborated by the infra-red spectral shifts of selected phosphorus compounds[43].

Previous experience[1] with the cleavage of di- and triphosphates by nitrogen-containing reagents, and the ability of HF to cleave condensed phosphates[42] strongly indicates that our DCCI–HF reagent combination will not be suitable for the derivatization and GC analysis of inorganic pyrophosphates and substituted condensed phosphates of biological interest; unfortunately, these species still remain inaccessible to quantitative GC analysis.

In conclusion, we have discovered that the sequential DCCI–HF reagent system reported here is particularly well suited for the dehydroxy-fluorination of phosphate diesters and that the substitution of hydroxyl by fluorine leads to advantageous changes in the GC properties of this stable and volatile phosphate derivative. By itself, this looks like a rather esoteric and very limited piece of scientific information until one realizes that there are many known commercial and military chemicals which are quite similar to the phosphate diester structure, namely, pesticides and nerve gases. Most known nerve gases are related to methylphosphonic acid, $CH_3P(O)(OH)_2$,

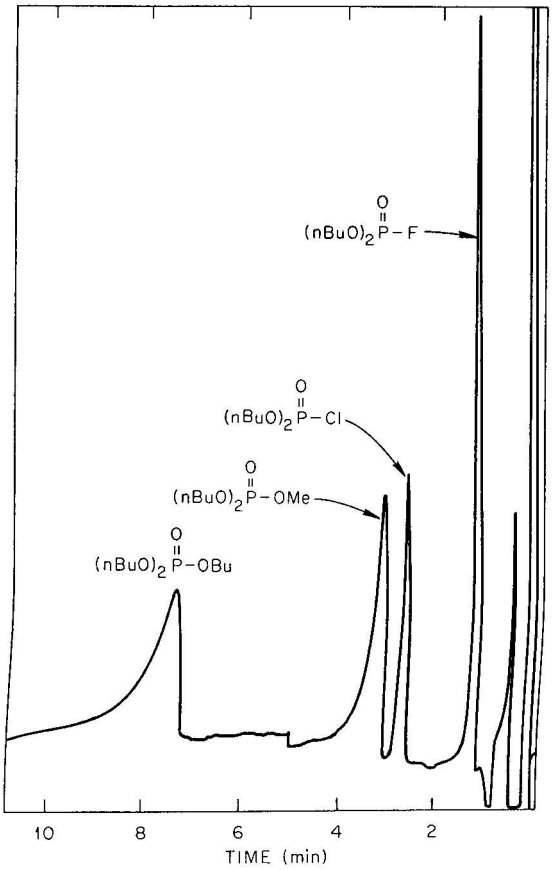

Fig. 2. GC resolution of DBP derivatives. (See Table II for RRT data). Bu = C_4H_9; Me = CH_3.

whereas many commercial organophosphorus pesticides are derivatives of phosphoric acid, $HOP(O)(OH)_2$ [44]. It is not surprising that such nerve gases and pesticides form a variety of hydroxylated substances on hydrolysis. Hydrolysates such as dialkylphosphates, methylphosphonic acid, and phosphoric acid are commonly converted into more volatile compounds for GC analysis by treatment with a diazoalkane in methanol or diethyl ether solution[12,13,17,45], or by co-injection with quaternary

TABLE II

RELATIVE RETENTION TIMES (RRT) FOR MODEL DERIVATIVES OF DBP

$(BuO)_2P(O)X$	*RRT**
X = F	0.20
X = H	0.32
X = Cl	0.38
X = OCH_3	0.44
X = OTMS	0.46
X = OC_4H_9	1.00

* Normalized to retention time of TBP (8.0 min).

ammonium salts[15,16]. We believe our DCCI–HF procedure is a safer and more convenient method than these techniques and that it is applicable to a wide range of hydroxyphosphates at minimal sample sizes. Also, since fluoro-organic chemistry is making an increasing impact on the biomedical and health-related sciences, we suggest that this method be tried in any situation where dehydroxy-fluorination might be useful to synthesize fluoro-analogues of important biochemical agents[46]. However, once again we warn that certain fluoro compounds, especially of the fluorophosphorus type, can be deadly poisons[47]. Hence, extreme caution must be exercised in preparing them above the nmol level used in this work.

ACKNOWLEDGEMENTS

This work was supported in part by the Atomic Energy Commission (contract no. AT-(40-1)-2825), the National Science Foundation (grant GP-2671) and Vanderbilt University. W.H.G. is also grateful for fellowship support from the E. I. du Pont de Nemours & Co., the Eastman-Kodak Co., and Vanderbilt University as well as for educational assistance from the Veterans Administration. Lastly, we owe special thanks to our colleague, Professor R. E. Rummel, for the many ways he has assisted this research.

REFERENCES

1 W. H. Griest and T. W. Martin, *J. Chromatogr.*, 148 (1978) 405.
2 M. Zinbo and W. R. Sherman, *Tetrahedron Lett.*, (1969) 2811.
3 W. C. Butts and W. T. Rainey, Jr., *Anal. Chem.*, 43 (1971) 538.
4 D. R. Matthews, W. D. Shults, M. R. Guerin and J. A. Dean, *Anal. Chem.*, 43 (1971) 1582.
5 T. Hashizume and Y. Sasaki, *Anal. Biochem.*, 15 (1966) 199.
6 T. Hashizume and Y. Sasaki, *Anal. Biochem.*, 15 (1966) 346.
7 T. Hashizume and Y. Sasaki, *Anal. Biochem.*, 21 (1967) 316.
8 T. Hashizume and Y. Sasaki, *Anal. Biochem.*, 24 (1968) 232.
9 D. J. Harvey and M. G. Horning, *J. Chromatogr.*, 76 (1973) 51.
10 A. D. Hortin, *J. Chromatogr. Sci.*, 10 (1972) 125.
11 W. W. Wells, in H. S. Kroman and S. R. Bender (Editors), *Theory and Application of Gas Chromatography in Medicine and Industry*, Grune and Stratton, New York, 1968, pp. 169–181.
12 D. Blair and H. R. Roderick, *J. Agr. Food Chem.*, 24 (1976) 1221.
13 C. G. Daugherton, D. G. Crosby, R. L. Garnas and D. P. H. Hsieh, *J. Agr. Food Chem.*, 24 (1976) 236.
14 F. C. Wright, *J. Agr. Food Chem.*, 23 (1975) 820.
15 F. C. Churchill, D. N. Ku and J. W. Miles, *J. Agr. Food Chem.*, 26 (1978) 1108.
16 J. W. Miles and W. C. Dale, *J. Agr. Food Chem.*, 26 (1978) 480.
17 E. M. Loves and D. E. Bradway, *J. Agr. Food Chem.*, 25 (1977) 75.
18 A. I. Vogel. *A Textbook of Practical Organic Chemistry*. Wiley, New York, 1956, pp. 969–970.
19 H. Schlenk and J. L. Gellerman, *Anal. Chem.*, 32 (1960) 1412.
20 T. W. Mastin, G. R. Norman and E. A. Weilmuenster, *J. Amer. Chem. Soc.*, 67 (1945) 1662.
21 H. McCombie and B. C. Saunders, *Nature (London)*, 157 (1946) 287, 776.
22 W. R. Supina, *The Packed Column in Gas Chromatography*, Supelco, Bellefonte, Pa., 1974, pp. 91–94.
23 *Operating Note, Phosphorus Detector Model 15150-S*, Hewlett-Packard, Böblingen/Württemberg, G.F.R., 1970.
24 I. G. Young, *Amer. Lab.*, 7 (1975) 11.
25 R. F. Coward and P. Smith, *J. Chromatogr.*, 61 (1971) 329.
26 W. H. Griest, *A Study of the Derivatization and Analysis of Nucleotides by Gas–Liquid Chromatography, Ph.D. Thesis*, Vanderbilt University, Nashville, Tenn., 1975, pp. 109–121.

27 B. C. Saunders and G. J. Stacey, *J. Chem. Soc., London*, (1948) 695.
28 S. B. Hartley, W. S. Holmes, J. K. Jacques, M. F. Mole and J. C. McCoubrey, *Quart. Rev., Chem. Soc.*, 17 (1963) 204.
29 J. J. G. Cadogan, *J. Chem. Soc., London*, (1961) 3067.
30 A. Deutsch and O. Fernö, *Nature (London)*, 156 (1945) 604.
31 H. S. Aaron, R. T. Uyeda, H. F. Frack and J. I. Miller, *J. Amer. Chem. Soc.*, 84 (1962) 617.
32 F. S. Fawcett, C. W. Tullock and D. D. Coffman, *J. Amer. Chem. Soc.*, 84 (1962) 4275.
33 W. Lange and R. Livingston, *J. Amer. Chem. Soc.*, 69 (1947) 1073.
34 V. W. Lange, *Z. Anorg. Chem.*, 214 (1933) 44.
35 R. Whittman, *Angew. Chem., Int. Ed. Engl.*, 1 (1962) 213.
36 E. Cherbuliez, in G. M. Kosolapoff and L. Maier (Editors), *Organic Phosphorus Compounds*, Vol. 15, Wiley-Interscience, New York, 1973, p. 211.
37 C. A. Dekker and H. G. Khorana, *J. Amer. Chem. Soc.*, 76 (1954) 3522.
38 M. Smith, J. G. Moffatt and H. G. Khorana, *J. Amer. Chem. Soc.*, 80 (1958) 6204.
39 H. G. Khorana, *Some Recent Developments in the Chemistry of Phosphate Esters of Biological Interest*, Wiley, New York, 1961, p. 128ff.
40 H. G. Khorana and A. R. Todd, *J. Chem. Soc., London*, (1953) 2257.
41 A. Karmen, *J. Chromatogr. Sci.*, 7 (1969) 541.
42 A. Hood and W. Lange, *J. Amer. Chem. Soc.*, 72 (1950) 4956.
43 D. E. C. Corbridge, in M. Grayson and E. J. Griffith (Editors), *Topics in Phosphorus Chemistry*, Vol. 6, Interscience, New York, 1969, pp. 260, 261, 337.
44 A. Verweij, H. L. Boter and C. E. A. M. Degenhardt, *Science*, 204 (1979) 616.
45 A. I. Vogel, *Practical Organic Chemistry*, Longmans Green, London, 3rd ed., 1970.
46 T. B. Patrick, *J. Chem. Educ.*, 56 (1979) 228.
47 H. E. Christensen, E. J. Fairchild, B. S. Carroll and R. J. Lewis (Editors), *Registry of Toxic Effects of Chemical Substances*, U.S. Department of Health, Education and Welfare, Rockville, Md., June 1976.

Journal of Chromatography, 192 (1980) 185–192

CHROM. 12,561

QUANTITATIVE DETERMINATION OF NATURAL DIPALMITOYL LECITHIN WITH DIMYRISTOYL LECITHIN AS INTERNAL STANDARD BY CAPILLARY GAS–LIQUID CHROMATOGRAPHY

ALFRED LOHNINGER

Research Institute of Traumatology of the AUVA, Donaueschingenstrasse 13, A-1200 Vienna (Austria)

and

ALEXEJ NIKIFOROV

Institute of Organic Chemistry, University of Vienna, Vienna (Austria)

(First received May 23rd, 1979; revised manuscript received November 23rd, 1979)

SUMMARY

A quantitative determination of 1,2-dipalmitoyl-*sn*-glycero-3-phosphocholine from dog lungs by means of the corresponding diacyl glycerol trimethylsilyl ether derivative with 1,2-dimyristoyl-*sn*-glycero-3-phosphocholine as internal standard was carried out by gas–liquid chromatography with glass capillary columns. The individual diacyl glycerol species were identified by using a combination of gas–liquid chromatography and mass spectrometry. In a total of 32 determinations percent deviations from the mean value between $\pm$ 2.0 and $\pm$ 4.4% were achieved. By using glass capillary columns instead of conventional columns the time required for an analysis was reduced to *ca.* 30% and separation was considerably improved. Thus the diacyl glycerol species from PC-32 were separated according to both the 1,2 and 1,3 positional isomerism and the degree of saturation of the acyl radicals.

INTRODUCTION

In several diseases such as the respiratory distress syndrome (RDS) of the newborn[1–4] or the adult RDS —the socalled shock lung[5,6]— the lung disfunction is at least in part the result of an impairment of the lung surfactant system. Dipalmitoyl lecithin (DPPC) is generally accepted as the major active component of the pulmonary surfactant[4,7–9]. There is strong evidence that the reduction of DPPC is characteristic of these pulmonary infections. A treatment resulting in an increase in the phospholipid synthesis requires a quantitative determination of 1,2-dipalmitoyl-*sn*-glycero-3-phosphocholine (DPPC) which has to be as exact as possible and which can be carried out in serial analyses.

The usual methods of determining disaturated phosphatidylcholine species comprise separating the corresponding diacyl glycerol acetates by argentation thin-layer chromatography (TLC)[10–13] or by adduction with mercury acetate or osmium tetroxide combined with column chromatography or TLC, respectively[9,14,15].

Gas–liquid chromatography (GLC) with conventional columns has been used to separate the 3-*sn*-phosphatidylcholine species from various biological sources by means of the corresponding diacyl glycerol acetates[16–19] or trimethylsilyl (TMS) ether derivatives[20].

Ogino *et al.*[21] characterized 3-*sn*-phosphatidylcholine species from fetal rat and rabbit lungs as TMS ether (PC_{30}–PC_{34}) by a combination of GLC and mass spectrometry (MS).

This paper describes a method for the quantitative determination of DPPC in lung tissue with 1,2-dimyristoyl-*sn*-glycero-3-phosphocholine as internal standard by GLC with glass capillary columns.

In accordance with the results of other authors, dimyristoyl lecithin could not be detected in natural lecithins[20,21]. This was shown in a series of samples without the internal standard. The use of other internal standards, such as dialkyl or 1-acyl-2-alkyl-*sn*-glycero-3-phosphocholine, has not proved possible as it is well established that plasmanylcholine also occurs in nearly all natural sources of phospholipids. As considerably better separation was achieved with glass capillary than with conventional columns, it was possible to separate the DPPC from the other 3-*sn*-phosphatidylcholine species having the same number of carbon atoms. The individual components were identified by GLC–MS.

EXPERIMENTAL

Apparatus

A Carlo Erba Fractovap 2350 gas chromatograph equipped with a hydrogen flame detector in connection with a System 1 Integrator was used for the quantitative analyses of diacyl glycerols (Carlo Erba, Milan, Italy). The samples were analysed on a SE-30 column (12 m × 0.25 mm I.D.). The injection port and detector temperature were maintained at 350°. The oven temperature was programmed to rise from 24° to 300° at a rate of 4°/min. Hydrogen was used as carrier gas at a flow-rate of 40 cm/sec.

An Ultraturax (IKA-Werk, Staufen, G.F.R.), a Kontes Micro-Ultrasonic Cell Disruptor (Kontes, Vineland, N.J., U.S.A.) and a Camag Lonomat III (Camag, Muttenz, Switzerland) were used.

A direct coupling of the glass capillary column with a Varian MAT 311A mass spectrometer in connection with a Varian 166 spectrosystem was used for the identification of the individual diacyl glycerol species. The temperature of the interface was 350°, the pressure in the ion source was $5 \cdot 10^{-6}$ Torr at a helium flow-rate of 3 ml/min. At an electron energy of 70 eV and an electron current of 3 mA every 0.7 sec, a mass spectrum in the range 20–800 mass units was recorded and evaluated by means of the spectrosystem.

Procedure

The lungs of dogs were bled *in situ* with a physiological NaCl solution, were removed immediately afterwards and homogenized with an Ultraturax in 40 volumes of chloroform–methanol (2:1) and extracted overnight under nitrogen. The tissue lipid extracts were washed using the method of Folch *et al.*[22].

Thin-layer chromatography. Aliquots of samples were applied as bands with

1,2-dimyristoyl-*sn*-glycero-3-phosphocholine (100 μg) on previously cleaned TLC plates. The plates were developed in chloroform–methanol–water (60:35:5), dried and the 3-*sn*-phosphatidylcholine fraction was removed from the plates.

Enzymatic hydrolysis. The 1,2-diacyl-*sn*-glycerols of 3-*sn*-phosphatidylcholine were obtained by digestion with phospholipase C from *Bacillus cereus*. After removal from the TLC plates, the 3-*sn*-phosphatidylcholine samples were dried under nitrogen and 2.5 ml of the 0.1 *M* tris buffer, (pH 7.4, 0.03 *M* with respect to $CaCl_2$) was added[23,24]. After sonication for *ca.* 15 sec, 10 μg of phospholipase C and 2.5 ml of diethyl ether were added and the mixture was stirred. After 3 h, when the reaction was complete, the ether layer was separated and the water layer was re-extracted five times with 2.5 ml of ether. The pooled ether extracts were dried under nitrogen.

Silylation. The TMS ethers of 1,2-diacyl-*sn*-glycerols were prepared by reacting (at room temperature for 1 h) with pyridine–hexamethyldisilazane–chlorotrimethylsilane (12:5:2)[20]. The resulting TMS ether solutions were used directly for subsequent analyses.

Reagents. Chloroform, methanol, pyridine, hexamethylsilazane, chlorotrimethylsilane and diethyl ether were obtained from Merck (Darmstadt, G.F.R.). Phospholipase C from *B. cereus* was obtained from Boehringer (Mannheim, G.F.R.). 1,2-Dilauroyl-*sn*-glycero-3-phosphocholine and 1,2-dimyristoyl-*sn*-glycero-3-phosphocholine, 1,2-dipalmitoyl-*sn*-glycerol, 1,3-dipalmitoyl-*sn*-glycerol, 1,2-dimyristoyl-*sn*-glycerol were obtained from Sigma (St. Louis, Mo., U.S.A.). 1-Palmityl-*sn*-glycerol, 1,3-dioleyl-*sn*-glycerol, 1-palmityl-3-oleyl-*sn*-glycerol and 1-stearoyl-3-oley-*sn*-glycerol were obtained from Analabs, a subsidiary of New England Nuclear (Boston, Mass., U.S.A.).

RESULTS AND DISCUSSION

Fig. 1 shows a representative chromatogram of a mixture of standards of 1,2- and 1,3-diacyl glycerols. On non-polar silicone phases, GLC with glass capillary

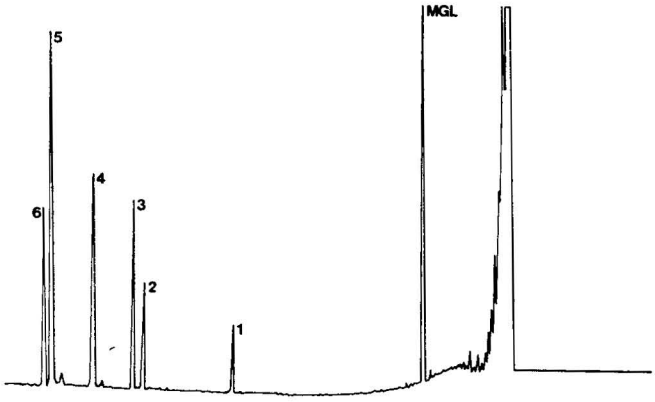

Fig. 1. GLC of reference 1,2- and 1,3-diacyl-*sn*-glycerols as TMS ethers. MGL = Palmitoyl-*sn*-glycerol; 1 = 1,3-dimyristoyl-*sn*-glycerol; 2 = 1,2-dipalmitoyl-*sn*-glycerol; 3 = 1,3-dipalmitoyl-*sn*-glycerol; 4 = 1-palmitoyl-3-oleoyl-*sn*-glycerol; 5 = 1,3-dioleoyl-*sn*-glycerol; 6 = 1-stearoyl-3-oleoyl-*sn*-glycerol. Column, 12-m SE-30, 150°–300°, programmed at 10°/min, carrier gas hydrogen.

columns permits the separation of the 3-*sn*-phosphatidylcholine species having the same number of carbon atoms according to both the 1,2 and 1,3 positional isomerism and the degree of saturation of the acyl radicals.

A good separation of the corresponding 1,2-diacyl glycerols from PC-32 was achieved on a 12-m SE-30 column, as illustrated in Fig. 2.

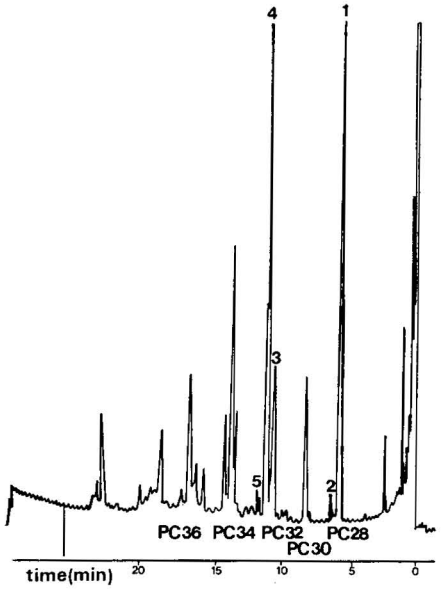

Fig. 2. GLC of the corresponding diacyl glycerols as TMS ethers from dog lung 3-*sn*-phosphatidylcholine. 1 = 1,2-Dimyristoyl-*sn*-glycerol; 2 = 1,3-dimyristoyl-*sn*-glycerol; 3 = 1-palmitoyl-2-palmitoleyl-*sn*-glycerol; 4 = 1,2-dipalmitoyl-*sn*-glycerol; 5 = 1,3-dipalmitoyl-*sn*-glycerol. Column, 12-m SE-30, 240°–300° programmed at 4°/min, carrier gas hydrogen.

Quantitative determinations

The reproducibility of the quantitative determination of dipalmitoyl lecithin with dimyristoyl lecithin as internal standard was confirmed with eight different lung samples in duplicated tests. Each individual sample was analysed twice. The greatest deviation from the mean in these duplicated tests was 4.4%, and the average reproducibility achieved was $\pm$ 3% (Table I).

GLC method with glass capillary columns used as described with non-polar silicone phases (SE-30 and OV-1) can bring about a separation sufficient to carry out a quantitative determination of the 1,2-dipalmitoyl-*sn*-glycerol. By use of the mercury adduction method or argentation TLC, the 3-*sn*-phosphatidylcholine species can be separated according to the number of double bonds but not according to the number of carbon atoms. The saturated 3-*sn*-phosphatidylcholine species isolated by these methods contain other fatty acids in addition to palmitic acid, in particular myristic acid and stearic acid.

The following values for the percentage of palmitic acid in the fatty acids of the disaturated phosphatidylcholine of the lung have been obtained: 67.7 (ref. 14), 80–98 (ref. 10), 95 (ref. 7) and 73 (ref. 15). Henderson and Hackett[25] found that 90%

TABLE I

RELATIVE STANDARD DEVIATION OF EIGHT DIFFERENT LUNG SAMPLES IN DOUBLE TESTS (A, B); EACH INDIVIDUAL SAMPLE WAS ANALYSED TWICE (a, b VALUES)

D = percent deviation.

Sample	*DPL (mg/g dry weight)*		*D (%)*	*D (A + B) (%)*
	(a)	*(b)*		
1 A	7.00	6.70	±2.2	±2.7
B	7.07	6.85	±1.6	
2 A	5.59	5.42	±1.6	±3.4
B	5.80	5.66	±1.4	
3 A	4.54	4.72	±2.0	±2.0
B	4.72	4.60	±1.3	
4 A	5.17	4.90	±2.6	±4.4
B	5.35	5.12	±2.2	
5 A	4.41	4.08	±3.9	±3.9
B	4.28	4.08	±2.4	
6 A	6.86	6.86	±0.0	±3.3
B	7.33	7.33	±0.0	
7 A	9.85	10.10	±1.3	±2.2
B	10.02	9.69	±1.7	
8 A	9.62	10.12	±2.6	±2.6
B	9.72	10.12	±2.0	

of the disaturated fraction was present as 1,2-dipalmitoyl-*sn*-glycerol-3-phosphocholine. In addition to the varying percentage of DPPC in the disaturated fraction the quantitative evaluation by densitometry or by measuring the fluorescence on different plates results in a greater standard deviation[26] than the deviation to be expected in a quantitative determination according to the present method.

A more precise determination of DPPC is possible by GLC determination of the composition of the fatty acids (after digestion with phospholipase A) in the α- and β-positions of the 3-*sn*-phosphatidylcholine. When comparing the determination of the diacyl-*sn*-glycerol species by GLC with glass capillary columns and the determination of the fatty acid composition in the α- and β-positions of the 3-*sn*-phosphatidylcholine, the times required for isolating the 3-*sn*-phosphatidylcholine and for enzymatic digestion are approximately the same, whereas the analysis according to the method described in the present paper is considerably shorter than the determination of the fatty acid composition in the α- and β-positions of the 3-*sn*-phosphatidylcholine. Since 1-myristoyl-2-palmitoyl-*sn*-glycero-3-phosphocholine seems to be present in quantitatively significant amounts, the percentage of the palmitic acid in the fatty acids of the β-position cannot be directly correlated with DPPC.

Myher and Kuksis[20] separated natural diacyl-*sn*-glycerols by GLC with packed columns containing 3% Silar 5-CP on Gas-Chrom Q. The long time required for the analysis (*ca.* 100 min as compared to 20 min according to the method described in this paper) results in wider peaks and thus renders the quantitative evaluation more difficult[27].

The mass spectra of some 1,2- and 1,3-diacyl-*sn*-glycerols have already been described[21,28]. In principle, the identification of the 1,2- and 1,3-positional isomerism

is possible owing to the differences in the mass spectra. The most important information disclosed by the mass spectrum are: the molecular weight (by means of the M−15 ion), the identification of the individual fatty acids by the RCO and RCO+74 ions, respectively, as well as the identification of the 1,3-derivatives by the preferred formation of the $M-RCOOCH_2$ ion[28].

The use of *tert.*-butyl-dimethylsilyl ethers of diacyl glycerols as reported by Myher *et al.*[29] enhances the ion intensities in higher mass ranges, thus making these derivatives more sensitive for characterization. However, for routine analytical use, more time consuming steps are necessary.

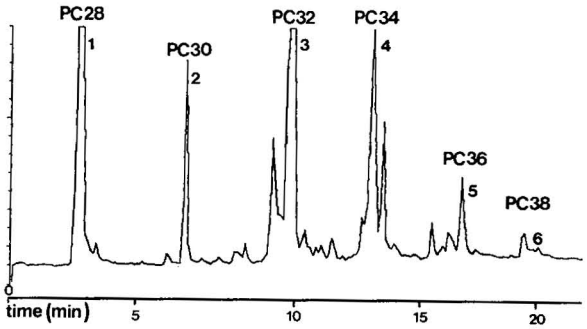

Fig. 3. A portion of the computer-reconstructed sum plot in the range from PC-28 to PC-38 recorded by GLC–MS (TMS derivatives).

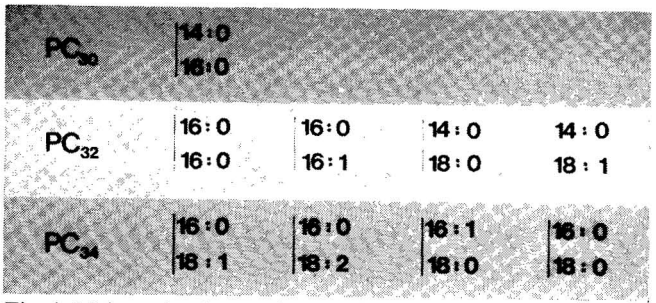

Fig. 4. Main molecular species of PC-30–PC-34 of dog lung 3-*sn*-phosphatidylcholine.

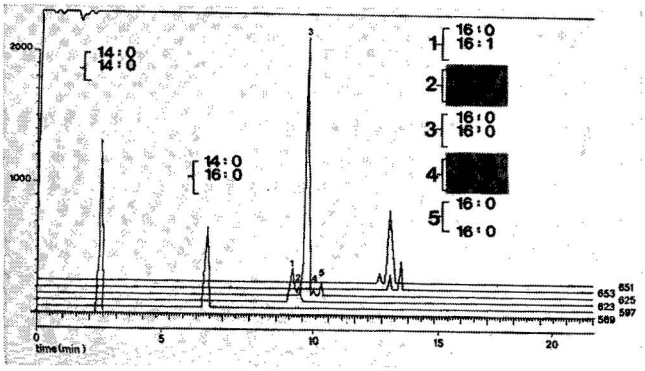

Fig. 5. $M^+ - 15$ ion profiles of dog lung 3-*sn*-phosphatidylcholine of the sum plot from Fig. 3. PC-28 (dimyristoyl-*sn*-glycerol) TMS derivative was used as internal standard.

Fig. 3 shows the sum plot in the range from PC-28 to PC-38 reconstructed by the computer which is correlatable to the gas chromatogram. The different PC-32 species to be expected in principle are shown in Fig. 4.

The ion profiles of the M−15 ions in Fig. 5 show that by means of the capillary column not only the mono-unsaturated 1,2- and 1,3-PC-32 species but also the corresponding saturated 1,3-isomers may be separated from the saturated 1,2-species (which corresponds to DPPC). It also seems to be possible to separate 1-myristoyl-2 stearoyl species from the 1,2-dipalmitoyl species.

In addition, the formation of undesired 1,3-isomers may be suppressed to a large extent by using HMDS–TMS–pyridine as silylating reagent. The mass spectrum of the 1,2-dipalmitoyl-*sn*-glycerol shown in Fig. 6 correlates clearly with the one cited in literature which was recorded with direct inlet[28]. This confirms the correct identification of the peaks. The identification of the PC-34–PC-38 species will be published elsewhere.

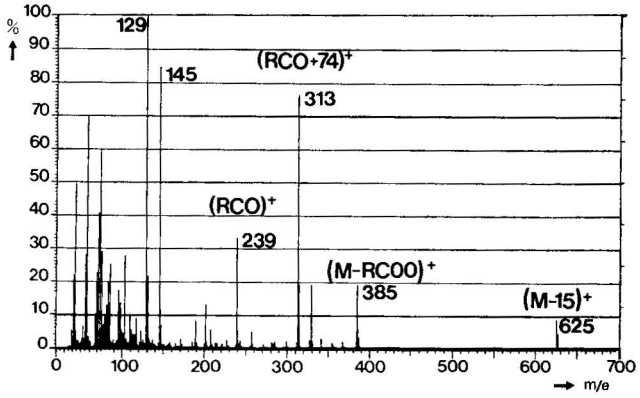

Fig. 6. Mass spectrum of 1,2-dipalmitoyl-*sn*-glycerol TMS ether obtained by GLC–MS from dog lung 3-*sn*-phosphatidylcholine.

CONCLUSION

The internal standard method described proved to be reliable in determining DPPC in lung tissue. Compared with other methods, the determination by GLC with glass capillary columns permits an exact direct determination of DPPC with a mean percent deviation from the mean of $\pm$ 3%, the time required for the GLC analysis being as short as *ca.* 20 min.

ACKNOWLEDGEMENTS

The authors are indebted to Doz. Dr. G. Schlag, Director of the Research Institute of Traumatology of the AUVA, for his interest and criticism. We also wish to thank Mr. A. Piegler for technical assistance. This work was supported by a grant from the Lorenz-Böhler-Forschungs-Fond, and Fonds zur Förderung der wissenschaftlichen Förschung, "Projects" Nos. 2696 and 3306.

REFERENCES

1 F. H. Adams, T. Fujiwara and H. Latta, *Biol. Neonate*, 17 (1971) 198.
2 R. V. Kotas, P. M. Farrell, R. E. Ulane and R. A. Chez, *J. Appl. Physiol.*, 43 (1977) 92.
3 P. M. Farrell and R. V. Kotas, *Adv. Pediatric*, 23 (1976) 213.
4 L. M. G. van Golde, *Amer. Rev. Resp. Disease*, 114 (1976) 977.
5 P. von Wichert, U. Wiegers, W. Stephan, A. Huck, P. Eckert and K. Riesner, *Resp. Exp. Med.*, 172 (1978) 223.
6 A. Lohninger, A. Nikiforov, H. Redl, G. Schlag and G. Schnells, *Europ. Surgical Res.*, 10, Suppl. 1 (1978) 36.
7 R. Mason, G. Huber and M. Vaughan, *J. Clin. Invest.*, 51 (1972) 68.
8 M. F. Frosolono, B. L. Charms, R. Pawlowski and S. Slivka, *J. Lipid Res.*, 11 (1970) 439.
9 R. J. King, J. Ruch and J. A. Clements, *J. Appl. Physiol.*, 35 (1973) 778.
10 D. F. Tierney, J. A. Clements and H. J. Trahan, *Amer. J. Physiol.*, 213 (1967) 671.
11 G. A. E. Arvidson, *Europ. J. Biochem.*, 4 (1968) 478.
12 L. M. G. van Golde, V. Tomasi and L. L. M. van Deenen, *Chem. Phys. Lipids*, 1 (1967) 282.
13 L. J. Morris, *J. Lipid Res.*, 7 (1966) 717.
14 T. E. Morgan and L. H. Edmunds, Jr., *J. Appl. Physiol.*, 22 (1967) 1012.
15 D. B. Gail, H. Steinkamp and D. Massard, *Resp. Physiol.*, 33 (1978) 289.
16 A. Kuksis, W. C. Breckenridge, L. Marai and O. Stachnyk, *J. Lipid Res.*, 10 (1969) 25.
17 L. Marai and A. Kuksis, *J. Lipid Res.*, 10 (1969) 141.
18 A. Kuksis and L. Marai, *Lipids*, 2 (1967) 217.
19 A. Kuksis, W. C. Breckenridge, L. Marai and O. Stachnyk, *J. Amer. Oil Chem. Soc.*, 49 (1968) 537.
20 J. J. Myher and A. Kuksis, *J. Chromatogr.*, 37 (1975) 138.
21 H. Ogino, T. Matsumura, K. Satouchi and K. Saito, *Biomed. Mass Spectrom.*, 4 (1977) 326.
22 J. Folch, M. Lees and G. H. S. Stanley, *J. Biol. Chem.*, 226 (1957) 497.
23 B. Samuelsson and K. Samuelsson, *J. Lipid Res.*, 10 (1969) 47.
24 O. Renkonen, *J. Amer. Oil Chem. Soc.*, 42 (1965) 298.
25 R. F. Henderson and N. A Hackett, *Biochem. Med.*, 20 (1978) 98.
26 J. Kirchner, *J. Chromatogr.*, 82 (1973) 101.
27 A. Kuksis, *Fette-Seifen-Anstrichm.*, 2 (1971) 130.
28 M. Barber, R. J. Chapman and A. W. Wolstenholme, *J. Mass Spectrom. Ion Phys.*, 1 (1968) 98.
29 J. J. Myher, A. Kuksis, L. Marai and S. K. F. Yeung, *Anal. Chem.*, 50 (1978) 557.

Journal of Chromatography, 192 (1980) 193–198

CHROM. 12,613

SIMPLE ANION-EXCHANGE CHROMATOGRAPHY FOR THE DETERMINATION OF ADENINE NUCLEOTIDES BY USING AG MP-1 RESIN

DAR-SAN HSU and SIDNEY S. CHEN

Department of Obstetrics and Gynecology, Long Island Jewish-Hillside Medical Center, New Hyde Park, N.Y. 11042 and Health Sciences Center, State University of New York at Stony Brook, Stony Brook, N.Y. 11794 (U.S.A.)

(First received September 10th, 1979, revised manuscript received December 6th, 1979)

SUMMARY

A simple ion-exchange chromatography with AG MP-1 resin (a strong basic anion-exchange resin of macroporous copolymer of styrene and divinylbenzene) for the assay of adenine nucleotides is described. AMP, ADP and ATP can be quantitatively resolved in a linear HCl gradient (0–0.08 *N*).

A milder HCl gradient between 0 and 0.02 *N* is able to separate cyclic AMP from AMP. The described method is not only useful in the purification of the nucleotides but also convenient in the detection of other contaminated nucleotides.

INTRODUCTION

Conventional ion-exchange chromatography using an anion-exchange resin, Dowex 1, for the analysis of adenine and other nucleotides[1–5] has the disadvantage of eluting the individual nucleotide in a large volume and is time consuming. At present, this technique has been replaced by high-performance liquid chromatography for its sensitivity and speed. However, the latter method requires expensive chromatographic equipment, and the column using pellicular ion-exchange systems has limited capacity[6,7]. Recently, Khym[8,9] described a method using a short column of Aminex A-27 (a conventional styrene-type anion-exchange resin of small particle size, 12–15 μm), to operate at a lower pressure and low-cost chromatographic equipment. In this paper, we revive conventional ion-exchange chromatography using AG MP-1 (a strong basic anion-exchange resin of a macroporous styrene-type anion-exchange resin) for the determination of adenine nucleotides. This not only improves but also simplifies the procedures of the conventional chromatographic technique, and can be used conveniently for the quantitation of adenine nucleotides in biological fluids and tissues, and assay of many enzymatic reactions which involve adenine nucleotides as substrates. The technique is also useful in the purification of nucleotides in a large quantity.

EXPERIMENTAL

Chemicals

AG-1 anion-exchange resin (200–400 mesh) and AG MP-1 anion-exchange resin (200–400 mesh) were obtained from Bio-Rad Labs. (Richmond, Calif., U.S.A.). Adenine nucleotides were obtained from Sigma (St. Louis, Mo., U.S.A.) or ICN Pharmaceuticals (Plainview, N.Y., U.S.A.).

Procedure

A 2-g amount of AG MP-1 resin was packed in a small column with distilled water (3.5 × 0.9 cm). A thick filter paper disc was then placed on the top of the resin. The elution was done by a linear gradient of HCl by interconnecting two 250-ml flasks filled to the 225-ml mark, one with distilled water and the other with 0.3 *N* HCl. The eluent was delivered to the column by a peristaltic pump from the mixing flask or by hydrostatic pressure at a flow-rate of 2.5 ml/min. The nucleotides in the effluent were continuously monitored through a flow cell of 10 mm light path at 257 nm using a Beckman double beam spectrophotometer.

After a run, the column was regenerated by washing the column with water for at least 20 min. Usually two columns were used alternatively so that while one was in use, the other was washing. The flow-rate was measured at the outlet of the flow cell.

Quantitation of peaks

Two methods were used. One was by comparing the area of each peak with the respective peak of standard nucleotide. A calibration curve was made with each standard nucleotide for each column.

The other method was by peak height and half-height width of the peak according to the equation[6,9]:

$$\text{Amount (nmoles)} = \frac{A_{\text{max.}} \cdot W_{\frac{1}{2}} \cdot F \cdot 1066}{\varepsilon_{257}}$$

where $A_{\text{max.}}$ is the maximal absorbance, $W_{\frac{1}{2}}$ is the width measured at the middle of peak (min), F is the flow-rate in ml/min and ε_{257} is the molar extinction coefficient of each nucleotide at 257 nm, 1066 is an equation constant.

The molar extinction coefficients used are 15 for AMP and ADP and 14.7 for ATP at 257 nm and pH 2 (ref. 10). The total adenine nucleotides in a standard solution was calculated by measurement of the total absorbance at 259 nm using the molar extinction coefficient of $15.4 \cdot 10^3$ in a neutral solution.

RESULTS AND DISCUSSION

Comparison of elution pattern using AG-1 and AG MP-1 resins

AG-1 resin was analytical grade of Dowex 1 resin which was generally used in the conventional ion-exchange chromatography for nucleotides. It gave broadening, tailing and unsymmetrical peaks. On the contrary, AG MP-1 resin gave sharp peaks at milder HCl concentration, as shown in Fig. 1.

AG-1, AG MP-1 and Aminex A-27 are all strongly basic anion-exchange

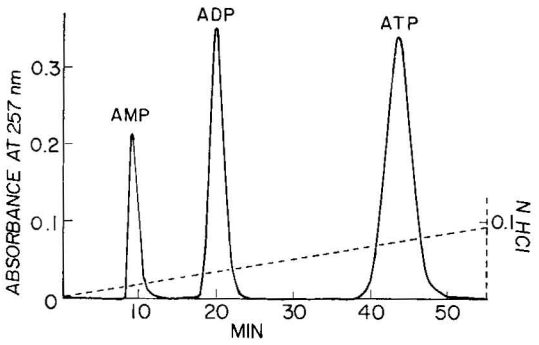

Fig. 1. Chromatogram for adenine nucleotides on AG MP-1 resin column. This curve represented a typical chromatogram for AMP, ADP and ATP. The peaks corresponded to 53.17 nmoles of AMP, 124.78 moles of ADP and 221.52 nmoles of ATP as calculated with the given equation. The broken line was the concentration of HCl gradient.

resins with quaternary ammonium groups attached to a styrene–divinylbenzene copolymer lattice. Aminex A-27 used by Khym[8,9] is a finely sized spherical beads of AG-1 resin while AG MP-1 is a highly crosslinked copolymer with high content of divinylbenzene.

Quantitation

The quantity of a nucleotide is linearly proportional to the area of peak obtained from the chromatogram. The difference obtained from two similar columns used was minimal. Since the same size of column and amount of resin were used, the difference was mainly caused by the flow-rate. If the results were corrected for the flow-rate of each column and calculated according to the equation given under Experimental, an identical curve could be obtained.

Purities of commercial adenine nucleotides

Table I shows the results of adenine nucleotides analyses from Sigma and ICN Pharmaceuticals. All were obtained as crystalline sodium salts. The determined purities for ADP were far from the manufacturers' specifications.

It was reported that solid ADP in storage would convert partially into AMP and ATP[11]. It is evident from Table I that this conversion is extensive during the storage in refrigerator. The first two lots of ADP were obtained from Sigma, 2 years and 1 year ago, respectively. The last ADP was freshly obtained from ICN Pharmaceuticals.

Modification of the elution gradient for the analysis of cyclic adenine monophosphate

Using HCl gradient elution described in the experimental protocol, cyclic AMP was eluted from the column at the position close to AMP. To separate cyclic AMP from AMP, the HCl gradient was modified as follows. The elution was started with 225 ml water in a mixing flask interconnecting to another flask containing 225 ml HCl. As shown in Fig. 2, this HCl gradient of lower concentration eluted AMP and cyclic AMP separately out of the column. After elution for 30 min, the mixing flask was disconnecting from the other flask and connecting to a flask containing 190 ml

TABLE I

CHROMATOGRAPHIC ANALYSIS OF PURITY OF NUCLEOTIDES

C.P. = Chromatographically pure.

Source of nucleotide	*Lot No.*	*Manufacturer's specification (%)*	*ATP (%)*	*ADP (%)*	*AMP (%)*
ATP, Sigma Equine muscle	76C-7360	99–100	98.00	1.56	0.45
ATP, ICN	8073	C.P.	96.04	1.66	2.30
AMP, ICN Muscle	6340	C.P. (99–100)	0	0.46	99.54
ADP, Sigma Grade III Yeast	86C-7530	95–99	3.63	74.00	22.50
ADP, Sigma Grade III Yeast	113C-7070	95–99	2.30	84.20	13.40
ADP, ICN	2923	—	1.84	91.19	6.97

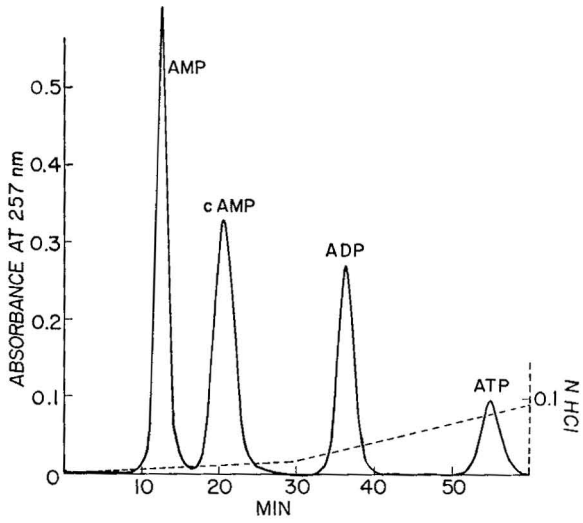

Fig. 2. Chromatogram for adenine nucleotides using HCl gradient of lower concentration. The peaks were identified as AMP, cyclic AMP, ADP and ATP. Amounts of each nucleotide as calculated with the equation were: AMP, 25.58; cyclic AMP, 192.72; ADP, 122.15; and ATP, 56.85 nmoles. Two-step HCl gradient was used. The milder HCl gradient could separate cyclic AMP from AMP.

of 0.4 *N* HCl. This last gradient eluted out ADP and ATP separately in 30 min. The resulting chromatogram is shown in Fig. 2.

Sample volume and salt effect

In a neutral solution containing low salt concentration, nucleotides can be applied to the column in a large volume. In 5 ml 0.02 *M* Tris–HCl buffer, pH 7.4, NaCl at a concentration lower than 0.2 *M* did not interfere with the absorption of AMP to the column. However, 0.25 *M* NaCl resulted in 8% loss of AMP; while 0.4 *M*, 80%.

Nucleotides in 3% trichloroacetic acid were not absorbed on the column; however, they were completely absorbed after the solution was neutralized with Tris-base. For the analysis of solution containing high concentration of protein, it was, therefore, treated as follows before applying to the column. To a sample solution, an equal amount of ice-cold 6% trichloroacetic acid was added. After thoroughly mixed, the mixture was centrifuged to remove the precipitated protein. An aliquot of the supernatant solution was then neutralized with 2 *M* Tris-base (5:1, v/v), and applied to the column. Running the column for 10 to 20 min with water, and then HCl gradient was started as described.

Stability of the column

The column was very stable. Repeated use of a column for several hundred times over a half year did not result in any appreciable change in efficiency. Repacking was not necessary. When it became hard to apply samples because of continuous use for biological fluids, the column was treated in the following manner. The paper disc was removed, the resin bed was stirred and resettled, the column was washed with distilled water and a new filter paper was re-installed.

Purification of ATP using a large column

A large column (14 × 2.6 cm) packed with 50 g of AG MP-1 resin was used for the purification of ADP. A 236-g amount was dissolved in 2 ml of distilled water and absorbed on the column. The HCl gradient was established with 500 ml each of water and 0.3 *N* HCl. The flow-rate was 250 ml per h and 10-ml fractions were collected.

The resulting chromatogram is shown in Fig. 3. The nucleotides in the corresponding peak fractions were 93.4, 308 and 1.4 μmoles for AMP, ADP and

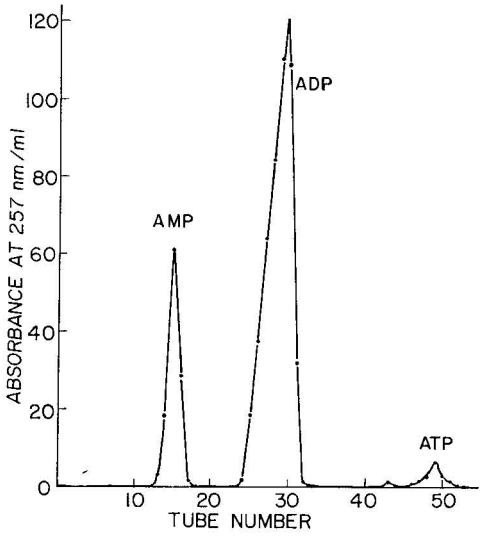

Fig. 3. Purification of ADP in a large chromatographic column. The absorbance was measured at 257 nm by diluting 10–50 μl of the effluent to 1 ml. The peaks were identified as ADP, AMP and ATP, respectively, by an analytical chromatography.

ATP, respectively. Two fractions, tubes 29 and 30, containing high ADP were combined and neutralized to pH 7.4 with Tris-base. Analytical column chromatography showed that it was pure and contained 7.78 m*M* ADP. Other ADP fractions, 25–28 and 31 were combined, neutralized and concentrated by ultrafiltration on a Diaflo UM-05 membrane to 9 ml. This was also chromatographically pure and contained 17 m*M* ADP. AMP fractions, tubes Nos. 14, 15 and 16, were combined, neutralized and concentrated by the ultrafiltration to 10.2 ml. The resulting solution was analyzed by the analytical chromatography to contain 9.25 m*M* AMP and to be pure. 97% was recovered by the ultrafiltration.

As shown in Fig. 3, two small peaks, tubes 43 and 49, corresponding to ATP peak were obtained. They could only be partially separated by analytical chromatography after being neutralized with Tris-base. This indicated a trace contamination of other nucleotides which could not be detected by the analytical chromatography. The first peak corresponded to 0.025% and the second peak to 0.35% of ATP calculated by the total absorbance. Therefore, this procedure is not only convenient and efficient for the purpose of purification but also can be used for the detection of trace amounts of contaminated nucleotides.

Since isolated nucleotides were in dilute HCl solutions, they could be converted to desirable cationic salts by neutralizing with proper bases. The neutralization could also be accomplished by passing the acid solution through Chelex 100 resin preconditioned to a desirable cationic form, and washing the resin with distilled water. Nucleotides were recovered in the void volume.

REFERENCES

1 W. E. Cohn and C. E. Carter, *J. Amer. Chem. Soc.*, 72 (1950) 4273.
2 W. E. Cohn and E. Volkin, *J. Biol. Chem.*, 203 (1953) 319.
3 R. B. Hurlbert, H. Schmitz, A. F. Brumn and V. R. Potter, *J. Biol. Chem.*, 209 (1954) 23.
4 N. G. Anderson, J. G. Green, M. L. Barber and Sr. F. C. Ladd, *Anal. Biochem.*, 6 (1963) 153.
5 T. Ben-Porat, A. Stere and A. S. Kaplan, *Biochim. Biophys. Acta*, 61 (1962) 150.
6 C. Horvath, *Methods Biochem. Anal.*, 21 (1973) 79.
7 P. R. Brown, *High-pressure liquid chromatography*, Wiley-Interscience, New York, 1973.
8 J. X. Khym, *J. Chromatogr.*, 97 (1974) 277.
9 J. X. Khym, *Clin. Chem.*, 21 (1975) 1245.
10 R. M. Bock, N. S. Ling, S. A. Morell and S. H. Lipton, *Arch. Biochem., Biophys.*, 62 (1956) 253.
11 H. V. Bergmeyer, *Methods of Enzymatic Analysis*, Vol. I, Verlag Chemie ,Weinheim and Academic Press, New York, London, 1974, pp. 525–527.

Journal of Chromatography, 192 (1980) 199–207

CHROM. 12,568

PERLOLINBESTIMMUNG IN GRÄSERN

J. SACHSE

Eidgenössische Forschungsanstalt für landwirtschaftlichen Pflanzenbau, 8046 Zürich (Schweiz)

(Eingegangen am 23. November 1979)

SUMMARY

Determination of perloline in grass species

A method was developed for the determination of the alkaloid perloline which occurs in different pasture grasses and is toxic to cattle and sheep.

Perloline was extracted with ethanol and hydrochloric acid, either partially purified by partitioning between an alkaline aqueous solution and chloroform or purified and further separated by thin-layer chromatography (TLC) and measured fluorometrically. The recovery after TLC separation was 96 $\pm 3\%$ when 250–2000 μg of the alkaloid were added to 5 g dried grass, poor in perloline.

The content of perloline was determined in cultivars of *Lolium perenne* L., *Lolium multiflorum* Lamk. and the hybrids between both species. The amounts found were in the range of 2 to 76 mg in 100 g dry matter. The deviation of the individual values from the mean was $\pm 3\%$ on the average.

EINLEITUNG

Das Alkaloid Perlolin, das in unterschiedlichem Ausmass in den Gräsern *Festuca arundinacea* Schreb., *Lolium temulentum* L., *Setaria lutescens* (Weigel) F. T. Hubb[1], *Lolium perenne* L.[2], *Lolium multiflorum* Lamk., *Dactylis glomerata* L. und *Phleum pratense* L.[3] neben anderen Alkaloiden vorkommt, wirkt auf Rinder und Schafe toxisch (tetanische Krämpfe "Raygrass Staggers Syndrome", Hemmung der Zelluloseverdauung)[4,5]. Dies kann eine Herabsetzung der tierischen Leistung und Herdenverluste zur Folge haben. Um einen Ueberblick über den Gehalt dieses Hauptalkaloids in den genannten Futtergräsern zu bekommen, ist eine Methode zur Bestimmung des Perlolins erforderlich.

Melville und Grimmett[2] schrieben 1941 über das Vorkommen von Perlolin in englischem Raygras auf Neuseeland. Ueber seine chemischen Eigenschaften, Struktur und Isolierung berichteten Reifer und Bathurst[3], Jeffreys und Sim[6], Jeffreys[1] sowie Bush und Jeffreys[7]. Zur quantitativen Erfassung des Perlolins liegen bereits einige Arbeiten vor[7–9]. Die Methode nach Shaffer *et al.*[10], die auf einer säulenchromatographischen Reinigung des Perlolins und einer fluorimetrischen Messung beruht, schien für unsere Probleme am geeignetsten, da sie empfindlicher und spezifischer als z.B. die kolorimetrische ist.

Die Erfahrungen bei der Bestimmung von Perlolin in Raygras, durch die eine Auswahl perlolinarmer Sorten ermöglicht und somit ein Beitrag zur Gesunderhaltung des genannten landwirtschaftlichen Viehbestandes geleistet wird, sollen hier mitgeteilt werden.

EXPERIMENTELLER TEIL

Als Untersuchungsmaterial dienten Grasproben aus dem ersten Aufwuchs eines Sortenversuchs, die an zwei verschiedenen Terminen geerntet wurden: englisches Raygras (*Lolium perenne* L.), italienisches Raygras (*Lolium multiflorum* Lamk.) und Hybriden aus beiden Arten.

Reagenzien

Aethanol 95%ig, denaturiert, Salzsäure etwa 1 *N*, Natronlauge 40%ig, Natriumkarbonat krist. rein, Chloroform rein, Salzsäure 37%ig p.a., Perlolinhydrochlorid, Tris(hydroxymethyl)-aminomethan p.a., Riboflavin für biochemische Zwecke Nr. 7609 (Merck, Darmstadt, B.R.D.), Phosphatpuffer pH 7, Kieselgel G Typ 60 für die Dünnschichtchromatographie (Merck), Säurefuchsin für die Mikroskopie (Merck 7629), *n*-Butanol p.a., Essigsäure 100%ig p.a.

Extraktion

2–5 g gefriergetrocknetes, fein gemahlenes Gras mit 50 ml denaturiertem Aethanol, der mit gleichem Volumen 1 *N* Salzsäure verdünnt wurde, unter Rückfluss 30 min und ein zweiten Mal mit 60 ml vom gleichen Lösungsmittel 20 min lang extrahieren. Den Rückstand jeweils abnutschen und mit wenig heissem Äthanol, verdünnt mit Wasser (1:1), nachwaschen. Die vereinten Extrakte am Rotationsverdampfer (Wasserbad 50°) so weit einengen, bis der Äthanol vollständig vertrieben ist. Den Rückstand mit heissem Wasser quantitativ in einen 250 ml Scheidetrichter spülen und mit konzentrierter Natronlauge auf pH 6 einstellen. Nach Zugabe von 2 g Natriumkarbonat krist. den Extrakt dreimal 2 min lang mit je 60 ml Chloroform im Halbdunkel ausschütteln. Die beiden Phasen durch Zentrifugieren trennen, die untere Chloroformphase in einem 250-ml Rundkolben auffangen, genau 0.5 ml Salzsäure 37%ig p.a. zugeben und am Rotationsverdampfer unter Lichtschutz eindampfen. Den Rückstand mit warmem Äthanol, verdünnt mit Wasser (1:1), in einen 50 ml Messkolben spülen und nach dem Erkalten bis zur Marke auffüllen. Diese Untersuchungslösung (= Lösung A) kann bis zur Messung einige Tage bei −20° aufbewahrt werden.

Fluorimetrische Messung

Gerät. Spektrofluorimeter Aminco Bowman, Xenonlampe, Photomultiplier 1 P 21; Ausgangsspalt am ersten Monochromator 2 mm, Eingangsspalt am zweiten Monochromator 2 mm; Anregungswellenlänge 450 nm, Emissionswellenlänge 511 nm, Fluoreszenzküvetten 1 cm.

Eichgerade. Die Ausgangslösung, 1 mg Perlolinhydrochlorid* in 100 ml

* Das Perlolinhydrochlorid wurde uns von Herrn Dr. J. A. D. Jeffreys, University of Strathclyde, Glasgow, Great Britain, grosszügig zur Verfügung gestellt, wofür wir bestens danken.

Äthanol–Wasser (1:1), nach Tabelle I verdünnen, so dass die Perlolinkonzentration im Bereich von 0.004 bis 0.2 μg/ml zu liegen kommt, wobei zu beachten ist, dass vor dem Auffüllen des Messkolbens 10 Vol.% einer 0.05 *M* wässrigen Tris(hydroxymethyl)–aminomethanlösung (= Trispuffer) zuzugeben sind. Als Blindprobe dient Äthanol–Wasser (1:1) mit 10 Vol.% Trispuffer.

TABELLE I

VERDÜNNUNGEN

Stammlösung	*Verdünnung (= A)*	*Verdünnung aus A*	*Verdünnen mit*
1 mg Perlolin in 100 ml	1:50	1:1 bis 1:50	Äthanol–Wasser (1:1)
50 ml Probelösung	1:10 bis 1:25	1:10 bis 1:25	Äthanol–Wasser (1:1)
DC-Fleck mit 50 ml eluiert	1:5 bis 1:10		Äthanol–Wasser (1:1)
5 mg Riboflavin in 100 ml	2:25	1:25	Phosphatpuffer pH 7

Zur späteren Eichung des Fluorimeters statt Perlolin Riboflavin bei gleicher Anregungs- und Emissionswellenlänge wie für Perlolin verwenden. 5 mg Riboflavin für biochemische Zwecke in 100 ml Phosphatpuffer pH 7 unter Erwärmen, evtl. mit Ultraschall, lösen. Nach zwei weiteren Verdünnungen (s. Tabelle I) ergibt sich bei dem von uns benutzten Gerät eine relative Intensität von 4.6. Als Blindprobe dient die oben erwähnte Äthanol–Wasser–Trispuffer-Mischung. Das Fluorimeter vor dem Messen mit der Riboflavin-Lösung jeweils auf die entsprechende relative Intensität zur Erreichung konstanter Messbedingungen einstellen.

Messung der Probe. In einen 25-ml Messkolben 1 ml Untersuchungslösung A pipettieren, je nach Perlolinkonzentration nach Tabelle I verdünnen, kurz vor dem Messen 10 Vol.% Trispuffer zufügen und mit Äthanol–Wasser (1:1) auffüllen. Die Messung unter den aufgeführten Bedingungen durchführen.

Dünnschichtchromatographische Reinigung des Perlolins. 40 ml der Untersuchungslösung A am Rotationsverdampfer eindampfen, den Rückstand mit genau 5 ml Äthanol 95%ig aufnehmen (= Untersuchungslösung B). Für eine Dünnschichtplatte 20 × 20 cm 5.5 g Kieselgel G Typ 60 für die Dünnschichtchromatographie in 20 ml Lösungsmittel (18 ml Äthanol + 2 ml Wasser) suspendieren und ausgiessen. Nach dem Trocknen an der Luft die Platte bei 130° 30 min aktivieren und bis zum Gebrauch im Exsiccator aufbewahren. Je nach der Perlolinkonzentration 100 bis 300 μl der Untersuchungslösung B als Band auftragen. Ausserdam 50 μl einer Lösung von 10 mg Säurefuchsin für die Mikroskopie in 25 ml Äthanol–Wasser (1:1) gelöst auf den Start als Leitsubstanz applizieren. Fliessmittel: *n*-Butanol–Essigsäure–Wasser 6:1:2 (9 modif.) ohne Kammersättigung. Platte über Nacht entwickeln (Laufzeit für eine Strecke von 18 cm mindestens 7 h). Das aufgetragene Säurefuchsin wird unvollständig in drei kräftige rote Hauptflecken (R_F 0; 0.06; 0.14) und einen obersten roten blassen Fleck (R_F 0.31) aufgetrennt. Zwischen letzterem und dem intensiv roten Fleck (R_F 0.14) liegt als gelbes Band das gesuchte Perlolin (s. Fig. 1). Nach sorgfältigem Trocknen der Platten, den Perlolinfleck abschaben und in einem Allihnschen Filterröhrchen D 4 mit heissem Äthanol–Wasser (1:1) eluieren. Das Eluat in einem 50 ml Messkolben auffangen, die Lösung evtl. zum Messen nach Tabelle I verdünnen und zuletzt mit 10 Vol.% Trispuffer versetzen. Die Messbedingungen bleiben dieselben wie für die Untersuchungslösung A.

TABELLE II

PERLOLINGEHALT IN RAYGRÄSERN

Sorte	*Ernte 23. Mai 1978*				*Ernte 29. Mai 1978*			
	*mg Perlolin/100 g TS***		*Abweichung** (±%)	*mg Perlolin/100 g TS nach DC*	*mg Perlolin/100 g TS***		*Abweichung** (±%)	*mg Perlolin/100 g TS nach DC*
	Einzelwerte	*Mittelwert*			*Einzelwerte*	*Mittelwert*		
Englisches Raygras								
Barvestra	19.6	19.1	2.4		22.7	22.1	2.6	
	18.7				21.5			
Cropper	23.9				31.2	31.0	0.7	30.8
					30.8			
Grimalda	78.1	75.1	3.5	72.6	68.6	67.2	2.1	65.8
	72.6				65.8			
Gremie	25.4	25.7	1.6	26.1	25.1	25.1	0.2	25.1
	26.1				25.0			
Reveille	33.8	33.8	0	33.8	24.6	24.7	0.4	24.8
	33.8				24.8			
Melino	20.1	21.0	3.8		20.8	20.8	0.3	
	21.8				20.9			
Pablo	3.3	3.0	9.5		8.1	8.2	0.2	8.2
	2.7				8.2			
Vigor	2.3	2.4	3.7		3.5	3.3	6.9	
	2.4				3.0			

Ital. Raygras								
Turilo	9.7				28.0	26.7	4.8	
					25.4			
Lemtal	7.7	8.6	8.5	9.0	9.7	10.4	4.4	
	9.3				10.9			
Tetila	29.9	31.9	5.8	33.8	23.3	22.9	1.8	22.5
	33.8				22.5			
Meritra	25.8				19.9		1.8	19.2
					19.2	19.6		
Lipo	22.0	23.0	4.4		16.7	16.8	0.7	
	24.1				16.9			
Hybrid-Raygras								
Sabel	76.1	73.1	4.0	70.1	54.2	52.9	2.4	
	70.0				51.6			
Sabrina	53.6	53.3	0.5	53.4	50.6	50.5	0.2	50.3
	53.1				50.4			

* Abweichung $\pm$ % = Abweichung der Einzelwerte vom Mittelwert.
** TS = Trockensubstanz.

ERGEBNISSE

Die Extraktion des Perlolins aus gefriergetrocknetem Pflanzenmaterial ist vollständiger als aus solchem, das bei 60° getrocknet wurde. Die extrahierten Perlolinmengen liessen sich ausserdem durch Kochen der gemahlenen Gräser erhöhen im Vergleich mit denen, die durch Rühren bei Raumtemperatur gewonnen wurden[10]. Weiterhin konnte die Alkaloidausbeute durch Zugabe von Salzsäure zum Extraktionsmittel gesteigert werden, das auf einem besseren Aufschluss des Zellmaterials und des Alkaloids sowie auf seiner Stabilisierung beruhen könnte. Die erhöhte Menge an Begleitstoffen muss bei der Extraktion in der Siedehitze in Kauf genommen werden. Die Äthanolkonzentration von etwa 50% [10] wurde beibehalten, da diese für die Perlolinextraktion ausreichend ist und weniger Begleitstoffe erfasst als Äthanol höherer Konzentration.

Bei den säulenchromatographischen Versuchen an Dowex MSC-1 nach Shaffer *et al.*[10] mussten die Bedingungen wegen des höheren Extraktgehaltes geändert werden. Jedoch stellten wir bereits bei der Chromatographie des reinen Perlolins an Dowex MSC-1 fest, dass ein Teil irreversibel gebunden oder zerstört wird. Ausserdem störte das Quellen, Schrumpfen und das Sicherwärmen des Harzes durch die wechselnden Eluenten. Um den Verlust des nicht sehr stabilen Alkaloids zu umgehen, sahen wir von einer Säulenchromatographie ab. Der gewonnene Extrakt wurde vom Alkoholanteil durch Eindampfen im Vakuum befreit, alkalisiert und mit Chloroform mehrfach ausgeschüttelt. Durch den Zusatz von Salzsäure zum erhaltenen Chloroformextrakt wird die im alkalischen Milieu, besonders unter Lichteinfluss, instabile Perlolinbase wieder in die stabilere Salzform überführt. Nach dem Verdampfen des salzsauren Chloroforms wurde der Rückstand mit Äthanol–Wasser (1:1) aufgenommen und mit dem gleichen Lösungsmittel entsprechend verdünnt. Nach Zugabe von Trispuffer beträgt der pH der zu messenden Lösung 9. Die Konzentration des Äthanols und des Puffers sind in dieser Lösung konstant zu halten, da hiervon einmal die Dissoziaten des Puffers und des Alkaloids und somit die Intensität der Fluoreszenz abhängen[10]. Wird Perlolin aus einer wässrigen alkalischen Lösung mit Chloroform ausgeschüttelt und seine Fluoreszens direkt in letzterem gemessen, so liegen die Maxima der Anregungs- und Emissionsspektren bei 467 bzw. 522 nm. Die Intensität der Fluoreszenz dieser Lösung ist gegenüber der in sauerstoffhaltigen alkoholischen Lösungen erhöht. Da aber die Fluoreszenz des Perlolins in alkalischem Chloroform durch die Bestrahlung sehr rasch abnimmt, ist von der Messung in diesem Lösungsmittel abzuraten. In dem Äthanol–Wasser–Trispuffer-Gemisch nimmt die Fluoreszenz nach zwei Stunden 5% ab. Im Konzentrationsbereich von 0.004 bis 0.8 μg Perlolin/ml ergeben die gefundenen Werte graphisch dargestellt eine Gerade. Es empfiehlt sich aber, die Messung in stark verdünnten Lösungen vorzunehmen, weil bei höheren Konzentrationen durch innere Absorption eine teilweise Fluoreszenzlöschung eintreten kann.

Zur wiederholten Eichung des Fluorimeters wurde das nicht käufliche Perlolin durch Riboflavin, in Phosphatpuffer gelöst, ersetzt. Da die Maxima seines Anregungs- und Emissionsspektrums sehr nahe bei denen des Perlolins, nämlich bei 464 und 520 nm, liegen, ist diese Substanz besonders für diesen Zweck geeignet. Die Konzentration wurde so gewählt, dass die erzielte relative Intensität in der Mitte der benutzten Eichgeraden liegt.

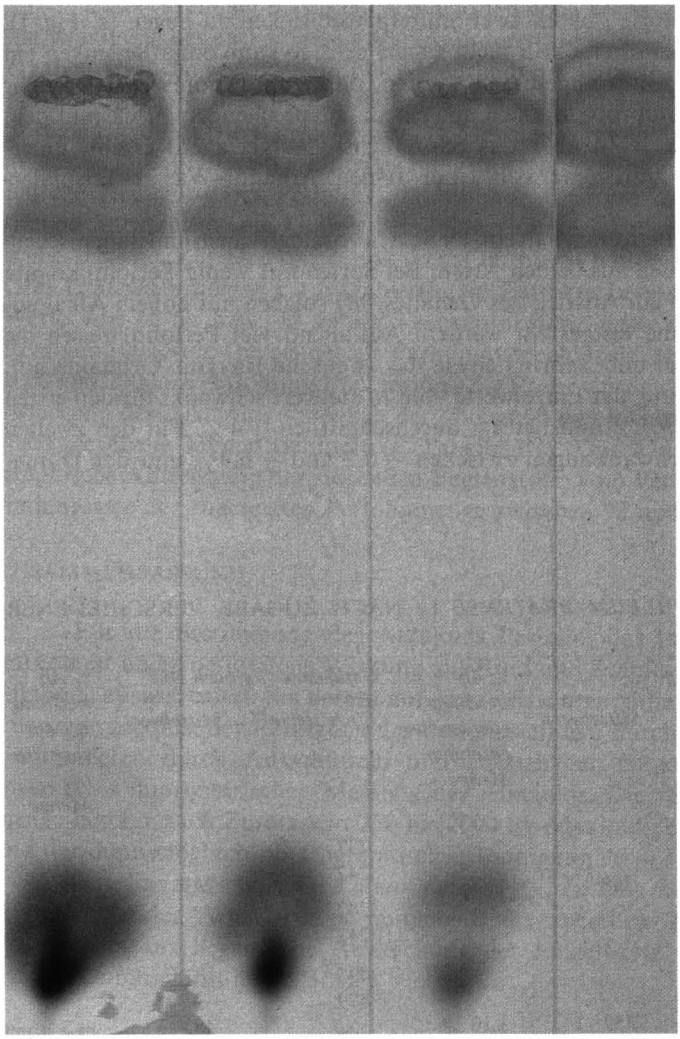

Fig. 1. Dünnschichtchromatogramm eines *Lolium*-Extraktes auf Kieselgel. Fliessmittel: *n*-Butanol–Essigsäure–Wasser (6:1:2), Laufzeit 15 h. Linke Bahn = Blindprobe; gelber Fleck zwischen den roten Säurefuchsinflecken = Perlolin.

Mit Hilfe der Dünnschichtchromatographie wurde geprüft, ob die direkte Messung des Perlolins nach dem Ausschütteln mit Chloroform durch Begleitstoffe zu hohe Werte liefert. Perlolin ist auf der Dünnschichtplatte bei Tageslicht als gelber, im UV-Licht als schmutziggelber Fleck (R_F 0.23) sichtbar. Der R_F-Wert des Perlolins ist umso höher je mehr Begleitstoffe auf der Platte mitlaufen. Als Alkaloidreagenzien eignen sich Kaliumjodoplatinat[11], mit dem Perlolin bräunlichgrün angefärbt wird, und Dragendorff-Reagenz[12], das einen orangefarbenen Fleck hervorruft. Proben mit geringem Perlolingehalt ergeben ohne Besprühen trotz der Auftragsmenge von 300 μl schwer erkennbare Flecken. Es wurde deshalb Säurefuchsin als Leitsubstanz verwendet. Der Perlolinfleck kommt unter den aufgeführten Bedingungen auf eine farb-

stofffreie Fläche zwischen die oberen zwei Säurefuchsinflecken zu liegen (s. Fig. 1). Sollte die Trennung vom Säurefuchsin nicht scharf sein, so kann ohne Bedenken ein Teil des roten Farbfleckes mit abgeschabt werden, da er die Fluoreszenz in keiner Weise beeinflusst. Die Blindprobe, die sich aus einem entsprechenden Fleck (auf dem Start wurde keine Probe, wohl aber das Säurefuchsin aufgetragen) ergibt, unterscheidet sich in ihrer Fluoreszenz von einer reinen Äthanol–Wasser–Trispuffer-Lösung sehr gering.

Tabelle II zeigt den Perlolingehalt einiger Sorten von englischem und italienischem Raygras sowie von Hybriden aus beiden Arten. Bei Sorten mit wenig Perlolin konnte beim zweiten Erntetermin ein Anstieg des Gehaltes, bei solchen mit hohem Alkaloidvorkommen eine Abnahme festgestellt werden. Auffallend viel Perlolin weisen die beiden Hybridgräser Sabel und Sabrina sowie das englische Raygras Grimalda auf. Die prozentuale Abweichung der Einzelwerte vom Mittelwert schwankt für den ersten Erntetermin von 0 bis $\pm 9.5\%$ und beträgt durchschnittlich $\pm 4\%$. Für den zweiten Erntetermin liegen die Schwankungen zwischen ± 0.2 und $\pm 6.9\%$ und der Durchschnitt bei $\pm 2\%$.

TABELLE III

PERLOLINGEHALT IN *PHLEUM PRATENSE* L. NACH ZUGABE VERSCHIEDENER ALKALOIDMENGEN

Perlolin-zugabe§ *(µg/5 g Probe)*	*Gefundene (µg)*		*% Abweichung von der zugesetzten Menge*	*Gefundene (µg nach DC***)*		*% Abweichung von der zugesetzten Menge*
	*Einzelwerte**	*Mittelwert*		*Einzelwerte***	*Mittelwert*	
250	275 262	268	+ 7	237 242 242 242	241	−4
500	552 552	552	+10	495 479 487 472	483	−3
1000	1190 1040	1115	+12	957 957 927 880	930	−6
2000	1910 2000	1955	− 2	2012 1987 2032 1987	2005	0

* Die Einzelwerte ergeben sich aus Doppelbestimmungen.

** Jeder Einzelwert entspricht einem DC-Fleck, je zwei Werte beziehen sich auf den gleichen Extrakt wie in Rubrik 2.

*** DC = Dünnschichtchromatographie.

§ Berechnet als Perlolinhydrochlorid.

Extrakte einiger Raygrassorten wurden noch der Dünnschichtchromatographie zur Reinigung des enthaltenen Perlolins unterworfen. Die anschliessenden Messungen ergaben, dass die gefundenen Werte innerhalb des Fehlerbereiches gut mit denen, die ohne vorherige Isolierung des Perlolins ermittelt wurden, übereinstimmen. Für eine Sortenauswahl dürfte daher die direkte Messung ohne Dünnschichtchromatographie ausreichend sein. Exakte Untersuchungen erfordern allerdings eine chromatographische Reinigung des Perlolins, da störende Einflüsse auf die Fluoreszenz durch fremde Substanzen aus komplexem Pflanzenmaterial nicht von vornherein auszuschliessen sind. Zur Demonstration dieses Problems wurde ein anderes perlolinarmes Gras (*Phleum pratense* L.) extrahiert. Die Extrakte besassen eine Fluoreszenz, die Werte von 60 μg bzw. 13 μg/5 g Trockensubstanz nach der chromatographischen Reinigung lieferten (berechnet als Perlolinhydrochlorid). Nach Zusatz von 250, 500, 1000 und 2000 μg Perlolinhydrochlorid zu 5 g Probe wurden ohne chromatographische Isolierung des Alkaloids abzüglich der obigen 60 μg maximal 12% mehr Perlolin als die zugegebene Menge ermittelt (s. Tabelle III). Durch die dünnschichtchromatographische Abtrennung der störenden Begleitstoffe vom Perlonin kommt die Wiederfindungsrate der zugesetzten Perlolinmenge zwischen 93 und 100% zu liegen.

ZUSAMMENFASSUNG

Für die Bestimmung des Alkaloids Perlolin, das in verschiedenen Gräsern vorkommt und eine toxische Wirkung auf Rind und Schaf ausüben kann, wurde eine Methode ausgearbeitet. Sie beruht auf einer salzsauren, äthanolischen Extraktion des Pflanzenmaterials, der Reinigung des Perlolins einmal durch Ausschütteln allein und zum anderen durch Ausschütteln und zusätzlicher Dünnschichtchromatographie sowie einer fluorimetrischen Messung des Alkaloids. Die wiedergefundene Perlolinmenge beträgt nach Zusatz von 250 bis 2000 μg Alkaloid zu 5 g perlolinarmen Gras und der dünnschichtchromatographischen Reinigung 96 $\pm$3%.

Perlolinvorkommen in *Lolium perenne* L., *Lolium multiflorum* Lamk. und in Hybriden beider Arten werden mitgeteilt, die zwischen 2 und 76 mg pro 100 g Trockensubstanz liegen. Die Abweichung der Einzelwerte vom Mittelwert beläuft sich im Durchschnitt auf $\pm$3%.

LITERATUR

1 J. A. D. Jeffreys, *J. Chem. Soc. (London)*, (1964) 4504.
2 J. Melville und R. E. R. Grimmett, *Nature (London)*, 148 (1941) 782.
3 I. Reifer und N. O. Bathurst, *N. Z. J. Sci. Technol., Sect. B*, 24 (1942) 155.
4 A. J. Aasen, C. C. J. Culvenor, E. P. Finnie, A. W. Kellock und L. W. Smith, *Aust. J. Agr. Res.*, 20 (1969) 71.
5 L. P. Bush, H. Burton und J. A. Boling, *J. Agr. Food. Chem.*, 24 (1976) 869.
6 J. A. D. Jeffreys und G. A. Sim, *Proc. Chem. Soc. London*, (1963) 171.
7 L. P. Bush und J. A. D. Jeffreys, *J. Chromatogr.*, 111 (1975) 165.
8 N. O. Bathurst, I. Reifer und E. M. Clare, *N. Z. J. Sci. Technol., Sect. B*, 24 (1942) 161.
9 C. E. Gentry, R. A Chapman, L. Henson und R. C. Buckner, *Agron. J.*, 61 (1969) 313.
10 S. R. Shaffer, M. Williams, B. J. Harmon, E. E. Pickett und G. B. Garner, *J. Agr. Food Chem.*, 23 (1975) 346.
11 E. Stahl, *Dünnschichtchromatographie*, Springer, Berlin, Heidelberg, New York, 1967, S. 837, Nr. 141.
12 E. Stahl, *Dünnschichtchromatographie*, Springer, Berlin, Heidelberg, New York, 1967, S. 829, Nr. 90.

Journal of Chromatography, 192 (1980) 208–211

CHROM. 12,619

Note

Correction for deviation from the Lambert-Beer law in the quantitation of thin-layer chromatograms by photodensitometry

DONALD T. DOWNING and ANNA M. STRANIERI

Department of Dermatology, University of Iowa College of Medicine, Iowa City, Iowa 52242 (U.S.A.)

(First received August 13th, 1979; revised manuscript received December 13th, 1979)

In a previous communication[1] it was shown that quantitative thin-layer chromatography (TLC) of lipids can be carried out so as to produce a linear relationship between the amounts of lipid and the photodensitometric peak areas obtained on scanning the acid-charred chromatograms. Furthermore, a single straight line represented this relationship for a variety of lipids provided that the results were expressed in terms of the weight of carbon contained in each quantity of lipid. Under these conditions, quantitative analysis of lipid mixtures was carried out without the use of reference compounds or the construction of standard curves. However, this was true only if the chromatographic adsorbent was first scored into narrow (6–7 mm) lanes so as to prevent the expansion of spot width with distance of migration during development or with the amount of lipid present in a spot. This allowed for a constant relationship between spot width and the length of the densitometer light beam.

In the previous study the densitometric peak areas obtained by triangulation, involving the usual (height $\times$ width) calculation, were linearly related to the quantity of lipid chromatographed. This could imply that the system of transmission photodensitometry obeyed the Lambert-Beer law, such that the optical density was linearly related to the amount of material (carbon) encountered by the light beam. However, the favorable correlation actually resulted from automatic correction for non-linearity of optical density provided by the strip-chart recorder employed (Varicord Model 42B; Photovolt, N.Y., U.S.A.). This consisted of an adjustable, quasiexpontial recorder response, instead of a truly linear response, relative to optical density. Photodensitometers from other manufacturers usually have a fixed response which is calibrated to be linear with optical density, so that deviations from the Lambert-Beer law are troublesome, especially as most modern instruments are useable over much wider ranges of optical density.

Several previous investigators have devised mathematical techniques for the correction of deviations in optical density encountered in thin-layer densitometry. Goldman and Goodall[2,3] used the theory of Kubelka and Munk[4] to calculate the nature and extent of deviations from the Lambert-Beer law which are to be expected from the light-scattering nature of chromatographic thin-layers. They then devised empirically an equation approximating the Kubelka-Munk expression and found that the still-complex calculation provided linear analyses over a limited range of sample quantity. Treiber[5] showed that neither the Lambert-Beer law nor the simulation

of the Kubelka-Monk expression gave linear results but that a more complex expression derived from both gave very much better results.

The present study provides a very much simpler correction factor for use with linearly-calibrated photodensitometers in carrying out quantitative TLC.

EXPERIMENTAL

Chromatographic plates

The 20 × 20 cm glass plates were spread with a 0.25 mm layer of silica gel G (E. Merck, Darmstadt, G.F.R.) using a Quickfit-Reeve Angel plate leveller and spreader. The layers were dried at 120° for 2 h, cooled, and then cleansed by development in chloroform–methanol (2:1). Before use the adsorbent layer was ruled into vertical lanes 6 mm wide.

Standard chromatograms

Solutions of pure docosanol, cholesteryl oleate, oleic acid and triolein (Applied Science Labs., State College, Pa., U.S.A.) of known concentration in toluene were combined and then diluted to produce a series of solutions in which 4 μl aliquots contained 1, 2, 4, 8, 12, 16, 24 and 32 μg of each lipid. Three such aliquots from each solution were applied to three separate lanes on each chromatographic plate, using a capillary pipet. The chromatograms were then developed to 19 cm in hexane–ether–acetic acid (80:20:1). After drying, each chromatographic plate was sprayed with 50% sulfuric acid and placed on an aluminum slab (20 × 20 × 0.65 cm) lying on a cold electric hotplate (Model HP-A1915B; Thermolyne, Dubuque, Iowa, U.S.A.). The hotplate was adjusted to a setting ("500") found to eventually produce a temperature of 220°, and then switched on. After 50 min, when the maximum degree of charring had been obtained and all of the sulfuric acid had been driven off, the system was allowed to cool to room temperature.

Photodensitometry

The light beam in the densitometer (Clifford Model 445; Corning Medical Products, Medfield, Mass., U.S.A.) was adjusted to illuminate the chromatograms from below with a rectangle of light 1 mm wide and just long enough (5 mm) to extend across the chromatographic lanes. The instrument was trimmed electronically so that when a photographic step tablet (Kodak No. 2) was laid on a blank, adsorbent-coated chromatographic plate and scanned, the recorder response was linear with optical density over the full range of the optical standard (0–3 O.D.). When chromatograms were subsequently scanned, the "zero" and "span" adjustments were set so that when the darkest spot on a plate was scanned the peak produced by the recorder just occupied the full width of the strip chart. The full series of chromatograms on the plate was then scanned without changing these parameters. This procedure was facilitated by an automatic plate scanner provided with the instrument which allowed all of the chromatographic lanes to be scanned in succession without intervention.

Each of the peaks on the recorder output was triangulated and the height (h) and width (w) measurements of the triangles were used for calculations either according to the conventional formula $hw/2$ or variations in which the height parameter was adjusted exponentially, as in $h^x w/2$. The adjusted peak areas obtained in this

way were plotted against the weight of carbon calculated to be present in the amounts of each lipid applied to the chromatograms.

RESULTS AND DISCUSSION

Table I shows the height and width of the triangles constructed around each of the chromatographic peaks on one of the sets of densitometer scans. Fig. 1 shows that when the areas of the triangles were obtained by the conventional calculation and then plotted against the quantities of lipid carbon applied to the chromatograms, the results deviated severely from linearity and each lipid produced a distinctly separate curve. The deviations were such as to indicate that the optical density (peak height) of the chromatographic spots increased at a rate that was less than linear relative to the increasing weights of lipid carbon. It was found by empirical means that the correlations became linear when the triangulation height of each peak was raised to the power 1.4 before calculation of the areas of the triangles, as shown in Fig. 2.

TABLE I

PEAK DIMENSIONS OBTAINED IN TRIANGULATION OF THE DENSITOMETER SCANS OF THE THIN-LAYER CHROMATOGRAMS ON ONE PLATE

Amount of lipid applied (μg)	*Peak dimensions (mm)*							
	Docosanol		*Oleic acid*		*Triolein*		*Cholesteryl oleate*	
	Height	*Width*	*Height*	*Width*	*Height*	*Width*	*Height*	*Width*
	8.0	2.6	4.0	3.9	4.0	4.0	5.0	4.1
1	8.0	2.7	4.0	4.2	4.5	3.9	5.0	4.2
	8.0	2.6	4.0	4.3	4.0	4.2	5.0	4.3
	14.5	2.7	8.0	4.2	8.0	4.1	9.0	4.2
2	16.0	2.6	8.0	4.3	8.0	4.2	9.0	4.2
	14.0	2.9	8.0	4.3	8.0	4.1	9.0	4.1
	24.0	2.8	14.0	4.3	14.5	4.2	16.0	4.4
4	24.0	2.8	15.0	4.3	14.0	4.3	16.0	4.3
	23.0	3.0	14.0	4.4	14.5	4.1	15.0	4.4
	34.5	3.2	23.0	4.8	24.0	4.5	26.5	4.7
8	35.5	3.3	23.0	5.1	24.0	4.6	26.0	4.7
	34.5	3.2	24.0	4.9	24.0	4.4	26.0	4.5
	44.0	3.4	29.0	5.2	31.0	4.6	33.0	4.8
12	43.0	3.4	29.0	5.3	31.0	4.6	33.0	4.7
	44.0	3.4	29.0	5.3	31.0	4.6	33.5	4.7
	50.5	3.5	35.0	5.6	37.0	4.7	40.0	5.0
16	50.5	3.5	35.5	5.6	38.5	4.7	40.5	5.0
	51.0	3.5	35.5	5.6	38.0	4.7	41.5	4.7
	63.0	4.1	43.5	6.4	49.0	5.0	54.0	5.2
24	62.0	4.1	45.0	6.4	50.5	4.8	55.0	5.1
	63.0	4.0	47.0	6.4	50.5	5.0	53.0	5.3
	69.0	4.1	51.5	6.7	57.5	5.2	62.0	5.2
32	69.0	4.2	51.5	6.7	58.5	5.1	63.0	5.3
	66.0	4.3	51.0	6.8	57.5	5.2	60.0	5.6

Furthermore, the results for all of the compounds then fell on a single straight line, even when the amounts of each lipid chromatographed were so excessive (24 and 32 μg) as to severely distort the shapes of the spots which they gave rise to after charring. In the normal practise of the technique described here, not more than 10 μg of any lipid would be applied to one of the chromatographic lanes.

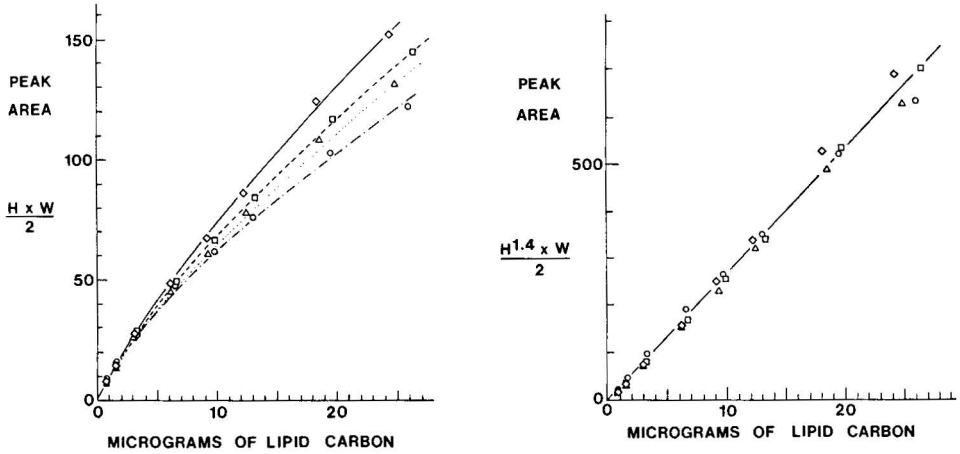

Fig. 1. Relationship between the weights of lipid carbon applied to chromatograms and the areas of the photodensitometer peaks obtained by the normal triangulation procedure for: ◇, oleic acid; □, cholesteryl oleate; △, triolein; ○, docosanol.

Fig. 2. Relationship between the weights of lipid carbon applied to chromatograms and the areas of the photodensitometer peaks obtained by the modified triangulation procedure for: ◇, oleic acid; □, cholesteryl oleate; △, triolein; ○, docosanol.

The present results confirm the previous report[1] that conditions can be found under which quantitative TLC can be performed without the continual use of reference compounds. It is apparent that accurate photodensitometric quantitation depends upon either an appropriate correction factor (mathematical or electronic) for deviation from the Lambert-Beer law or extensive use of reference compounds for the construction of a standard curve for each lipid to be assayed. The inherent non-linearity of the photodensitometric assay of thin-layer chromatograms appears often to have been overlooked, perhaps because the instrument (Photovolt) most commonly used by developers of the procedure provided an electronic correction.

ACKNOWLEDGEMENT

This study was supported in part by Research Grant No. AM 07388 from the National Institutes of Health, U.S. Public Health Service.

REFERENCES

1 D. T. Downing, *J. Chromatogr.*, 38 (1968) 91.
2 J. Goldman and R. R. Goodall, *J. Chromatogr.*, 32 (1968) 24.
3 J. Goldman and R. R. Goodall, *J. Chromatogr.*, 40 (1969) 345.
4 P. Kubelka and F. Munk, *Z. Tech. Physik.*, 12 (1931) 593.
5 L. R. Treiber, *J. Chromatogr.*, 100 (1974) 123.

Journal of Chromatography, 192 (1980) 212–215

CHROM. 12,632

Note

Gas chromatographic separations of dialkyl barbiturate derivatives

ROBERT D. BUDD

Rancho Los Amigos Hospital, 7601 E Imperial Highway, Downey, Calif. 90242 (U.S.A.)

(First received November 7th, 1979; revised manuscript received December 19th, 1979)

Numerous gas chromatographic (GC) procedures have been published for the analysis of barbiturates as free acids and as N,N-dialkyl derivatives. A review article by Jain and Cravey[1] details much of the literature on this subject. Retention times have been reported for free acid barbiturates[2,3] and various derivatives such as: N,N-dimethyl[3], N,N-diethyl[4] and N,N-dibutyl[5]. Recently the retention times for N,N-dialkyl derivatives (dimethyl through didecyl) of aprobarbital, phenobarbital and secobarbital on a 3% SE-30 column were published[6].

Previous work has shown that alkylated barbiturates exhibit less tailing and absorption to GC columns than do the free acid barbiturates[1]. It is also known that under the same GC conditions that a free acid barbiturate will have a longer retention time than that same barbiturate as its N,N-dimethyl derivative and about the same retention time as its N-ethyl-N-propyl derivative[6].

This study was undertaken to determine the relationship between the length of the N-alkyl groups and the separation of several barbiturates (allylbarbital, amobarbital, butabarbital, pentobarbital, phenobarbital, and secobarbital), which are commonly analyzed for by GC due to their extensive use and abuse[7].

EXPERIMENTAL

Reagents

The N,N-dimethylformamide dialkyl acetals used to prepare the barbiturate derivatives were obtained from Aldrich (Milwaukee, Wisc., U.S.A.), while the alcohols used were obtained from Fisher Scientific (Pittsburgh, Pa., U.S.A.) and J. T. Baker (Phillipsburg, N.J., U.S.A.).

Procedure

The following barbiturate solutions in chloroform were prepared (10 μg/ml of each barbiturate included): the common barbiturates (allylbarbital, amobarbital, butabarbital, ibomal, pentobarbital, phenobarbital and secobarbital); heptabarbital and ibomal; and alphenal and ibomal.

The N,N-dialkylated derivatives of the barbiturates were prepared on-column through the use of the appropriate N,N-dimethylformamide dialkyl acetals and *n*-alkyl alcohols as described in our earlier work[6]. The dimethyl through dipropyl derivatives were made by injecting 1 μl of the barbiturate solution and 1 μl of the

appropriate N,N-dimethylformamide dialkyl acetal together into the 3% SE-30 column. The higher derivatives (dibutyl through dioctyl) were made by injecting 1 μl of the barbiturate solution, 1 μl of N,N-dimethylformamide dineopentyl acetal, and 1 μl of the appropriate alcohol together into the column. The retention times (*RT*) and relative retention times (*RRT*) were determined for each barbiturate derivative prepared.

RESULTS AND DISCUSSION

The N,N-dialkyl derivatives from dimethyl through dioctyl of a solution containing allylbarbital, amobarbital, butabarbital, ibomal, pentobarbital, phenobarbital, and secobarbital were synthesized on a 3% SE-30 column. These barbiturates (except for ibomal) were chosen for study because they are commonly used and, therefore, commonly subject to analysis by GC. *RT* and RRT values of these derivatives are shown in Table I. It can be seen that the *RRT* values for each barbiturate derivative remain essentially constant. It can also be seen that butylation and

TABLE I

RETENTION TIMES OF DIALKYL BARBITURATE DERIVATIVES ON 3% SE-30

Conditions: 6 ft. × 2 mm (I.D.) glass column packed with 3% SE-30 on Chromosorb W AW DMCS (80–100 μm). Oven temperature, 200°; injector 240° and detector 250°.

Dialkyl derivative		*Drug*						
		Allylbarb	*Butabarb*	*Amobarb*	*Pentobarb*	*Secobarb*	*Ibomal*	*Phenobarb*
Methyl	*RT* (min)	1.3	1.3	1.6	1.8	2.1	2.8	3.9
	RRT	0.48	0.48	0.56	0.64	0.75	1.00	1.42
Ethyl	*RT*	1.9	1.9	2.1	2.4	2.8	3.9	4.8
	RRT	0.48	0.48	0.54	0.62	0.72	1.00	1.23
Propyl	*RT*	3.3	3.3	3.7	4.2	4.9	6.8	8.4
	RRT	0.48	0.48	0.54	0.62	0.71	1.00	1.23
Butyl	*RT*	5.7	5.9	6.6	7.7	8.6	12.0	14.8
	RRT	0.48	0.50	0.55	0.64	0.72	1.00	1.24
Amyl	*RT*	11.1	11.6	12.8	14.6	16.5	23.1	28.3
	RRT	0.48	0.50	0.55	0.63	0.71	1.00	1.23
Hexyl	*RT*	20.9	22.1	23.9	27.9	30.7	43.5	52.6
	RRT	0.48	0.51	0.55	0.64	0.70	1.00	1.21
Heptyl	*RT*	40.8	43.6	46.8	53.8	60.6	84.9	103.9
	RRT	0.48	0.51	0.55	0.63	0.71	1.00	1.22
Octyl	*RT*	81.2	87.2	93.1	108.0	121.7	168.8	203.8
	RRT	0.48	0.52	0.55	0.64	0.72	1.00	1.21

higher alkylations lead to a separation of allylbarbital and butabarbital that is not obtained with shorter derivatives (Fig. 1). The separation is slight, as the *RRT* values still remain essentially constant.

An interesting, although unexplained, anomaly occurred in the case of phenobarbital where the dimethyl derivative had a significantly longer *RRT* than the other seven dialkyl derivatives (Table I). Further investigation of this anomaly was undertaken. Three possible explanations to the problem were proposed: (1) This property

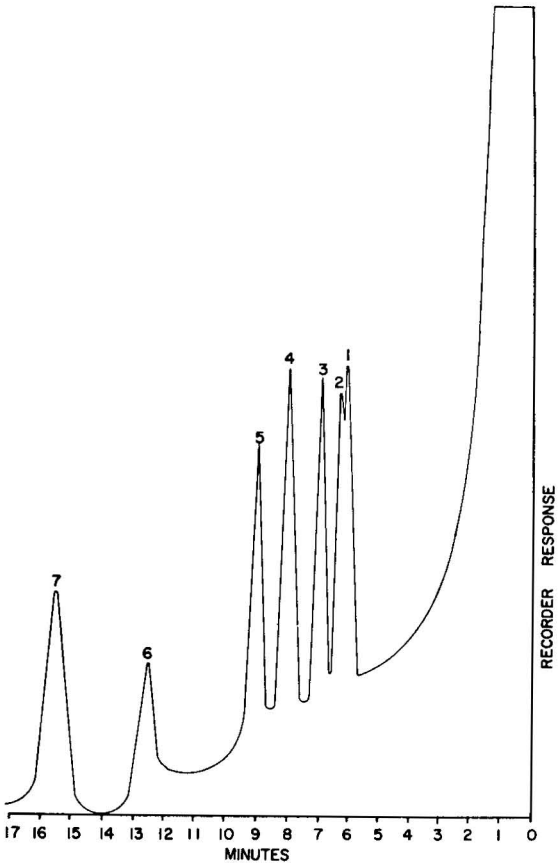

Fig. 1. Butylated barbiturates on 3% SE-30 glass column, 6 ft. × 2 mm, 195°; injector 270°; detector 280°; range 10^{-11}; attenuation × 32, injection: 1 μl containing 0.1 g/l each of the dibutyl derivatives of (1) allylbarbital, (2) butabarbital, (3) amobarbital, (4) pentobarbital, (5) secobarbital, (6) ibomal and (7) phenobarbital.

may occur for all barbiturates, but may only be observable for those barbiturates with long retention times (longer than ibomal); (2) it may occur for all barbiturates containing a 5-phenyl group; or (3) it may occur for only phenobarbital (5-ethyl-5-phenylbarbital). To investigate these possibilities, derivatives were made of heptabarbital (5-ethyl-5-(1-cyclohepten-1-yl)-barbital and alphenal (5-allyl-5-phenylbarbital), which both have longer retention times than ibomal. The *RRT* values of these barbiturates were compared with obimal (Table II). The *RRT* values for alphenal behaved as those of phenobarbital, while the *RRT* values of heptabarbital behaved as those of ibomal and the other barbiturates. Thus the anomaly must be related to the 5-phenyl group.

The synthesis of derivatives other than dimethyl allows differentiation of mephobarbital (1-methylphenobarbital) from phenobarbital, narconumol (1-methylaprobarbital) from aprobarbital, and metharbital (1-methylbarbital) from barbital. Thus, although dimethyl derivatives are the most frequently used derivatives in GC

TABLE II

RETENTION TIMES OF DIALKYL BARBITURATE DERIVATIVES

Conditions: 3ft. × 2 mm (I.D.) glass column packed with 3% SE-30 on Chromosorb W AW DMCS (80–100 μm). Oven temperature, 140°; injector 270° and detector 280°.

	Retention times (min)			*Relative retention times*		
	Ibomal	*Heptabarb*	*Alphenal*	*Ibomal*	*Heptabarb*	*Alphenal*
Dimethyl	3.85	9.4	7.78	1.0	2.4	2.0
Diethyl	5.9	13.5	10.2	1.0	2.3	1.7
Dipropyl	12.1	27.25	21.2	1.0	2.3	1.7
Dibutyl	26.45	61.9	45.35	1.0	2.3	1.7
Diamyl	64.8	—	111.0	1.0	—	1.7
Dihexyl	147.0	328.1	245.7	1.0	2.2	1.7
Ethyl propyl	8.1	18.5	13.85	1.0	2.3	1.7
Propyl butyl	17.15	—	29.0	1.0	—	1.7
Methyl ethyl	4.7	11.25	8.95	1.0	2.4	1.9
Methyl propyl	6.5	—	12.5	1.0	—	1.9
Methyl butyl	9.6	—	18.4	1.0	—	1.9
Methyl amyl	15.0	—	28	1.0	—	1.9
Methyl hexyl	25.2	57.4	45.5	1.0	2.3	1.8
Dihydrogen	8.95	19.7	23.1	1.0	2.2	2.6

procedures[1] and have the shortest retention times at a given temperature (Table I), the formation of barbiturate derivatives other than dimethyl may be advantageous for several reasons: (1) The shorter *RRT* for phenobarbital, (2) separation of allylbarbital from butabarbital, (3) differentiation of mephobarbital from phenobarbital, and (4) their ready formation[5–6].

It has been found that the dibutyl derivatives are the derivatives of choice since they are the shortest alkyl derivatives giving separation of allylbarbital and butabarbital.

REFERENCES

1 N. C. Jain and R. H. Cravey, *J. Chromatogr. Sci.*, 12 (1974) 228–236.
2 D. J. Berry, *J. Chromatogr.*, 86 (1973) 89–105.
3 N. C. Jain, R. D. Budd, T. C. Sneath, D. M. Chinn and W. J. Leung, *Clin. Tox.*, 9 (1976) 221–233.
4 J. MacGee, *Clin. Chem.*, 17 (1971) 587–591.
5 R. H. Greely, *Clin. Chem.*, 20 (1974) 192–194.
6 R. D. Budd, *Clin. Tox.*, in press.
7 R. D. Budd, *Amer. J. Drug Alcohol Abuse*, in press.

Journal of Chromatography, 192 (1980) 216–221

CHROM. 12,608

Note

Identification des produits de pyrolyse de la *cis*-décaline

P. BREDAEL et D. RIETVELDE

Université Libre de Bruxelles, Service de Chimie Générale-Radioactivation, Faculté des Sciences Appliquées, 50 Avenue F. D. Roosevelt, 1050 Bruxelles (Belgique)

(Reçu le 25 octobre 1979; manuscrit modifié reçu le 10 décembre 1979)

Dans un précédent article[1], nous avons déjà décrit le craquage thermique des décalines entre 873 et 1223 °K. Les résultats obtenus montraient la formation de quantités importantes de composés aromatiques légers, atteignant 34% en poids à 1173 °K.

Les mesures effectuées permettaient de penser que les composés aromatiques étaient issus de cycloalcanes et cycloalcènes, eux-mêmes formés dans une étape précédente du mécanisme de pyrolyse de la décaline.

L'objet du présent travail est d'identifier les premiers composés formés lors de la pyrolyse qui, par leurs mécanismes propre de craquage thermique, mèneront aux hydrocarbures aromatiques.

PARTIE EXPÉRIMENTALE

Les expériences ont été réalisées tout d'abord dans un appareillage de pyrolyse à pression atmosphérique décrit dans la Fig. 1. Le réacteur en verre de silice, d'un diamètre intérieur de 6 mm permet un temps de séjour dans le réacteur de 0.2 sec minimum.

Un appareillage de pyrolyse instantanée dans lequel un microréacteur de 1 mm de diamètre intérieur est directement raccordé sur le bloc d'injection d'un chromatographe en phase gazeuse, décrit dans la Fig. 2, et permettant d'atteindre des temps de séjour dans le réacteur de $5 \cdot 10^{-4}$ sec a également été utilisé.

Les conditions de travail et d'analyse sont rassemblées dans le Tableau I.

RÉSULTATS ET DISCUSSIONS

Les résultats obtenus sont illustrés dans les Figs. 3 et 4.

Deux séries de mesures ont été réalisées. L'une dans l'appareil 1, à 923 °K, entre 0.6 et 1.4 sec de temps de séjour dans le réacteur (Fig. 3); l'autre dans l'appareil 2, pour $5 \cdot 10^{-3}$ sec de temps de séjour dans le réacteur, entre 935 et 1055 °K (Fig. 4).

Les Tableaux II et III rassemblent les produits identifiés par référence aux indices de Kovats préalablement déterminés et confimés par la littérature[2].

Les diagrammes présentés montrent clairement que les produits initiaux de craquage sont le 1,7-octadiène, le cyclohexène, le 1,3-cyclohexadiène, l'éthyl-1,4-

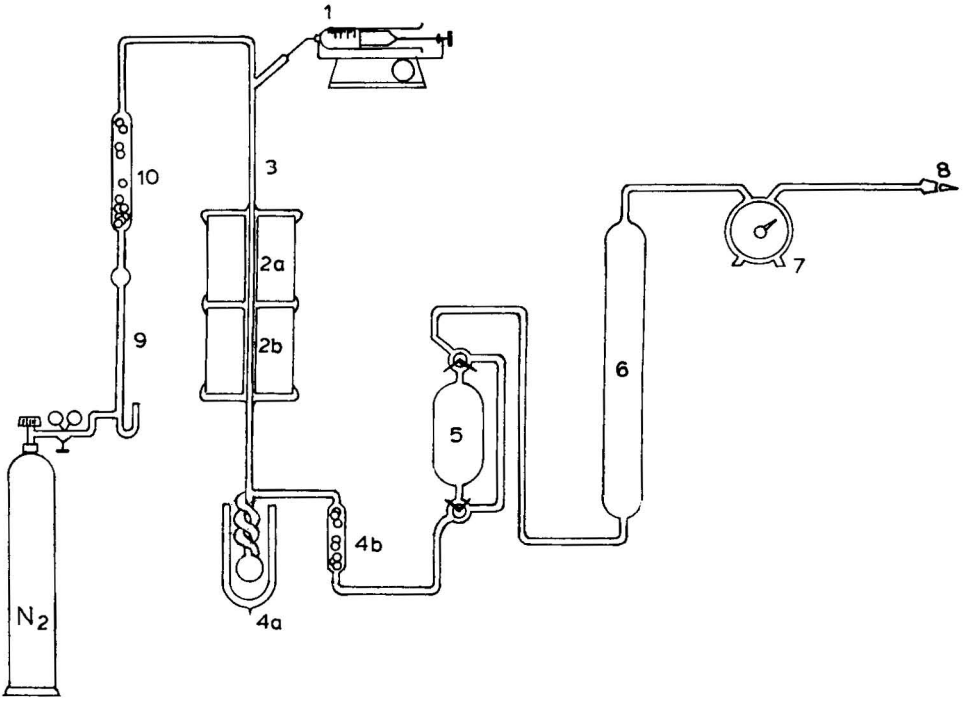

Fig. 1. Pyrolyse de la *cis*-décaline; appareil de pyrolyse classique (t = 0.2 sec). 1 = Injecteur; 2a = four 200°, 2b = four 550→1000°; 3 = réacteur; 4a, 4b = pièges à liquides; 5 = piège à gaz; 6 = ampoule à gaz de 5 l; 7 = compteur à gaz; 8 = cheminée; 9 = débitmètre à bulle de savon; 10 = silica gel.

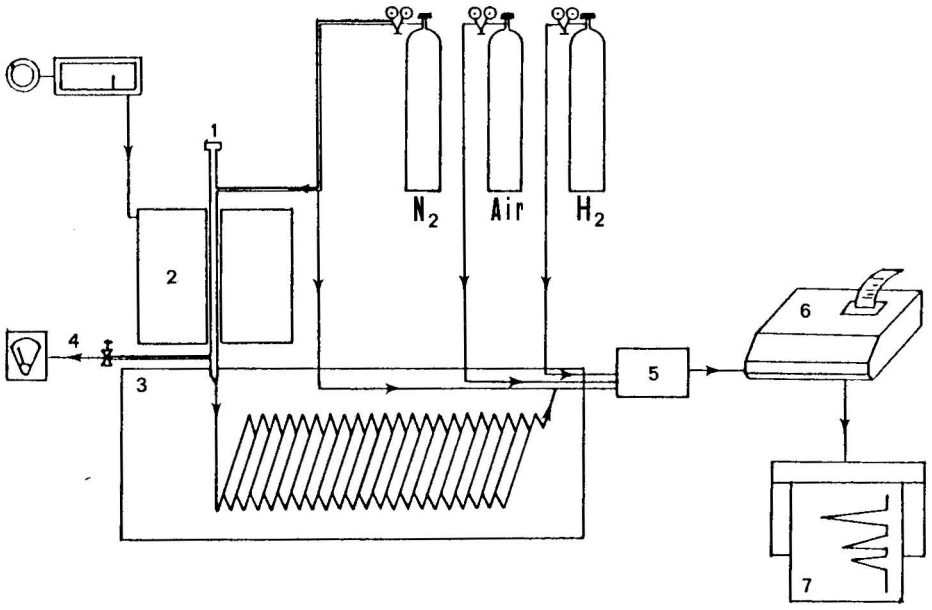

Fig. 2. Pyrolyse de la *cis*-décaline; appareil de pyrolyse instantanée (10^{-4} sec $\leqslant t \leqslant 10^{-2}$ sec). 1 = Injecteur; 2 = four de pyrolyse; 3 = chromatographe; 4 = diviseur de débit; 5 = detecteur; 6 = intégrateur; 7 = enregistreur.

TABLEAU I

PYROLYSE DE LA *cis*-DÉCALINE

Conditions de travail et d'analyse des sous produits.

	Analyse des gaz de pyrolyse		*Analyse des liquides de pyrolyse*
	H_2	CH_4, C_2H_4, C_3H_6, C_4H_8, $1,3\text{-}C_4H_6$	
Appareil 1			
Diamètre du réacteur (mm)	6	6	6
Temps de séjour (sec)	0.2→2	0.2→2	0.2→2
Température de pyrolyse (°K)	873→1373	873→1373	873→1373
Colonne	Charbon actif	Alumine	Capillaire polyphényl-éther, 100 m × 0.1 mm
Température de colonne (°C)	180	150	80
Gaz vecteur	N_2	He	N_2
Détecteur	Thermistances	Catharomètre	Détecteur à ionisation de flamme
Appareil 2			
Diamètre du réacteur (mm)	1	1	1
Temps de séjour (sec)	$5\cdot10^{-4}\rightarrow10^{-2}$	$5\cdot10^{-4}\rightarrow10^{-2}$	$5\cdot10^{-4}\rightarrow10^{-2}$
Température de pyrolyse (°K)	873→1273	873→1273	873→1273
Colonne	Capillaire SE-30, 100 m × 0.5	Capillaire SE-30, 100 m × 0.5 mm	Capillaire SE-30, 100 m × 0.5 mm
Température de colonne (°C)	80	80	80

TABLEAU II

PYROLYSE DE LA *cis*-DÉCALINE

Identification des produits de pyrolyse sur polyphényléther, 80 °C.

No. pic	*Nom du composé*	I_K *polyphényléther 80 °C*
2	1,3-Butadiène	
3	Isoprène	602
4	1,3-Cyclopentadiène	694
5	Cyclopentane	660
6	Cyclopentène	674
7	1-Méthyl cyclopentène	707
8	2,4-Hexadiène	770
9	Cyclohexène	788
10	1,3-Cyclohexadiène	806
11	Benzène	827
12	Méthyl cyclohexène	840
13	1,4-Cyclohexadiène	847
14	Méthyl cyclohexène	870
15	Méthyl-1,4-cyclohexadiène	884
16	Éthyl cyclohexane	890
17	?	897
18	?	908
19	1,7-Octadiène	916
20	Toluène	

TABLEAU III

PYROLYSE DE LA *cis*-DÉCALINE

Identification chromatographique et produits de pyrolyse sur SE-30, 80 °C.

No. pic	*Nom du composé*	I_K *SE-30*
1	Méthane	
2	Éthylène	
3	Propène	
4	1,3-Butadiène	
5	?	
6	Méthylbutènes	
7	?	
8	1,4-Pentadiène	480
9	1-Pentène	492
10	Isoprène	507
11	1,3-Cyclopentadiène	540
12	Cyclopentène	561
13	1,5-Hexadiène	577
14	2-Méthyl-1-Pentène	590
15	1,4-Hexadiène	596
16	2-Méthyl-2-pentène	607
17	1,3-Hexadiène	619
18	2-Méthyl-1,3-cyclopentadiène	640
19	1-Méthylcyclopentène	651
20	Benzène	659
21	1,3-Cyclohexadiène	671
22	Cyclohexène	685
23	2,4-Diméthyl-1,3-pentadiène	696
24	1,4-Cyclohexadiène	706
25	?	715
26	?	722
27	Vinylcyclopentane	727
28	Méthylcyclohexane	735
29	Éthylcyclopentane	740
30	Méthyl-1-cyclohexène	743
31	1-Éthylcyclopentène	756
32	Toluène	762
33	1-Méthylcyclohexène	771
34	1,7-Octadiène	779
35	1-Octène	789
36	Octène	793
37	?	798
38	Diméthylcyclohexène	816
39	Vinylcyclohexane	824
40	Diméthylcyclohexène	829
41	4-Vinyl-1-Cyclohexène	833
42	Éthylbenzène	854
43	2,5-Diméthyl-2,4-hexadiène	861
44	Éthylidène cyclohexane	869
45	1-Éthylcyclohexène	872
46	Styrène	879
47	*o*-Xylène	884
48	1-Nonène	888
49	Nonène	891
50	1-Éthyl-1,4-cyclohexadiène	901

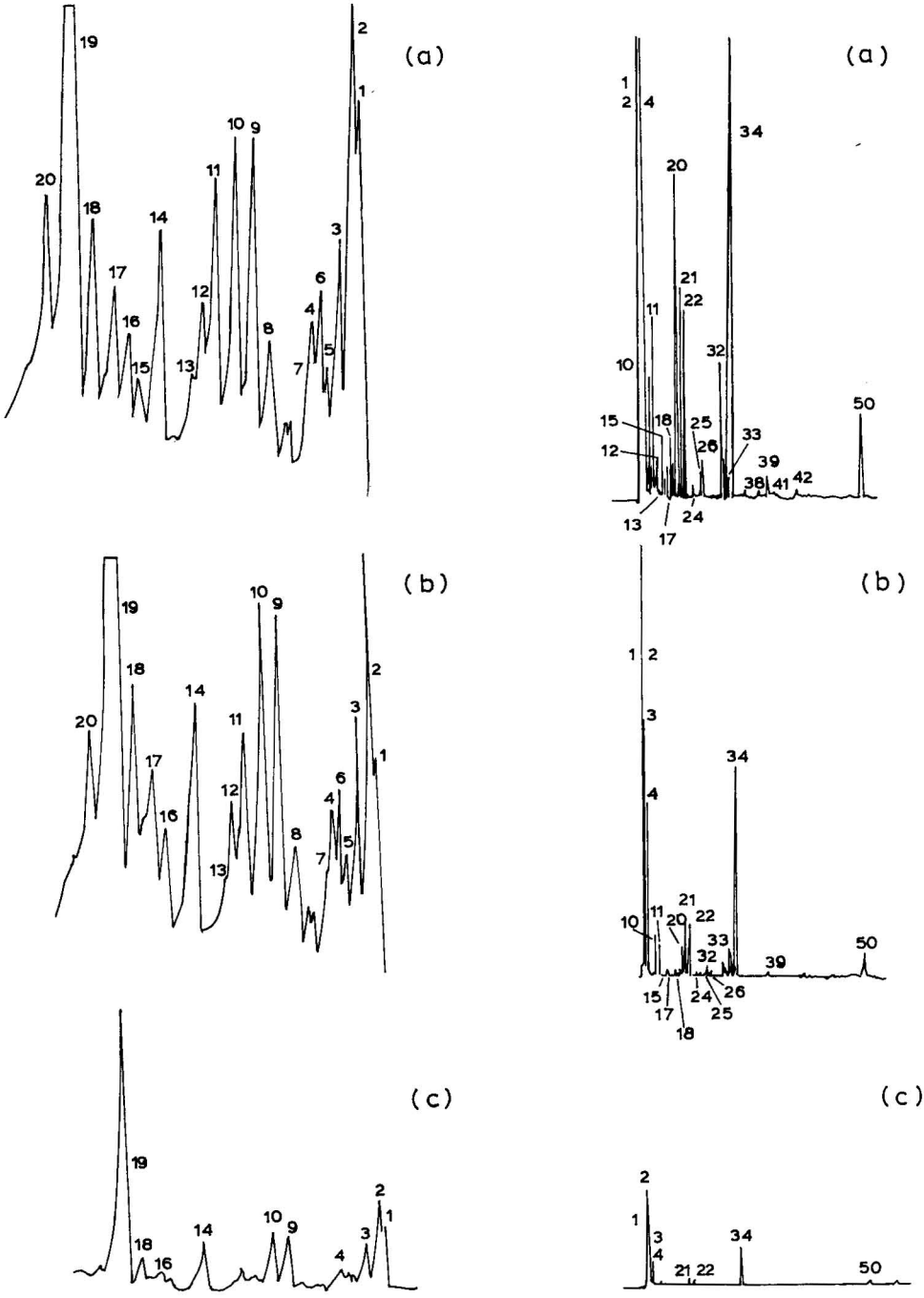

Fig. 3. Pyrolyse de la *cis*-décaline à 923 °K. (a) 1.4 sec; (b) 0.9 sec; (c) 0.6 sec.

Fig. 4. Pyrolyse instantanée de la *cis*-décaline ($t = 5 \cdot 10^{-3}$ sec). (a) 1055 °K; (b) 1009 °K; (c) 935 °K.

cyclohexadiène, l'éthylène et le 1,4-butadiène. Ces composés, à plus haute température, donnent lieu à la formation de composés alicycliques à 5 et 6 carbones dans le cycle et à des α, ω oléfines, lesquels par déshydrocyclisation se transforment en hydrocarbures aromatiques tels le benzène, le toluène, l'éthylbenzène et le styrène qui prédominent à partir de 1123 °K (ref. 1).

CONCLUSIONS

Deux séries de mesures effectuées l'une à faible temps de séjour ($5 \cdot 10^{-3}$ sec) entre 935 et 1055 °K et l'autre à basse température (923 °K) pour des temps de séjour de 0.6 à 1.4 sec ont été réalisées.

On a ainsi pu mettre en évidence le 1,7-octadiène, le cyclohexène et le 1,3-cyclohexadiène comme produits initiaux issus de la pyrolyse de la *cis*-décaline. Ces composés, par l'intermédiaire d'alkylcycloalcènes à 5 et 6 carbones dans le cycle, mènent aux hydrocarbures aromatiques légers précédemment observés.

Les résultats obtenus confirment le chemin réactionnel déjà proposé et montrent bien que la pyrolyse de la *cis*-décaline passe par une rupture des deux cycles, soit totale en 1,7-octadiène, soit partielle en cyclohexène, avec production d'éthylène et de 1,3-butadiène.

BIBLIOGRAPHIE

1 P. Bredael et D. Rietvelde, *Fuel*, 58 (1979) 215–218.
2 P. G. Robinson et A. L. Odell, *J. Chromatogr.*, 57 (1971) 11–17.

Journal of Chromatography, 192 (1980) 222–227

CHROM. 12,637

Note

High-performance liquid chromatography of amino acids, peptides and proteins

XXI*. The application of preparative reversed-phase high-performance liquid chromatography for the purification of a synthetic underivatised peptide

C. A. BISHOP**, D. R. K. HARDING, L. J. MEYER and W. S. HANCOCK

Department of Chemistry, Biochemistry and Biophysics, Massey University, Palmerston North (New Zealand)

and

M. T. W. HEARN

Immunopathology Group, Medical Research Council of New Zealand, Medical School, P.O. Box 913, Dunedin (New Zealand)

(Received December 27th, 1979)

During the past few years, reversed-phase high-performance liquid chromatography (HPLC) has emerged as a powerful technique for analysing the purity of underivatised peptides[1–8]. In recent theoretical and experimental studies[9–13], a number of different approaches have been explored by which secondary solution equilibria, *e.g.* pH and ion-pairing, of underivatised peptides can be manipulated to influence selectivity and resolution of these substances on microparticulate reversed-phase supports. In particular, the addition of hydrophilic and hydrophobic counterionic species to the mobile phase at low pH has proved very useful for the analysis of underivatised peptides of widely different intrinsic polarities.

Currently a wide variety of peptides are being synthesised for use in biological investigations[14]. A major difficulty with these syntheses has been the production of high purity products in gram quantities. In the past, liquid chromatographic techniques such as ion-exchange and gel filtration have been used for purification of the products of solid phase or solution phase peptide syntheses. These techniques tend to be slow, exhibit low separation efficiencies and can result in low recoveries. Fully protected peptides have been successfully purified[15] using preparative normal-phase HPLC on porous silica gel microparticles with sample sizes 5 g and larger. However, with these packing materials unprotected peptides show poor resolution, long retention times and generally low recoveries.

It is the purpose of this report to show that it is also possible to purify gram quantities of underivatised peptides by reversed-phase HPLC using polyethylene car-

* Part XX: ref. 8.

** To whom correspondence should be addressed.

tridges, containing 10–20 μm octadecylsilica particles, which can be radially compressed. A model tetrapeptide, L-leucyl–glycyl–glycyl–glycine, (L-Leu(Gly)$_3$), extensively used for intestinal transport studies[16], was prepared by standard solution phase methods and purified to homogeneity by this preparative HPLC approach. The time for the chromatographic separation for up to 10 g of the tetrapeptide was under 30 min.

EXPERIMENTAL

Apparatus

A Waters Assoc. (Milford, Mass., U.S.A.) HPLC system was used for the analytical separations. This consisted of two M6000A solvent delivery units, an M660 solvent programmer and a U6K universal liquid chromotograph injector, coupled to an M450 variable wavelength UV Spectrophotometer (Waters Assoc.) and an Omniscribe two-channel chart recorder (Houston Instruments, Austin, Texas, U.S.A.). A μBondapak C_{18} column (10 μm, 30 cm $\times$ 4 mm I.D.) purchased from Waters Assoc. was used for all analyses. Sample injections were made using a Microliter 802 syringe (Hamilton, Reno, Nev., U.S.A.).

The preparative separations were carried out on a Waters Assoc. Prep LC/System 500 instrument with a built in refractive index detector and recorder. An M450 variable wavelength detector (Waters Assoc.) was connected in series with the refractive index detector, and coupled to an Omniscribe two-channel recorder (Houston Instruments). A Waters Assoc. Prep PAK-500-C_{18} cartridge (75 μm mean particle size 30 cm $\times$ 5.7 cm) was used for the purification. Sample injections were made using a Gastight 1010W syringe (Hamilton).

For both analytical and preparative work solvents were filtered using a Pyrex filter holder (Millipore, Bedford, Mass., U.S.A.) while peptide samples were filtered using a Swinney Filter (Millipore). Millipore HA grade, 0.45 μm filters were used at all times for solvent and sample preparation, except for filtration of the methanol when a Millipore FH grade filter was used.

Chemicals

Water was glass-distilled. Methanol was drum-grade (I.C.I., Wellington New Zealand) and distilled before use. Trifluoroacetic acid (TFA) (Halocarbon Products, Hackensack, N.J., U.S.A.) was also distilled before use. The tetrapeptide, L-Leu(Gly)$_3$, was prepared by a standard solution phase synthetic method, the details of which will be reported elsewhere. A commercial sample of L-Leu(Gly)$_3$ was purchased from Vega Biochemicals (Tucson, Ariz., U.S.A.). Glycine and L-leucine were obtained from BDH (Poole, England).

Methods

Analytical HPLC was carried out at a flow-rate of 1.5 ml/min using 0.05% TFA in water, pH 2.3, as mobile phase.

All chromatography was carried out at room temperature (*ca.* 22°). Peptides were dissolved in the mobile phase at a concentration of 5 mg/ml and 10–25 μl volumes injected onto the columns. Similarly, 25 μl aliquots from the preparative HPLC runs were analysed under identical elution conditions with and without the commercial standard present.

For the preparative separations, a flow-rate of 100 ml/min was maintained (back pressure 100 p.s.i.). The mobile phase, water–methanol–TFA (95:5:0.05) was degassed completely by vacuum aspiration or by a helium gas purge. The crude sample was loaded in amounts between 1 and 10 g in 10 ml of the eluting solvent. Immediately after collection each fraction was neutralised to pH 7 with ammonium hydroxide, concentrated on a rotary evaporator and lyophilised.

RESULTS AND DISCUSSION

The analytical HPLC profile of the crude product from the solution synthesis of L-Leu(Gly)$_3$ is shown in Fig. 1a. As has been noted previously[4,17] with other peptides, the peak shape obtained for the crude L-Leu(Gly)$_3$ as well as the commercial standard (Fig. 1b) with mobile phases containing TFA is poor compared to that obtained with orthophosphate systems[1,11] at a similar pH. However, TFA was chosen as the hydrophilic ion-pairing reagent on account of its apparent volatility as the ammonium salt, a property which should allow it to be removed at the final step of the purification, by lyophilisation. The resolution of the peaks is not optimal but represents a maximal loading before resolution is lost completely. Lowering the sample size dramatically improved the resolution but would give no indication of a maximum loading weight of the product for use on the preparative system.

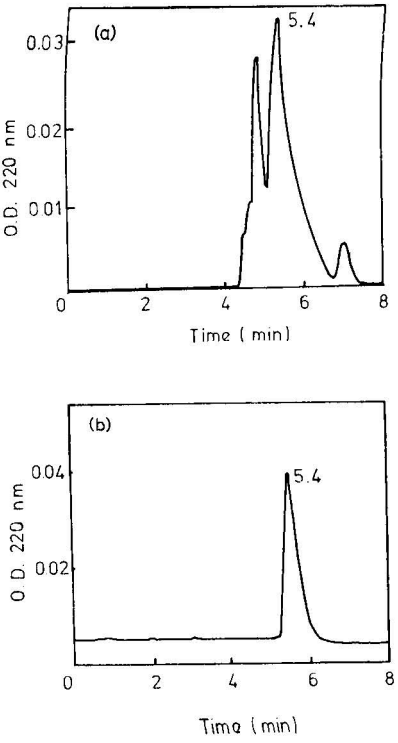

Fig. 1. The elution profile of the crude synthetic L-Leu(Gly)$_3$ (a) and the commercially obtained standard L-Leu(Gly)$_3$ (b). Chromatographic conditions: Column, μBondapak C_{18}; mobile phase, water–0.05% TFA, pH 2.3; flow-rate, 1.5 ml/min.

Fig. 2 shows the preparative HPLC chromatogram for the separation of 1 g of the crude tetrapeptide product. Following analytical HPLC of the collected fractions (Fig. 3) a close correlation between the profiles obtained under analytical and preparative conditions was apparent. The degree of separation achieved during the preparative purification is easily discerned. The major component evident in the HPLC analysis of the fraction 5 had a retention time identical to authentic L-Leu(Gly)$_3$. To improve resolution, the leading edge of the preparative fraction 5 was recycled under the same elution conditions and fractions 6, 7, 8 and 9 (Fig. 2) were collected. Only 2 l of solvent were required for this preparative run which was completed in 27 min including the recycle. In view of the excellent separation of L-Leu(Gly)$_3$ from other contaminants at the one gram scale, the sample load was subsequently increased to 10 g of crude product without loss of resolution. The purified tetrapeptide, recovered from the major recycled peak (Fig. 2, fraction 8), had a coincident retention time under analytical HPLC conditions to that of L-Leu(Gly)$_3$ standard. (*cf.* Fig. 3, fractions 5 and 8 with Fig. 1b).

A known amount of the purified product was loaded onto the preparative system in the absence of any ion-pairing reagent and collected, lyophilised and reweighed. Recovery was greater than 95%. The product obtained after lyophilisation of fraction 8 exhibited an unretained peak corresponding to a small amount of ammonium TFA which resisted repeated lyophilisation. The product could, however, be easily desalted by rechromatography on the preparative system equilibrated in

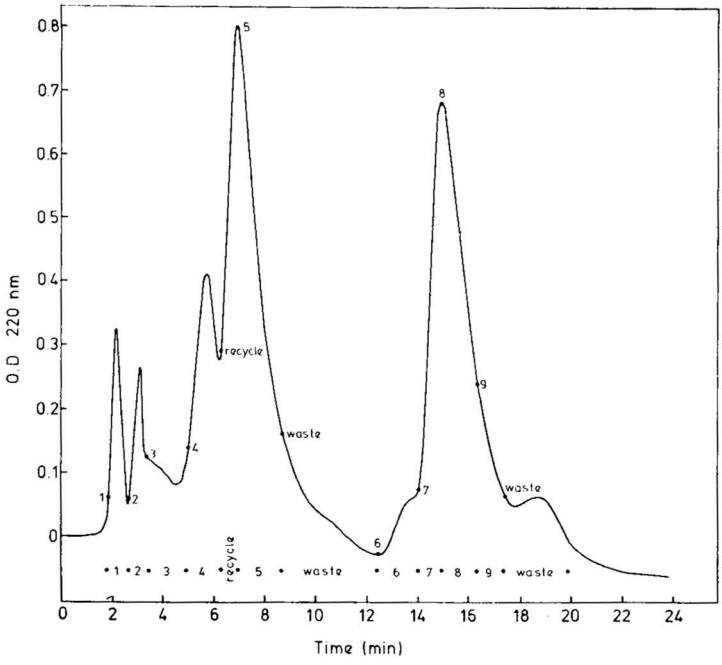

Fig. 2. The elution profile of the preparative purification of 1 g crude L-Leu(Gly)$_3$. Chromatographic conditions: Column, Prep PAK-500/C$_{18}$ cartridge; mobile phase, water–methanol–TFA (95:5:0.05), pH 2.3; flow-rate, 100 ml/min.

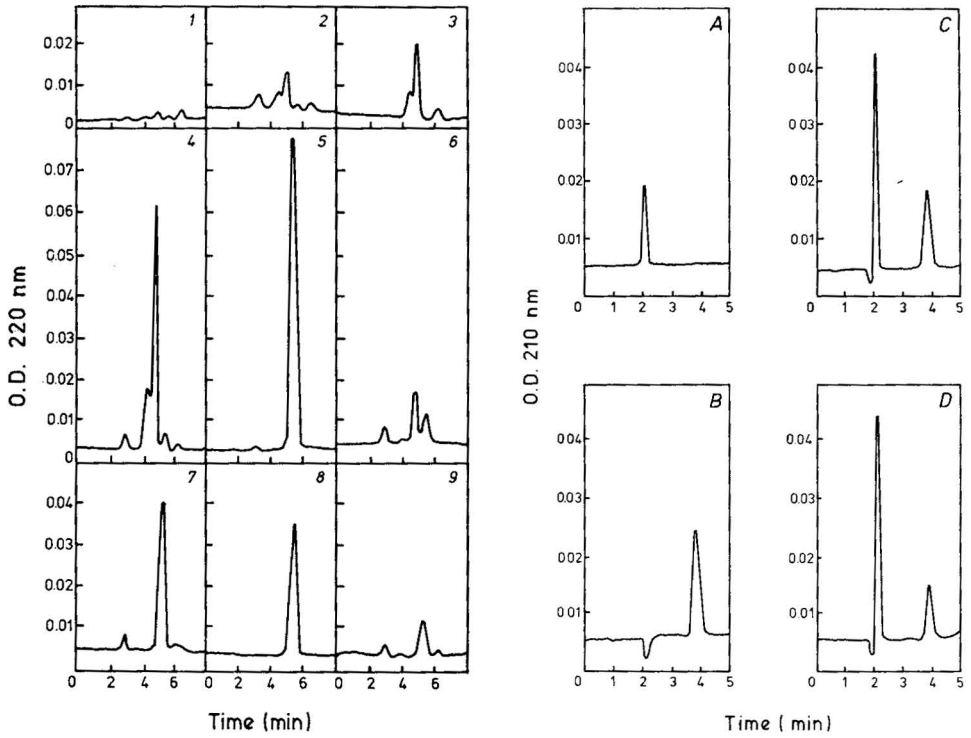

Fig. 3. The analytical HPLC profiles of the collected fractions (1–9) from the preparative separation of the crude L-Leu(Gly)$_3$. Chromatographic conditions as in Fig. 1.

Fig. 4. The elution profiles of the amino acid analysis by HPLC. (A) Glycine, (B) L-leucine, (C) the hydrolysate of the L-Leu(Gly)$_3$ obtained by preparative HPLC, (D) the hydrolysate of the commercial standard. Chromatographic conditions as in Fig. 1.

water–methanol (9:1) without the TFA present. Under these elution conditions the L-Leu(Gly)$_3$ was obtained, following lyophilisation, free of solvent contaminants.

Further positive identification of the purified product was achieved by N.M.R. and mass spectrometry. Analytical reversed-phase HPLC using several mobile phases containing ion-pairing reagents of different polarities[9,12,13] failed to reveal any peptide impurities in the recovered product. A sample of the purified peptide was hydrolysed and subjected to amino acid analysis by both conventional autoanalyser techniques and reversed-phase HPLC. The latter technique, as has been reported previously[18], is particularly useful to distinguish constituent underivatised amino acids differing in hydrophobicity. As can be seen from Fig. 4 both the commercial standard and the purified synthetic peptide show, following hydrolysis, exact correlation with the standard constituent amino acids, glycine and leucine.

Based on the above observations with the model peptide, we consider that the rapid and extremely efficient purifications of underivatised peptides in quantities up to at least 10 g should now be possible by means of preparative reversed-phase HPLC using inexpensive solvents, in reasonable volumes and with excellent recoveries of the desired product. In a subsequent paper the purification by this means of a range of biologically active synthetic underivatised peptides will be described.

ACKNOWLEDGEMENTS

We wish to thank Mrs. C. Smart for expert technical assistance. This investigation was supported in part by Medical Research Council (New Zealand) Grant No. 77-30 and National Heart Foundation of New Zealand Award No. 153. We also wish to acknowledge the generous equipment grant made by Waters Assoc. (New Zealand) which made this work possible.

REFERENCES

1 W. S. Hancock, C. A. Bishop, R. L. Prestidge, D. R. K. Harding and M. T. W. Hearn, *Science*, 200 (1978) 1168.
2 E. Lundanes and T. Greibrokk, *J. Chromatogr.*, 149 (1978) 241.
3 S. Terabe, R. Konaka and K. Inouye, *J. Chromatogr.*, 172 (1979) 163.
4 J. E. Rivier, *J. Liquid Chromatogr.*, 1 (1978) 343.
5 M. J. O'Hare and E. C. Nice, *J. Chromatogr.*, 171 (1979) 209.
6 J. Rivier, R. Kaiser and R. Galyean, *Biopolymers*, 17 (1978) 1927.
7 E. C. Nice and M. J. O'Hare, *J. Chromatogr.*, 162 (1979) 401.
8 M. T. W. Hearn, C. A. Bishop, W. S. Hancock, D. R. K. Harding and G. D. Reynolds, *J. Liquid Chromatogr.*, 2 (1979) 1.
9 M. T. W. Hearn, B. Grego and W. S. Hancock, *J. Chromatogr.*, 185 (1979) 429.
10 M. T. W. Hearn, *Advan. Chromatogr.*, 18 (19) in press.
11 W. S. Hancock, C. A. Bishop, R. L. Prestidge, D. R. K. Harding and M. T. W. Hearn *J. Chromatogr.*, 153 (1978) 391.
12 W. S. Hancock, C. A. Bishop, L. J. Meyer, D. R. K. Harding and M. T. W. Hearn, *J. Chromatogr.*, 161 (1978) 291.
13 W. S. Hancock, C. A. Bishop, J. E. Battersby, D. R. K. Harding and M. T. W. Hearn, *J. Chromatogr.*, 168 (1979) 377.
14 A. Loffet (Editor), *Peptides 1976*, University of Brussels, Brussels, 1976.
15 T. F. Gabriel, J. Michalewsky and J. Meienhofer, *J. Chromatogr.*, 129 (1976) 287.
16 Y. C. Chung, D. B. A. Silk and Y. S. Kim, *Clin. Sci.*, 57 (1979) 1.
17 C. E. Dunlap, III, S. Gentleman and L. I. Lowney, *J. Chromatogr.*, 160 (1978) 191.
18 W. S. Hancock, C. A. Bishop and M. T. W. Hearn, *Anal. Biochem.*, 92 (1978) 170.

Journal of Chromatography, 192 (1980) 228–231

Chrom. 12,620

Note

Ligand-exchange chromatography

I. Resolution of L- and D-proline on a copper(II)–proline complex bound to microparticulate silica gel

K. SUGDEN, C. HUNTER and G. LLOYD-JONES

Reckitt and Colman Ltd., Pharmaceutical Division, Dansom Lane, Kingston-upon-Hull HU8 7DS (Great Britain)

(First received October 3rd, 1979; revised manuscript received December 13th, 1979)

Of the two principal methods for achieving chromatographic resolution of amino acid enantiomers the conventional one involves reaction with a chiral compound to form diastereoisomers with subsequent separation by gas (GC)[1,2] or ion-exchange[3] chromatography. This method has the disadvantage in quantitative analysis in that derivatisation procedures can lead to the formation of interfering artefacts or result in racemisation of the enantiomers. The alternative method, involving on-column formation of diastereoisomers by interaction with optically active stationary phases is less likely to lead to racemisation and has been used extensively to resolve racemic acid esters by GC[4–9]. Some literature reports indicate that D- and L-amino acids can also be directly resolved by liquid chromatography using either a chiral eluent[10] or a ligand-exchange technique involving a copper(II)–proline complex bound to either a styrene–divinylstyrene copolymer[11] or an acrylamide porous gel[12]. This paper describes a rapid and efficient separation achieved by high-performance liquid chromatography using a copper(II)–proline complex bound to microparticulate silica gel.

EXPERIMENTAL

Preparation of the chiral stationary phase

LiChrosorb SI 60 (5 μm silica gel) (BDH, Poole, Great Britain) was refluxed with 2 *M* hydrochloric acid for 4 h, filtered, washed with water and acetone and dried in an oven at 110° for 16 h. The acid-washed material (10 g) was suspended in dry dioxane (200 ml) and 3-chloropropyltrichlorosilane (4 ml) was added. The mixture was refluxed for 4 h, filtered, washed with dioxane, water and acetone and dried on a water pump. The silanized silica gel was suspended in chloroform–methanol (85:15) (200 ml) containing L-proline (3 g), potassium iodide (1 g) and diisopropylethylamine (2.8 ml). The mixture was refluxed for 17 h, filtered, washed with methanol and acetone and dried on a water pump.

Column

The chiral phase was packed, as a methanol slurry, into a 25 × 0.46 cm I.D. stainless-steel tube using a Magnus P5000 Slurry Packing Unit (Magnus Scientific, Sandbach, Great Britain). The copper(II)–proline complex was formed *in situ* by eluting the column with a mobile phase of 1 m*M* copper(II) acetate.

Apparatus

A Waters Model 6000A constant flow pump (Waters Assoc., Northwich, Great Britain) was used to provide mobile phase flow and an ACS ultraviolet detector model 750/11 (Applied Chromatography System, Luton, Great Britain), fitted with a 240 nm filter, was employed to monitor column eluent.

RESULTS AND DISCUSSION

The surface of the silica gel was chemically modified and then activated by the elution of Cu^{2+} to give a structure of the type:

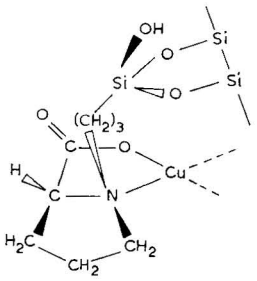

The amount of L-proline bound to the silica gel was determined by elemental analyses (Table I) which, from the percentage carbon figures, indicate a 67.5% conversion of the silanized intermediate. Atomic absorption analysis of the complexed phase indicate that it contained 0.17% (w/w) copper.

TABLE I

ELEMENTAL ANALYSIS OF THE CHEMICALLY MODIFIED SILICA GEL

Sample	*C (%, w/w)*	*H (%, w/w)*	*N (%, w/w)*
Silanized intermediate	2.10	0.75	−0.02
3-Prolylpropyl–silica gel	3.62	0.89	0.27

The chiral phase was initially evaluated in the absence of any bound Cu^{2+} using water only as the mobile phase and was found to give capacity factors, k' >15 with both L- and D-proline. On the introduction of 1 m*M* ammonium acetate into the mobile phase elution of the amino acid was rapid ($k' = 1.4$) but resolution of the two isomers was not observed. With 1 m*M* copper (II) acetate as the mobile phase, however, ligand exchange occurred and the L- and D- isomers were resolved

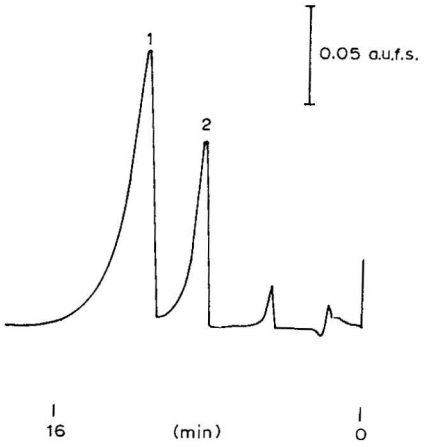

Fig. 1. Separation of D-proline (1) and L-proline (2). Column, copper (II)–proline complex bound to LiChrosorb 5 μm silica gel, 25 × 0.46 cm I.D. Mobile phase, 1 mM copper(II) acetate (pH 4.6) delivered at 3 ml min^{-1}. Detection, UV at 240 nm.

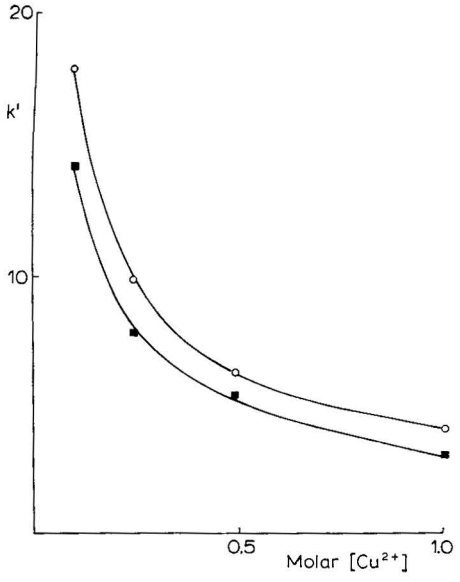

Fig. 2. Effect of Cu^{2+} ionic strength of the mobile phase on the k' values of D-(○) and L-proline (■).

(Fig. 1). Some peak tailing was observed and was thought to be due to the slow kinetics of ligand exchange in the bound metal coordination sphere.

The absolute retention of the proline isomers is inversely dependent upon the Cu^{2+} ionic strength of the mobile phase (Fig. 2) but, over the range studied, resolution is largely unaffected. The presence of Cu^{2+} in the mobile phase has the advantage that it allows the amino acids to be eluted as their copper(II) complexes, which exhibit a wavelength of maximum absorption of 240 nm, and thus avoids the need

to use end-absorption to achieve good sensitivity. The on-column limit of detection was found to be 400 ng L-proline at this wavelength.

The mobile phase pH range over which this chiral stationary phase can be successfully employed is narrow; at pH <3.9, the copper(II)–proline complex is unstable whereas at pH >5.6 column efficiency is observed to deteriorate.

Some work has been carried out using mobile phases containing other metal ions, such as Zn^{2+}, but complexation with the stationary phase has been found to be minimal with no observable resolution of the enantiomers.

L- and D-3,3-dimethylprolines have been completely resolved using the copper(II)-complexed stationary phase and partial resolution has been achieved with L- and D-phenylalanines. Attempts to resolve the isomers of histidine, alanine and glutamic acid have as yet proved unsuccessful but with further development the procedure may well prove to be useful as a method for the rapid evaluation of the stereochemical purity of α-amino acids.

ACKNOWLEDGEMENT

The authors would like to acknowledge the assistance provided by Dr. R. Henson during the course of this work.

REFERENCES

1 E. Gil-Av, R. Charles and G. Fischer, *J. Chromatogr.*, 17 (1965) 408.
2 B. Halpern and J. W. Westley, *Chem. Commun.*, (1965) 246.
3 J. M. Manning and S. Moore, *J. Biol. Chem.*, 243 (1968) 5591.
4 W. Parr, C. Yang, E. Bayer and E. Gil-Av., *J. Chromatogr. Sci.*, 8 (1970) 591.
5 S. Nakaparksin, P. Birrell, E. Gil-Av and J. Oró, *J. Chromatogr. Sci.*, 8 (1970) 177.
6 B. Feibush, *Chem. Commun.*, (1971) 544.
7 R. Brazell, W. Parr, F. Andrawes and A. Zlatkis, *Chromatographia*, 9 (1976) 57.
8 *Gas-Chrom® Newsletter*, Vol. 19, No. 5, Applied Science Lab., State College, Pa., 1978, p. 2.
9 R. Charles, U. Beitler, B. Feibush and E. Gil-Av., *J. Chromatogr.*, 112 (1975) 121.
10 P. E. Hare and E. Gil-Av., *Science*, 204 (1979) 1226.
11 V. A. Kavankov and Yu. A. Zolotarev, *J. Chromatogr.*, 155 (1978) 295.
12 B. Lefebvre, R. aUdebert and C. Quivoron, *J. Liq. Chromatogr.*, 1 (1978) 761.

Journal of Chromatography, 192 (1980) 232–235

CHROM. 12,594

Note

Purification of grape polyphenoloxidase with hydrophobic chromatography

KIMBERLY W. WISSEMANN* and C. Y. LEE

Department of Food Science and Technology, Cornell University, New York State Agricultural Experiment Station, Geneva, N.Y. 14456 (U.S.A.)

(Received December 4th, 1979)

The oxidation reaction associated with the darkening of damaged tissue in fresh fruits and vegetables is catalyzed by the enzyme polyphenoloxidase (PPO) (monophenol, dihydroxyphenylalanine: oxygen oxidoreductase; E.C. 1.14.18.1). To better control the action of PPO in different fruit and vegetable products, it is necessary to characterize the enzyme isolated from those different sources. However, the isolation of PPO is difficult[1,2], and several methods for the purification of PPO have been reported with varying degrees of success[3–10].

In this report, hydrophobic chromatography is used to isolate and purify grape PPO. The use of hydrophobic chromatography for the separation of proteins[11–15] is relatively new; Flurkey and Jen[16] appear to be the first to use such columns to purify PPO. The use of hydrophobic chromatography as a rapid, reproducible and successful purification technique for grape PPO is presented in this paper.

MATERIALS AND METHOD

Enzyme extraction

The two varieties of grapes, Ravat 51 and Niagara, used in this study were grown in the vineyards at the New York State Agricultural Experiment Station, Geneva, N.Y.

The PPO was initially extracted from the grapes with acetone[16,17]. Acetone powders were prepared by homogenizing 200 g of fresh grapes with 300 ml of cold (−20°) acetone and 1% of polyethylene glycol (average mol.wt. 3000–3700). The seeds were discarded, and the remainder of the homogenate was filtered under suction, and washed with 150 ml of cold acetone. The marc was further extracted with 300 ml of cold acetone three more times.

The dried acetone powders were suspended in 100 volumes (w/v) of 0.05 *M* K_2HPO_4–1.0 *M* KCl buffer (pH 6.5) and stirred for 30 min at ambient temperature. The suspensions were then centrifuged in a Sorvall RC-5 refrigerated centrifuge at 12,000 *g* at 0° for 15 min and then filtered through glass wool. The filtrate was made

* Present address: Department of Food Science and Technology, Oregon Sate University, Corvallis, Ore. 97331, U.S.A.

1 *M* with respect to ammonium sulfate by adding solid crystals of the salt, adjusted to pH 6.5 and filtered through Whatman No. 4 filter paper (labeled "before-column extract").

Chromatography on phenyl Sepharose CL-4B

PPO was isolated and purified on a hydrophobic column in a manner similar to that of Flurkey and Jen[16] and Flurkey *et al.*[18]. Pre-swollen phenyl Sepharose CL-4B (Pharmacia, Uppsala, Sweden), a hydrophobic resin, was de-gassed and equilibrated in four volumes of de-aerated buffer, consisting of 1 *M* ammonium sulfate, 1 *M* KCl and 0.05 *M* K_2HPO_4 (pH 6.5). A 20-ml bed-volume column (20 × 1 cm I.D.) was packed, rinsed with buffer, and then 300 ml of the "before-column extract" were applied on to the column. The proteins bound to the hydrophobic resin were eluted by using eluents decreasing in buffer concentration in a batchwise manner: (A) 60 ml of buffer; (B) 32 ml of buffer + 8 ml of distilled and deionized water; (C) 24 ml of buffer + 16 ml of water; (D) 16 ml of buffer + 24 ml of water; (E) 8 ml of buffer + 32 ml of water; (F) 40 ml of a 50% solution of ethylene glycol; and (G) 40 ml of water. Each fraction (160 drops) collected was assayed for PPO activity, and its protein content was estimated by measuring the absorbance at 280 nm in a Varian Cary UV/visible spectrophotometer (Model 219) against a reference of the buffer solution. The most active fractions were combined, dialyzed against three changes of 0.01 *M* Na_2HPO_4 buffer of pH 6.5, freeze-dried, and then suspended in 10 ml of Na_2HPO_4 buffer (labeled "purified PPO extract").

Specific activity

The PPO activity was determined on 0.2 ml of the enzyme extract in 2.4 ml of 0.01 *M* Na_2HPO_4 buffer of pH 6.5 and 0.4 ml of 0.5 *M* catechol also prepared in the buffer. The increase in absorbance at 420 nm, at 25°, was measured against a reference of the same solution without the enzyme[19]. One unit of PPO activity is defined as the amount of enzyme that caused a 0.001 unit change in absorbance per min at 420 nm. The protein content (mg/ml) of the extract was determined by the method of Sutherland *et al.*[20] using bovine serum albumin as standard. The specific activity was expressed as Units of activity per mg of protein.

RESULTS AND DISCUSSION

The elution profile from the hydrophobic column is shown in Fig. 1 for Ravat PPO. The largest portion of PPO activity contained in one peak (fractions 68–75) was clearly separated from the bulk of the other material. The reproducibility of this purification step was excellent for both the Ravat and Niagara enzymes.

The purification procedure for Ravat PPO is summarized in Table I. Although the crude extract was not the primary step in the isolation process, it is included in Table I to emphasize the merits of the procedure. The preparation of the acetone powder achieved a 23-fold purification, and after the entire isolation an increase in the PPO specific activity of over 250-fold was obtained. The recovery (better than 100%) of PPO indicates the removal of an inhibitory substance or an activation of the enzyme during the isolation procedure. If the "before-column extract" is set at 100%, a 53% yield of PPO activity for Ravat was recovered in the most active

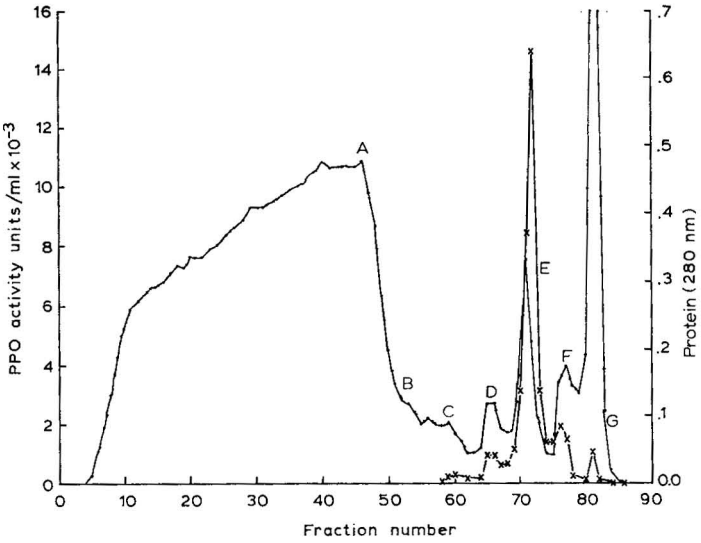

Fig. 1. Elution profile from a phenyl Sepharose CL-4B hydrophobic column for Ravat PPO activity (×—×, Units per ml); ●—●, protein content. The letters A–G indicate addition of a different eluent (see text).

TABLE I

PURIFICATION TABLE OF RAVAT 51 POLYPHENOLOXIDASE

Sample	*Volume (ml)*	*PPO activity (Units/ml)*	*Total Units*	*Protein (mg/ml)*	*Specific activity (Units/mg)*	*Yield (%)*	*Purification (α-fold)*
Crude extract*	200	908	181,600	6.50	140	—	1.0
Acetone powder buffer extract	350	1083	379,050	0.34	3185	—	23
"Before-column extract"	337	3250	1,096,875**	0.31	10,484	100**	75
After-column fractions 68–75	56	9267	583,821	0.28	33,096	53	236
"Purified PPO extract"	10	46,900	570,956	1.33	35,263	52	252

* The crude extract was prepared by homogenizing 100 g of grapes with 100 ml of Na_2HPO_4 buffer.

** There was an increase in the total Units, therefore the percentage yield was based on the "Before-column extract".

fractions. Further studies on the biochemical properties of the Ravat and Niagara PPO enzymes, using disc gel electrophoresis revealed that the purified PPO extract was almost nearly homogeneous.

REFERENCES

1 D. S. Bendall and R. P. F. Gregory, in J. B. Pridham (Editor), *Enzyme Chemistry of Phenolic Compounds*, Pergamon Press, New York, 1963, p. 7.

2 A. G. Mathew and H. A. Parpia, *Advan. Food Res.*, 19 (1971) 75.
3 M. Kidron, E. Harel and A. M. Mayer, *Phytochemistry*, 16 (1977) 1050.
4 E. Harel, A. M. Mayer and Y. Shain, *Phytochemistry*, 4 (1965) 783.
5 E. Harel, A. M. Mayer and E. Lehman, *Phytochemistry*, 12 (1973) 2649.
6 D. Kertesz and R. Zito, *Biochim. Biophys. Acta*, 96 (1965) 447.
7 D. Racusen, *Can. J. Bot.*, 48 (1970) 1029.
8 N. D. Benjamin and M. W. Montgomery, *J. Food Sci.*, 38 (1973) 799.
9 V. Kahn, *Phytochemistry*, 15 (1976) 267.
10 N. Rivas and J. R. Whitaker, *Plant Physiol.*, 52 (1973) 501.
11 B. H. Hofstee, *Anal. Biochem.*, 52 (1973) 430.
12 S. Hjertén, *J. Chromatogr.*, 87 (1973) 325.
13 S. Hjertén, J. Rosengren and S. Pählman, *J. Chromatogr.*, 101 (1974) 281.
14 J. Rosengren, S. Pählman, M. Glad and S. Hjertén, *Biochim. Biophys. Acta*, 412 (1975) 51.
15 S. Shaltiel, *Methods Enzymol.*, 34 (1974) 126.
16 W. H. Flurkey and J. J. Jen, *J. Food Sci.*, 43 (1978) 1826.
17 N. S. Dizik and F. W. Knapp, *J. Food Sci.*, 35 (1970) 282.
18 W. H. Flurkey, L. W. Young and J. J. Jen, *J. Agr. Food Chem.*, 26 (1978) 1474.
19 J. D. Ponting and M. A. Joslyn, *Arch. Biochem.*, 19 (1948) 47.
20 E. W. Sutherland, C. F. Cori, R. Haynes and N. E. Olsen, *J. Biol. Chem.*, 180 (1949) 825.

Journal of Chromatography, 192 (1980) 236–239

CHROM. 12,586

Note

One-step purification of human leukocyte elastase by biospecific affinity chromatography at subzero temperatures

KRISTOFFER K. ANDERSSON, CLAUDE BALNY* and PIERRE DOUZOU

INSERM U-128, BP 5051, 34033 Montpellier Cedex (France)

and

JOSEPH G. BIETH

Laboratoire d'Enzymologie, Faculté de Pharmacie, 74 Route du Rhin, 64700 Illkirch-Graffenstaden (France)

(First received September 24th, 1979; revised manuscript received December 5th, 1979)

We have previously shown[1] that it is possible to perform biospecific affinity chromatography with a "true" substrate under non-turnover conditions, by using subzero temperatures in fluid media. The enzyme system used was porcine pancreatic elastase, which can be selectively absorbed on and desorbed from an affinity column supporting the artificial specific substrate, L-trialanine-*p*-nitroanilide.

In the present paper we show that this affinity column may be used for the one-step purification of elastase from a crude extract of granules from human leukocytes.

EXPERIMENTAL

Reagents

Porcine pancreatic elastase, succinyl-L-trialanine-*p*-nitroanilide, L-trialanine-*p*-nitroanilide, *N*-acetyl-L-tryptophan ethyl ester, Sepharose 6B CL, 1,4-butanediol-diglycidyl ether (Bioxirane), and ethylene glycol were prepared or purchased as previously described[1]. Bovine α-chymotrypsin was obtained from Worthington (Freehold, N.J., U.S.A.).

The granule extract of human leukocytes was obtained by the procedure of Baugh and Travis[2] and was stored at −20° in 0.2 *M* sodium acetate buffer, pH 4, until used. The procedure of Baugh and Travis was also used to obtain the mixture of human leukocyte elastase iso-enzymes using affinity chromatography on Trasylol–Sepharose**.

When buffers (Tris–hydrochloric acid or sodium acetate) were used in mixed hydro-organic solvents at various temperatures, the pa_H was calculated as described previously[3,4] (a_H being the protonic activity in mixed solvents).

---

* To whom correspondence should be addressed.

** Trasylol is the trade name for basic pancreatic trypsin inhibitor.

Chromatography

The Sepharose 6B CL was activated with diglycidyl ether and L-trialanine-*p*-nitroanilide was coupled as described before[1]. The chromatographic column[1] had an inner diameter of 6 mm, and the temperature was regulated with a Colora bath (from $+20$ to $-30 \pm 0.2°$). Usually 1 ml of affinity adsorbent was used for each experiment. During the elution, the flow-rate through the column was 5 ml/h. The eluted fractions (1 ml) were collected at 4°.

Assay procedure

Enzyme activities were measured spectrophotometrically at 25° with a Beckman Acta III spectrophotometer equipped with a thermostated cell compartment[5]. Elastase activity was determined at 410 nm with succinyl-L-trialanine-*p*-nitroanilide[6]. Chymotrypsin activity was measured with N-acetyl-L-tryptophan ethyl ester (2 m*M*) at 300 nm and pH 8.5, in 0.1 *M* Tris–HCl containing 5% (v/v) of ethylene glycol. This method can detect α-chymotrypsin at concentrations as low as 1 n*M* (ΔOD/min = $6 \cdot 10^{-4}$). Protein concentration was measured by the micromethod of Bradford[7] using porcine pancreatic elastase as a standard.

RESULTS AND DISCUSSION

The conditions used to adsorb pancreatic elastase on the column (*i.e.* Tris–HCl pH 9.2, 4 *M* NaCl, $-14°$) could not be used for the binding of human leukocyte elastase, because 5–10% of the substrate bound on the column was hydrolysed during the adsorption of the latter enzyme. This result is rather surprising for the leukocyte enzyme, which is usually considered a poorer catalyst than pancreatic elastase. Indeed, Twumasi and Liener[8] have shown that the former hydrolyses succinyl-L-trialanine-*p*-nitroanilide 40 times slower than does the latter. We therefore determined the kinetic parameters of the Michaelis-Menten equation (k_{cat} and K_m)[1] for the hydrolysis of L-trialanine-*p*-nitroanilide by leukocyte elastase. At pH 8 and 25° we found k_{cat} and K_m values of 0.045 sec^{-1} and 1.4 m*M*, respectively. The substrate bound on the affinity columns has thus a k_{cat} value with leukocyte elastase which is five times greater than that observed with pancreatic elastase[9]. This higher turnover number does not solely account for the very rapid hydrolysis of the substrate during the chromatographic adsorption. For this reason, we considered the possibility that the NaCl present in our adsorption buffer enhances the enzyme activity. We discovered that ionic strength indeed stimulates markedly the elastase-catalysed hydrolysis of L-trialanine-*p*-nitroanilide: at pH 8, 25°, the rate is increased by a factor of *ca.* 12 in the presence of 4 *M* NaCl. These effects are now under investigation[11].

In order to slow down this high turnover, we decided to adsorb the enzyme at pH 5. Under these conditions (0.1 *M* sodium acetate buffer, 4 *M* NaCl) only 0.5% and 0.05% of substrate is hydrolysed at $+4°$ and at $-14°$, respectively. When elution was started immediately after the sample was poured on to the column, only 80% of the total elastase activity was bound to the adsorbent. Column flow was therefore stopped for 1 h before elution was initiated, in order to achieve complete adsorption of the enzyme.

The experiments described lead to the following technique for the one-step purification of human leukocyte elastase. 100 μl of crude granular extract (1 mg of

protein) are mixed with 500 μl of 0.1 *M* sodium acetate buffer, pH 5, containing 4 *M* NaCl. This mixture is cooled to $-14°$ and applied to the chromatographic column previously equilibrated with the same buffer at the same temperature. This sample is applied to the column at a flow-rate of 1 ml/h. After 1 h, impurities are eluted with 20 ml of the same buffer. Elastase is then desorbed from the column with a mixture of equal volumes of ethylene glycol and 0.2 *M* sodium acetate buffer, pa_H 5.0, without NaCl, at the same temperature. The pa_H is adjusted after mixing[4].

The elution profile contained a single peak with good coincidence of protein and activity (Fig. 1). The elastase activity is recovered with a yield of *ca.* 85%. Activity measurements of the combined fractions showed that this preparation had the same specific activity at $\pm 5\%$ (measured with succinyl-L-trialanine-*p*-nitroanilide) as the enzyme prepared following the procedure of Baugh and Travis[2]. In addition, no cathepsin G activity (*i.e.* chymotrypsin-like activity) could be detected. The isolation procedure of Baugh and Travis uses Trasylol–Sepharose and yields elastase contaminated by the chymotrypsin-like enzyme cathepsin G; this may be subsequently removed by CM cellulose chromatography[2]. In order to achieve a one-step purification with Trasylol–Sepharose, cathepsin G must first be removed by precipitation at low

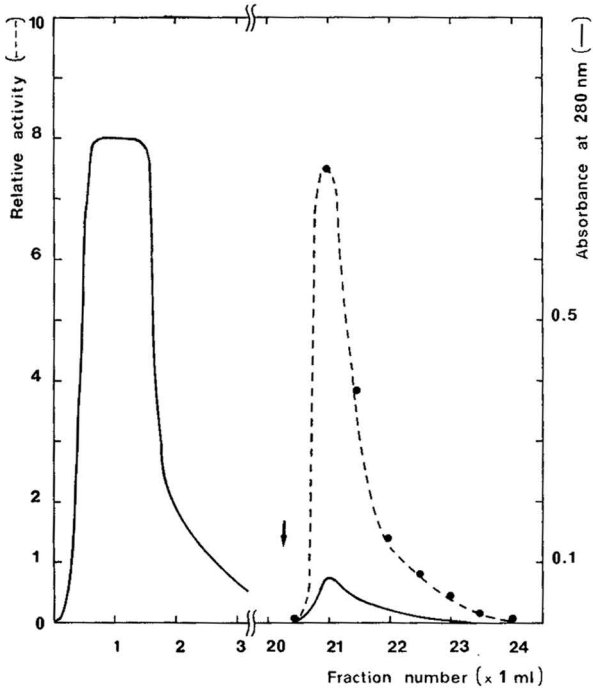

Fig. 1. Elution pattern of human leukocyte elastase from the affinity column (1 × 0.6 cm I.D.). Elastase was fixed with 0.1 *M* sodium acetate (pH 5.0) and 4 *M* NaCl, and eluted with 50% (v/v) ethylene glycol, 0.1 *M* sodium acetate (pa_H 5.0). During the chromatography the temperature was maintained at $-14°$. The arrow indicates the introduction of the elution buffer. The eluted activity was measured at 25° in 0.2 *M* Tris–HCl (pH 8.0) and 5 *M* NaCl in presence of 2% (v/v) ethylene glycol. At the eluted peak tube, the corresponding activity in 0.2 *M* Tris buffer (pH 8.0) at 25° is 20 mU. 1 U of elastase activity corresponds to the hydrolysis of 1 μmole of substrate per minute under the above conditions.

ionic strength[2]. This additional step is not necessary with the affinity chromatography system described here. However, we do not wish to stress the relative merits of the two procedures. We wish to emphasize that we have been able to demonstrate that affinity chromatography at subzero temperatures using a true substrate[1] is a feasible procedure for a real purification problem.

Our technique may be particularly suited for purifying trace amounts of elastases from other sources. In this connection, it is worthwhile noticing that macrophage elastase, which has never been purified, reacts with succinyl-L-trialanine-*p*-nitroanilide[10].

ACKNOWLEDGEMENTS

We thank Dr. P. Lestienne for the preparation of the leukocyte granule extract. This work was supported by grants from INSERM (C.R.L. 78.1.038.3), CNRS and the Fondation pour la Recherche Médicale Française.

REFERENCES

1 C. Balny, C. Le Doucen, P. Douzou and J. G. Bieth, *J. Chromatogr.*, 168 (1979) 133.
2 R. J. Baugh and J. Travis, *Biochemistry*, 15 (1976) 836.
3 P. Douzou, *Cryobiochemistry, an Introduction*, Academic Press, New York, 1977.
4 C. Larroque, P. Maurel, C. Balny and P. Douzou, *Anal. Biochem.*, 73 (1976) 9.
5 P. Maurel, F. Travers and P. Douzou, *Anal. Biochem.*, 57 (1974) 555.
6 J. G. Bieth, B. Spiess and C. G. Wermuth, *Biochem. Med.*, 11 (1974) 350.
7 M. M. Bradford, *Anal. Biochem.*, 72 (1976) 248.
8 D. Y. Twumasi and I. E. Liener, *J. Biol. Chem.*, 252 (1977) 1917.
9 J. G. Bieth and C. G. Wermuth, *Biochem. Biophys. Res. Commun.*, 53 (1973) 383.
10 H. de Crémoux, W. Hornebeck, M. C. Jaurand, J. Bignon and L. Robert, *J. Pathol.*, 125 (1978) 171.
11 C. Boudier, K. K. Andersson, C. Balny and J. G. Bieth, *Biochem. Med.*, (1980) in press.

Journal of Chromatography, 192 (1980) 240–246

CHROM. 12,627

Note

Modifizierte Darstellung von Fettsäure-2-naphtacylestern und ihre Fluoreszenz-Detektion in der Hochleistungs-Flüssigkeits-Chromatographie

W. DISTLER

Poliklinik für Zahnerhaltung und Parodontologie, Biochemisches Labor, Friedrich-Alexander-Universität Erlangen, Glückstrasse 11, D-8520 Erlangen (B.R.D.)

(Eingegangen am 14. Dezember 1979)

In den letzten Jahren sind zahlreiche Methoden zur Bestimmung und Trennung von Carbonsäuren mit Hilfe der Hochleistungs-Flüssigkeits-Chromatographie (HPLC) ausgearbeitet worden. Wegen der geringen UV-Absorption der Carbonsäuren ist bei geringen Mengen eine Derivatisierung unerlässlich. In Standardwerken wie Lawrence und Frei[1] und Blau und King[2] wird eine Übersicht über geeignete Derivate zur UV-Detektion bzw. Fluoreszenzdetektion gegeben. Diese Entwicklung wird weitergeführt durch Synthese neuer UV-absorbierender Derivate wie z.B. N-Chlormethylphtalimide[3] und fluoreszierender Derivate wie Ester des 4-Bromomethyl-7-Methoxycumarin[4–6].

Die chromatographische Trennung derartiger Derivate lässt sich am einfachsten mit Hilfe der Gradienten-Elution an nicht polaren stationären Phasen vom reversed-phase Typ durchführen.

In der vorliegenden Arbeit wird die Eignung der schon länger bekannten 2-Naphtacylester[8] für die Fluoreszenzdetektion und ein modifiziertes Verfahren für die Veresterung von Natrium-Salzen kurzkettiger Carbonsäuren aus biologischem Material beschrieben.

EXPERIMENTELLES

Reagenzien und Chemikalien

Alle organischen Lösungsmittel waren handelsüblich (Merck, Darmstadt, B.R.D.) p.a. Qualität, Acetonitril für die HPLC war frisch destilliert, trockenes Acetonitril wurde unter Rückfluss über Calciumhydrid gekocht und unter Wasserausschluss destilliert, trockenes Dimethylformamid wurde im Vakuum destilliert. 2-Bromacetonaphton (Aldrich, Milwaukee, Wisc., U.S.A.) wurde ohne weitere Reinigung verwendet. Kryptofix 221 (4,7,13,16,21-penta-oxa-1,10-diazabicyclo(8,8,5)-tricosan) (Merck) war unter Stickstoff in wasserfreien Acetonitril gelöst. Alle verwendeten Säuren bzw. Natrium-Salze waren handelsüblich p.a. (Merck).

Apparatur

Benutzt wurde ein Hochleistungs-Flüssigkeits-Chromatograph HP 1080 A (Hewlett-Packard). Als Detektoren wurden verwendet ein Zweistrahlspektrometer

HP 1030 B (baugleich mit Schöffel SF 770) der gleichen Firma und ein Spektralfluorometer SFM23LC (Kontron) mit getrennt abstimmbarem Exitations- und Emissionsmonochromatoren. Als Trennsäule diente eine 250 × 3 mm I.D., 10 μm C_{18} LiChrosorb Fertigsäule (Merck).

Derivatisierung

Das aus Stoffwechseluntersuchungen mit Hilfe der Warburg-Methode erhaltene Säuregemisch (20 nMol–80 μMol) wurde mit 0.01 *M* Natriumhydroxyd gegen Phenolphtalein neutralisiert und nach Abtrennung der Bakterien gefriergetrocknet. Die gefriergetrockneten Rückstände, die neben Natriumchlorid, Natriumhydrogen carbonat und verschiedenen Mono- und Polysacchariden die Natriumsalze der Carbonsäuren enthielten, wurden unter striktem Wasserausschluss mit 8 ml einer 0.01 *M* Lösung von 2-Bromacetonaphton (80 μMol) in trockenem Acetonitril 60 min im Ultraschallbad sehr fein suspendiert. Nach der Ultraschallbehandlung wurden 20 μl einer 0.2 *M* Lösung von Kryptofix 221 in trockenem Acetonitril und 2 ml trockenes Dimethylformamid zugegeben. Die Veresterungsansätze wurden unter Wasserausschluss 60 min unter Rückfluss gekocht, abfiltriert und unter Auswaschen des Filters mit Acetonitril auf 20 ml aufgefüllt. Eine Verdünnung 1:2 dieser Proben kann direkt am Chromatographen injiziert werden. Sind in der Probe Naphtacylester von Dicarbonsäuren wie z.B. Bernsteinsäure vorhanden, empfiehlt es sich wegen der Schwerlöslichkeit dieser Ester die Proben auf 60 ml aufzufüllen und den Rückstand (Natriumchlorid, Natriumbromid) auszukochen.

Im Spurenbereich (<50 nMol) ist es empfehlenswert, die Gesamtlösungsmittelmenge des Veresterungsansatzes auf 4 ml zu beschränken und entsprechend konzentrierte Reagenzienlösungen einzusetzen. Der Überschuss an Derivatisationsreagenz sollte nicht mehr als 10% betragen.

Präparative Darstellung von Standardsubstanzen

Um geeignete Standardsubstanzen zu gewinnen, wurden die Naphtacylester von Milchsäure, Ameisensäure, Essigsäure, Buttersäure und Valeriansäure analog zu üblichen Verfahren der Darstellung von Phenacylestern[9] im 20 mMol Masstab synthetisiert. Nach Umkristallisieren und chromatographischer Prüfung auf Reinheit wurden sie massenspektrometrisch charakterisiert.

Bernsteinsäure-bis-naphtacylester lässt sich nur in Anlehnung an die analytische Derivatisierung im wasserfreiem Medium mit Kryptofix als Katalysator in guten Ausbeuten herstellen, wie auch schon Durst *et al.*[10] mit Kronenverbindungen als Katalysatoren zeigen konnten.

ERGEBNISSE UND DISKUSSION

Derivatisierung

Die Ausbeuten der Derivatisierungsreaktion wurden chromatographisch mit Hilfe externer Standardisierung bestimmt. Beim Einsatz reiner Natriumsalze von Carbonsäuren werden im Bereich zwischen 10 μMol und 100 μMol Ausbeuten über 98% erhalten. Die Reaktionsdauer bis zur vollständigen Veresterung betrug *ca.* 45 min, sie wurde chromatographisch verfolgt. Bei Proben biologischer Herkunft wurde die Wiederfindungsrate durch Zugabe von Buttersäure als interner Standard

bestimmt. Die Wiederfindungsraten schwankten zwischen 65% und 94%. Ein möglicher Grund für diese deutlich verschlechterten Wiederfindungsraten dürfte der hohe Anteil von Fremdsubstanzen wie Monosaccharide, Polysaccharide und anorganischen Salzen in den Proben biologischer Herkunft sein, die den Ablauf der heterogenen Reaktion stören.

Die Katalyse der Veresterungsreaktion durch Poly-oxa-diaza-makro bicyclen (Warenzeichen Kryptofix) erfolgt nach dem gleichen Prinzip wie bei den von Durst *et al.*[11] eingeführten Kronenäthern. Die gebildeten Kryptatverbindungen werden im Vergleich zu monocyclischen Polyäthern wie z.B. 18-Krone-6 als stabiler und selektiver[12] in der Bildung beschrieben. Durch die Komplexbindung des Na^+ im Hohlraum des bicyclischen Diamins kommt es zur Ausbildung eines getrennten Ionenpaares, wobei das Anion, also der Säurerest, eine gesteigerte Nucleophilie erlangt. Dadurch wird die nucleophile Substitution des Bromatoms im Bromacetonaphton durch einen Säurerest wesentlich erleichtert. Bei Versuchen, die Derivatisierung analog zu Durst *et al.*[10,11] zu katalysieren, wurden bei Proben biologischer Herkunft etwas schlechtere Wiederfindungsraten gefunden.

Störend macht sich bemerkbar, dass durch die Ausbildung eines Natrium-Kryptats alle vorliegenden Anionen der im Derivatisierungsansatz befindlichen Natriumsalze grössere nucleophile Kraft gewinnen. Dies gilt vor allem für Natriumchlorid, das aus biochemischen Untersuchungen in die Proben gelangt.
Gemäss Gleichung 1

$$\text{Ar–CO–CH}_2\text{Br} + \text{NaCl} \xrightarrow{\text{Kryptofix}} \text{Ar–CO–CH}_2\text{Cl} + \text{NaBr} \qquad (1)$$

tritt eine Umhalogenisierung des Derivatisierungsreagenze in starkem Masse auf. In gleicher Weise bewirken Spuren von Wasser, vor allem wässrige Alkalien, den Austausch des Bromatoms gegen eine Hydroxyl-Gruppe. Im Falle des α-Brom-2-acetonaphtons konnten sowohl das entsprechende α-Chlor-2-acetonaphton als auch das α-Hydroxy-2-acetonaphton isoliert und massenspektrometrisch charakterisiert werden. Daneben entstehen, allerdings in weit geringerer Menge, weitere Nebenprodukte deren Struktur nicht aufgeklärt wurde. Die Neigung zu derartigen Nebenprodukten nimmt mit gesteigerter Labilität des Bromatoms von 2-Naphtacylbromid über Phenacylbromid, *p*-Bromphenacylbromid bis *p*-Nitrophenacylbromid zu.

Spektroskopische Eigenschaften

Das UV-Spektrum von Milchsäurenaphtacylester zeigt das Hauptmaximum bei 246 nm mit Nebenmaxima bei 280.5 nm mit einer Schulter bei 290 nm und einem weiteren flachen Maximum bei 335 nm. Sowohl bei 246 nm als auch bei 280.5 nm lässt sich Fluoreszenz anregen mit einem Emissionsmaximum bei 450 nm. Das Anregungsmaximum liegt bei 290 nm, der Wellenlänge der ausgeprägten Schulter der ersten Nebenmaximums des UV-Spektrums. UV- und Fluoreszenzspektrum von Milchsäurenaphtacylester sind in Fig. 1 dargestellt. Bromacetonaphton, Chloracetonaphton und Hydroxyacetonaphton zeigen keine Fluoreszenz. Die Fluoreszenzintensität der homologen Carbonsäurenaphtacylester nimmt mit steigender C-Zahl ab. Durch diese Ergebnisse ist eine Fluoreszenzdetektion von 2-Naphtacylestern möglich und gleichzeitig die Störung durch Nebenprodukte beseitigt. Die Fluoreszenzintensität der Naphtacylester ist um etwa den Faktor $5 \cdot 10^{-2}$ geringer als die der von

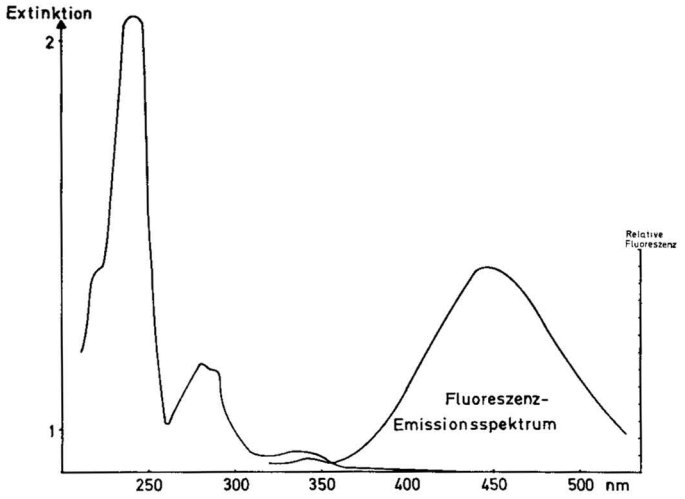

Fig. 1. UV- und Fluoreszenzemissionsspektrum von Milchsäurenaphtacylester. Lösungsmittel 40% Acetonitril in Wasser.

Dünges beschriebenen 4-Methylen-7-methoxycumarinester[4] (BMC-Ester). Die Nachweisempfindlichkeit für Milchsäurenaphtacylester beträgt 1 ng/10 μl Injektionsvolumen, für Valeriansäurenaphtacylester liegt sie bei 20 ng/10 μl.

Chromatographische Trennung

Trennungen von Phenacyl- und Naphtacylestern sind in der Literatur beschrieben. Die meisten Trennungen erfolgten auf reversed-phase Material[7,8,10,13], eine neuere Arbeit[14] beschreibt die Trennung auf Kieselgel. Die wohl am besten geeignete Trenntechnik ist das Arbeiten auf reversed-phase Säulen unter Einsatz eines Wasser–Acetonitrilgradienten. Fig. 2 zeigt das Chromatogramm einer Eichmischung, wie sie zur externen Standardisierung benutzt wurde.

Fig. 3 zeigt das Chromatogramm der gleichen Eichmischung, aber über den hinter den UV-Detektor angeschlossenen Fluoreszenzdetektor detektiert. Die geringe Zeitverschiebung der Peaks ergibt sich aus der Länge der Verbindungskapillare. Im Fluoreszenzchromatogramm fehlt der Peak des Bromacetonaphtons. Die Chromatogramme eines Blindwertes, der unter peinlichem Ausschluss von Wasser und Natriumchlorid hergestellt wurde und des Parallelansatzes, der mit 20 μl Wasser versetzt wurde und Natriumchlorid aus isotonischer Natriumchlorid-Lösung enthielt, sind in Fig. 4 übereinander gezeichnet. Man erkennt deutlich das Auftreten der Nebenprodukte. α-Hydroxy-2-acetonaphton erscheint bei einer Retentionszeit (RT) von 2.14 min, α-Chlor-2-acetonaphton bei RT = 7.12 min, ein Wert, der mit dem Retentionswert für Propionsäurenaphtacylester interferiert. Eine Trennung ist bei isokratischer Arbeitsweise und Zusatz von 10% Dimethylformamid, allerdings auf Kosten der Trennzeit zu erreichen, wie in Fig. 5 dargestellt ist. Die Chromatogramme einer typischen Probe aus biologischen Material, nämlich aus 8 mg (Nassgewicht) Zahnplaque, sind in Fig. 6 wiedergegeben. Milchsäure ist dominierend, daneben werden Ameisen, Essig- und Propionsäure gefunden. Bei UV-Detektion wird das im Peak mit RT = 6.93 min mit enthaltene α-Chloracetonaphton mit erfasst und täuscht zu

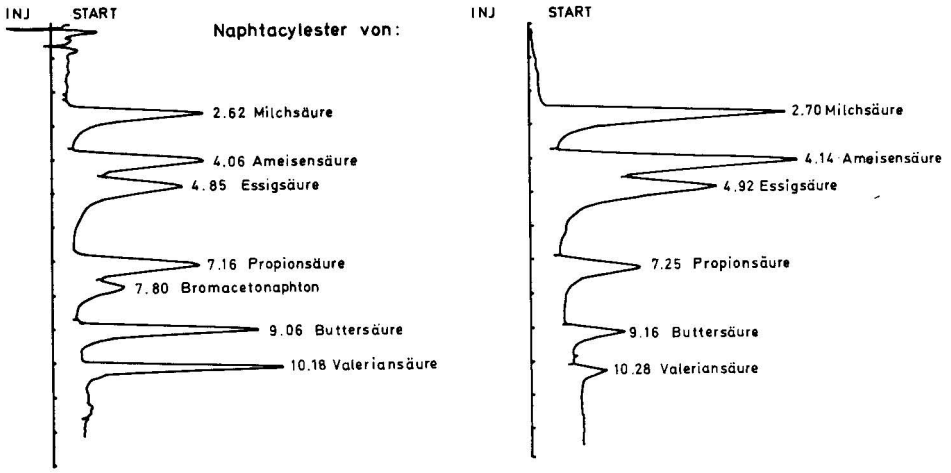

Fig. 2. Trennung von Fettsäurenaphtacylestern. Säule, 250 × 3 mm I.D., C_{18} LiChrosorb 10 μm; Temperatur, 35°; mobile Phase: Wasser–Acetonitril; konvexer Gradient von 38% Acetonitril auf 75% Acetonitril; Flussrate, 2 ml/min; Injektionsvolumen 20 μl ≈ je 200 ng Fettsäurenaphtacylester; UV-Detektor 245 nm.

Fig. 3. Trennung von Fettsäurenaphtacylestern. Bedingungen wie in Fig. 2. Fluoreszenzdetektor, λ_{ex} = 290 nm und λ_{em} = 450 nm.

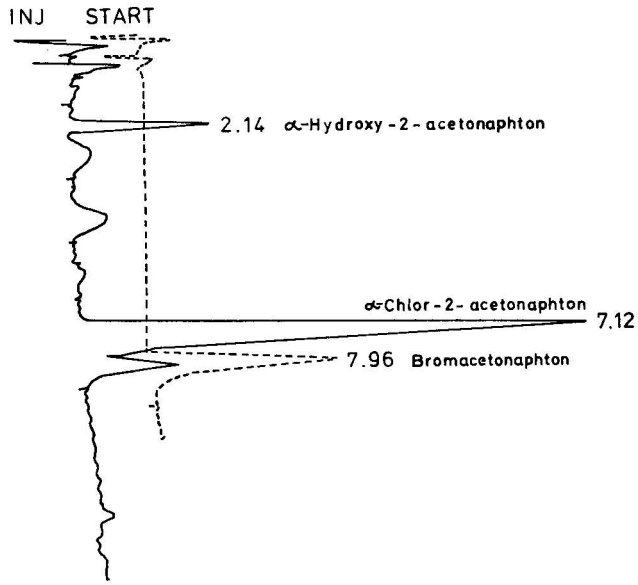

Fig. 4. Chromatogramme von Veresterungsblindwerten. – – –, unter Ausschluss von Wasser und Natriumchlorid; ———, Veresterungsansatz enthielt 20 μl Wasser und Natriumchlorid, aus physiologischer Kochsalzlösung. Sonstige Bedingungen wie in Fig. 2.

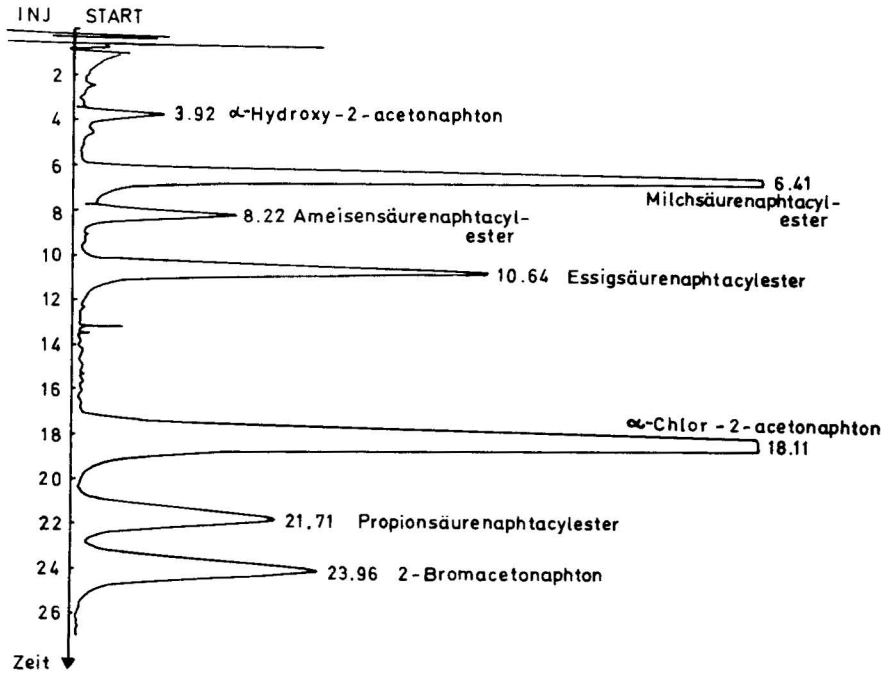

Fig. 5. Isokratische Trennung von Naphtacylestern, α-Hydroxyacetonaphton und α-Chloracetonaphton. Mobile Phase, 25% Acetonitril und 10% Dimethylformamid in Wasser. Sonstige Bedingungen wie in Fig. 2.

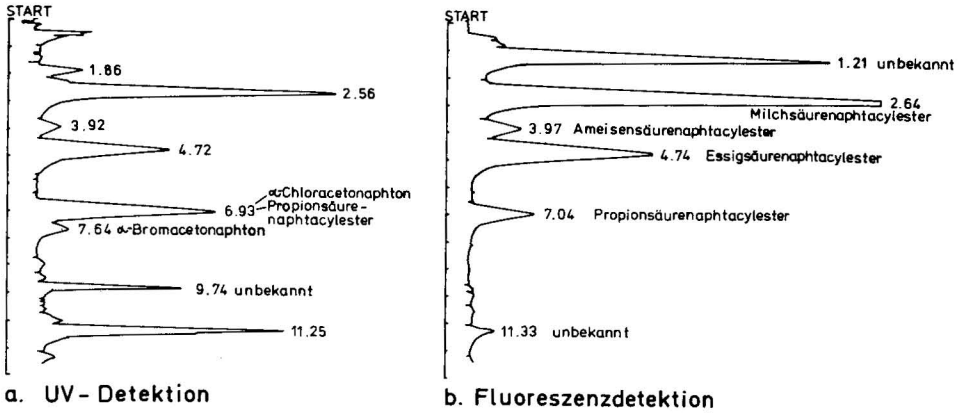

Fig. 6. Naptacylester aus *in vivo* gebildeten Säuren aus 8 mg (Nassgewicht) Plaque nach Zuckerspülung. Injektionsvolumen 10 µl. Sonstige Bedingungen wie in Fig. 2.

hohe Werte für Propionsäurenaphtacylester vor. Bei Fluoreszenzdetektion entfällt diese Störung, ebenso die Peaks bei RT = 9.74 min und RT = 1.86 min, dagegen tritt ein neuer Peak einer unbekannten fluoreszierenden Substanz bei RT = 1.21 min auf. Die Substanz bei RT = 11.25 min bzw. 11.33 min ist noch nicht identifiziert, es dürfte sich um eine weitere Säure handeln.

DANK

Ich danke der Deutschen Forschungsgemeinschaft für eine Sachbeihilfe. Frau A. Flach, Frau U. Degiorgio und Frau E. Zitterbart bin ich für ihre zuverlässige experimentelle Mithilfe zu Dank verpflichtet. Besonders danken möchte ich Prof. Dr. A. Kröncke, Poliklinik für Zahnerhaltung und Parodontologie, Erlangen, der durch sein Interesse und seine wohlwollende Hilfsbereitschaft diese Arbeit ermöglicht hat.

LITERATUR

1 J. F. Lawrence und R. W. Frei, *Chemical Derivatization in Liquid Chromatography*, Elsevier, Amsterdam, Oxford, New York, 1976.
2 K. Blau und G. S. King, *Handbook of Derivatives for Chromatography*, Heyden & Son, London, 1977.
3 W. Lindner und W. Santi, *J. Chromatogr.*, 176 (1979) 55.
4 W. Dünges, *Anal. Chem.*, 49 (1977) 442.
5 W. Dünges und N. Seiler, *J. Chromatogr.*, 145 (1978) 483.
6 S. Lam und E. Grushka, *J. Chromatogr.*, 158 (1978) 207.
7 H. Engelhard und H. Elgass, *J. Chromatogr.*, 158 (1978) 249.
8 M. J. Cooper und M. W. Anders, *Anal. Chem.*, 46 (1974) 1849.
9 *Organikum*, VEB Deutscher Verlag der Wissenschaften, Berlin, 6. Aufl., 1967, S. 190.
10 E. Grushka, H. D. Durst und E. J. Kikta, jr., *J. Chromatogr.*, 112 (1975) 673.
11 H. D. Durst, M. Milano, E. J. Kikta, S. A. Counelly und E. Grushka, *Anal. Chem.*, 47 (1975) 1797.
12 J. M. Lehn und J. P. Sauvage, *Chem. Commun.*, (1971) 440.
13 H. C. Jordi, *J. Liquid Chromatogr.*, 1 (1978) 215.
14 J. Weatherston, L. M. MacDonald, T. Blake, M. H. Benn und Y. Y. Huang, *J. Chromatogr.*, 161 (1978) 347.

Journal of Chromatography, 192 (1980) 247–249

CHROM. 12,600

Note

Measurement of the formation of paracetamol and *p*-nitrophenol glucuronides *in vitro*, by ion-pair high-performance liquid chromatography

B. I. KNIGHT and G. G. SKELLERN

Drug Metabolism Research Unit, Department of Pharmaceutical Chemistry, University of Strathclyde, Glasgow G1 1XW (Great Britain)

(Received December 6th, 1979)

Uridine diphosphate glucuronyltransferase (UDPGT) (E.C. 2.4.1.17) catalyses the glucuronidation of endogenous and foreign substances[1], which, in most mammalian species, is the most important of the synthetic metabolic reactions. In the course of investigating whether or not certain drugs and their metabolites are conjugated by liver microsomal UDPGT preparations *in vitro*, it was necessary to ascertain the activity of the enzyme preparation under identical incubation conditions. For this purpose, assays by high-performance liquid chromatography (HPLC) were developed to measure the formation of glucuronides of two known substrates of UDPGT (*p*-nitrophenol and paracetamol) by injecting aliquots of incubation mixtures directly on to a reversed-phase HPLC column; elution was with a mobile phase containing an ion-pairing reagent in aqueous methanol.

EXPERIMENTAL

Chemicals

p-Nitrophenol (PNP), *p*-nitrophenyl-β-D-glucuronide (PNP-G), uridine diphosphoglucuronic acid (UDPGA), uridine monophosphate (UMP) and uridine were obtained from Sigma (Poole, Great Britain). Paracetamol and tetrabutylammonium hydroxide (TBAH) were obtained from BDH (Poole, Great Britain). Paracetamol-β-D-glucuronide (P-G) was a gift. Tetrabutylammonium phosphate (TBAP) was prepared by titrating TBAH with 10% phosphoric acid to pH 7.5.

HPLC apparatus and conditions

A Spectra-Physics liquid chromatograph (Model 3500B), with ultraviolet detection at 254 and 280 nm, in conjunction with a Leeds-Northrup dual-pen recorder was used. Samples were injected on to a column (10 × 0.50 cm) slurry-packed with ODS-Spherisorb (5 μm mean particle size). The mobile phase was 5 m*M* TBAP in either methanol–water (5:95, v/v) for P-G or methanol–water (12:88, v/v) for PNP-G; it was delivered at a flow-rate of 0.8 ml min^{-1}.

Incubation conditions

A guinea pig-liver microsomal preparation (1 ml) prepared with 154 m*M* KCl according to the method of Graham and Wood[2] and containing either 2 or 5 mg

of protein per ml suspended in 154 m*M* KCl, was added to a solution (0.4 ml) of UDPGA and either PNP or paracetamol in 0.1 *M* KH_2PO_4–KOH buffer solution of pH 7.1. The resulting solution was incubated at 37°. The final concentrations of substrate (PNP or paracetamol) and of UDPGA were 0.6 m*M* and 4.0 m*M*, respectively. Aliquots (100 μl) of the incubation mixture were removed at zero time and at appropriate intervals up to 2 h, then centrifuged in tapered 10-ml test-tubes to sediment microsomal protein; aliquots (3 μl) of the supernatant solutions were injected on to the HPLC column. Control incubations contained heat-denatured (5 min at 100°) protein.

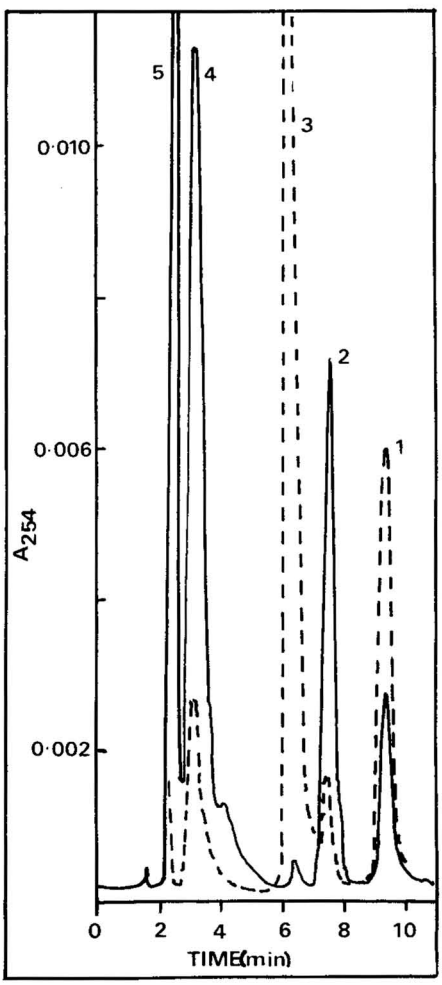

Fig. 1. Chromatograms recorded during the *in vitro* glucuronidation of paracetamol at 2 min (broken line) and 30 min (solid line) from the start of incubation. Peaks: 1 = paracetamol; 2 = P-G; 3 = UDPGA; 4 = UMP; 5 = uridine.

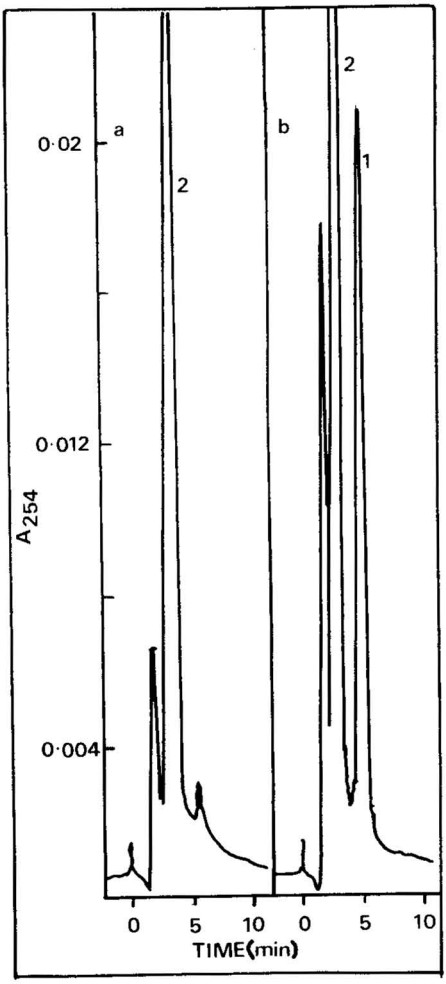

Fig. 2. Chromatograms recorded during the *in vitro* glucuronidation of PNP at 2 min (a) and 20 min (b) from the start of incubation. Peaks: 1 = PNP-G; 2 = UDPGA. Unconjugated PNP is retained on the column.

RESULTS AND DISCUSSION

A recent method[3] for the determination of PNP-G in urine by reversed-phase HPLC was unsuitable in our hands for *in vitro* glucuronidation studies, as PNP-G could not be separated from UDPGA.

In the work reported here, the methanol–water ratio of the mobile phase was adjusted to separate the components of the incubation media. With paracetamol as substrate, both the formation of the glucuronide (P-G) and the decrease in the paracetamol concentration can be monitored simultaneously (see Fig. 1). However, with PNP as substrate, PNP is retained on the column under the conditions described, whereas PNP-G has a retention time of 5 min (see Fig. 2).

The method described would also be suitable for studying another enzyme present in rat-liver microsomal preparations, UDPGA pyrophosphatase[4], which hydrolyses UDPGA and hence might interfere with glucuronidation.

In general, the need for an ion-pairing reagent in the mobile phases arises because most glucuronides are insufficiently lipophilic to be retained on a reversed-phase column. This method is applicable to a variety of substrates, as the retention times of their glucuronides can be adjusted by altering the proportion of methanol in the mobile phase. Therefore, studies on UDPGT may be performed without being limited to the few substrates for which published assays are available.

ACKNOWLEDGEMENT

This work was supported by a grant from the Scottish Hospital Endowments Research Trust.

REFERENCES

1 G. J. Dutton, in G. J. Dutton (Editor), *Glucuronic Acid: Free and Combined*, Academic Press, London, 1966, p. 229.
2 A. B. Graham and G. C. Wood, *Biochim. Biophys. Acta*, 311 (1973) 45.
3 G. Diamond and A. J. Quebbemann, *J. Chromatogr.*, 177 (1979) 368.
4 A. B. Graham and G. C. Wood, *Biochim. Biophys. Acta*, 276 (1972) 392.

Journal of Chromatography, 192 (1980) 250–252

CHROM. 12,599

Note

Thin-layer chromatographic estimation of 2,4-xylenol in 2,5-xylenol

JOSE PHILIP and LESTER CHAFETZ

Analytical Research Laboratories, Parke-Davis Division, The Warner-Lambert Company, Morris Plains, N.J. 07950 (U.S.A.)

(Received December 10th, 1979)

2,5-Xylenol is the starting material in synthesis of gemfibrozil, 2,2-dimethyl-5-(2,5-xylyloxy)valeric acid. Studies on the purity of this investigational hypolipemic agent showed the presence of small amounts of its 2,4-xylyloxy isomer, a process contaminant from 2,4-xylenol in the starting material. Although a rather tedious and lengthy gas chromatographic method was developed for detection and estimation of the isomer in the experimental drug, estimation of the 2,4-xylenol content of the 2,5-xylenol used in the synthesis was considered to be most definitive.

Attempts to purify 2,5-xylenol by crystallization and to separate the 2,5- and 2,4-isomers by gas–liquid chromatographic, high-performance liquid chromatographic and thin-layer chromatographic (TLC) methods were unsuccessful owing to the closely similar physical properties of the isomers. Crump separated *p*-nitrophenylazo derivatives of isomeric phenols by paper partition chromatography[1] and by TLC on alkali-impregnated plates[2]. An operationally simpler TLC system is described here, wherein the azo dye derivatives are made by coupling the xylenols with commercially available *p*-nitrobenzenediazonium fluoborate. As expected, 2,4-xylenol couples exclusively at the 6-position, and the predominant product for 2,5-xylenol is the 4-azo dye. A description of the TLC method and evidence obtained in characterization of the reaction products are presented below.

EXPERIMENTAL AND RESULTS

Determination of 2,4-xylenol in 2,5-xylenol

Weigh 25 mg of the 2,5-xylenol under test and transfer it to a 15-ml centrifuge tube. Dissolve 2,4-xylenol in 0.1 *M* sodium hydroxide to obtain a concentration of *ca.* 0.5 mg per ml, and transfer 0.05 ml (25 μg) and 0.5 ml (250 μg) to similar tubes. Add 5 ml of 0.1 *N* sodium hydroxide to each tube and mix, then add 2 ml of water and 50 mg of *p*-nitrobenzenediazonium fluoborate and mix on a Vortex mixer for 2–3 min. Add 0.75 ml of 1 *N* hydrochloric acid, then extract with 3 ml of hexane–chloroform (7:3), with shaking for 5 min; centrifuge, and collect the top layer. Apply 20 μl of each solution *ca.* 2.5 cm from one edge of a TLC plate (20 × 20 cm) coated with a 0.25-mm layer of silica gel GF, and develop the plate in the hexane–chloroform (7:3) until the solvent front has ascended *ca.* 15 cm, then air-dry the plate, and spray it with 1 *M* methanolic tetrabutylammonium hydroxide. Estimate the amount of

2,4-xylenol in the lane from the 2,5-xylenol by comparison with the two standards (0.1% and 1%). The azo dye from 2,4-xylenol has an R_F of *ca.* 0.3, and is well resolved from the dyes from 2,5-xylenol, which show R_F values from the origin to less than 0.2. (Development of the chromatogram can be followed by the orange spots of the azo dyes; these are changed to purple and intensified when treated with alkali.)

Characterization of azo dyes

6-(4-Nitrophenylazo)-2,4-xylenol was prepared by adding 3 g of *p*-nitrobenzenediazonium fluoborate to a solution of 2 g of 2,4-xylenol in 100 ml of 0.1 *M* sodium hydroxide and stirring for 5 min. The solution was acidified by dropwise addition of concentrated hydrochloric acid and extracted with 50 ml of chloroform, and the extract was washed with three 25-ml portions of water and then evaporated to dryness. The residue, which gave essentially one spot on TLC, was recrystallized once from aqueous acetic acid and twice from glacial acetic acid to yield dark pink crystals, which were washed with cold water and dried in a vacuum oven at 90°. Elemental analysis, mass spectra and nuclear magnetic resonance (NMR) studies gave results consistent with the structure assigned.

Calculated for $C_{14}H_{13}N_3O_3$: C = 61.99, H = 4.79, N = 15.49
Found: C = 61.27, H = 4.93, N = 15.46

The mass spectrum showed a molecular ion at *m/e* 271 (the molecular weight) and additional peaks for fragments *m/e* 149, 121, 91 and 77. NMR in deuterochloroform showed peaks at 2.28 and 2.36 ppm (diagnostic of two aromatic methyls), at 7.1 and 7.55 ppm (indicating protons at the 3- and 5-positions on the xylenol ring), at 7.87 to 8.37 ppm (for the four protons on the 4-nitrophenyl moiety) and at 12.83 ppm for the proton on the xylenol -OH group.

4-(4-Nitrophenylazo)-2,5-xylenol was prepared similarly, except that the reaction was allowed to proceed for 25 min. The residue was impure by TLC. It was purified by introducing 150 mg of it, in chloroform, into a glass column (37 cm × 3.2 cm I.D.) packed with SilicAR®-CC-4 (Mallinckrodt, St. Louis, Mo., U.S.A.) slurried in toluene, eluting with toluene and monitoring the fractions visually. The major component was chromatographed on a similar column, using chloroform for elution. The eluate was evaporated to dryness, and the residue was recrystallized from aqueous methanol to give brown crystals, which melted at 225–227°. Elemental analysis, mass spectra and NMR spectra were consistent with the assigned structure.

Calculated for $C_{14}H_{13}N_3O_3$: C = 61.99, H = 4.79, N = 15.49
Found: C = 61.51, H = 4.87, N = 15.46

The mass spectrum showed a molecular ion at *m/e* 271 and was similar to that obtained for the azo dye from 2,4-xylenol. NMR in deuterochloroform showed peaks at 2.17 and 2.60 ppm (for the two aromatic methyls), a peak at 4.98 ppm (for the -OH proton), peaks at 6.64 and 7.50 ppm (diagnostic of the protons at the 6- and 3-positions of the xylenol ring) and at 7.78 to 8.28 ppm (for the four protons of the 4-nitrophenyl moiety).

ACKNOWLEDGEMENTS

We are grateful to Messrs. Charles Childs and R. Bruce Scott of Parke-Davis, Ann Arbor, Mich., U.S.A., for analyses of the samples.

REFERENCES

1 G. B. Crump, *J. Chromatogr.*, 10 (1963) 21–28.
2 G. B. Crump, *Anal. Chem.*, 36 (1964) 2447–2451.

Vol. 192, No. 1

journal of chromatography news section

APPARATUS

N-1390

PACKARD-BECKER 433 GAS CHROMATOGRAPH

The latest addition to Packard-Becker's range of microprocessor-controlled GC instruments is the Model 433 which features a compact printer/plotter. This unit is built into the system's separate control station, and produces the analysis reports on one sheet. The format can be selected before or after the analysis. The entire process is directed from the control station with its chromatography-labelled keyboard and display. The system has storage capacity for 20 programs, each with a capacity of 15 time-based instructions. Calculation methods

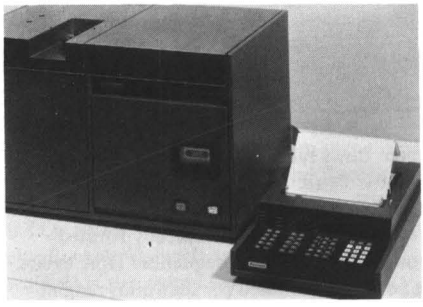

optionally available include area normalization with correction factors, internal standard, external standard, and automatic (re)calibration. The 433 system has interchangeable analytical modules (oven covers with injection ports, columns and detectors), plug-in flow and pressure regulators and detectors. New in the detector program is the flame photometric detector.

N-1376

BROCHURE ON DANI GAS CHROMATOGRAPHS

DANI has available a brochure with compact information on the company's line of Series 3200 gas chromatographs. The DANI Series 3200 gas chromatographs are produced in four basic different configurations having different detectors (TCD, TCD with amplifier, FID, ECD). All DANI Series 3200 gas chromatographs are single-column isothermal versions in the standard configuration.

N-1409

HAMILTON PRECISE FLUID HANDLING AND MEASURING DEVICES

More than 1000 different precision measuring and dispensing products for research applications are described in the Hamilton catalog "Precise Fluid Handling and Measuring Devices". Included are a range of Microliter® syringes and special application syringes, valves and fittings, automatic and manual dispensers, and accessories such as septa, columns and gauges for gas and liquid chromatography. Several products in the catalog are new, including the Microlab P, a microprocessor pipette and the Precision Liquid Dispenser-II, with single- or dual-channel operation. Other new products are the Multi-Pak, a package of metal-handled syringes, the Terasaki dispenser, a flow meter, and GC and LC accessories.

For further information concerning any of the news items, apply to the publisher, using the reply cards provided, quoting the reference number printed at the beginning of the item.

N-1401

SYRINGE FOR POLLUTION ANALYZERS

The Hamilton Company introduced a push-button, semi-automatic constant rate syringe, Model CR-700, for injection into CO_2, CO, SO_2, NO_2 and TOC analyzers. The Hamilton CR-700 is claimed to be equivalent in performance to larger and more complex devices that cost much more. Designed especially for use in environmental testing laboratories where procedures are run for carbon, SO_2 or NO_2 content, the CR-700 delivers identical sample volumes and injection rates regardless of operator skill. The gas-tight and liquid-tight syringe permits volume selection in increments as small as 0.1 µl with a repeatable and resettable accuracy of ± 1.0%. The CR-700-50 has a capacity of 2.0 to 50.0 µl. Other standard capacities include 1.0 to 20.0 µl, and 10.0 to 200.0 µl.

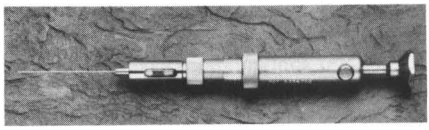

N-1408

CAPILLARY DISPENSER

The CAMAG capillary dispenser system opens possibilities to use disposable glass capillaries efficiently in quantitative conventional and high-performance TLC analysis. The system is easy to handle and offers the precision of sample positioning required for automatic chromatogram scanning. By pushing the pipette holder into the mouth of the dispenser it is loaded with a disposable capillary. After the capillary has been filled with sample solution the holder is placed in the magnet head of a CAMAG Nanomat from where it descends on to the layer surface at an adjusted speed and for a regulated contact time. With the automatic repetition device of the Nanomat the capillary content can be delivered in small increments so that comparatively large volumes are applied as small spots. Pipette holders and capillaries in dispensing magazines are available in the sizes 0.5, 1, 2, 3, and 5 µl.

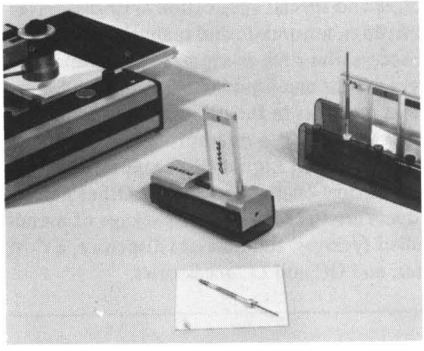

N-1411

GRADIENT GENERATOR

A gradient generator developed by Hamilton makes possible the preparation of linear gradients for use in HPLC and in classic column chromatography. The device combines an electronic digital timer with a miniature inert valve and an accurate electric valve driver. Depending upon the application parameters, samples ranging in size of 0.5 to 10.0 µl can be introduced into systems having pressures up to 5000 p.s.i.

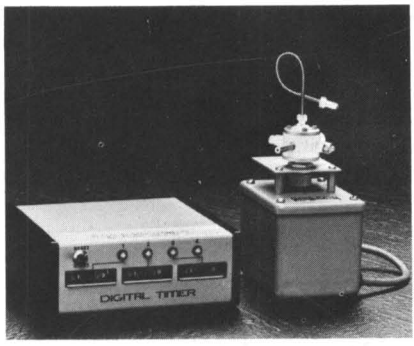

Sample flows range from a simple on-off to four-way distribution. The timer portion of the device can produce up to four step gradients wherein the valve is electronically rotated through all positions in sequence. Time cycles can be pre-determined for durations ranging from 1.0 sec up to 200.0 min, with typical accuracies of ± 0.008 sec. Cycles can be reprogrammed or over-ridden on demand, and indicator lights make possible visible status checks. The sample flow patterns are changed in 1.5 sec.

N-1362

ALLTECH CATALOG NO. 30

From Alltech Associates is available the chromatography catalog No. 30. The catalog describes in more than 160 pages the Alltech program on chromatography which ranges from pocket calculators to vacuum pumps. The catalog gives a good description of the various types of GC and HPLC columns in the Alltech program, and also includes information on Alltech products for control and maintenance of the chromatographic instrumentation.

N-1370

HAMILTON CATALOG

More than 1000 products for industrial, medical and chemical research are described in a 56-page catalog from Hamilton. Included are a broad range of syringes, valves and fittings, automatic and manual dispensers, and accessories such as septa, columns and gauges for gas and liquid chromatography. New are the programmable microprocessor pipette Microlab P and the Precision Liquid Dispenser-II with single- or dual-channel operation.

N-1396

DENSITOMETER FOR TLC

The SD 3000 spectrodensitometer from the Schoeffel Instruments Division of Kratos, Inc. is described in an 8-page brochure. The SD 3000 is a thin-layer chromatogram scanner capable of making absorbance and fluorescence measurements of spotted thin-layer separations on TLC plates, paper, or film, as well as agarose gels, disc gels, slab gels and electrophoretic media. It is also suited for the analysis of HPTLC plates. The SD 3000 may be operated in either the single-beam or double-beam ratio mode. The instrument is modular in design, permitting the user to choose from an array of compatible accessories according to application. The accessories include the necessary carriers for various media, and an electronic reporting integrator for quantitative analysis reports.

N-1400

HPLC GUARD COLUMNS

Available from Rheodyne, Inc. are guard columns using disposable cartridges. The company estimates that use of these guard columns will reduce total column costs about 50% by protecting expensive analytical columns. The cartridges last about 10 times as long as pellicular guard column packings because they are packed with totally porous particles with a diameter of 10 μm. This packing not only catches harmful particles but captures also strongly absorbed compounds before they reach the analytical column. The cartridges are 3 cm long and operate at pressures up to 7000 p.s.i. Cartridges with ten different packings are available to match the stationary phase with that of the analytical column.

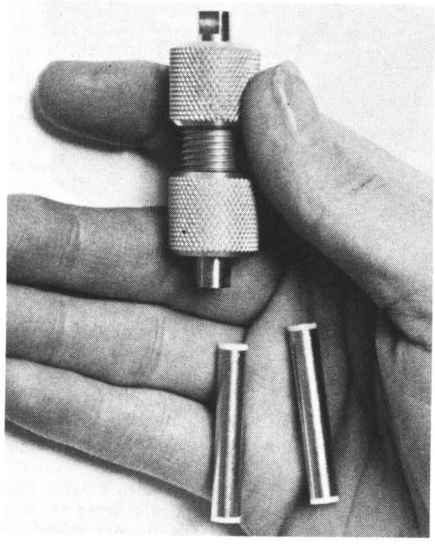

N-1406

PACKARD 430 BROCHURE

From Packard-Becker BV is available a brochure describing the Model 430 gas chromatography system. The brochure gives extended information on this GC instrument, with the built-in dual-channel integrating and printing system, the advanced analytical hardware, based on the analytical module concept, and on the MDSS (Multi Dimensional Switching System) for multidimensional analysis.

N-1403

ANALYSIS OF PCBs IN TRANSFORMER OILS

Analytical Instrument Development, Inc., have developed a field analysis scheme and instrumentation for on-site measurement of polychlorinated biphenyls (PCBs) in transformer fluids. The technique utilizes a portable electron-capture gas chromatograph. The self-contained batteries and gas supply permit at least eight hours of transformer fluid analysis. With an inherent sensitivity of 20 pg PCB, the technique provides results from 2 ppm to several percent.

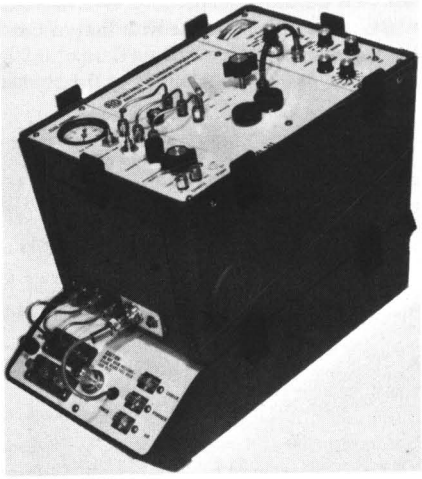

N-1375

REFRACTOMONITOR III

The RefractoMonitor III from LDC is a sensitive double-beam Fresnel-type refractive index detector for liquid chromatography. The minimum detectable refractive index difference is 4×10^{-8} at 0.5 sec time constant. The cell volume is 0.5 μl with standard gasket. The differential refractive index range of the instrument lies between 2×10^{-6} and 1024×10^{-6} RI units full scale in 10 binary steps. The drift rate is typically less than 4×10^{-7} RI units per hour. The Refracto Monitor III has an output to a recorder or to a computer.

N-1380

TLC EDUCATIONAL KIT

A complete TLC educational kit designed and equipped to provide "hands-on" training for students and analytical technicians, is available from Analtech. The kit includes an instruction manual which covers the basic TLC procedures step-by-step. It includes a pre-developed TLC plate with complete analysis. An assortment of TLC plates is provided with a development chamber, plate rack, disposable micropipettes, test dye kit and saturation pads.

MEETING

EXPOCHEM '80, an international exposition of analytical instrumentation in the industrial and biomedical fields, will be held at the Astrohall in Houston, Texas on October 6–9, 1980.

The technical programme will consist of presentations by the leading authorities in most areas of analytical chemistry from throughout the world. Topics to be included are: emission spectroscopy, automation, environmental analysis, new instrumentation, surface analysis, pharmaceutical analysis and data treatment. The chromatography section will be represented by the 15th International Symposium on Advances in Chromatography which will be included as part of EXPOCHEM '80. Current developments in gas chromatography, high performance liquid chromatography, high performance thin-layer chromatography and gas chromatography–mass spectrometry will be presented. Intensive short courses on a variety of subjects will be given on the weekend prior to the exposition.

Inquiries regarding exhibition space, technical programme or short courses should be directed to: Dr. Albert Zlatkis, Chemistry Department, University of Houston, Texas 77004, U.S.A. or phone (713) 749-2623.

GENERAL INFORMATION

(A leaflet *Instructions to Authors* can be obtained by application to the publisher.)

Types of Contributions. The following types of papers are published in the *Journal of Chromatography* and the section on *Biomedical Applications:* Regular research papers (Full-length papers), Short communications and Notes. Short communications are preliminary announcements of important new developments and will, whenever possible, be published with maximum speed. Notes are usually descriptions of short investigations and reflect the same quality of research as Full-length papers, but should preferably not exceed four printed pages. For reviews, see page 2 of cover under Submission of Papers.

Manuscripts. Manuscripts should be typed in double spacing on consecutively numbered pages of uniform size. The manuscript should be preceded by a sheet of manuscript paper carrying the title of the paper and the name and full postal address of the person to whom the proofs are to be sent. Authors of papers in French or German are requested to supply an English translation of the title of the paper. As a rule, papers should be divided into sections, headed by a caption (*e.g.*, Summary, Introduction, Experimental, Results, Discussion, etc.). All illustrations, photographs, tables, etc. should be on separate sheets.

Title. The title of the paper should be concise and informative. Since titles are widely used in information retrieval systems, care should be taken to include the key words. The title should be followed by the authors' full names, academic or professional affiliations, and the address of the laboratory where the work was carried out. If the present address of an author is different from that mentioned, it should be given in a footnote. Acknowledgements of financial support are *not* to be made in a footnote to the title or name of the author, but should be included in the Acknowledgements at the end of the paper.

Summary. Full-length papers and Review articles should have a summary of 50–100 words which clearly and briefly indicates what is new, different and significant. In the case of French or German articles an additional summary in English, headed by an English translation of the title, should also be provided. (Short communications and Notes are published without a summary.)

Illustrations. The figures should be submitted in a form suitable for reproduction, drawn in Indian ink on drawing or tracing paper. One original and two photocopies are required. Attention should be given to any lettering (which should be kept to a minimum) and to spacing on axes of graphs in order to ensure that numbers etc. remain legible after reduction. Axes of a graph should be clearly labelled. The figures should preferably be of such a size that the same degree of reduction can be applied to all of them. Photographs should have good contrast and intensity. Sharp, glossy photographs are required to obtain good halftones. References to the illustrations should be included in appropriate places in the text using arabic numerals. Each illustration should have a legend, all the *legends* being typed (with double spacing) together on a *separate sheet*. If structures are given in the text, the original drawings should be supplied. Coloured illustrations are reproduced at the author's expense, the cost being determined by the number of pages and by the number of colours needed. The written permission of the author and publisher must be obtained for the use of any figure already published. Its source must be indicated in the legend.

References. References should be numbered in the order in which they are cited in the text, and listed in numerical sequence on a separate sheet at the end of the article. The numbers should appear in the text at the appropriate places in square brackets. In the reference list, periodicals [1], books [2], multi-author books [3] and proceedings [4] should be cited in accordance with the following examples:

1 A. T. James and A. J. P. Martin, *Biochem. J.*, 50 (1952) 679.
2 L. R. Snyder, *Principles of Adsorption Chromatography*, Marcel Dekker, New York, 1968, p. 201.
3 H. C. S. Wood and R. Wrigglesworth, in S. Coffey (Editor), *Rodd's Chemistry of Carbon Compounds, Vol. IV, Heterocyclic Compounds*, Part B, Elsevier, Amsterdam, Oxford, New York, 2nd ed., 1977, Ch. 11, p. 201.
4 E. C. Horning, J.-P. Thenot and M. G. Horning, in A. P. De Leenheer and R. R. Roncucci (Editors), *Proc. 1st Int. Symp. Quantitative Mass Spectrometry in Life Sciences, Ghent, June 16–18, 1976*, Elsevier, Amsterdam, Oxford, New York, 1977, p. 1.

Abbreviations for the titles of journals should follow the system used by *Chemical Abstracts*. Articles not yet published should be given as "in press", "submitted for publication", "in preparation" or "personal communication". The *Journal of Chromatography; Journal of Chromatography, Biomedical Applications* and *Chromatographic Reviews* should be cited as *J. Chromatogr.*

Proofs. One set of proofs will be sent to the author to be carefully checked for printer's errors. Corrections must be restricted to instances in which the proof is at variance with the manuscript. "Extra corrections" will be inserted at the author's expense.

Reprints. Fifty reprints of Full-length papers, Short communications and Notes will be supplied free of charge. Additional reprints can be ordered by the authors. An order form containing price quotations will be sent to the authors together with the proofs of their article.

News. News releases of new products and developments, and information leaflets of meetings should be addressed to: The Editor of the News Section, Journal of Chromatography/Journal of Chromatography, Biomedical Applications, Elsevier Scientific Publishing Company, P.O. Box 330, 1000 AH Amsterdam, The Netherlands.

Advertisements. Advertisement rates are available from the publisher on request. The Editors of the journal accept no responsibility for the contents of the advertisements.

H.P.L.C.?

Du Pont has got what you're looking for.

We've got the experience.

Since introducing the first commercial High Performance Liquid Chromatograph in 1969, Du Pont has continued to lead the field in this important separation technique.

Today, Du Pont offers the most versatile range of HPLC and HP Preparative LC systems available anywhere.

We've got the performance.

Some of the recent advances you'll find in our HPLC systems include microprocessor control, precision gradient programming, state-of-the-art detectors, automatic samplers, built-in diagnostics and self-contained "memory" for ready recall of up to 8 stored analytical programmes.

It all adds up to unbeatable high performance. Speed. Reliability. Superb reproducibility. Excellent resolution of peaks. And of course, ease of operation.

And Du Pont "Zorbax" columns ensure highest performance throughout the analysis.

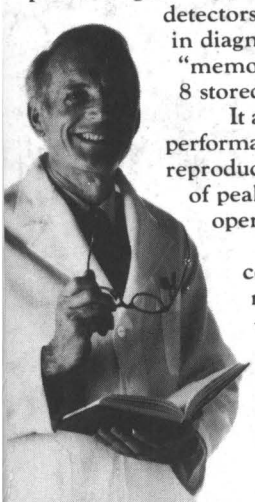

We've got the versatility.

Because Du Pont HPLC systems are designed and built on a modular basis, you can start with a basic system and add on at a later date according to your needs, and your budget.

Modules currently available include gradient, autosampler, SEC data analyser, automated sample processor plus several detectors and accessories. A wide range of "Zorbax" columns is also available.

We've got the reputation.

As one of the world's leading manufacturers of precision analytical instruments, Du Pont enjoys an outstanding reputation for product quality and service support.

Ask any of our customers. Or better still, contact Du Pont now and get the facts first hand.

Free book.

If you're seriously considering the purchase of a new HPLC system within the next 6-9 months, a fascinating book on Liquid Chromatography written by a leading Du Pont authority could be yours free, just by inviting our representative to call. Simply complete and return the coupon before December 31 to qualify.

Du Pont de Nemours International S.A.
Room N102/P.O. BOX
CH-1211 Geneva 24, Switzerland-Tel. (022) 27 81 11

Du Pont Instruments DU PONT

I intend to buy a new HPLC system within the next 6-9 months. Please ask your representative to phone for an appointement.

NAME: _____

POSITION: _____

COMPANY/INSTITUTION: _____

ADDRESS: _____

TEL.: _____ JC

Post to: Du Pont de Nemours International S.A., **"Dept. F.R"**, Room N102-P.O. BOX-CH-1211 Geneva 24, Switzerland.